The Journal of American Science

ISSN 1545-1003

Volume 5 - Number 4 (Cumulated No. 20), July 30, 2009, ISSN 1545-1003

Marsland Press, Michigan, The United States

The Journal of American Science

The ***Journal of American Science*** is an international journal with a purpose to enhance our natural and scientific knowledge dissemination in the world under the free publication principle. Any valuable paper that describes natural phenomena and existence or any reports that convey scientific research and pursuit is welcome. Papers submitted could be reviews, objective descriptions, research reports, opinions/debates, news, letters, and other types of writings that are nature and science related. All the manuscripts will be processed in a professional peer review. After the peer review, the journal will make the best efforts to publish all the valuable works as soon as possible.

Introductions to Authors

1. General Information

(1) Goals: As an international journal published both in print and on internet, *The Journal of American Science* is dedicated to the dissemination of fundamental knowledge in all areas of nature and science. The main purpose of *The Journal of American Science* is to enhance our knowledge spreading in the world under the free publication principle. It publishes full-length papers (original contributions), reviews, rapid communications, and any debates and opinions in all the fields of nature and science.

(2) What to Do: *The Journal of American Science* provides a place for discussion of scientific news, research, theory, philosophy, profession and technology - that will drive scientific progress. Research reports and regular manuscripts that contain new and significant information of general interest are welcome.

(3) Who: All people are welcome to submit manuscripts in any fields of nature and science.

(4) Distributions: Web version of the journal is freely opened to the world, without any payment or registration. The journal will be distributed to the selected libraries and institutions for free. For the subscription of other readers please contact with: editor@americanscience.org or americansciencej@gmail.com or editor@sciencepub.net

(5) Cost: This journal will be no charge for the manuscript contributors. If the author needs hard copy of the journal, it will be charged for US$100/issue to cover the printing and mailing fee.

(5) Advertisements: The price will be calculated as US$400/page, i.e. US$200/a half page, US$100/a quarter page, etc. Any size of the advertisement is welcome.

2. Manuscripts Submission

(1) Submission Methods: Electronic submission through email is encouraged and hard copies plus an IBM formatted computer diskette would also be accepted.

(2) Software: The Microsoft Word file will be preferred.

(3) Font: Normal, Times New Roman, 10 pt, single space.

(4) Indent: Type 4 spaces in the beginning of each new paragraph.

(5) Manuscript: Don't use "Footnote" or "Header and Footer".

(6) Cover Page: Put detail information of authors and a short title in the cover page.

(7) Title: Use Title Case in the title and subtitles, e.g. "**Debt and Agency Costs".**

(8) Figures and Tables: Use full word of figure and table, e.g. **"Figure 1.** Annul Income of Different Groups**", Table 1. Annual Increase of Investment".**

(9) References: Cite references by "last name, year", e.g. "(Smith, 2003)". References should include all the authors' last names and initials, title, journal, year, volume, issue, and pages etc.

Reference Examples:

Journal Article: Hacker J, Hentschel U, Dobrindt U. Prokaryotic chromosomes and disease. Science 2003;301(34):790-3.

Book: Berkowitz BA, Katzung BG. Basic and clinical evaluation of new drugs. In: Katzung BG, ed. Basic and clinical pharmacology. Appleton & Lance Publisher. Norwalk, Connecticut, USA. 1995:60-9.

(10) Submission Address: editor@sciencepub.net, Marsland Company, P.O. Box 21126, Lansing, Michigan 48909, The United States, 517-980-4106.

(11) Reviewers: Authors are encouraged to suggest 2-8 competent reviewers with their name and email.

2. Manuscript Preparation

Each manuscript is suggested to include the following components but authors can do their own ways:

(1) Title page: including the complete article title; each author's full name; institution(s) with which each author is affiliated, with city, state/province, zip code, and country; and the name, complete mailing address, telephone number, facsimile number (if available), and e-mail address for all correspondence.

(2) Abstract: including Background, Materials and Methods, Results, and Discussions.

(3) Key Words.

(4) Introduction.

(**5) Materials and Methods**.

(**6) Results**.

(**7) Discussions**.

(**8) References**.

(**9) Acknowledgments**.

Journal Address:
Marsland Press
2158 Butternut Drive
Okemos, MI 48864
The United States
Telephones: 347-321-7172; 718-404-5362; 517-349-2362
Emails: editor@americanscience.org; americansciencej@gmail.com; sciencepub@gmail.com
Websites: http://www.americanscience.org; http://www.sciencepub.net; http://www.sciencepub.org

The Journal of American Science

ISSN 1545-1003

Volume 5 - Number 4, July 30, 2009

Cover Page, Introduction, Contents, Call for Papers, All papers in one file

Welcome to send your manuscript(s) to: americansciencej@gmail.com.

CONTENTS

For back issues of *the Journal of American Science*, click here.

Emails: editor@americanscience.org; americansciencej@gmail.com

Himalayan Mouse-Hare *Ochotona roylei* : A Neglected Himalayan Wild Species?

Ritesh Joshi

Doon Institute of Engineering and Technology, 9th Mile Stone, Shyampur,
Rishikesh, Dehradun, 249 204, Uttarakhand, India
ritesh_joshi2325@yahoo.com

Abstract: In order to generate primary information about Himalayan mouse-hare *Ochotona roylei*, an in-depth survey was carried out in Tungnath area, Garhwal Himalaya. Mouse hares are tail less Himalayan rodents and generally ranging usually from 2200 to 3500 meter above sea level. A short migration has been observed during winter season from higher to lower elevations of the mountain region basically in search of food and for mating needs. The home range was measured to 1.5 Km^2 during favourable conditions and average movement was observed to be 70 meters in a single day. Feeding behaviour of this Himalayan mammal is very exemplary and food generally comprises of medicinal plant species (*Picrorhiza kurrooa, Saussurea costus, Aconitum heterophyllum, Angelica glouca* and *Allium spp*.) and dry grasses. In sub alpine areas where less snowfall was occurred, animal's movement activities were observed through out the year whereas in high altitude areas where ground surface was completely covered with snow, its movement activities were restricted to some extent. It was recommended that more studies are required on its behaviour, which can conclude about its movements during the winter especially in snow fed areas. [Journal of American Science 2009;5(4):1-6]. (ISSN: 1545-1003).

Key words: Himalayan Mouse-hare, *Ochotona roylei*, Garhwal Himalaya, behaviour, conservation

1. Introduction

Central Himalaya is recognized as a rich bio-diversity center due to its different climatic conditions, which provides variety of ecosystems with floral as well as faunal diversity. Himalayan mountain system includes 18,500 plant species, 241 mammals, 528 birds, 149 reptiles and 74 amphibian species (Ghosh, 1996). The diversity index of both plant and animal appears to be very significant including many of the primitive, new evolving wild species. Few of them are also categorized under threatened category mainly due to escalated rate of developmental and anthropogenic activities.

Presently several species of Himalayan wild animals have become extinct and many more are on the verge of extinction. Due to poor accessibility and rigid climatic conditions very less studies have been carried out on Himalayan mammals in high altitude (sub alpine and alpine) areas. Also in the absence of detailed studies and monitoring it appears too conjectural, to assume that the Himalayan wild animals are either migratory or resident. The order Lagomorpha comprises of two families, the Leporidae (hares and rabbits) and the Ochotonidae (mouse-hares). Mouse-hares (*Ochotona roylei*) are small tail less animal with short, broad, rounded ears and short legs (Figure 1). They are only restricted to the Himalayas, the mountains and steppes of central Asia and the mountains of western North America (Prater, 1998). Still no single document is available, which will focus on the conservation issues of this mammal and hence an attempt has been made to document the primary information regarding to its behaviour from sub alpine region (Tungnath) of Garhwal Himalaya. Besides, an effort has also been made to trace out their distribution in some other parts of Garhwal Himalaya. Mouse-hares are commonly called as 'Runda' and ranging usually from 2200 to 3500 meter above sea level. The body size varies from 15 to 20 centimeters in length and 5 to 7 centimeters in height. This animal shows both the characters of mouse and hare, therefore, may be an inter-connective link between the mouse and hare.

2. Study Area

The present investigation was carried out at Tungnath area [30°14' N latitude and 79°13' E longitude] of Garhwal Himalaya, altitude lies between 2200 to 3500 meter above sea level (Figure 2 & 3). The adverse climatic condition of study area reveals about maximum 26°C to minimum -4°C air temperature, intensive solar intensity (2500 lux in September to 79200 lux in May), high wind velocity, heavy frost, blizzards and low air

pressure throughout the year except few months of the summer season. Precipitation is found to be in the form of snow, hail and sometime heavy rain. Soil type is loam / sandy loam, light gray to brown in colour at lower altitude and sandy with large debris above the 3500 meter of height. Surface soil pH ranges between 4-8 and 5-7 (Acidic). The study area is also enriched with myriad types of floral as well as of faunal diversity. Tungnath alpine region consist about 171 species of different grasses, sedges, monocots, short forbs, medium forbs, tall forbs and shrubs and most of them are medicinal (Nautiyal et al., 2001). Some important flora comprises of *Rhododendron* spp. (Buransh), *Querques* spp. (Baanj), *Cedrus deodara* (Devdar), *Pinus* spp. (Kail) and *Abies pindraw* (Raga). The major wild animals found in this area are *Panthera uncial* (Snow Leopard), *Selenarctos thibentanus* (Himalayan Black Bear), *Moschus moschiferus* (Musk deer), *Martes flavigula* (Himalayan Yellow throated Martin), *Capra ibex* (Himalayan Ibex), *Hermitragus jemlahicus* (Himalayan Thar), *Lophophorus impejanus* (Himalayan Monal Pheasant) and *Pucrasia macrolopha* (Koklass Pheasant).

3. Observations

Himalayan Mouse- hares are not the highly wide-ranging animal but traversing more distances to fulfill their basic requirements as per different seasons and environmental conditions. As local inhabitation in Garhwal Himalayan region is mainly concentrated around the alpine and timberline regions, therefore, this mouse-hare is frequently seen around these areas. A short migration has been observed during winter season from higher to lower elevations of the mountain region basically in search of food and for mating needs. The home range was measured to 1.5 Km^2 during favourable conditions and average movement was observed to be 70 meters in a single day.

During winter (mid-December to mid-March) when entire study area is covered by snow, mouse-hare lives under the blanket of snow and fulfills their feeding requirements by the food materials collected and stored during the pre-winter period. This reflects towards the hibernation behaviour of animal and helps them adaptable to the adverse and unfavorable climatic condition during the winter in snowfed areas. In sub alpine areas where less snowfall was occurred, animal's movement activities were observed through out the year whereas in high altitude areas where ground level was completely covered with snow its movement activities were restricted to some extent. More research studies are required on its behaviour, which can conclude about its movements during the winter especially in snow fed areas. At Thangu (Sikkim, 3700 m asl) mouse hares are common in summer, but disappear completely during winter and it was suggested that there may be some movement to lower levels (Prater, 1998).

Feeding is one of the prime characteristics of animals, which directly link with their local movements and long-term migration. As the high altitude area are important source of many economically important medicinal plants this tail less mouse–hare generally feed on valuable parts of the medicinal plants, sometimes these are also observed to feed on ferns and small grasses of pasture lands. Among the medicinal and aromatic plants *Picrorhiza kurrooa, Saussurea costus, Aconitum heterophyllum, Angelica glouca* and *Allium spp*. are important ones. It was observed during the course of investigation that this rodent shows a typical feeding behaviour. During the pre winter period animal collects several types of medicinal plants and their different parts (leaves, roots, fruits and flowers) and stores them in their small burrows and den situated in between big pieces of stones (Figure 4). Dry grasses are a preffered item during this period as this can be utilized for a long period of time. This may helps them to utilize the stored food during unfavorable conditions, when whole of the area is covered by snow. As per the observations of the present study it was revealed that these mouse-hares are entirely dependent upon the natural food available in forest areas and near to human habitation areas, as the area does not comprises of any agricultural land.

The Himalayan mouse-hare population in the country has been adversely affected by the fragmentation of natural habitats, which leads to considerably limiting its frequent movement. It was observed that mouse-hare is slowly losing its habitat due to rapid increase in anthropogenic activities near to Tungnath area [Figure 5]. According to local people perceptions mouse hares are more commonly seen before last 4-5 years than today. Although no any evidences of human-animal conflict has been observed currently but unfortunately the number seems to decrease than the scenario of few previous years. This might be co-related with the studies on endangered medicinal and aromatic plant diversity. Till today no single research work has been carried out on its

ecological aspects and this Himalayan rodent becomes neglected wild species in Garhwal Himalaya. According to a preliminary report their breeding habits are also unrecorded (Prater, 1998).

The future of the Himalayan mouse-hare in this region thus depends on the long-term research studies on its behaviour and on the management practices inside the region, where this animal generally live as well as in formulating a clear cut action plan for their long term survival. Presently, mainly due to the loss of natural habitat and human encroachment into the deeper forest regimes of high altitude areas many plants are categorized under threatened category or are on the verge of extinction. This has caused a serious problem for maintaining the biological diversity status of alpine region.

(1)

(3)

(4)

(5)

Figure 1) *Ochotona roylei*: A flagship species of Garhwal Himalaya, 3) Overview of study area, 4) Himalayan mouse hare in its den under rocky clusters & 5) Anthropogenic activities around Tungnath area.

4. Recommendations

1. It has been observed at different locations that tourists are not careful and aware about the dumping of remains of food items. These dumps not only attract the mouse-hare but it also attracts few other herbivore wild animals, which generally lead to drastic change in their behaviour. Several times animal may also died due to indigestion and subsequent blockage of intestine. Tourist must be motivated regarding to environmental pollution and conservation.
2. Studies are required to be conducted regarding to altitude-wise distribution of mouse hare, which will be helpful in concluding its exact status whether animal is endangered, vulnerable or rare.
3. Eco-development and conservation education activities through organizing training programmes and workshops can provide better management strategies.
4. Grazing by horses, mules and other domestic animals is another major problem and it should be controlled in some of the habitats where population of mouse hares still exists.
5. It is recommended that during the summer when large number of tourist visit to Tungnath area, hoardings must be placed regarding to environmental conservation, which will be helpful in creating awareness among local people and tourist about the conservation issues of Himalayan biological diversity.

Acknowledgements:

The author is highly thankful to the Director and Dr. R. K. Maikhuri, Scientist Incharge (Garhwal Unit) of the G. B. Pant Institute of Himalayan Environment and Development for their valuable support and cooperation during the investigation period. Thanks are also due to Dr. S. N. Bahuguna, Department of Zoology, HNB Garhwal University for providing valuable inputs during the investigation period. Chairman and Director, Doon Institute of Engineering and Technology are highly acknowledged for providing necessary facilities during the study period.

Correspondence to:

Ritesh Joshi

Doon Institute of Engineering and Technology, 9th Mile Stone, Shyampur, Rishikesh, Dehradun, 249 204, Uttarakhand, India

Telephone: + 91 135 2454353 (O)

Email: ritesh_joshi2325@yahoo.com

References

[1] Ghosh, A.K. 1996. Himalayan fauna with special reference to endangered and endemic species. In: Himalayan biodiversity: action plan (Dhar, U. ed.), Himavikas publication, Nainital. pp. 53-59.

[2] Prakash, I. 1978. Handbook of vertebrate pest control. ICAR Publication. pp. 1-95.

[3] Prater, S.H. 1998. The book of Indian animals. Bombay Natural History Society, Oxford University Press.

ISSN: 1545-1003

The journal of American Science

Normal paper structure for the Journal of American Science:

Each manuscript is suggested to include the following components but authors can do their own ways:

(1) The complete article title.
(2) Each author's full name; institution(s) with which each author is affiliated, with city, state/province, zip code, and country; and the name, complete mailing address, telephone number, facsimile number (if available), and email address for all correspondence.
(3) **You must put at least one email address under the authors' address.**
(4) Abstract: including Background, Materials and Methods, Results, and Discussions, 100-300 words preferred.
(5) Key Words.
(6) Introduction.
(7) Materials and Methods.
(8) Results.
(9) Discussions.
(10) Acknowledgments.
(11) Correspondence to.
(12) References.

Description of Manuscript Preparation and Format:

(1) Software: Microsoft Word file.
(2) Font: Normal, Times New Roman, 10 pt, single space.
(3) Indent: 8 spaces in the beginning of each new paragraph.
(4) Manuscript: Don't use "Footnote" or "Header and Footer".
(5) Spelling check: Do spelling check when you finish.
(6) Color: Email and website addresses are blue, and all other contents are black.
(7) Abstract: 100-300 words are preferred, and remember to add "[The Journal of American Science. 2009;x(x):xx-xx]. (ISSN 1545-1003)" in the end of abstract.
(8) Page setup: Margins: top 72 pt, bottom 72 pt. left 72 pt, right 72 pt.
(9) Paper size: Letter, width 612 pt, height 792 pt.
(10) Layout: Header 36 pt, Foot 36 pt.
(11) Title: Use Title Case in the title and subtitles, e.g. "Debt and Agency Costs".
(12) Figures and Tables: Use full word of figure and table, e.g. "Figure 1. Annul Income of Different Groups", Table 1. Annual Increase of Investment".
(13) References: Cite 10-20 references preferred, by "last name, year", e.g. "(Smith, 2003)". References should include all the authors' last names and initials, title, journal, year, volume, issue, and pages etc.
(14) *Reference Examples*: Journal Article: Hacker J, Hentschel U, Dobrindt U. Prokaryotic chromosomes and disease. Science 2003;301(34):790-3.
(15) Book: Berkowitz BA, Katzung BG. Basic and clinical evaluation of new drugs. In: Katzung BG, ed. Basic and clinical pharmacology. Appleton & Lance Publisher. Norwalk, Connecticut, USA. 1995:60-9.
(16) Insert page number by bottom / center.
(17) Header for odd: Marsland Press Journal of American Science 2009;x(x):xx-xx.
(18) Header for even: short title Family name of the first author, et al.
(19) Footer: http://www.americanscience.org americansciencej@gmail.com.
(20) Submission Address: sciencepub@gmail.com, editor@sciencepub.net, Marsland Press, P.O. Box 21126, Lansing, Michigan 48909, The United States, 347-321-7172.

Probability of Estimating a Large Earthquake Occurrence in Yangon and Its Surrounding Areas Using Historical Earthquake Data

Yin Myo Min Htwe [1,2], SHEN WenBin [2,*]

1. Department of Meteorology and Hydrology, Office Building No-5, Ministry of Transport, Naypyidaw, Myanmar
2. Department of Geophysics, School of Geodesy and Geomatics, Wuhan University, 129 Luoyu Road, Wuhan, Hubei 430079, China

wbshen@sgg.whu.edu.cn; jianyou.wu007@gmail.com;

Abstract: Seismologists try to predict how likely it is that an earthquake will occur, with a specified time, place, and magnitude. Earthquake prediction also includes calculating how a strong ground motion will affect a certain area if an earthquake does occur. Estimation of the probability of a large earthquake occurring in the time interval is a difficult problem in the conventional method of earthquake prediction; it is given some distribution of observed interval times between large earthquakes. In this paper, it is estimated the interval time for the next large earthquake, assuming the conditional probability of an earthquake occurrence as a maximum, which can or cannot occur in the next 30, 50, 80, 100 and 200 years since the occurrence of the last large earthquake. The probability distribution of the earthquake model and the method of predicting the annual probability are applied by using historical data on large earthquakes in Yangon and its surrounding areas, and the probability of the future earthquake in the region is suggested. [Journal of American Science 2009;5(4):7-12]. (ISSN: 1545-1003).

Key words: probability, conditional probability of earthquake, annual probability

1. Introduction

Myanmar is one part of a long active tectonic belt extending from Himalayas to the Sunda Trench (Vigny et al. 2003; Myanmar Earthquake Committee, 2005). Historically, Myanmar has experienced many earthquakes (Maung Thein, 1994). The probabilistic prediction of the next large earthquake in Myanmar might be significant. Such a prediction must rely on the observations of phenomena which are related to large earthquakes. Prediction is usually probabilistic in nature to allow for observed differences in individual repeated times and uncertainties in the parameters used in the calculations.

Earthquake prediction is inherently statistical (Lindh, 2003). Although some people continue to think of earthquake prediction as the specification of the time, place and magnitude of a future earthquake; it has been clear for at least two decades that this is an unrealistic and unreasonable definition. Earthquake prediction is customarily classified into long-term, intermediate-term and short-term (Snieder et al. 1997; Committee on the Science of Earthquakes, 2003; and Sykes et al. 1999). Long-term earthquake prediction is to predict the possible shocks occurring in a special region for the period of several years to over ten years in the future (Su Youjing, 2004). The reality is that the earthquake prediction starts from long-term forecasts of place and magnitude, with very approximate time constrains, and progresses, at least in principle, to a gradual narrowing of the time window as data and understanding permit. Thus, knowledge of present tectonic setting, historical records, and geological records are studied to determine locations and recurrence intervals of earthquakes (Nelson, 2004). A method of long-term prediction, which has been studied extensively in connection with earthquakes, is the use of probability distributions of recurrence times on individual faults or fault segments (Ferraes, 2003).

Two kinds of time-dependent models have been proposed: time-predictable and slip-predictable (Ferraes, 2003). In a time-predictable pattern the time between events is proportional to the magnitude of the preceding event, and therefore the date but not the magnitude of the next event can be predicted (Zoller et al, 2007). In a slip-predictable model the time between events is proportional to the magnitude of the following event, and the magnitude of the next event can be predicted, but the date cannot be predicted. In this model, the probability of earthquake occurrence during a period of interest, which is referred to as conditional probability,

is related to the elapsed time since the last major event and the average recurrence interval between major earthquakes. In time-interval based prediction, it is given some kind of assumed distribution of interval times and knowing the elapsed time since the last large event.

2. Probability Distribution of Earthquake Models

The probability distribution curves have three different models: characteristic earthquake model, time-predictable model and random model (Martel, 2002). The probability of events depends on the probability density distribution that is sampled and the sampling method.

In fact, we can not tell exactly when an earthquake occurs, because we do not have a theoretical model that successfully describes earthquake recurrence, so we adopt probability distributions based on the earthquake history which for most faults is short (only a few recurrences) and complicated. As a result, various distributions grossly consistent with the limited history are used and can produce quite different estimates.

Time-predictable model states that an earthquake occurs when the fault recovers the stress relieved in the most recent earthquake (Murray et al, 2002). Unlike time-independent models (for example, Poisson probability), the time-predictable model is therefore often preferred when adequate data are available, and it is incorporated in hazard predictions for many earthquake-prone regions. Time-predictable model is dividing the slip in the most recent earthquake by the fault slip rate in approximating the expected time to the next earthquake and only can predict the time of the next earthquake, not the magnitude of the next earthquake.

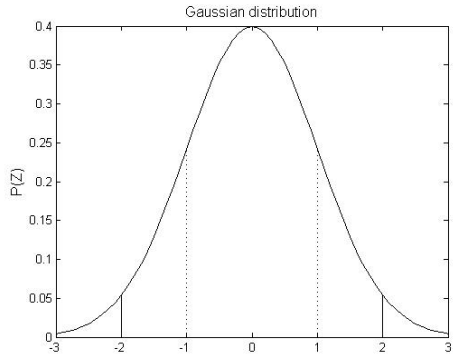

Figure 1 Gaussian or normal (bell curve) distribution.

Gaussian distribution approach can be used with any assumed probability density function. The simplest is to assume that the earthquake recurrence follows the familiar Gaussian or normal (bell curve) distribution

$$p(t,\tau,\sigma)=\frac{1}{\sigma\sqrt{2\pi}}\exp\left[\frac{-1}{2}\left(\frac{t-\tau}{\sigma}\right)^2\right] \quad (1)$$

This distribution is often described by using the normalized variable $z=(t-\tau)/\sigma$ that describes how far it is from its mean in terms of the standard deviation.

3. Conditional Probability

The purpose of this section is to provide a brief synopsis of conditional probability of event occurrence, $P(\Delta t/t)$, and to discuss some applications of conditional probability. The equations of conditional probability are applied to predict the occurrence of the next large earthquake in Yangon and its surroundings.

Given an interval of t years since the occurrence of the previous event, the probability of failure can be determined before time $t+\Delta t$ .The conditional probability $P(t<T\le t+\Delta t/T>t)$, which is the probability that an earthquake occurs during the next Δt interval, is

$$P(\Delta t|t)=\frac{P(t<T\le t+\Delta t)}{P(T\ge t)} \quad (2)$$

In terms of the probability density of T, say f, we have

$$P(t<T\le t+\Delta t)=\int_t^{t+\Delta t} f(s)ds \quad (3)$$

and

$$P(T\ge t)=\int_t^{\infty} f(s)ds \quad (4)$$

Substituting equations (3) and (4) in equation (2), one gets

$$P(\Delta t|t)=\frac{\int_t^{t+\Delta t} f(s)ds}{\int_t^{\alpha} f(s)ds} \quad (5)$$

Equation (5) provides a reasonable approach for estimating the seismic hazard on a fault or fault-segment and makes the underlying probability distribution of the earthquake recurrence time intervals normal (Ferraes, 2003).

4. Prediction of the annual probability of a large earthquake

There are total 22 large earthquakes from 527 AD to 1930 AD happened in and around the Yangon City

of Myanmar (Myanmar Earthquake Committee, 2005). The data set includes 527, 615, 652, 736, 813, 875, 986, 1059, 1161, 1269, 1286, 1348, 1396, 1457, 1464, 1570, 1644, 1757, 1768, 1912, 1917 and 1930.

Based on the time period between the oldest event listed above and the 1930 event, the average (mean) recurrence interval for large earthquakes can be calculated as follows:

Mean Recurrence Interval = (1930-527) years/ 21number of recurrence interval (6)

= 67 years.

The earthquakes are not occurring at a perfectly regular pace. The recurrence times between each successive pair of earthquakes are 88, 37, 84, 77, 62, 111, 73, 102, 108, 17, 62, 48, 61, 7, 106, 74, 113, 11, 144, 5, 13.

When we calculate the standard deviation of the 21 recurrence intervals associated with the 22 earthquakes, the following equation is used

$$\sigma = \sqrt{\frac{\sum_{i=1}^{n}(R_i - R^*)^2}{n-1}} \quad (7)$$

where σ is the standard deviation, R_i is the recurrence time between a given pair of events, R^* is the mean recurrence interval, and n is the number of recurrence intervals. Thus, the standard deviation σ is 40 years.

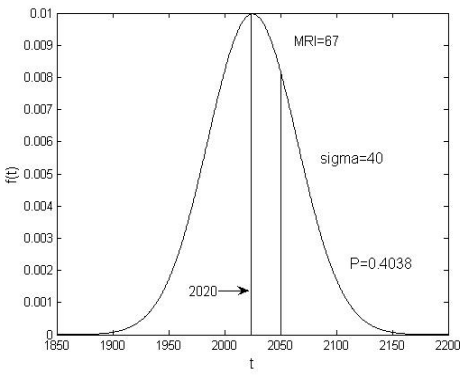

Figure 2 Probability of an Earthquake.

Assuming target year is 2020, how many years have elapsed since the last large earthquake in Myanmar is expressed as

2020-1930 = 90 years (8)

The mean recurrence interval of the years:

90-67 = 23 years (9)

The mean recurrence interval of the standard deviations:

23years/40years = 0.58 standard deviations (10)

We will now suppose the distribution of the recurrence intervals is normally distributed about the mean recurrence interval. On a supplied paper, plot the equation

$$f(t) = \frac{1}{\sigma\sqrt{2\pi}} \exp \frac{-(t-t^*)^2}{2\sigma^2} \quad (11)$$

where $f(t)$ is normal distribution, t is time, t^* is the mean, and σ is the standard deviation. Plot this for $0 \le t \le 250$ years.

Suppose the year is 2020–23 years (0.58 standard deviations) of the mean recurrence interval. In 30 years it would have 7 years (or 7/40 = 0.18 standard deviations) past the mean recurrence interval. The area under the probability density curve from the mean to 0.58 standard deviations of the mean is 0.219. The area under the probability density curve from the mean to 0.18 standard deviations past the mean is 0.0714. The area under the probability density curve from 0.58 standard deviations of the mean to ∞ is 0.5 + 0.219. So:

P= (0.219+0.0714)/ (0.5+0.219) = 40% (12)

Now suppose we consider the earthquakes to be distributed randomly (i.e. they are characterized by a Poisson distribution). Then the probability of an earthquake occurrence does not depend on how much time has elapsed since the last earthquake. The probability of "x" number of earthquakes occurring in a given interval of time t is given by:

$$P(x) = \frac{(vt)^2 e^{-vt}}{x!} \quad (13)$$

where "v" is the average rate of occurrence. So if the average recurrence interval is 67 years, the probability of getting 1 event in 67 years is:

$$P(1) = \frac{(\frac{1 \text{ event}}{67 \text{ yrs}} 67 \text{ yrs})^1 e^{-(\frac{1 \text{ event}}{67 \text{ yrs}} 67 \text{ yrs})}}{1!} \quad (14)$$

$$= e^{-1} = 37\ \%$$

The probability of getting one event in 30 years is:

$$P(1) = \frac{(\frac{1 \text{ event}}{67 \text{ yrs}} 30 \text{ yrs})^1 e^{-(\frac{1 \text{ event}}{67 \text{ yrs}} 30 \text{ yrs})}}{1!} \quad (15)$$

$$= (30/67)(e^{-30/67})$$

$$= 29\ \%$$

Thus the probability of getting no event in 30 years is:

$$p_{No}(1) = 1 - p(1) = 71\% \quad (16)$$

where " p_{No} " is the probability of getting no event.

Similarly, the probability of getting one event and no event in 50 years, 80 years, 100 years and 200 years is listed in table 1.

Finally, we have found the probability of getting one event and no event for next 30 years, 50 years, 80 years, 100 years and 200 years as shown by figures 3 and 4.

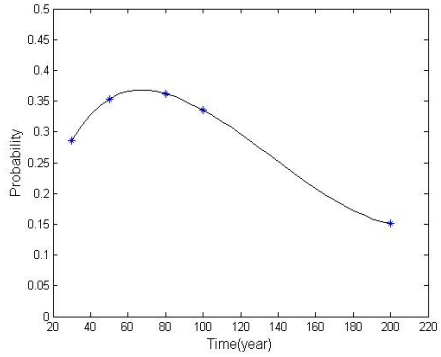

Figure 3 Probability of getting one event.

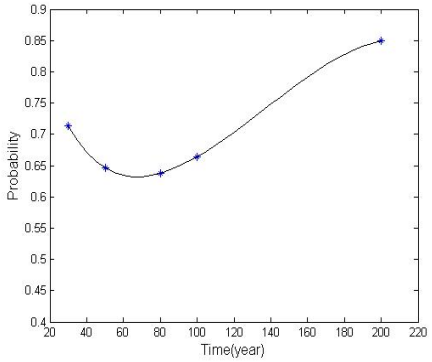

Figure 4 Probability of getting no event.

Table 1. The probability of getting event

No	Time (Years)	Probability of getting one event (%)	Probability of getting no event (%)
1	50	35	65
2	80	36	64
3	100	34	66
4	200	15	85

5. Conclusion

We have determined a time interval for the occurrence of the next large earthquake in Yangon City and its surroundings, using the conditional probability of earthquake occurrence and the annual probability method based on the historical earthquake data. First, the probability predictions are provided for next 30 years by using the prediction of the annual probability method, and then the predictions for next 50 years, 80 years, 100 years and 200 years. The prediction of the annual probability of "the big one" method tells the occurrence of the probability of the next large earthquake in 30 years, 50 years, 80 years, 100 years and 200 years in Yangon and its surrounding areas. In this paper, the time predictable pattern is used and consequently the time of event occurrence is estimated.

Acknowledgement:

Y.M.M. Htwe expresses his sincere gratitude to U Tint Lwin Swe, Engineering Geology Department, Yangon Technological University, Myanmar, for his persistent support in this study. This study is supported by the Natural Science Foundation of China (Grand No.40637034; 40574004)

Correspondence to:

WenBin Shen, Department of Geophysics, School of Geodesy and Geomatics, Wuhan University, 129 Luoyu Road, Wuhan 430079, China.
Tel.: 0086-027-68778857; Fax: +86-027-68778825
E-mail:; wbshen@sgg.whu.edu.cn;
or Yin Myo Min Htwe
Department of Meteorology and Hydrology
Office Building No-5, Ministry of Transport,
Naypyidaw, Myanmar
Telephone: 0095-067-411250;
E-mail: jianyou.wu007@gmail.com

References

[1] Vigny C, Socquet A., Rangin C, Chamot-Rooke N, Pubellier, M, Bouin M N, Bertrand G., Becker M. Present-day crustal deformation around Sagaing fault, Myanmar. J. Geophys. Res. 2003, 108(B11): 2533.

[2] Myanmar Earthquake Committee. Introduction to the Sagaing fault. Myanmar Earthquake Bureau, 2005.

[3] Maung Thein. Myanmar and earthquake disaster. Department of Geology, Yangon Art and Science University, 1994.

[4] Lindh AG.. The nature of earthquake prediction. U. S. Geological Survey, 2003.

[5] Snieder R, Van Eck T. Earthquake prediction: A political problem? Department of Geophysics, Utrecht University, Netherlands, 1997.

[6] Committee On The Science Of Earthquakes. Living on an active Earth: Perspectives on earthquake science. National Research Council of the National Academies 2003: 54-65.

[7] Sykes LR, Shaw BE, Scholz CH. Rethinking earthquake prediction, Pure Appl. Geophys. 1999, 155: 207- 232.

[8] Su Y. A brief introduction on development and scientific

thoughts of earthquake prediction. Developments of Earthquake Prediction 2004: Part-2.

[9] Nelson SA. Earthquake prediction and control. Lecture Notes, Tulane University 2004.

[10] Ferraes SG.. Probabilistic prediction of the next large earthquake in the Michoacan fault-segment of the Mexican subduction zone. Mexico Geofisica Internacional 2003; 42(1): 69-81

[11] Zoller G., Ben- Zion Y., Holschneider, M. and Haiz, S. Estimating recurrence times and seismic hazard of large earthquakes on an individual fault. Geophys. J. Int. 2007; 170: 1300-1310

[12] Martel S. Recurrence intervals and probability (18). University of Hawaii, 2002.

[13] Murray J, Segall P. Testing time-predictable earthquake recurrence by direct measurement of strain accumulation and release. Nature 2002; 419: 287-291.

ISSN: 1545-1003

The journal of American Science

Normal paper structure for the Journal of American Science:

Each manuscript is suggested to include the following components but authors can do their own ways:

(1) The complete article title.
(2) Each author's full name; institution(s) with which each author is affiliated, with city, state/province, zip code, and country; and the name, complete mailing address, telephone number, facsimile number (if available), and email address for all correspondence.
(3) **You must put at least one email address under the authors' address.**
(4) Abstract: including Background, Materials and Methods, Results, and Discussions, 100-300 words preferred.
(5) Key Words.
(6) Introduction.
(7) Materials and Methods.
(8) Results.
(9) Discussions.
(10) Acknowledgments.
(11) Correspondence to.
(12) References.

Description of Manuscript Preparation and Format:

(1) Software: Microsoft Word file.
(2) Font: Normal, Times New Roman, 10 pt, single space.
(3) Indent: 8 spaces in the beginning of each new paragraph.
(4) Manuscript: Don't use "Footnote" or "Header and Footer".
(5) Spelling check: Do spelling check when you finish.
(6) Color: Email and website addresses are blue, and all other contents are black.
(7) Abstract: 100-300 words are preferred, and remember to add "[The Journal of American Science. 2009;x(x):xx-xx]. (ISSN 1545-1003)" in the end of abstract.
(8) Page setup: Margins: top 72 pt, bottom 72 pt. left 72 pt, right 72 pt.
(9) Paper size: Letter, width 612 pt, height 792 pt.
(10) Layout: Header 36 pt, Foot 36 pt.
(11) Title: Use Title Case in the title and subtitles, e.g. "Debt and Agency Costs".
(12) Figures and Tables: Use full word of figure and table, e.g. "Figure 1. Annul Income of Different Groups", Table 1. Annual Increase of Investment".
(13) References: Cite 10-20 references preferred, by "last name, year", e.g. "(Smith, 2003)". References should include all the authors' last names and initials, title, journal, year, volume, issue, and pages etc.
(14) *Reference Examples*: Journal Article: Hacker J, Hentschel U, Dobrindt U. Prokaryotic chromosomes and disease. Science 2003;301(34):790-3.
(15) Book: Berkowitz BA, Katzung BG. Basic and clinical evaluation of new drugs. In: Katzung BG, ed. Basic and clinical pharmacology. Appleton & Lance Publisher. Norwalk, Connecticut, USA. 1995:60-9.
(16) Insert page number by bottom / center.
(17) Header for odd: Marsland Press Journal of American Science 2009;x(x):xx-xx.
(18) Header for even: short title Family name of the first author, et al.
(19) Footer: http://www.americanscience.org americansciencej@gmail.com.

Submission Address: sciencepub@gmail.com, editor@sciencepub.net, Marsland Press, P.O. Box 21126, Lansing, Michigan 48909, The United States, 347-321-7172.

Comparison of Direct and Indirect Boundary Element Methods for the Flow Past a Circular Cylinder with Constant Element Approach

Muhammad Mushtaq[1,*], Nawazish Ali Shah[1], Ghulam Muhammad[1]

1 Department of Mathematics, University of Engineering & Technology, Lahore – 54890 Pakistan
mushtaqmalik2004@yahoo.co.uk

Abstract: In this paper, a comparison of direct and indirect boundary element methods is applied for calculating the flow past(i.e. velocity distribution) a circular cylinder with a constant element (i.e a new) approach. To check the accuracy of the method, the computed flow velocity is compared with the analytical solution for the flow over the boundary of a circular cylinder. [Journal of American Science 2009;5(4):13-16]. (ISSN: 1545-1003).
Keywords: Boundary element methods, Flow past, Velocity distribution, Circular cylinder, Constant element

1. Introduction

From the time of fluid flow modeling, it had been struggled to find the solution of a complicated system of partial differential equations (PDE) for the fluid flows which needed more efficient numerical methods. With the passage of time, many numerical techniques such as finite difference method, finite element method, finite volume method and boundary element method etc. came into beings which made possible the calculation of practical flows. Due to discovery of new algorithms and faster computers, these methods were evolved in all areas in the past. These methods are CPU time and storage hungry. One of the advantages is that with boundary elements one has to discretize the entire surface of the body, whereas with domain methods it is essential to discretize the entire region of the flow field. The most important characteristics of boundary element method are the much smaller system of equations and considerable reduction in data which is prerequisite to run a computer program efficiently. These method have been successfully applied in a number of fields, for example elasticity, potential theory, elastostatics and elastodynamics (Brebbia, 1978; Brebbia and Walker, 1980).Furthermore, this method is well–suited to problems with an infinite domain. From above discussion, it is concluded that boundary element method is a time saving, accurate and efficient numerical technique as compared to other numerical techniques which can be classified into direct boundary element method and indirect boundary element method. The direct method takes the form of a statement which provides the values of the unknown variables at any field point in terms of the complete set of all the boundary data. Whereas the indirect method utilizes a distribution of singularities over the boundary of the body and computes this distribution as the solution of integral equation. The direct boundary element method was used for flow field calculations around complicated bodies (Morino et al.,1975;Mushtaq,2008). While the indirect method has been used in the past for flow field calculations surrounding arbitrary bodies (Hess and Smith, 1967; Hess, 1973, Muhammad 2008)

2. Velocity Distribution

Let a circular cylinder be of radius 'a' with center at the origin and let the onset flow be the uniform stream with velocity U in the positive direction of the x-axis as shown in figure (1).

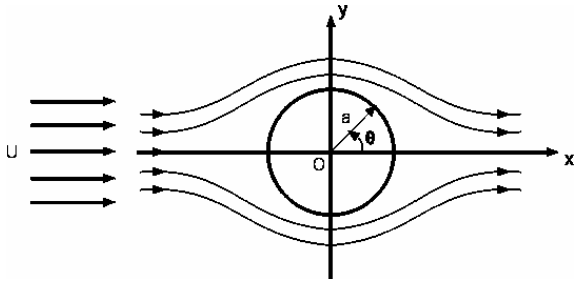

Figure 1: Flow past a circular cylinder

The magnitude of the exact velocity distribution over the boundary of the circular cylinder is given by (Milne-Thomson, 1968; Shah, 2008)

$$\left|\vec{V}\right| = 2aU \sin\theta \qquad (1)$$

where θ is the angle between the radius vector and the positive direction of the x–axis.

Now the condition to be satisfied on the boundary of the circular cylinder is (Muhammad,2008; Mushtaq,2008)

$$\hat{n} \cdot \vec{V} = 0 \qquad (2)$$

where $\hat{n}$ is the unit normal vector to the boundary of the cylinder.

Since the motion is irrotational, $\vec{V} = -\nabla\Phi$ where Φ is the total velocity potential. Thus equation (2) becomes

$$\hat{n} \cdot (-\nabla\Phi) = 0$$

or $$\frac{\partial\Phi}{\partial n} = 0 \qquad (3)$$

Now the total velocity potential Φ is the sum of the perturbation velocity potential and the velocity potential of the uniform stream $\phi_{u.s.}$

i.e. $\Phi = \phi_{u.s} + \phi_{c.c}$ (4)

or $\frac{\partial \Phi}{\partial n} = \frac{\partial \phi_{u.s}}{\partial n} + \frac{\partial \phi_{c.c}}{\partial n}$

Which on using equation (3) becomes

$$\frac{\partial \phi_{c.c}}{\partial n} = -\frac{\partial \phi_{u.s}}{\partial n} \quad (5)$$

But the velocity potential of the uniform stream is

$$\phi_{u.s} = -U x \quad (6)$$

$$\frac{\partial \phi_{u.s}}{\partial n} = -U \frac{\partial x}{\partial n}$$

$$= -U (\hat{n} \cdot \hat{i}) \quad (7)$$

Thus from equations (5) and (7),

$$\frac{\partial \phi_{c.c}}{\partial n} = U (\hat{n} \cdot \hat{i}) \quad (8)$$

or $$\frac{\partial \phi_{c.c}}{\partial n} = U \frac{x}{\sqrt{x^2 + y^2}} \quad (9)$$

Equation (9) is the boundary condition which must be satisfied over the boundary of the circular cylinder.

Now for the approximation of the boundary of the circular cylinder, the coordinates of the extreme points of the boundary elements can be generated within the computer program as follows:

Divide the boundary of the circular cylinder into m elements in the clockwise direction by using the formula

$$\theta_k = \frac{(m+3) - 2k}{m} \pi, \quad k = 1, 2, \ldots, m \quad (10)$$

Then the coordinates of the extreme points of these m elements are Calculated from

$$\left.\begin{aligned} x_k &= a \cos \theta_k \\ y_k &= a \sin \theta_k \end{aligned}\right\} \quad k = 1, 2, \ldots, m \quad (11)$$

Take m = 8 and a = 1.

In the case of constant boundary elements where there is only one node at the middle of the element and the potential ϕ and the potential derivative $\frac{\partial \phi}{\partial n}$ are constant over each element and equal to the value at the middle node of the element.

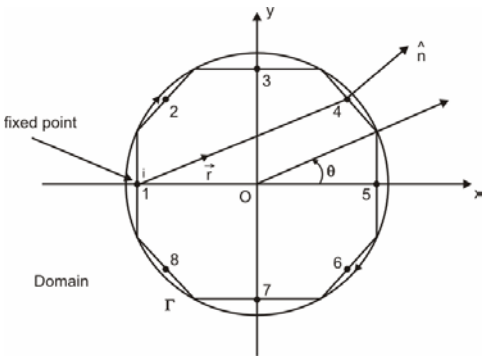

Figure 2. Discretization of the circular cylinder into 8 constant boundary elements

The coordinates of the middle node of each boundary element are given by

$$\left.\begin{aligned} x_m &= \frac{x_k + x_{k+1}}{2} \\ y_m &= \frac{y_k + y_{k+1}}{2} \end{aligned}\right\} \quad k, m = 1, 2, \ldots, 8 \quad (12)$$

And therefore the boundary condition (9) in this case takes the form

$$\frac{\partial \phi_{c.c}}{\partial n} = U \frac{x_m}{\sqrt{x_m^2 + y_m^2}}$$

The velocity U of the uniform stream is also taken as unity.

The following tables show the comparison of the direct and indirect boundary element methods for computed and analytical velocity distributions over the boundary of a circular cylinder for 8,16 and 32 constant boundary elements.

Table 1: The comparison of the computed velocity with exact velocity over the boundary of a circular cylinder using 8 constant boundary elements.

Element	x-Coordinate	y-Coordinate	Computed Velocity Using DBEM	Computed Velocity Using IBEM	Analytical Velocity
1	-.79	.33	.80718E+00	.82884E+00	.76537E+00
2	-.33	.79	.19487E+01	.20010E+01	.18478E+01
3	.33	.79	.19487E+01	.20010E+01	.18478E+01
4	.79	.33	.80718E+00	.82884E+00	.76537E+00
5	.79	-.33	.80718E+00	.82884E+00	.76537E+00
6	.33	-.79	.19487E+01	.20010E+01	.18478E+01
7	-.33	-.79	.19487E+01	.20010E+01	.18478E+01
8	-.79	-.33	.80718E+00	.82884E+00	.76537E+00

Table 2: The comparison of the computed velocity with exact velocity over the boundary of a circular cylinder using 16 constant boundary elements .

Element	x-Coordinate	y-Coordinate	Computed Velocity Using DBEM	Computed Velocity Using IBEM	Analytical Velocity
1	-.94	.19	.39524E+00	.39785E+00	.39018E+00
2	-.80	.53	.11256E+01	.11330E+01	.11111E+01
3	-.53	.80	.16845E+01	.16956E+01	.16629E+01
4	-.19	.94	.19870E+01	.20001E+01	.19616E+01
5	.19	.94	.19870E+01	.20001E+01	.19616E+01
6	.53	.80	.16845E+01	.16956E+01	.16629E+01
7	.80	.53	.11256E+01	.11330E+01	.11111E+01
8	.94	.19	.39524E+00	.39785E+00	.39018E+00
9	.94	-.19	.39524E+00	.39785E+00	.39018E+00
10	.80	-.53	.11256E+01	.11330E+01	.11111E+01
11	.53	-.80	.16845E+01	.16956E+01	.16629E+01
12	.19	-.94	.19870E+01	.20001E+01	.19616E+01
13	-.19	-.94	.19870E+01	.20001E+01	.19616E+01
14	-.53	-.80	.16845E+01	.16956E+01	.16629E+01
15	-.80	-.53	.11256E+01	.11330E+01	.11111E+01
16	-.94	-.19	.39524E+00	.39785E+00	.39018E+00

Table 3: The comparison of the computed velocity with exact velocity over the boundary of a circular cylinder using 32 constant boundary elements .

Element	x-Coordinate	y-Coordinate	Computed Velocity Using DBEM	Computed Velocity Using IBEM	Analytical Velocity
1	-.99	.10	.19667E+00	.19699E+00	.19604E+00
2	-.95	.29	.58244E+00	.58339E+00	.58057E+00
3	-.87	.47	.94583E+00	.94738E+00	.94279E+00
4	-.77	.63	.12729E+01	.12750E+01	.12688E+01
5	-.63	.77	.15510E+01	.15535E+01	.15460E+01
6	-.47	.87	.17695E+01	.17724E+01	.17638E+01
7	-.29	.95	.19200E+01	.19232E+01	.19139E+01
8	-.10	.99	.19968E+01	.20001E+01	.19904E+01
9	.10	.99	.19968E+01	.20001E+01	.19904E+01
10	.29	.95	.19200E+01	.19232E+01	.19139E+01
11	.47	.87	.17695E+01	.17724E+01	.17638E+01
12	.63	.77	.15510E+01	.15535E+01	.15460E+01
13	.77	.63	.12729E+01	.12750E+01	.12688E+01
14	.87	.47	.94583E+00	.94738E+00	.94279E+00
15	.95	.29	.58244E+00	.58339E+00	.58057E+00
16	.99	.10	.19667E+00	.19699E+00	.19603E+00
17	.99	-.10	.19667E+00	.19699E+00	.19603E+00
18	.95	-.29	.58243E+00	.58339E+00	.58057E+00
19	.87	-.47	.94583E+00	.94738E+00	.94279E+00
20	.77	-.63	.12729E+01	.12750E+01	.12688E+01
21	.63	-.77	.15510E+01	.15535E+01	.15460E+01
22	.47	-.87	.17695E+01	.17724E+01	.17638E+01
23	.29	-.95	.19200E+01	.19232E+01	.19139E+01
24	.10	-.99	.19968E+01	.20001E+01	.19904E+01
25	-.10	-.99	.19968E+01	.20001E+01	.19904E+01
26	-.29	-.95	.19200E+01	.19232E+01	.19139E+01
27	-.47	-.87	.17695E+01	.17724E+01	.17638E+01
28	-.63	-.77	.15510E+01	.15535E+01	.15460E+01
29	-.77	-.63	.12729E+01	.12750E+01	.12688E+01
30	-.87	-.47	.94583E+00	.94738E+00	.94279E+00
31	-.95	-.29	.58244E+00	.58339E+00	.58057E+00
32	-.99	-.10	.19666E+00	.19698E+00	.19604E+00

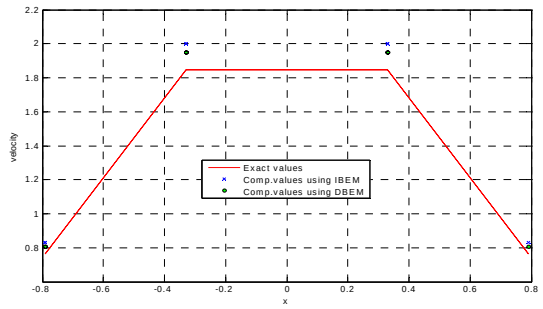

Figure 3. Comparison of computed and analytical velocity distributions over the boundary of a circular cylinder using 8 boundary elements with constant element approach.

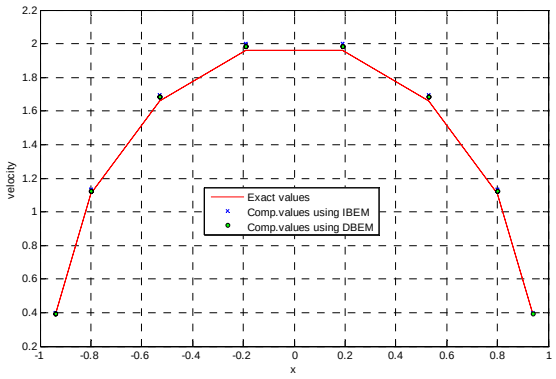

Figure 4. Comparison of computed and analytical velocity distributions over the boundary of a circular cylinder using 16 boundary elements with constant element approach.

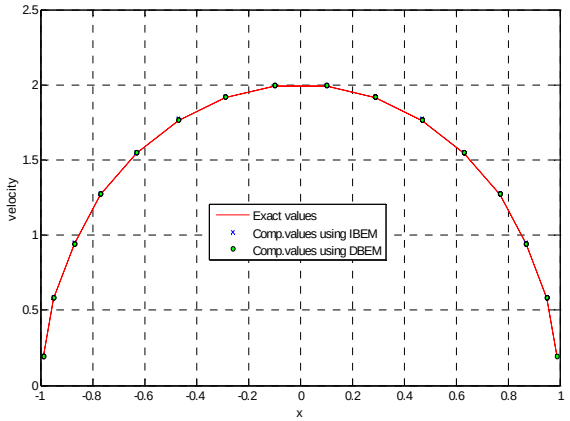

Figure 5. Comparison of computed and analytical velocity distributions over the boundary of a circular cylinder using 32 boundary elements with constant element approach.

3. Conclusion

A direct and indirect boundary element methods have been applied for the calculation of flow past a circular cylinder with a constant element (i.e. a new) approach. The calculated flow velocities obtained using these methods are compared with the analytical solutions for flow over the boundary of a circular cylinder . It is found that the results obtained with the direct boundary element method for the flow past are excellent in agreement with the analytical results for the body under consideration.

Acknowledgement

We are thankful to the University of the Engineering & Technology, Lahore – Pakistan for the financial support.

Correspondence to :

Muhammad Mushtaq

Assistant Professor, Department of Mathematics, University of Engineering & Technology, Lahore-54890 Pakistan. Telephone : 0092-42-9029214

Email: mushtaqmalik2004@yahoo.co.uk

References

[1]. Hess, J.L. and Smith, A.M.O.: "Calculation of potential flow about arbitrary bodies", Progress in Aeronautical Sciences, Pergamon Press 1967,8: 1-158.

[2]. Hess, J.L.: "Higher order numerical solutions of the integral equation for the two-dimensional Neumann problem", Computer Methods in Applied Mechanics and Engineering, 1973 :1-15.

[3]. Morino, L., Chen, Lee-Tzong and Suciu,E.O.: "A steady and oscillatory subsonic and supersonic aerodynamics around complex configuration", AIAA Journal,1975, 13(3): 368-374.

[4]. Milne-Thomson, L.M.: "Theoretical Hydrodynamics", 5th Edition, London Macmillan & Co. Ltd., 1968,158-161.

[5]. Brebbia, C.A.: "The Boundary element Method for Engineers", Pentech Press 1978.

[6]. Brebbia, C.A. and Walker, S.: " Boundary Element Techniques in Engineering" , Newnes-Butterworths 1980.

[7]. Shah, N.A. "Ideal Fluid Dynamics", A–One Publishers, Lahore–Pakistan 2008,362-366.

[8] Muhammad, G., Shah, N.A., & Mushtaq, M.: "Indirect Boundary Element Method for the Flow Past a Circular Cylinder with Linear Element Approach", International Journal of Applied Engineering Research 2008,3(12):1791-1798.

[9] Mushtaq, M., Shah, N.A., & Muhammad, G.: "Comparison of Direct and Indirect Boundary Element Methods for the Flow Past a Circular Cylinder with Linear Element Approach", Australian Journal of Basic and Applied Sciences 2008,2(4):1052-1057.

Bioremediation of Oil Refinery Effluent By Using Scenedesmus Obliquus

Rajasulochana, P*, Dhamotharan, R**, Murugesan, S*** and Rama Chandra Murthy A#
* Lecturer, Dept. of Industrial Biotechnology, Bharath Institute of Higher Education and Research, Chennai, Tamil Nadu, India.
**PG and Research Dept. Plant Biology & Plant Biotech, Presidency College, Chennai, Tamil nadu, India.
***PG and Research Dept. of Plant Biology and Plant Biotechnology, Unit of Environmental Sciences and Algal Biotechnology, Pachaiyappa's College, Chennai 30, Tamil nadu, India.
Scientist, Structural Engineering Research Centre, CSIR Campus, Taramani, Chennai, Tamil Nadu, India, 600 113. India.
*** - Corresponding author,** prajasulochana@yahoo.co.in, 91-9444222678

ABSTRACT: The contamination of groundwater, surface water and air with hazardous and toxic chemicals is one of the major problems in the industrialized world faces today. One among many new technologies to deal with this major problem is bioremediation. Bioremediation, the use of microorganisms or microbial processes to degrade environmental contaminants. Present investigation focuses on the bioremediation of oil refinery effluent by using micro algae. In order to select organism for the treatment process, micro algal populations were collected at different places from where the effluent was collected; isolated and identified by using the standard manual and were maintained in Bold Basal Medium (BBM). To study the role of micro algae in oil refinery effluent, the following protocols were employed. i) Effluent treated with Scenedesmus obliquus and ii) Effluent without Scenedesmus obliquus (control). Various physicochemical parameters such as pH, alkalinity, hardness, iron content, COD, BOD and free ammonia were estimated. It is observed that Scenedesmus obliquus proved to be an efficient removal of most of the parameters including COD and BOD. Results obtained for various parameters are critically analyzed and compared with those of similar investigations reported by various researchers. [The Journal of American Science. 2009; 5(4): 17-22].

Keywords: Refinery effluent, Bioremediation, *Scenedesmus obliquus*

1. INTRODUCTION

Industrialization has long been accepted as a hallmark of civilization. However, the fact remains that industrial emanations have been adversely affecting the environment. Industrial effluents containing toxic and heavy metals drawn into river, which is often source of drinking water for another town downstream. Corporation/Municipal water treatment facilities in most of the developing countries, at present are not equipped to remove traces of heavy metals, consequently exposing every consumer to unknown quantities of pollutants in the water they consume. The main sources of heavy metal pollution are mining, milling, petro chemical industries, discharging a variety of toxic metals into the environment. Although the removal of toxic heavy metals from industrial waste waters has been practiced for several decades, the cost effectiveness of the most common physico-chemical processes such as oxidation and reduction, chemical precipitation, filtration, electrochemical treatment, evaporation, ion-exchange and reverse osmosis is limited. The need to remediate these sites has led to the development of new technologies that emphasize the destruction of the pollutants rather than the conventional approach of disposal. Bioremediation, the use of microorganisms or microbial processes to degrade environmental contaminants, is among these new technologies. Bioremediation has numerous applications, including clean-up of ground water, soils, lagoons, sludges, and process-waste streams.

Micro algae are used in wastewater bio-treatments (Oswald, 1992), as food for humans and animals (Becker, 1992), as feed in aquacultures Lora-Vilchis et al., 2004), for the production of pigments (Johnson and An, 1991) and in agriculture (Metting, 1992). Bioremediation, the use of microorganisms or microbial processes, is one among the new technologies. The bioremediation has been proven successful in numerous applications especially treating petroleum contaminated soils Gazyna et al., 2005). Bioremediation strategies for typical hazardous wastes are illustrated by Satinder et al. (2006). Petrochemical plants generate an aqueous effluent containing various conventional pollutants as well as specific petrochemicals and intermediates. The present study focuses on the bioremediation of oil refinery effluent by using a micro alga.

Present investigation focuses on the bioremediation of oil refinery effluent by using micro algae. In order to select organism for the treatment process, micro algal populations were collected at different places from where the effluent was collected; isolated and identified by using the standard manual and were maintained in Bold Basal Medium (BBM). To study the role of micro algae in oil refinery effluent, the following protocols were employed. i) Effluent treated with Scenedesmus obliquus and ii) Effluent without Scenedesmus obliquus (control). Various physicochemical parameters such as pH, alkalinity, hardness, iron content, COD, BOD and free ammonia were estimated. It is observed that Scenedesmus obliquus proved to be an efficient removal of most of the parameters including COD and BOD. Results obtained for various parameters are critically analyzed and compared with those of similar investigations reported by various researchers.

2. MATERIALS AND METHODS

Oil refinery effluent was collected from Ennore, a suburb of Chennai, India. In order to select organism for treatment process, micro algal populations were collected at different places from where the effluent was collected, isolated and identified by using the standard manual and were maintained in Bold Basal Medium (BBM) (Nichols and Bold, 1965).

The taxa collected and identified as *Chroococcus, Oscillatoria, Lyngbya, Scenedesmus, Scytonema and Spirulina* sp indicates the polluted status of the water body. Among various micro algae, *Scenedesmus obliquus,* have alone acclimatized well with oil refinery effluent. For the present investigation, *Scenedesmus obliquus* was selected for treatment process. To study the role of micro alga in oil refinery effluent, the following protocols were employed. i) The effluent treated without *Scenedesmus obliquus* (control) and ii) The effluent was treated with *Scenedesmus obliquus*. These experiments were conducted in duplicate and repeated three times.

Two ml of uniform suspension of *Scenedesmus obliquus* was added as initial inoculums in each flask containing 1 liter of effluent. The experiment was conducted under controlled conditions (temperature 27 ± 2º C) with a light intensity of 2000 lux, provided from overhead cool light white fluorescent tubes (16L+8D) for the total duration of 15 days. The samples were analyzed periodically on every 5th day for various physico-chemical parameters by using standard methods[1]. The results of the physico-chemical parameters were analysed using one way Analysis of Variance (ANOVA) followed by Tukey HSD test.

3. RESULTS AND DISCUSSION

All physico-chemical parameters were quantified for 0^{th}, 5^{th}, 10^{th} and 15^{th} day respectively are shown in Table 1. The following conclusions/observations can be made w.r.t Table 1.

In the present study, the colour of effluent treated with *Scenedesmus obliquus* changed from blackish to greenish yellow from the seventh day on wards and completed turned green. These changes in colour and odour of the oil refinery effluent may be due to the action of algae which decomposed the organic matter present in the effluent and made the water clear. These findings are in concordant with Verma and Madamwar (2002). There is no work reported on decolourization using micro algae.

The total dissolved solids (TDS) in the effluent treated with *Scenedesmus obliquus* were reduced to 6.10 percent. The TDS value of the oil refinery effluent was found to be exceeding the limit prescribed by CPCB (1995) in the raw effluent which could be attributed to various environmental factors responsible for the reduction of the diversity of aquatic life and oxygen depletion.

The electrical conductivity of the treated effluent was reduced to 7.43 percent by *Scenedesmus obliquus.* The higher level of electrical conductivity in the raw effluent could be attributed to the use of inorganic chemicals in oil refinery. Such low electrical conductivity could be attributed to the presence of organic compounds in the effluent.

Interestingly, the pH of the oil refinery effluent treated with *Scenedesmus obliquus* increased from 5.75 to 6.52. The present study shows that pH increased on the 3^{rd} day itself. Manoharan and Subramanian (1992b, 1993) found a rise in pH value up to the tenth day of growth in paper mills wastewater. The values of pH in the effluent discharged indicated that it was well within the permissible limits of CPCB (1995). In the present study, pH was found to increase in the oil refinery effluent treated with the alga, whereas there was no change in the pH of the untreated effluent.

The alkaline nature of the effluent showed a gradual reduction. The alkalinity of the effluent was reduced to 44.0 percent by *Scenedesmus obliquus*. Alkalinity was found to be high which is harmful to aquatic organism (Nemerow, 1978). The

ability to utilize bicarbonate was also demonstrated with a variety of algae Beardall et al., 1976).

Hardness in the effluent would make it unsuitable for industrial purposes as it may cause the scaling of equipment (Goel, 2000). The total hardness was reduced to 6.34 percent by *Scenedesmus obliquus* with the result of an efficient nutrient uptake of micro algae. Saravanan et al.,(1998) reported that the total hardness was due to Na, K, Ca etc, and would affect the oil refinery wastewater treatment plants. Calcium and magnesium were reduced to 10.83 and 13.73 percent especially when the oil refinery effluent was treated with *Scenedesmus obliquus* with the result of an efficient uptake of alga. The reduction was noticed from the third day till the fifteenth day of growth and after was almost stabilized latter. Sengar et al.,(1990) in their study on purification of river water by algae found a reduction of 67.10 percent of calcium and 67.40 per cent of potassium.

In the present study, 39.27 percent of iron was removed when the effluent was treated with *Scenedesmus obliquus*.

The alga *Scenedesmus obliquus* was also more effective in the removal of (94.97 percent) free ammonia from the oil refinery effluent. The toxicity of ammonia is generally dependent on pH, oxygen concentration and temperature (Cote, 1976).

Chlorides are generally considered one of the major pollutants in the effluents which are difficult to be removed by conventional biological treatment methods. But it was also reduced (47.96 percent) by the experimental alga. Uma and Subramanian (1990) recorded a 30 percent chloride reduction under laboratory conditions by Halo bacterium and only an additional reduction of 12-17 percent with cyanobacteria in the ossein effluent.

The sulphate content in the effluent treated with *Scenedesmus obliquus* was found to be reduced to 26.02 percent. The reduction of sulphate in the effluent and its uptake by micro algae were reported by Mittal and Sengar (1989).

The phosphate and silica levels in the treated effluent were found to have increased to 78.02 and 41.92 percent respectively. The increase in the phosphate with all carbon sources was appreciably low at higher NH_4^+-N concentrations in the waste, but it was quite high at low concentration. Doran and Boyle (1979) reported that 90 percent of phosphorus removal by the activated algae was due to chemical precipitation. The increase of silica was due to the unavailable form of silica converted into the available form.

Oil and grease, if discharged into treated effluents, can create unsightly floating matter and films on water surfaces. It may also interfere with biological life forms on surface water (Metcalf, 1991). In the present study, 99.85 percent of oil and grease was removed when the effluent was treated with *Scenedesmus obliquus*. In wastewater treatment, much of oil and grease floats can be generally removed by mechanical skimming. Though the amount of oil and grease is found to be in negligible, their continuous discharge into the aquatic ecosystem could also destroy the nursery ground of a variety of fishes.

The discharges of BOD in to receiving environments with the limited assimilative capacity sometimes reduce the dissolved oxygen concentrations to the levels below those required for aquatic biota, and it is in this condition that BOD is considered pollutant. The BOD and COD levels of the treated effluent were reduced significantly. In the present study the BOD level was reduced to 16.66 percent by *Scenedesmus obliquus*, and the COD level to 82.80 percent. It can be observed that the reduction in BOD was less compared to the reduction in COD. It is because the degradation sought was through biological activity and not through any chemical agent. Moreover, the presence of organic matter will promote anaerobic leading to the accumulation of toxic compounds in water bodies. This is in accordance with the work of Panneerselvam (1998) and Prabakar (1999). The reduction of BOD and COD levels might occur due to the removal of the dissolved organic compounds and derivatives to some extent from the effluent during the treatment process. The present investigation showed high levels of COD in both untreated and treated effluent, which would render the aquatic body unsuitable for the existence of aquatic organism (Goel, 2000) due to the reduction in the dissolved oxygen content.

4. CONCLUSION

The bioremediation of the pollution load of the oil refinery effluent with *Scenedesmus obliquus* can be used as an effective technology in the reduction of pollutants like inorganic and organic compounds. Furthermore, the better performance in field conditions gave positive indication of their usefulness in the treatment of oil refinery effluent. It is a simple, sensitive, biological, and rapid effluent treatment agent. The system, when standardized would not only be economical but also eco-friendly and sustainable. The information generated would help to scale up the process and moreover, to assess the economic feasibility of the technology.

Table 1 Physico-chemical parameters of oil refinery effluent

Parameter	Control	5th Day	10 th Day	15 th Day	F-Value	P-Value
TDS	1868±18.08[d]	1833±10.77[c]	1793±9.53[b]	1754±6.81[a]	100.717	0.0000**
Conductivity	2625±11.95[d]	2565±13.34	2500±9.47[b]	2430±10.7[a]	322.163	0.0000**
pH	5.75±0.07[d]	6.02±0.07[c]	6.28±0.07[b]	6.52±0.07[a]	139.147	0.0000**
Alkalinity	100±3.91[d]	85±4.94[c]	68±6.23[b]	56±4.00[a]	94.370	0.0000**
Tot. Hardness	1025±7.24[d]	1003±8.90[c]	980±4.73[b]	960±5.55[a]	102.943	0.0000**
Calcium	240±1.41[c]	240±1.41[c]	228±4.98[b]	214±3.16[a]	94.639	0.0000**
Magnesium	102±2.61[d]	98±1.41[c]	93±2.61[b]	88±1.41[a]	50.340	0.0000**
Iron	4.71±0.07[d]	4.11±0.06[c]	3.50±0.12[b]	2.86±0.08[a]	558.969	0.0000**
Free Ammonia	8.96±0.14[d]	6.13±0.25[c]	3.21±0.19[b]	0.45±0.12[a]	2454.486	0.0000**
Chloride	492±9.55[d]	414±8.65[c]	332±13.91[b]	256±13.11[a]	469.691	0.0000**
Sulphate	196±4.69[d]	179±4.20[c]	161±6.57[b]	145±6.23[a]	96.223	0.0000**
Phosphate	1.58±0.10[a]	3.34±0.20[b]	5.21±0.09[c]	7.19±0.16[d]	1672.715	0.0000**
Silica	38±4.05[a]	47.21±1.89[b]	56.25±1.84[c]	65.43±3.49[d]	93.922	0.0000**
Oil & Grease	4±0.16[d]	2.62±0.08[c]	1.41±0.11[b]	0.01±.0.00[a]	1600.736	0.0000**
BOD	239.83±5.12[d]	226±5.52[c]	212±3.94[b]	200±1.96[a]	93.773	0.0000**
COD	407±11.81[d]	295±8.29[c]	180±8.42[b]	70±14.17[a]	1056.562	0.0000**

** Denotes significant at 1 % level; Different alphabet between days denotes significant at 5 % level

5. REFERENCES

Beardall, J. D., Mukerji, D., Glover, H. E. and Morris, I., 1976. The path of carbon in photosynthesis by marine phytoplankton. J Phycol, 1:134-141.

Becker, E. W., 1992. Micro-algae for human and animal consumption. In: Micro-algal Biotechnology, edited by Borowitzka M A & Borowitzka L J (Cambridge University Press ,Cambridge.), 222–256.

Cote, R. P., 1976. The effects of petroleum refinery liquid wastes on aquatic life. with special emphasis on the Canadian environment. National Research Council of Canada, NRC Associate Committee on Scientific Criteria for Environmental Quality, Ottawa, Ontario, Canada K1A 0R6, publication number 15021.

CPCB., 1995. Pollution control: acts, rules and modifications issued there under central pollution control board. New Delhi, India.

Doran, M. D. and Boyle, W. C., 1979. Phosphorus removal by activated algae. Wat, 13: 805-812.

Gazyna Plaza, Grzegorz Nalecz-Jawecki, Krzysztof Ulfig, Robin, L. Brigmon., 2005. Assessment of genotoxic activity of petroleum hydrocarbon-bioremediated soil. Ecotoxicology and Environmental Safety, 62:415-420.

Goel, P. K., 2000. Water pollution, causes, effects and control. (New age international (P) Ltd. Publ., New Delhi, India).

Johnson, E. A. and An, G. H., 1991. Astaxanthin from microbial sources. Crit Rev Biotechnol, 11:297–326.

Lora-Vilchis, M. C., Robles-Mungaray, M., and Doctor, N., 2004. Food value of four micro algae for juveniles of Lion's paw scallop Lyropecten subnodosus (Sowerby, 1833). J World Aquaculture Soc, 35:297–303.

Manoharan, C and Subramanian, G. 1992b. Sewage – cyanobacteria interaction. A case study. Indian J Environ pro, 12: 251–258.

Manoharan, C and Subramanian, G., 1993. Feasibility studies on using cyanobacteria in ossein effluent treatment. Indian J Env Hlth, 35:88-96.

Metting, B., 1992. Micro-algae in agriculture In: Micro-algal Biotechnology. edited by Borowitzka M A & Borowitzka L J (Cambridge University Press, Cambridge) 288–304.

Metcalf Eddy, 1991. Wastewater Engineering: Treatment, Disposal, Reuse. 3rd Edition. (McGraw-Hill, Toronto).

Mittal, S. and Sengar, R. M. S., 1989. Toxic effect of sulphate and its uptake in algae. Natl Acad Sci Lett, 12:17-19.

Nemerow, N. L., 1978. Industrial water pollution: origins, characteristics and treatment. (Addision-Wesley Publishing company Inc., Philipines).

Nichols, H. W. and Bold, H. C., 1965. Trichosarcina polymorpha gen.et .sp. F. Phycol, 1: 34-8.

Oswald, W. J., 1992. Micro-algae and waste-water treatment In: Micro-algal Biotechnology. edited by Borowitzka M A & Borowitzka L J (Cambridge University Press, Cambridge), 305–328.

Panneerselvam, A, 1998. Studies on sago industry effluent and its bioremediation using the white-rot fungus. Phanerochaete chrysosporum (Burds). Ph.D. Thesis, University of Madras, India.

Prabakar, K., 1999. Bioremediation of sugar and distillery effluents. Ph.D Thesis, University of Madras, India..

Saravanan, S., Saravanan, A., Elangovan, N. and Kalichelvan, P.T., 1998. Decolourization of tannery effluent of Flavobacterium sp. EK. Indian J Environ Protection, 19:19-24.

Satinder, K., Brar, Verma, M., Surampalli, R. V., Misra, K., Tyagi, R. D. et al., 2006. Bioremediation of Hazardous wastes – A Review. Practical periodical of hazardous, toxic and radioactive waste management, 10:59-72.

Sengar, R. M. S., Sharma, K. D. and Mittal, S., 1990. In Vitro Studies for the publication of river water by algae treatment. Geobios, 17:77 - 81.

Uma, L., and Subramanian, G., 1990. Effective use of cyanobacteria in effluent treatment. National symposium on cyanobacterial in nitrogen fixation, New Delhi, 437-443.

Verma, P., and Madamwar, D., 2002. Comparative study on transformation of azo dyes by different white rot fungi. Indian J Biotechnol, 1:393-396.

ISSN: 1545-1003

The journal of American Science

Normal paper structure for the Journal of American Science:

Each manuscript is suggested to include the following components but authors can do their own ways:

(1) The complete article title.
(2) Each author's full name; institution(s) with which each author is affiliated, with city, state/province, zip code, and country; and the name, complete mailing address, telephone number, facsimile number (if available), and email address for all correspondence.
(3) **You must put at least one email address under the authors' address.**
(4) Abstract: including Background, Materials and Methods, Results, and Discussions, 100-300 words preferred.
(5) Key Words.
(6) Introduction.
(7) Materials and Methods.
(8) Results.
(9) Discussions.
(10) Acknowledgments.
(11) Correspondence to.
(12) References.

Description of Manuscript Preparation and Format:

(1) Software: Microsoft Word file.
(2) Font: Normal, Times New Roman, 10 pt, single space.
(3) Indent: 8 spaces in the beginning of each new paragraph.
(4) Manuscript: Don't use "Footnote" or "Header and Footer".
(5) Spelling check: Do spelling check when you finish.
(6) Color: Email and website addresses are blue, and all other contents are black.
(7) Abstract: 100-300 words are preferred, and remember to add "[The Journal of American Science. 2009;x(x):xx-xx]. (ISSN 1545-1003)" in the end of abstract.
(8) Page setup: Margins: top 72 pt, bottom 72 pt. left 72 pt, right 72 pt.
(9) Paper size: Letter, width 612 pt, height 792 pt.
(10) Layout: Header 36 pt, Foot 36 pt.
(11) Title: Use Title Case in the title and subtitles, e.g. "Debt and Agency Costs".
(12) Figures and Tables: Use full word of figure and table, e.g. "Figure 1. Annul Income of Different Groups", Table 1. Annual Increase of Investment".
(13) References: Cite 10-20 references preferred, by "last name, year", e.g. "(Smith, 2003)". References should include all the authors' last names and initials, title, journal, year, volume, issue, and pages etc.
(14) *Reference Examples*: Journal Article: Hacker J, Hentschel U, Dobrindt U. Prokaryotic chromosomes and disease. Science 2003;301(34):790-3.
(15) Book: Berkowitz BA, Katzung BG. Basic and clinical evaluation of new drugs. In: Katzung BG, ed. Basic and clinical pharmacology. Appleton & Lance Publisher. Norwalk, Connecticut, USA. 1995:60-9.
(16) Insert page number by bottom / center.
(17) Header for odd: Marsland Press Journal of American Science 2009;x(x):xx-xx.
(18) Header for even: short title Family name of the first author, et al.
(19) Footer: http://www.americanscience.org americansciencej@gmail.com.
(20) Submission Address: sciencepub@gmail.com, editor@sciencepub.net, Marsland Press, P.O. Box 21126, Lansing, Michigan 48909, The United States, 347-321-7172.

Evaluation of synthetic unit hydrograph methods for the development of design storm hydrographs for Rivers in South-West, Nigeria

Adebayo, Wahab Salami[1], Solomon, Olakunle Bilewu[1], Ayanniyi .Mufutau Ayanshola[1] and Sikiru Folahan Oritola,[2]

1. Department of Civil Engineering,University of Ilorin, P.M.B 1515, Ilorin, Nigeria
2. Department of Civil Engineering, F.U.Technology, P.M.B 65, Minna, Nigeria

awsalami2006@yahoo.co.uk

Abstract: This report presents the establishment of appropriate method of synthetic unit hydrograph to generate ordinates for the development of design storm hydrographs for the catchment of eight selected rivers located in the South West Nigeria. Unit hydrographs were developed based on Snyder, Soil Conservation Service (SCS) and Gray methods; while the SCS curve Number method was used to estimate the cumulative rainfall values for storm depth of different return periods. The peak storm hydrographs corresponding to the excess rainfall values were determined based on the unit hydrograph ordinates established. The peak storm hydrograph flows obtained based on the unit hydrograph ordinate determined by Snyder for 20-yr, 50-yr, 100-yr, 200-yr and 500-yr, return period varies from 112.63m^3/s and 13364.30m^3/s, while those based on the SCS varies from 304.43m^3/s and 6466.84m^3/s and those based on Gray varies from 398.06m^3/s and 2607.42m^3/s for the eight watersheds. The analysis shows that the values of peak flows obtained by Gray and SCS methods for five watershed were relatively close, while the values of peak flows obtained by Gray and Snyder methods for two watershed were relatively close and the values of peak flows obtained by Snyder and SCS methods for only one watershed was relatively close. This inferred that SCS method can be used to estimate ordinate required for the development of peak storm hydrograph of different return periods for the river watersheds considered. [Journal of American Science 2009;5(4):23-32] (ISSN: 1545-1003).

Keywords: Synthetic unit hydrograph, storm hydrograph, storm duration, River catchment and return periods

1. Introduction

In many parts of the world, rainfall and runoff data are seldom adequate to determine a unit hydrograph of a basin or watershed. This situation is common in Nigeria due to lack of gauging stations along most of the rivers and streams. Generally, basic stream flow and rainfall data are not available for planning and designing water management facilities and other hydraulic structures in undeveloped watershed. However, techniques have been evolved that allow generation of synthetic unit hydrograph. This includes Snyder's method, Soil Conservation Service (SCS) Method, Gray's Method and Clark's Instantaneous Unit Hydrograph Method. The peak discharges of stream flow from rainfall can be obtained from the design storm hydrographs developed from unit hydrographs generated from established methods. Warren et al (1972) described hydrograph as a continuous graph showing the properties of stream flow with respect to time, normally obtained by means of a continuous strip recorder that indicates stages versus time and is then transformed to a discharge hydrograph by application of a rating curve. Wilson (1990) observed that with an adjustment and well measured rating curve, the daily gauge readings may be converted directly to runoff volume. He also emphasized that catchment properties influence runoff and each may be present to a large or small degree. The catchment properties include area, slope, orientation, shape, altitude and also stream pattern in the basin. The unit hydrograph of a drainage basin, according to Varshney (1986) is defined as the hydrograph of direct runoff resulting from one unit of effective rainfall of a specified duration, generated uniformly over the basin area at a uniform rate. Arora (2004) defined 1-hr unit hydrograph as the hydrograph which gives 1 cm depth of direct runoff when a storm of 1-hr duration occurs uniformly over the catchment.

A vast amount of literature exists treating the various unit hydrograph methods and their development. Jones (2006) reported that Sherman in 1932 was the first to explain the procedure for development of the unit hydrograph and recommended that the unit hydrograph method should be used for watersheds of 2000 square miles (5000 km^2) or less. Chow et al (1988) discussed the derivation of unit hydrograph and its linear systems theory. Further more Viessman et al (1989), Wanielista (1990) and Arora (2004) presented the history and procedures for several unit hydrograph methods. Ramirez (2000) reported that the synthetic unit hydrograph of Snyder in 1938 was based on the study of 20 watersheds located in the Appalachian Highlands and varying in size from 10 to 10, 000 square miles (25 to 25000.0 km^2). Ramirez (2000) reported that the dimensionless unit hydrograph was developed by the Soil Conservation Service and obtained from the UH's for a great number of watersheds of different sizes and for many different locations. It was also stated by

Ramirez (2000) that the SCS dimensionless hydrograph is a synthetic UH in which the discharge is expressed as a ratio of discharge, Q, to peak discharge, Q_p and the time by the ratio of time, t, to time to peak of the UH, t_p. Wilson (1990) also reported that in 1938, Mc Carthy proposed a method of hydrograph synthesis but in that same year Snyder proposed a better known method by analyzing a larger number of basins in the Appalachian mountain region of the United States. Ogunlela and Kasali (2002) applied four methods of unit hydrographs generation to develop unit hydrograph for an ungaged watershed. The outcome of the study revealed that both Snyder and SCS methods were not significantly different from each other. Salami (2009) evaluated three methods of storm hydrograph development for the catchment of lower Niger River basin at downstream of Jebba Dam. The methods considered are Snyder, SCS and Gray methods, the statistical analysis, conducted at the 5% level of significance indicate significant differences in the methods except for Snyder and SCS methods which have relatively close values. This study also applied Snyder, SCS and Gray methods to develop unit hydrographs and subsequently used to generate peak storm hydrographs of rainfall depth of various return intervals through convolution. The peak flows obtained can be used for the design of hydraulic structures within the River Catchment.

2. Material and Methods

2.1 Study area

The watersheds of the river under consideration are located in South West Nigeria. Figure 1 is a map of Nigeria showing the location of the River catchment shaded. Rivers Fawfaw, Oba, Awon, Opeki, and Ogunpa are located in Oyo State, while Rivers Osun and Otin are located in Osun State and River Ogun is located in Ogun State.

2.2 Theory on Unit hydrograph methods

Theories on the applied methods of unit hydrographs are described and were used to synthesize the peak runoff. The methods are; Snyder's, Soil Conservation Service (SCS), and Gray methods.

2.2.1 Snyder's method

The method was used to determine the peak discharge, lag time and the time to peak by using characteristic features of the watershed. Ramirez (2000) reported that the hydrograph characteristics are the effective rainfall duration, t_r, the peak direct runoff rate Q_p, and the basin lag time, t_l. From these relationships, five characteristics of a required unit hydrograph for a given effective rainfall duration may be calculated. The five characteristics are the peak discharge per unit of watershed area, q'_p , the basin lag t'_l, the base time, t_b, and the widths, w (in time units) of the unit hydrograph at 50 and 75 percent of the peak discharge.The unit hydrograph parameters are estimated in accordance to Ramirez (2000) and Arora (2004).

Lag time, t_p

$$t_l = C_t\left(L * L_c\right)^{0.3} \qquad (1)$$

where t_l is lag time (hr) and C_t is a coefficient representing variations of watershed slope and storage. (Values of C_t range from 1.0 to 2.2, Arora (2004)). An average value of 1.60 is assumed for this catchment. Equation (1) gives the lag time, t_l for the watershed.

Unit-hydrograph duration, t_r (storm duration)

$$t_r = \frac{t_l}{5.5} \qquad (2)$$

From equation (2) the duration of the storm was obtained. However, if other storm durations are intended to be generated for the watershed, the new unit hydrograph storm duration (t'_r), the corresponding basin lag time ((t'_l) can be obtained from equation (3)

$$t_l^{'} = t_l + \left(\frac{t_r^{'} - t_r}{4}\right) \qquad (3)$$

Peak discharge, Q'_p

The peak discharge (**Q'_p**) was obtained from equation (4)

$$Q_p^{'} = \frac{2.78 * C_p * A}{t_l^{'}} \qquad (4)$$

where C_p is the coefficient accounting for flood wave and storage conditions.(Values of C_p range from 0.3 to 0.93, Arora (2004) with an average of 0.62 is assumed for this catchment).

Base time (days)

The base time was obtained from equation (5)

$$t_b = 3 + 3\left(\frac{t_l^{'}}{24}\right) \qquad (5)$$

The time width W_{50} and W_{75} of the hydrograph at 50% and 75% of the height of the peak flow ordinate were obtained based on equations (6) and (7) respectively in accordance to U.S Army Corps of Engineer (Arora, 2004). The unit of the time width is hr. Also the peak discharge per area (cumec/km^2) is given by equation (8)

$$W_{50} = \frac{5.9}{\left(q_p^{'}\right)^{1.08}} \qquad (6)$$

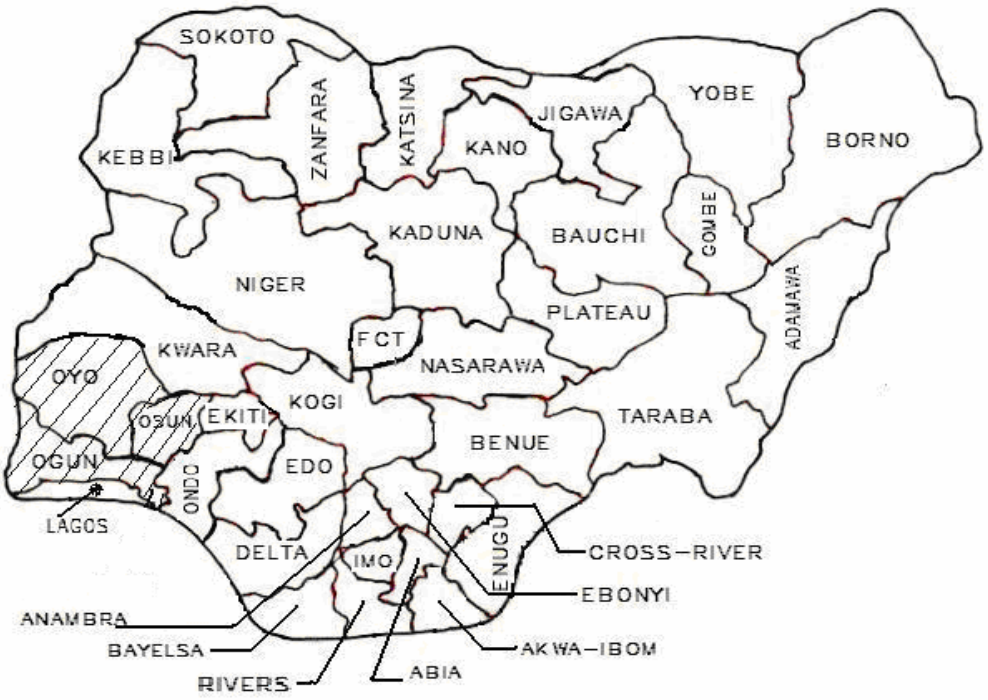

Figure 1 Map of Nigeria showing location of selected river catchments

$$W_{75} = \frac{3.4}{\left(q_p^{'}\right)^{1.08}} \qquad (7)$$

$$q_p^{'} = \frac{Q_p^{'}}{A} \qquad (8)$$

2.2.2 Soil Conservation Service (SCS) method

Raghunath (2006) reported that the US Soil Conservation Service in 1971 used many hydrographs from drainage areas of varying sizes and different geographical locations developed a dimensionless unit hydrograph. The peak discharge and the time to peak can be determined in accordance to Viessman et al (1989), Wanielista (1990), Ramirez (2000), SCS (2002), Ogunlela and Kasali (2002) and Raghunath (2006) as follows;

Peak discharge:

The peak discharge can be obtained through the equation (Ramirez (2000))

$$Q_p = \frac{0.208 * A * Q_d.}{t_p} \qquad (9)$$

where

Q_p = peak discharge (m^3/s)

The estimated values for both the peak discharge and time to peak were applied to the dimensionless hydrograph ratios in accordance to SCS and the points for the unit hydrograph were obtained (Raghunath , 2006) and used to develop the unit hydrograph curve.

2.2.3 Gray's method

The discharge was obtained through the dimensionalizing of the incomplete Gamma function Γ. The equation is given as (Viessman et al 1989; Ogunlela and Kasali, 2002).

$$Q_{t/P_R} = \frac{25.0(\gamma)^q}{\Gamma(q)}\left(e^{-\gamma\left(t/P_R\right)}\right)\left(\frac{t}{P_R}\right)^{q-1} \qquad (13)$$

where

Q_{t/P_R} = percent flow in 0.25 P_R at any given t/P_R value

q and γ = shape and scale parameters, respectively

Γ (q) = the gamma function of q which is equal to (q - 1)!

e = base of natural logarithm

P_R = period of rise (min)

t = time (min.)

Development of unit hydrograph

The Snyder's method was used to compute the lag time, unit hydrograph duration, peak discharge, time base and hydrograph time widths of peak flow by using the watershed characteristics obtained from the topographic map of the River catchment under consideration in accordance to Ramirez (2000) and Arora (2004). The parameters obtained are presented in Table1. The method of US Soil Conservation Service (SCS) for constructing synthetic unit hydrographs was based on a dimensionless hydrograph, which relates ratios of time to ratios of flow (Viessman et al., 1989) and Ramirez (2000). This method requires only the determination of the time to peak and the peak discharge. The calculated values for parameters t_p and q_p were applied to the SCS dimensionless unit hydrograph to obtain the corresponding unit hydrograph ordinates, the estimated unit hydrograph ordinates is presented in Table 2 to 9 based on the values of time to peak discharge (t_p) and peak discharge (q_p) for each river.

Table 1 Parameters for the generation of unit hydrograph (Snyder's method)

River watershed	L (km)	L_c (km)	t_L (hr)	t_r (hr)	Q_p (m^3/s)	T_b (hr)	A (km^2)	S (%)
Faw-Faw	11.80	6.40	5.86	1.07	13.54	89.57	46.00	0.59
Oba	23.50	10.00	8.23	1.50	78.53	96.70	375.00	0.39
Awon	35.60	20.00	11.48	2.09	60.52	106.44	403.00	0.34
Ogunpa	22.87	13.20	8.87	1.61	21.15	98.62	108.85	0.46
Opeki	43.50	20.00	12.19	2.22	81.31	108.57	575.00	0.21
Otin	36.00	16.00	10.77	1.96	76.01	104.31	475.00	0.36
Osun	47.50	15.00	11.48	2.09	175.66	106.44	1170.00	0.21
Ogun	600.00	315.00	61.25	11.14	574.13	255.73	20400.00	0.07

Table 2 Unit hydrograph ordinate for Fawfaw river watershed (SCS method)

T (hr)	0.00	1.05	2.09	3.14	4.18	5.23	6.27	7.32	8.36	9.41	10.45	11.50
Q (m^3/s)	0.00	19.68	45.77	30.21	14.65	7.09	3.43	1.65	0.82	0.41	0.18	0.0

Table 3 Unit hydrograph ordinate for Oba river watershed (SCS method)

T (hr)	0.00	2.09	4.18	6.27	8.36	10.46	12.55	14.64	16.73	18.82	20.91	23.00
Q (m^3/s)	0.00	80.20	186.50	123.09	59.68	28.91	13.99	6.71	3.36	1.68	0.75	0.00

Table 4 Unit hydrograph ordinate for Awon river watershed (SCS method)

T (hr)	0.00	3.02	6.04	9.07	12.09	15.11	18.13	21.16	24.18	27.20	30.22	33.24
Q (m^3/s)	0.00	59.63	138.68	91.53	44.38	21.50	10.40	4.99	2.50	1.25	0.55	0.00

Table 5 Unit hydrograph ordinate for Ogunpa river watershed (SCS method)

T (hr)	0.00	1.92	3.84	5.76	7.69	9.61	11.53	13.45	15.37	17.29	19.21	21.14
Q (m^3/s)	0.00	25.33	58.92	38.88	18.85	9.13	4.42	2.12	1.06	0.53	0.24	0.00

Table 6 Unit hydrograph ordinate for Opeki river watershed (SCS method)

T (hr)	0.00	4.26	8.52	12.78	17.04	21.30	25.56	29.82	34.08	38.34	42.60	46.86
Q (m^3/s)	0.00	60.37	140.39	92.66	44.92	21.76	10.53	5.05	2.53	1.26	0.56	0.00

Table 7 Unit hydrograph ordinate for Otin river watershed (SCS method)

T (hr)	0.00	3.00	6.01	9.01	12.02	15.02	18.03	21.03	24.04	27.04	30.05	33.05
Q (m^3/s)	0.00	70.69	164.40	108.50	52.61	25.48	12.33	5.92	2.96	1.48	0.66	0.00

Table 8 Unit hydrograph ordinate for Osun river watershed (SCS method)

T (hr)	0.00	4.56	9.12	13.67	18.23	22.79	27.35	31.91	36.47	41.02	45.58	50.14
Q (m^3/s)	0.00	114.79	266.95	176.19	85.42	41.38	20.02	9.61	4.81	2.40	1.07	0.00

Table 9 Unit hydrograph ordinate for Ogun river watershed (SCS method)

T (hr)	0.00	50.17	100.34	150.51	200.68	250.85	301.02	351.19	401.36	451.53	501.70	551.87
Q (m^3/s)	0.00	181.84	422.88	279.10	135.32	65.55	31.72	15.22	7.61	3.81	1.69	0.00

The Gray method required the determination of period of rise P_R, and other parameters require in solving equation (13). Other parameters determined are rainfall duration D, the volume of the unit hydrograph V, and the volume of dimensionless graph V_D. The parameters were obtained in accordance to the procedure stated by Viessman et al (1989), Ogunlela and Kasali (2002) and presented in Table 10.

Table 10 Parameter for development of unit hydrograph (Gray method)

River watershed	P_R (hr)	P_R/γ (hr)	D (hr)	Σcfs (10^4)	$V=V_D$ (10^6 m^3)
Faw-Faw	4.85	1.61	1.21	0.95	1.17
Oba	11.94	3.96	2.98	3.13	9.52
Awon	19.26	6.38	4.81	2.09	10.23
Ogunpa	10.70	3.54	2.67	1.02	2.76
Opeki	30.08	9.97	7.52	1.91	14.60
Otin	19.12	6.33	4.78	2.48	12.06
Osun	32.84	10.88	8.21	3.55	29.70
Ogun	739.99	245.18	185.00	2.75	518.00

Development of peak storm hydrographs

The established unit hydrographs ordinates were used to develop the storm hydrographs due to actual rainfall event over the watershed. Peak storm hydrographs for selected return periods (20yr, 50yr, 100yr, 200yr and 500yr) were developed through convolution. The maximum 24-hr rainfall depths of the different recurrence interval for the catchment under consideration are 174.2 mm, 205.0 mm, 232.3 mm, 262.73 mm and 309.0 mm respectively (Olofintoye et al, 2009). The storm hydrograph was derived from a multiperiod of rainfall excess called hydrograph convolution. It involves multiplying the unit hydrograph ordinates (U_n) by incremental rainfall excess (P_n), adding and lagging in a sequence to produce a resulting storm hydrograph. The SCS type II curve was used to divide the different rainfall data into successive equal short time events and the SCS Curve Number method was used to estimate the cumulative rainfall for storm depth of 20yr, 50yr, 100yr, 200yr and 500yr return period. The incremental rainfall excess was obtained by subtracting sequentially, the rainfall excess from the previous time events. The equations that apply to the SCS Curve Number method are given below (SCS, 2002).

$$Q_d = \frac{\left(P^* - I_a\right)^2}{P^* + 0.8S} \quad for\ P^* > 0.2S \qquad (14)$$

$$Q_d = 0 \quad for\ P^* \le 0.2S$$

I_a = initial abstraction $I_a = 0.2S$

$$S = \frac{25400}{CN} - 254 \qquad (15)$$

With the CN = 75 based on soil group B, small grain and good condition, S is estimated as 84.67 mm, while I_a is 16.94 mm. This implies that any value of rainfall less than 16.94 mm is regarded as Zero.

where
P* = accumulated precipitation (mm)
Q_d = cumulative rainfall excess, runoff (mm)

The storm hydrograph ordinates based on the rainfall depth of desire return periods were estimated from the unit hydrographs. The storm hydrograph peak flows obtained for the watersheds of Fawfaw, Oba, Awon, Ogunpa, Opeki, Otin, Osun and Ogun Rivers based on the three methods of synthetic unit hydrographs and various return periods are presented in

Table 10 to 17 respectively.

Table 10 Storm hydrograph peak flows for Faw-Faw River watershed (m^3/s)

Methods	Storm return periods				
	20yr, 24hr	50yr, 24hr	100yr, 24hr	200yr, 24hr	500yr, 24hr
Snyder	112.63	143.70	171.28	203.15	352.34
SCS	304.43	388.06	464.59	556.52	699.89
Gray	398.06	509.24	607.93	721.25	896.87

Table 11 Storm hydrograph peak flows for Oba River watershed (m^3/s)

Methods	Storm return periods				
	20yr, 24hr	50yr, 24hr	100yr, 24hr	200yr, 24hr	500yr, 24hr
Snyder	678.80	866.23	1030.03	1218.99	1510.35
SCS	1240.54	1581.35	1893.19	2267.81	2852.03
Gray	1318.61	1686.91	2013.82	2389.22	2970.98

Table 12 Storm hydrograph peak flows for Awon River watershed (m^3/s)

Methods	Storm return periods				
	20yr, 24hr	50yr, 24hr	100yr, 24hr	200yr, 24hr	500yr, 24hr
Snyder	555.52	707.11	839.52	992.08	1227.17
SCS	922.46	1175.88	1407.77	1686.34	2120.76
Gray	878.37	1123.71	1341.48	1591.55	1979.08

Table 13 Storm hydrograph peak flows for Ogunpa River watershed (m^3/s)

Methods	Storm return periods				
	20yr, 24hr	50yr, 24hr	100yr, 24hr	200yr, 24hr	500yr, 24hr
Snyder	180.44	230.26	273.80	324.02	401.46
SCS	391.89	499.55	598.06	716.40	900.96
Gray	427.21	546.54	652.46	774.08	962.56

Table 14 Storm hydrograph peak flows for Opeki River watershed (m^3/s)

Methods	Storm return periods				
	20yr, 24hr	50yr, 24hr	100yr, 24hr	200yr, 24hr	500yr, 24hr
Snyder	724.84	925.16	1100.29	1302.34	1613.93
SCS	933.81	1190.34	1425.08	1707.08	2146.84
Gray	802.54	1026.70	1225.66	1454.14	1808.21

Table 15 Storm hydrograph peak flows for Otin River watershed (m^3/s)

Methods	Storm return periods				
	20yr, 24hr	50yr, 24hr	100yr, 24hr	200yr, 24hr	500yr, 24hr
Snyder	672.80	858.83	1021.46	1209.10	1498.46
SCS	1093.50	1393.91	1668.80	1999.02	2513.93
Gray	1043.02	13334.35	1592.94	1889.88	2350.05

Table 16 Storm hydrograph peak flows for Osun River watershed (m^3/s)

Methods	Storm return periods				
	20yr, 24hr	50yr, 24hr	100yr, 24hr	200yr, 24hr	500yr, 24hr
Snyder	1558.63	1989.43	2366.10	2800.66	3470.81
SCS	1775.65	2263.46	2709.82	3246.04	4082.25
Gray	1495.47	1913.18	2283.94	2709.69	3369.48

Table 17 Storm hydrograph peak flows for Ogun River watershed (m^3/s)

Methods	Storm return periods				
	20yr, 24hr	50yr, 24hr	100yr, 24hr	200yr, 24hr	500yr, 24hr
Snyder	6018.71	7672.82	9120.66	10790.02	13364.33
SCS	2812.87	3585.63	4292.72	5142.16	6466.84
Gray	1157.25	1480.49	1767.39	2096.86	2607.42

The storm hydrograph peak flows of the same return periods for the catchment of the Rivers under consideration based on the three methods of synthetic unit hydrograph are presented in Figure 2 - 9 respectively. The figures show the relationships between the predicted design storm values using the three methods of synthetic unit hydrograph to generate the required ordinates used for the development of design storm hydrographs.

Figure 2 Comparison of peak storm hydrograph for Faw-Faw River

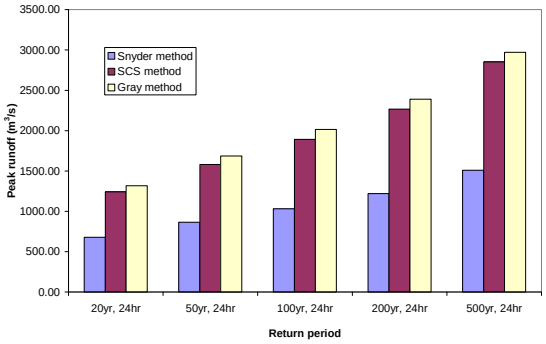

Figure 3 Comparison of peak storm hydrograph for Oba River

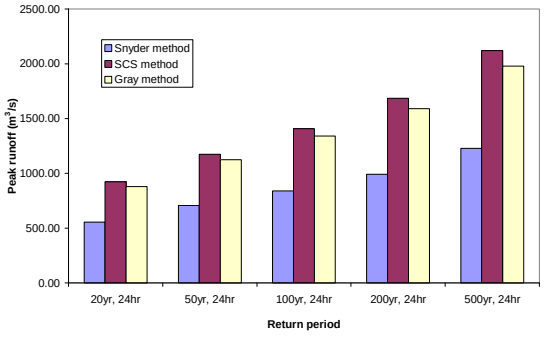

Figure 4 Comparison of peak storm hydrograph for Awon River

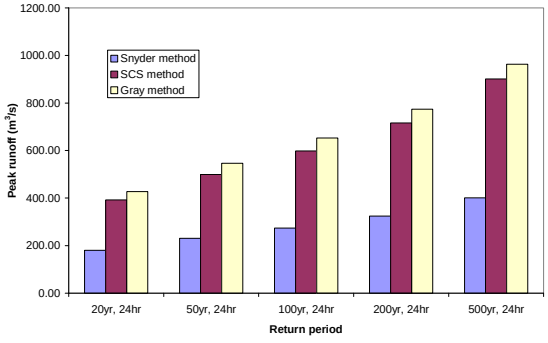

Figure 5 Comparison of peak storm hydrograph for Ogunpa River

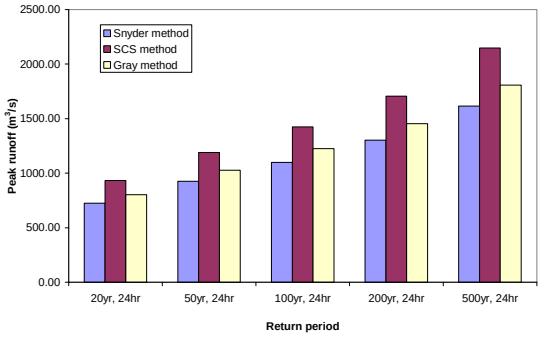

Figure 6 Comparison of peak storm hydrograph for Opeki River

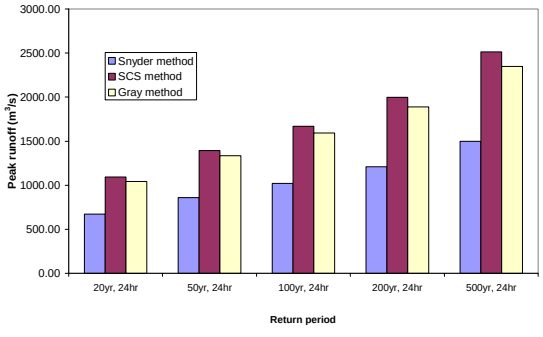

Figure 7 Comparison of peak storm hydrograph for Otin River

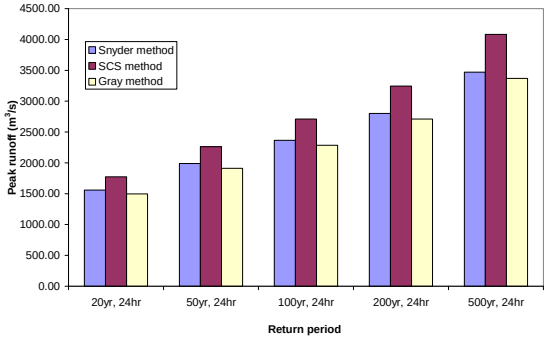

Figure 8 Comparison of peak storm hydrograph for Osun River

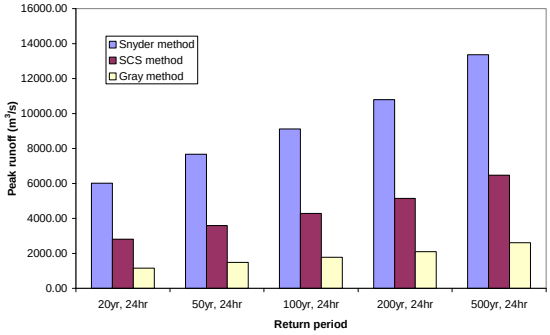

Figure 9 Comparison of peak storm hydrograph for Ogun River

Results and Discussion

Three methods of synthetic unit hydrograph were adopted to determine the ordinates for the development of peak storm hydrograph for Faw-Faw, Oba, Awon, Ogunpa, Opeki, Otin, Osun, and Ogun River watersheds. The methods are Snyder, SCS and Gray. The results from the synthetic unit hydrograph based on the three methods have already been presented in Tables 1 to 9. The storm hydrograph peak flows (m^3/s) for the eight watersheds are presented in Tables 10 to 17 based on Snyder, SCS, and Gray synthetic hydrograph ordinates respectively. The comparison of the storm hydrographs of the same return periods generated based on different synthetic unit hydrographs are presented in Figures 2 to 9 respectively. The results presented in the tables 10 - 17 and figures 2 - 9 shows that for Faw-Faw watershed, the values obtained for Gray method is higher by 71.80% and 23.14% than those of Snyder and SCS method respectively, while the value obtained with SCS method is higher by 63.31% than that of Snyder method. For Oba watershed, the values obtained for SCS method is higher by 45.88% and 5.45% than those of Snyder and Gray method respectively, while the value obtained with Gray method is higher by 48.83% than that of Snyder method. Also for Awon watershed, the values obtained for SCS method is higher by 40.66% and 5.25% than those of Snyder and Gray method respectively, while the value obtained with Gray method is higher by 37.38% than that of Snyder method. Likewise, for Ogunpa watershed, the value obtained for Gray method is higher by 58.02% and 7.81% than those of Snyder and SCS method respectively, while the value obtained with SCS method is higher by 54.46% than that of Snyder method. For Opeki watershed, the values obtained for SCS method is higher by 23.20% and 14.48% than those of Snyder and Gray method respectively, while the value obtained with Gray method is higher by 10.20% than that of Snyder method. For Otin watershed, the values obtained for SCS method is higher by 39.11% and 5.08% than those of Snyder and Gray method respectively, while the value obtained with Gray method is higher by 35.85% than that of Snyder method. For Osun watershed, the values obtained for SCS method is higher by 13.14% and 16.195% than those of Snyder and Gray method respectively, while the value obtained with Snyder method is higher by 3.50% than that of Gray method. For Ogun watershed, the values obtained for Snyder method is higher by 52.06% and 80.63% than those of SCS and Gray method respectively, while the value obtained with SCS method is higher by 59.06% than that of Gray method.

However, the percentage difference shows that for five watershed the values of peak flows obtained by SCS and Gray methods is fairly close (5.08 – 23.14%), while the percentage difference shows that for two watersheds, the values of peak flows obtained by Gray and Snyder method is fairly close (3.50 – 10.20%) and the percentage difference shows that for only one watershed the values of peak flows obtained by Snyder and SCS method to be fairly close. This inferred that Soil Conservation Service (SCS) method is favorably comparable with the other two methods. Based on this observation, it can be summarized that the SCS method can be useful in the generation of unit hydrograph ordinates required for the development of storm hydrograph within the catchment under consideration.

4. Conclusions

It has been noted that the watersheds under consideration have undergone notable eco-hydrological changes due to several developments along their course. This has replaced the natural ground surface, covered with grasses and has influenced its flow pattern. Based on the results obtained, it could be observed that the generation of unit hydrograph through synthetic methods has been found useful and effective. In some cases two methods give very close values. This implies that those two methods are highly efficient in estimating the parameters of the watershed which are required in the development of the unit hydrograph for the catchment considered. Conclusively, SCS method is recommended for use on this watershed since it is most comparable to other methods. The established unit and storm hydrographs can be used to compute the peak flows for the design of hydraulic structures within the catchment. The selection of peak storm hydrograph flows of the desire return period depend on the type of hydraulic structure in mind. For example, peak flow of 100 yr return period is required for the design of bridge, while 20 yr return period can be adopted for drainage culverts and minor bridges. It can also be inferred that synthetic unit hydrograph methods are suitable for the estimation of ordinates for the development of storm hydrograph for rivers that have small watershed, because it was observed that the bigger the watershed area the more the differences between the value obtained with different methods using the same return periods.

Acknowledgement:

The authors thanked the management of Techn – Consultants International Associates Ltd, (TCIA) Ilorin, Nigeria for involving us as part of the consulting team in executing the hydrological studies of Rivers in Osun State being Part of Research work under Water Supply & Sanitation Sector Reform Programme, Osun State Technical Unit, Osogbo, Nigeria.

Correspondence to:

Adebayo Wahab Salami and Solomon Olakunle Bilewu.
Department of Civil Engineering, University of Ilorin, P.M.B 1515, Ilorin, Nigeria
Telephone: 2348038219183 ; 2348035507690
E-mails: awsalami2006@yahoo.co.uk ; bilewuk@yahoo.com

References

[1] Warren V, Terence E.H and John W.K. Introduction to hydrology. Intext Educational Publishers, 2nd edition, New York, 1972, 106 – 141

[2] Wilson E.M Engineering Hydrology. Macmillan Press Ltd. 2nd edition Houndmills, Basingstoke, Hampshire and London. 1990, 172 -180

[3] Varshney R.S. Engineering Hydrology. NEM Chand & Bros, Roorkee (U.P), India. 1986

[4] Arora K.R. Irrigation, water power and water Resources Engineering. Standard Publishers Distributions, 1705-B, NAI SARAK, Delhi, 2004, 79-106

[5] Jones B.S. Five – minute unit hydrographs for selected Texas Watersheds. M.Sc Thesis in Civil Engineering submitted to the Graduate Faculty of Texas Tech. University. 2006

[6] Chow V.T, Maidment D.R and Mays. LW. Applied Hydrology: McGraw – Hill Publishing company, New York, 1988

[7] Viessman W, Knapp J.W and Lewis G.L. Introduction to Hydrology, Harper and Row Publishers, New York, 1989, 149 – 355.

[8] Wanielista M.P. Hydrology and Water Quantity Control. John Willey and Sons. Inc. (1990)

[9] Ramirez J.A. Prediction and Modeling of Flood Hydrology and Hydraulics. Chapter 11 of Inland Flood Hazards: Human, Riparian and Aquatic Communities. Edited by Ellen Wohl; Cambridge University Press. 2000

[10] Ogunlela A.O and Kasali. M.Y. Evaluation of four methods of storm hydrograph development for an ungaged watershed. Published in Nigerian Journal of Technological development. Faculty of engineering and Technology, University of Ilorin, Ilorin, Nigeria. 2002 (2); 25 – 34

[11] Salami A.W. Evaluation of Methods of Storm Hydrograph Development. International Egyptian Engineering Mathematical Society IEEMS, Zagazig University Publications. International e-Journal of Egyptian Engineering Mathematics: Theory and Application (http://www.ieems.net/iejemta.htm) 2009 (6); 17-28.

[12] Raghunath H.M. Hydrology: Principles, Analysis

and Design. New Age International (P) Limited, Publishers, New Delhi. 2nd edition. 2006

[13] SCS. Soil Conservation Service. Design of Hydrograph. US Department of agriculture, Washington, DC. 2002

[14] Olofintoye O.O, Sule BF and Salami AW. Best-fit Probability Distribution model for peak daily rainfall of selected Cities in Nigeria. New York Science Journal, 2009, 2(3),ISSN1554-020. (http://www.sciencepub.netyork)

Assessment of Basic Slag on Reduction of Fe and Al Toxicity in Acid Sulfate Soils under Various Moisture Regimes

Abul Hasnat Md. Shamim[1, 2], Md. Harunor Rashid Khan[3] and Takeo Akae[1]

[1]Department of Environmental Management Engineering, Faculty of Environmental Science and Technology, Okayama University, Okayama 700-8530, Japan
[2]School of Agriculture and Rural Development, Bangladesh Open University, Gazipur-1705
[3]Department of Soil, Water and Environment, Dhaka University, Dhaka-100, Bangladesh
E-mail: abulhasnats@yahoo.com, duharun@yahoo.com, akae@cc.okayama-u.ac.jp

Abstract: Acid sulfate soils (ASSs), which are one of the worst soils in the world, release huge amounts of acid and toxically high concentrations of metals, affecting biological activity in the soils as well as in the surrounding water environments, which requires sustainable measures for their reclamation. Accordingly, an incubation study was conducted with the topsoil of two different ASSs (Cheringa and Badarkhali) to assess the effects of basic slag (BS: size <1 mm; pH 9.6; Ca 20.8 %; Mg 9.8 %, etc.) on reduction of Fe and Al toxicity in ASSs. It is noted that BS is a byproduct of steel industry in Bangladesh and can be collected almost free of charge. These soils received BS at the rate of 0 (T_0), 11 (T_1), 22 (T_2) and 33 (T_3) t ha^{-1} under various moisture regimes (saturated condition M_1, i.e. 100 % moisture content, wetting-drying cycles of 100 and 50 % moisture M_2, and moisture at field condition M_3, i.e. 50 %). The impacts of these treatments on selected parameters in these soils were studied within180 days of incubation. The application of BS was found to be increased the pH of soils from 3.6 to 5.1 for Cheringa; 3.9 to 5.2 for Badarkhali soils at the end of incubation. These increments were more striking with the highest doses of BS under saturated moisture conditions in both of the soils. The treatments exerted significant ($p \leq 0.05$) effects on the decrement of Fe and Al ions in different period of incubation. The striking changes were recorded for the rate of decrements of Fe and Al ions, under saturated condition compared with the control after 180 days of incubation. These results suggest that the application of BS not only reduction of soil acidity but also to improve these soils at desirable pH (pH>5) levels in the same moisture conditions. [Journal of American Science 2009;5(4):33-42]. (ISSN: 1545-1003).

Keywords: acid sulfate soils, Fe and Al ions, basic slag, incubation time, moisture regimes.

1. Introduction

Acid sulfate soils (ASSs), which are one of the worst soils in the world, release huge amounts of acid and toxically high concentrations of metals, affecting biological activity in the soils as well as in the surrounding water environments (Gosavi et al., 2004; Mathew et al., 2001; Minh et al., 1997; Thawornwong and van Diest 1974). Acidification from ASSs cause a number of chemical, biological and physical problems arise such as aluminum and iron toxicities, decrease availability of phosphate, nutrient deficiencies, arrested soil ripening, hampered root growth, blockage of drains by ochre and corrosion of metal and concrete structures (AARD and LAWOO, 1992). The initial heavy rain on acid sulfate soils cause a 'first-flush' runoff and drainage of toxic water with properties including low pH, low concentration of dissolved oxygen and high concentration of dissolved aluminum which caused massive fish kill (Anon, 1990; Lin and Melville, 1994). The ASSs cause on- and off- site problems (Ritsema et al., 2000). On-site problems, which have been extensively reviewed (Dent 1986), include Al toxicity in drained soils, Fe and H_2S toxicity in flooded soils, salinity and nutrient deficiencies, especially decrease availability of phosphate. Engineering problems include (i) corrosion of steel and concrete and (ii) uneven subsidence, low bearing strength and fissuring leading to excessive permeability of unripe soils; blockage of drains and filters by ochre; and the difficulties of establishing vegetation cover on earthworks and restored land. Off-site problems stem from drainage effluents, earthworks, excavations, and mines. The acid drainage water carries Al released by acid weathering of soil minerals. Drainage waters may also be enriched in heavy metals and arsenic, a toxic cocktail endangering aquatic life and public health. Acid drainage and floodwaters may travel for many kilometers before they are neutralized. Acid drainage can have disastrous effects on freshwater and estuarine fishes, especially on invertebrates that are unable to escape. These soils could display a high agricultural potential if they were to be reclaimed by appropriate methods (Khan, 2000). Moreover, the reclamation of these soils may be difficult but very essential due to the formation of acidity during dry periods of the year and hampering not only crop growth but also destroying aquatic lives.The conventional reclamation by the application of lime and flash leaching in the proposed soils are not effective and

sustainable (Khan, 1994). Because, soil acidity produced by 1% oxidizable sulfur requires about 30 ton of $CaCO_3$ per ha (van Breemen, 1993). Usually ASSs contain 1-5% oxidizable sulfur and showed antagonistic effect on micronutrient levels as well as on the balance of basic cations in plants (Khan et al., 1996). Tri et al., (1993) revealed that construction of raised bed is the most important land management practices for acid sulfate soils. However, this practice has not enough success. Its success depends on several factors of the soils, their position and environmental conditions (AARD and LAWOO, 1992). Acidity and salinity problems relating to rice production in the studied acid sulfate soils were alleviated by the application of leaching. Khan and Adachi (1999) reported that reclamation of the soils through leaching enhanced the losses of basic cations from top soils, whereas increased acidic cations in the top soils by exchange reactions. After seven years of leaching practices on acid sulfate soils in Vietnam, Sterk (1993) reported that the acid content of the topsoils is not decreasing, which might be attributed to enrichment of acidic cations like aluminum in the top soils. Khan (1994) reported that leaching is an effective method for reclaiming both salinity and acidity of the soils but losses of basic cations through leaching should be considered for the greater success of reclamation. Takai et al., (1992) claimed that nutrient deficiency is an important factor for the improvement of acid sulfate soils. Khan (1994) revealed that for the reclamation and improvement of ASSs, BS would be effective to reduce acidity of the soils because BS was found to increase soil solution pH and optimized the concentration of some elements like Ca, Mg, P and Si, which are very essential/beneficial for crop production as well as alleviates the toxicity of Fe and Al. Moreover, there is evidence that high Ca and Si concentrations in drainage/waste waters protect fish against Al toxicity (Birchall et al., 1989). Potential ASSs may have high pH like 6 to 7 does not mean that the soils are safe because at that situation it may create H_2S, Fe and some organic acids problems (Kabir, 2005).

ASSs are of major environmental concern in many wetlands. Van Mensvoort and Dent (1998) claimed for about 24 M ha of ASSs of which about 0.7 M ha are located in different pockets of inundated coastal areas in Bangladesh where crop production is very low; some where the lands are unproductive though the soils have high agricultural potential (Khan, 2000). The nature and characteristics of these pockets of ASSs varied from place to place and even within pockets owing to the difference in mangrove vegetations and accumulation of sediments (Khan, et al., 2007). Since the ASSs can exert severe effects on surrounding ecosystems, immediate steps should be taken to improve these soils further (Khan, et al., 2002). Delayed effects of potential chemicals stored in the ASSs resulted in harmful effects, like a “chemical time bomb” on the associated environments (Khan and Adachi, 1999). It has recently been estimated that these affect some 100 million hectares (M ha) of land world-wide (Sheeran, 2003). For sustainable use ASSs, acceptable cost effective chemical reduction of the acidity is very essential. Soil acidity produced by one percent oxidizable sulfur after neutralization (3 to 30 t of $CaCO_3$ per ha, depending on clay content and mineralogy) by exchangeable cations requires about 30 t of $CaCO_3$ per ha (Van Breemen, 1993). Usually ASSs contains 1 to 5 % oxidizable sulfur which indicates a huge amount of lime would be needed. Generally calcite ($CaCO_3$) is used as agricultural lime but it is to some extent expensive. As a result farmers often become reluctant to ameliorate ASSs. With this objective BS, a low cost liming material was undertaken to use as an ameliorant of ASSs. From its suitability BS as a byproduct from the steel industry in Bangladesh can be collected almost free of charge. However, application of BS as agricultural lime is not well documented. Moreover, the reducing capacity and potentiality of the BS for the exchangeable cations in different ASSs are also not known but needed for its economic and sustainable budgeting for these problem soils (Khan, et al., 2002). Accordingly, agricultural limes such as BS were planned to incorporate into two ASSs under different moisture regimes.

Jintaridth, 2006 reported that deficiency in plant base minerals is an important factor when the reclamation and management practices are performed in ASSs. Takai, et al., (1992) also claimed that nutrient deficiency is an important factor for the improvement of ASSs. Dent (1986) reported that BS from the steel industry was effective in reducing the soil acidity and also economical if available locally. The application of BS in ASSs significantly increased soil pH, Ca and Mg with an associated decrease in Na, Fe and Al concentrations over time (Khan, et al., 2006a). This BS had a very high pH of 9.6 and contained 20.8 % Ca, 9.8 % Mg, and 12.8 % SiO_2 (Khan, et al., 2006b). They also added that the BS has been used on a small scale for the reclamation of ASSs in Bangladesh since 1985 and to-date there is no evidence of its harmful effects. The reclamation of these soils may be difficult but essential. Successful reclamation of the ASSs may result in the development of productive fields for crop growth. While poor soil reclamation may lead to creation of unfavorable soil conditions for crop growth and formation of actual ASSs, the real problem is resulted in the coastal tidal flat plain areas (Khan, et al.. 2006b). Cook, et al., (2006) reported that the progressive oxidation of organic matters, sulfides and increasing acidity in the profile of ASSs is not only decreasing bases in the soil solution but also strongly affect the fate/mobility of metals and metalloids in groundwater, posing threat to groundwater resources and health of

both terrestrial and aquatic ecosystems (Abou-Seeda, et al., 2002). In ASSs, water management is the key to soil management and proper water management can limit acidification (Khan, et al.. 2006b). However, the potentiality of BS for the reduction of ASSs and associated ion dynamics under variable soil moisture regimes and wetting-drying cycles should have much influence regarding sustainable reclamation and improvement of ASSs. Considering the above background, the present study was done in order to assess the remedying capacity of BS under various moisture regimes and its effects on the reduction of Fe and Al ions in the soils.

2. Methods and Materials

2.1 Incubation experiment

For assessing of BS on reduction of Fe and Al toxicity in ASSs under various moisture regimes, an incubation study was carried out in the laboratory of the Department of Soil, Water and Environment, University of Dhaka, Bangladesh during 2000 to 2001. Accordingly, an experiment was conducted for 180 days (six months) under saturated moisture condition (water content = 100 % by weight), moisture at field capacity (50 % by weight) and wetting-drying cycles of these treatments. It is mentioned that during the incubation experiment, the moisture contents was monitored and kept it at a fixed value by watering when it is required. The effects of these treatments with time were also considered for this experiment.

Table1: Some selected physical and chemical properties of the acid sulfate soils (depth 0-20 cm) before the incubation study.

Soil properties	Cheringa soil	Badarkhali soil
Texture	Silty clay loam	Silty clay loam
Moisture at field condition (vol. %)	48	49
Soil pH (Field)	3.8	4
Soil pH (Soil:Water=1: 2.5)	3.6	3.9
Soil pH (Soil:0.02 M $CaCl_2$=1.2.5)	3.3	3.4
Pyrite content (%)	7.3	6.6
Electrical Conductivity (1: 5 dS m^{-1})	18.5	19
Organic matter (Wet oxidation, g kg^{-1})	39.1	30.7
Available nitrogen (1.3 M KCl, mM kg^{-1})	3.6	3.3
Available phosphorus (0.02N H_2SO_4, mM kg^{-1})	0.1	0.11
CEC (1 M NH_4Cl: cmol kg-1, at pH 7.0)	17.2	18.5
Aluminium-saturation (1M NH_4Cl: %)	40.3	41.2
Iron-saturation (1M NH_4Cl: %)	8.3	7.1
Sodium-saturation (1M NH_4Cl: %)	12.4	13
Potassium-saturation (1M NH_4Cl: %)	1.4	1.6
Calcium-saturation (1M NH_4Cl: %)	1.8	1.9
Magnesium-saturation (1M NH_4Cl: %)	5.5	6.2
Water-soluble ions		
Sodium (Flame photometry: cmol kg^{-1})	3.01	3.2
Potassium (Flame photometry: cmol kg^{-1})	0.3	0.25
Calcium (*AAS: cmol kg^{-1})	0.3	0.37
Magnesium (AAS: cmol kg^{-1})	3.34	3.43
Iron (AAS: cmol kg^{-1})	0.35	0.31
Aluminium (ASS: cmol kg^{-1})	2.1	1.9
Sulfate ($BaCl_2$, : cmol kg^{-1})	4.86	4.2

*Atomic Absorption Spectrophotometer

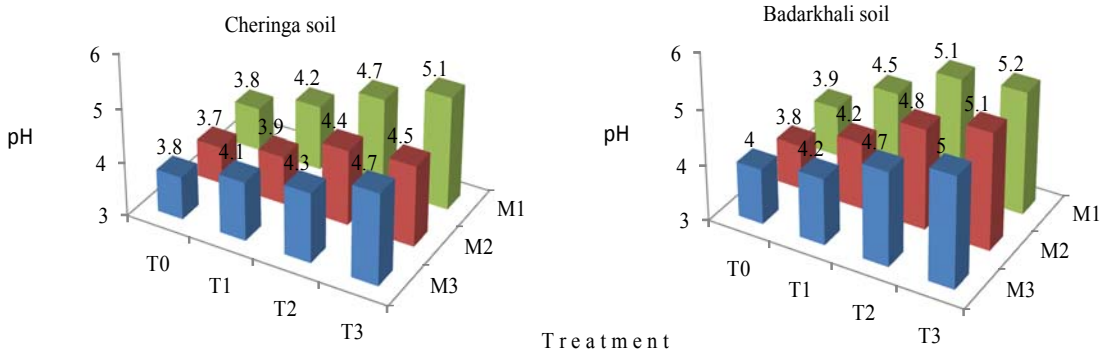

T0=Control; T1=Basic slag (BS)@11; T2=BS@22; T3=BS@33 t ha^{-1}; M1=Saturated condition; M2=Wetting-Drying cycle; and M3=Moisture at field condition

Figure 1 Effcets of basic slag and moisture regimes at the end of incubation times on pH in the soils.

Surface layer (Topsoils: depth 0 to 20 cm) of two different ASSs (Cheringa and Badarkhali) were collected from Cheringa and Badarkhali upazilas in Cox' Bazar district, Bangladesh. These soils were air-dried and grounded uniformly and passed through 2 mm (10 meshes) sieve and mixed thoroughly. Then fifty grams of each soil with respect to treatments was taken in a plastic bottle (10 cm height and 4 cm diameter). The four different doses of 0, 11, 22 and 33 t ha^{-1} of BS were considered for this study (the application rates were selected from feasible stand point of view). The BS was collected from a steel industry and then grounded to less than 1 mm sizes. The composition of basic slag (%)：SiO_2 12.8, Ca 20.8, Mg 9.8, Fe 11.3, Mn 0.04, PO_4 0.03, others 44.96 and pH 9.6 (Source: Laboratory of Soil Science, Institute for Plant Nutrition and Soil Science, University of Kiel, D-24109 Kiel, Germany, 1999). It was mixed thoroughly as per treatments. The distilled water was added at saturation condition of soil (by 50 ml), moist at field condition (by 20 ml) and at wetting-drying cycles (by 20 ml on drying and 50 ml on wetting). In wetting-drying cycle, the soil samples in the bottles were kept open to air under saturated condition for 15 days at room temperatures (25° to 30° C) for natural air drying towards field capacity during the following 30 days. The wetting-drying cycle was continuously repeated within every one and half months and maintained up to the end of the incubation period of 180 days. The desired levels of moisture in the soils in each bottle were maintained by the addition of distilled water (pH 6.7, EC 0.5 dS m^{-1}) when required. The soils were sampled in order to analyses the soil pH, ECe (EC of saturation extract of soil) and exchangeable cations at 1, 15, 45, 60, 90, 105, 135, 150, 180 days after incubation. There were 9 sets of bottles and each set contained 24 bottles (2 soils X 4 treatments X 3 replications), i.e. the numbers of total bottles were 216.

The soils were analyzed for textural class (pipette method; Day, 1965), pH (field, 1:2.5 water and 0.02 M $CaCl_2$: Jackson, 1973), ECe (Richards, 1954), organic carbon (wet combustion with $K_2Cr_2O_7$; Nelson and Somners, 1982), available nitrogen (micro-Kjeldhal method; Jackson, 1973); available phosphorus (0.02 N H_2SO_4, Spectrophotometry at 440 nm wave length; Olsen, et al., 1954), exchangeable cations (Jackson, 1973) such as Na^+, K^+ (Flame photometry), Ca^{2+}, Mg^{2+}, Fe^{2+} and Al^{3+} (atomic absorption spectrophotometry; Hesse, 1971), and CEC (Chapman, 1965). The level of significance of the different treatment means were calculated by Duncan's New Multiple Range Test (DMRT) and Least Significant Difference (LSD) Techniques (Zaman, et al., 1982).

3. Results and Discussion

The studied soils, namely Cheringa and Badarkhali (depth: 0-20 cm) showed a silty clay loam texture, initially low pH of 3.6 for the Cheringa and 3.9 for the Badarkhali soils, high ECe (18.5 for Cheringa and 19.0 dS m^{-1} for Badarkhali soils) and high amount of organic matter . Some selected physical and chemical properties of the studied ASSs (depth 0 to 20 cm) before the incubation study are given in Table 1.

3.1 Changes in soil pH

A significant ($p \leq 0.05$) positive increase in pH were determined with the increased rates of BS application in both the soils compared with the control where no BS was applied but the water content was maintained at field capacity (Figure 1). It is evident from the data that the initial low pHs of the soils was increased steadily with the highest doses of BS and the effects were more pronounced with the latter periods of incubation. The pH rose from 3.6 to 5.1 in Cheringa soil and 3.9 to 5.2 in Badarkhali soil after 180 days of incubation, which

revealed a wide and significant ($p \leq 0.05$) changes in soil pH were made by the application of BS in both the soils (Figure 1). The lower pHs were observed in the control treatments having moisture at field capacity as compared with those obtained from the saturated and wetting-drying cycle conditions. This might be due to having more oxidized conditions at field capacity than those of the other soil conditions. The release of acidic materials occurred from the break down of pyrite in more oxidized acid sulfate soils, reflecting the requirement of more liming materials to reduce more acidity in both the soils. The facts that these soils contain pyrite were reported by many researchers (Khan et al., 2006). In case of control, except for several initial increased trends within first 90 days, the almost unchanged values of soil pHs were found in both of the soils throughout the whole period of incubation of 180 days. Application of BS was found to be increased the soil pH linearly with their increase doses regardless of water contents and soil conditions. Khan, et al., (1996) reported that the application of BS at the rate of 12 t ha^{-1} in acid sulfate soil raised the soil pH from 5.3 to 7.4. The rise of soil pH in present study also remained almost similar range, which might be due to the washout of soluble sulfate and/or in the formation of insoluble sulfate compounds like gypsum, akaganeite (Bigham, et al., 1990).

The increase in soil pH or in other way, it can be expressed in the reducing capacity of BS by releasing exchangeable cations in the acid sulfate solution was found to be the highest after180 days of incubation with each of the moisture condition and treatment in both the soils. This might be due to the reduction of produced acids with the released basic ions with the passes of time and the slow releasing of basic ions from the BS might hold the steady increase in pHs of the soils. Throughout the incubation period, it was noticed that the potentiality of BS as a liming material will be effective for reducing the acidity of acid sulfate soils for long time. To maintain a reasonably good conditioned soil for growing crops, the soil should be amended at saturated soil condition followed by the application of BS at 33 t ha^{-1}. The BS was also reported effective in increasing soil pH as well as maintained favorable soil conditions **(**Abbaspour, et al., 2004; Alves, et al., 2006 and Khan, et al., 2006b).

3.2 Changes in water-soluble iron and aluminium

Iron is mostly a pH dependent element. The amount of water-soluble Fe was low throughout the incubation time and the quantity was found to be decreased with the increment of pH in both the soils as compared with the control (Figure 2). The leased amount of Fe were determined in the soils of high pH as a result of BS at 33 t ha^{-1} under saturated condition in both the soils followed by the condition of field capacity and wetting-drying cycle. The steepest fall in the concentration of the Fe were observed with the application of lime (Khan et al., 1996). They also reported that the concentration of K, Ca and Mg were increased while the concentration of Fe and Mn decreased in the ASSs.

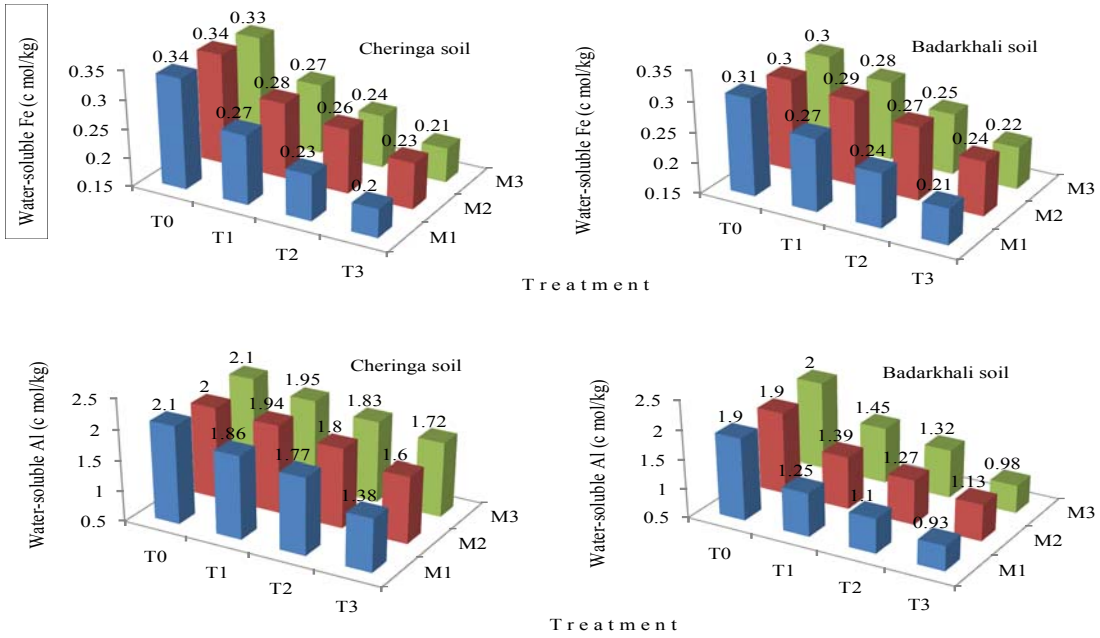

T0=Control; T1=Basic slag (BS)@11; T2=BS@22; T3=BS@33 t ha^{-1}; M1=Saturated condition; M2=Wetting-Drying cycle; and M3=Moisture at field condition

Figure 2 Effcets of basic slag and moisture regimes at the end of incubation times on water-soluble Fe and Al ions in the soils.

The availability of Al is also highly pH dependent, i.e. available at the lower pH value of <4.5 and the higher pH of > 10 (Donahue et al., 1987). With the amendments through BS, the pHs of both the soils were found to be increased strikingly as compared with the initial pHs, which resulted the low availability of Al. The amount of water-soluble Al in both the soils was found to be decreased under saturated condition. Cheringa soil was found to be content more, Al, which might be due to their initial high potential acidity as compared with Badarkhali soils. Application of BS of 33 and 22 t ha^{-1} were found to be effective in decreasing Al contents in both the soils regardless of moisture regimes. The BS at 33 t ha^{-1} exerted more detrimental effect regarding the availability of Al, which reduced to almost half of the amounts of its initial contents in these soils (Figure 2).

3.3 Changes in exchangeable iron and aluminium

The results showed that the contents of exchangeable iron remarkably decreased with time. The lowest content of Fe^{2+} was determined by the highest dose of BS (33 t ha^{-1}) under saturated conditions in both the soils where the corresponding pH rises at highest levels of 5.1 at Cheringa and 5.2 at Badarkhali soils (Figure 1). So, the exchangeable Fe^{2+} was found to have negative relationship with their corresponding pH.

The initial very high contents of exchangeable Al^{3+} in both the ASSs were found to be decreased strikingly with the higher dose of BS regardless of moisture regimes (Figure 3). The maintenance of saturated moisture condition of soil was found to be more suitable practice in order of decrement in contents of exchangeable Al^{3+} in both the soils followed by moisture at field capacity and wetting-drying cycle. The amounts of exchangeable Al^{3+} was very high in Badarkhali soil as compared with Cheringa soil, which might be due to the variation in their corresponding pH level. The lowest value of exchangeable Al^{3+} was recorded by the higher rates of BS (33 t ha^{-1}) as 3.56 c mol kg^{-1} in Cheringa soil and 3.32 c mol kg^{-1} in Badarkhali soil under the moisture at saturation condition. The second lowest contents were found for the condition of moisture at wetting-drying cycle (3.86 c mol kg^{-1} for Cheringa and 3.67 c mol kg^{-1} for Badarkhali soils) followed by the condition of field capacity (4.0 c mol kg^{-1} for Cheringa and 4.1 c mol kg^{-1} for Badarkhali soils) having the treatment of BS 33 t ha^{-1}. The lower doses of BS (11 and 22 t ha^{-1}) exerted comparatively the higher contents of exchangeable Al^{3+} in both the incubated ASSs. It was noticed that the exchangeable Al^{3+} in ASSs fell steeply as soon as pH rose above 4.0 (Gotoh and Patric, 1974; Hart, 1959). Moreover van Breemen (1973 and 1976) has shown that Al activity was inversely related to pH, increasing roughly 10 folds per unit pH decrease.

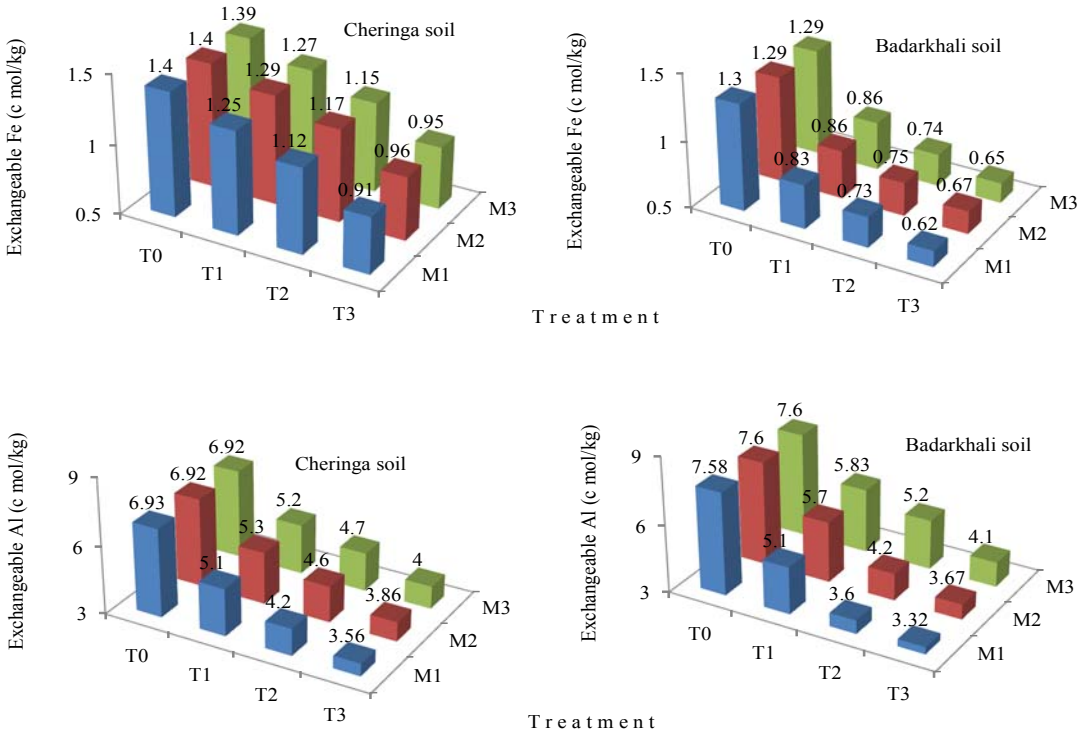

T0=Control; T1=Basic slag (BS)@11; T2=BS@22; T3=BS@33 t ha^{-1}; M1=Saturated condition; M2=Wetting-Drying cycle; and M3=Moisture at field condition

Figure 3 Effcets of basic slag and moisture regimes at the end of incubation times on Exchangeable Fe and Al ions in the soils.

4. Conclusions

From the results, it was revealed that the Fe and Al toxicity of the studied acid sulfate soils (ASSs) were remarkably decreased by the application of basic slag (BS). Moisture at saturated condition was found to be best for the reduction of these ions in both the soils, which will be supportive for planning of crop production on these soils. The highest dose (33 t ha^{-1}) of BS in Cheringa and Badarkhali ASSs were found to be reduced the acidity of these soils at desirable pH (pH>5) levels under same moisture conditions. The present findings suggest that by the use of BS or material rich in basic cations in these soils is a pre-requisite to be brought into productive land in order of quick reduction of acidity problems.

Acknowledgements

The research is carried out by the financial and technical supports of the Volkswagen Foundation (Ref.: 1/73802 dated 03.08.98) and Alexander von Humboldt (AvH) Foundation of Germany. The senior author also wishes to express appreciation to the Ministry of Education, Science, Culture and Sports, Government of Japan and the Graduate School of Environmental Science, Okayama University.

Correspondence to:
Abul Hasnat Md. Shamim
Ph. D Student
Graduate School of Environmental Science
Okayama University, Okayama 700-8530, Japan
Telephone and fax number: 0081-086-251-8874
E-mail: abulhasnats@yahoo.com

Received: 1/26/2009 / Revised: 14/07/2009

References

[1] Abbaspour A, Kalbasi M, Shariatmadari H. Effect of steel converter sludge as iron fertilizer and amendment in some calcareous soils. J. Plant Nutr. 2004; 27: 377-94.

[2] Abou-Seeda MH, EI-Ashry I. Assessment of basic slag as soil amelioration and their effects on the uptake of some nutrient elements by radish plants. Bulletin National Res. Centre (Cairo), 2002; 27: 491-506.

[3] Agency for Agricultural Research and Development (AARD) and The Land Water Research Group (LAWOO). Acid sulfate soils in the humid tropics: Simulation model and chemical processes to evaluate water management strategies. Wageningen, The Netherlands, 1992.

[4] Ahmed N, Wilson HW. Acid sulfate soils of Caribbean region-their occurrence, reclamation and use. Soil Sci. 1992; 153 (2):154-164.

[5] Alves MC, Paz Gonzalez A, Colorado G, Perecin Junior H, Vidal V. Influence of bio-solids rate on chemical properties of an Oxisol in Sao Paulo, Brazil. Common Soil Sci. Plant Anal. 2006; 37: 2481-93.

[6] Anon. Regional Research Program on relationship between epizootic ulcerative syndrome in fish and the environment. Network of aquaculture centers in Asia-Pacific, Bangkok. 1990.

[7] Bigham JM, Schwertmann U, Carlson L, Mural E. A poorly crystallized oxihydroxisulfate of iron formed by bacterial oxidation of Fe (II) in acid mine waters. GeoChin. CosoChim. Acta, 1990; 54: 2743-2758.

[8] Birchall JD, Exley C, Chappell JS, Phillips MJ. Acute toxicity of aluminium to fish eliminated in silicon-rich waters Nature, 1989; 338:146–148.

[9] Chapman HD. Cation exchange capacity. In: Methods of Soil Analysis. Part 2, Agron. Series 9. C.A. Black (ed.). Am. Soc. Agron., Publication, Madison, WI, USA. 1965; pp. 891-900.

[10] Cook TJ, Watkins R, Appleyard S, Vogwill R J. Acidification of groundwater caused by a falling water table in a sandy aquifer in the Perth Region, Western Australia. The 18th World Congress of Soil Science Abstract. July 9-15, Philadelphia, Pennsylvania, USA, 2006; pp. 680.

[11] Day PR. Particle fractionation and particle size analysis. In: Methods of Soil Analysis. Part 2, Agron. Series 9. C.A. Black (ed.). Am. Soc. Agron., Publication, Madison, WI, USA. 1965; pp. 545-566.

[12] Dent D. Acid sulfate soils: a Baseline for Research and Development. ILRI (International Land Reclamation and Improvement) Publication no. 39: Wageningen, The Netherlands, 1986; pp. 58.

[13] Donahue RL, Miller RW and Shickluma JC. Soils: an Introduction of Soils and Plant Growth. 5th Edn. Prentice-Hall of India Pvt. Ltd., New Delhi-110001, India, 1987. pp. 667.

[14] Gosavi K, Sammut J, Gifford S, Jankowski J. Macroalgal biomonitors of trace metal concentration in acid sulfate soil aquaculture ponds. Sci. Total Env. 2004; 25: 25-39.

[15] Gotoh, S and Patrick, WH. Transformation of iron ina waterlogged soil as influence by redox potential and pH. Soil Sci. Soc. Am. Proc. 1974; 38:66-71.

[16] Hart, MGR. Sulfur oxidation in tidal mangrove soils of Sierre leone. Plant Soil, 1959; 11:215-236.

[17] Hesse PR. A text Book of Soil Chemical Analysis. John Murry Publicatin, London, 1971.

[18] Jackson ML. Soil Chemical Analysis. Prentice Hall of India Pvt. Ltd., New Delhi, 1973; pp. 41-330.

[19] Jintaridth B. The role and effectiveness of Phospho-microorganisms with rock phosphate. The 18th World Congress of Soil Science Abstract, July 9-15, Philadelphia, Pennsylvania, USA. 2006; pp. 681.

[20] Kabir SM. Acid sulfate soil ecosystems and their sustainable management. Unpublished Ph.D thesis, University of Dhaka, Bangladesh. 2005; pp. 1-2.

[21] Khan HR, Blume H-P, Kabir SM, Bhuiyan MMA, Ahmed F, Syeed SMA. Quantification of the severity, reserve and extent of acidity in the twenty profiles of acid sulfate soils and their threats to environment. Soil & Environ., 2007 26 (in press).

[22] Khan H R, Kabir SM, Bhuiyan MMA, Blume H-P, Adach T, Oki Y, Islam KR. Physico-chemical amendments of acid sulfate soils for rice production in Bangladesh. The 18th World Congress of Soil Science Abstract, July 9-15, Philadelphia, Pennsylvania, USA. 2006a; pp. 682.

[23] Khan HR, Bhuiyan MMA, Kabir SM, Oki Y, Adachi T. Effects of selected treatments on the production of rice in acid sulfate soils in a simulation study. Jpn. J. Trop. Agr. 2006b; 50: 109-115.

[24] Khan HR, Bhuiyan MMA, Kabir SM, Ahmed F, Syeed SMA, Blume H-P. The assessment and management of acid sulfate soils in Bangladesh in relation to crop production. In: The restoration and management of derelict land, M. H. Wong and A. D. Bradshaw (Ed.), World Scientific Publishing Co. Pte. Ltd. UK, 2002; pp. 254-262.

[25] Khan HR, Rahman S, Hussain MS, Blume H-P. Response of rice to basic slag, lime, and leaching in two saline-acid sulfate soils in pot experiments. J. Plant Nutrition and Soil Science, Germany, 1996; 159: 549-555.

[26] Khan HR. (2000): Problem, prospects and future directions of acid sulfate soils. Proc. Inter. Conference on Remade Lands 2000, pp. 66-67. A. Brion and R.W. Bell (ed.). Nov. 30 to Dec. 2, 2000, Perth, Australia.

[27] Khan HR, Adachi T (1999): Effects of selected natural factors on soil pH and element dynamics studied in columns of pyretic sediments. Soil Science and Plant Nutrition, 45, pp. 783-793.

[28] Khan HR. Fundamental studies on reclamation and improvement of problem soils in relation to rice production. PhD thesis, Okayama University, Okayama 700, Japan, 1994.

[29] Khan HR, Rahman S, Hussain MS, Adachi T. Morphology and characterization of an acid sulfate soils from mangrove floodplain area of Bangladesh, Soil Phys. Cond. Plant Growth, Jpn, 1993; 68: 25-36.

[30] Lin C, Melville MD. Acid sulfate soil-landscape relationships in the Pearl River Delta, southern China. Catena, 1994; 22: 105-120.

[31] Mathew EK, Panda RK, Madhusudan N. Influence of sub-surface drainage on crop production and soil quality in a low-lying acid sulfate soil. Agr. Water Manage.; 2001; 47:191-209.

[32] Minh LQ, Tuong TP, van Mensvoort MEF, Bouma J. Contamination of surface water as affected by land use in acid sulfate soils in the Mekong River Delta, Vietnam. Agr. Ecosys. Env. 1997; 61: 19-27.

[33] Moore PA, Jr Attanandana T and Patrick WHJr. Factors affecting rice growth on acid sulfate soils. Soil Sci. Soc. Am. J., 1990; 54:1651-1656.

[34] Nelson DW, Sommers LE. Total carbon, organic carbon and organic matter. In: Methods of Soil Analysis. Part 2, Agron. Series 9. A.L. Page (ed.). Am. Soc. Agron. Publication Madison, WI, USA, 1982; pp. 539-579.

[35] Olsen SR, Cale CV, Watanabe, FS, Dean, L.A. Estimation of available phosphorus in soils by extraction with sodium bicarbonate. USDA Circ. 939, Washington, USA, 1954.

[36] Richards LA. Diagnosis and improvement of saline and alkali soils. In: USDA Handbook No. 60. US Govt. Print. Office, Washington, USA, 1954; pp. 84-156.

[37] Ritsema CJ, MEF, Van Mensvoort, DL Dent, Y, Tan H, Van Den-Bosch and ALM Van Wiji. Acid Sulfate Soils.p G121-154. *In* E.S. Malcome (Ed.) Hand Book of Soil Science, CRC Press, Washington D.C., 2000.

[38] Sheeran B Virosoil™ – An effective and lasting treatment for acid sulfate soils. Virotec. International Ltd. *www.virotec.com.,* 2003.

[39] Sterk, G. Leaching of acid from the top soils of raised beds on acid sulfate soils in Mekong Delta of Vietnam. Technical report no. (EEC project STD Vietnam, Department of Soil Science and Geology, WAU, Wageningen, The Netherlands, 1993.

[40] Takai Y, Vilarnsorn P, Stittbush C, Boonson A, Adachi T, Matsumoto S, Okazaki M, Sugi J. Soil amelioration trails in peat and acid sulfate soils. In Coastal low land ecosystems in the southern Thiland and Malaysia. Ed. K. Kyuma, et al. Publication By Showado Printing Co., Sakyku, Kyoto, Japan, 1992; pp. 318-335.

[41] Thawornwong N, van Diest A. Influence of high acidity and aluminum on the growth of low land rice. Plant Soil, 1974; 41: 141-159.

[42] Tri LQ, Nhan NV, Huizing HGJ, Van Mensvoort MEF. Present land use as basis for land evaluation in two Mekong Delta districts. In Selected Papers of the Ho Chi Minh City Symposium on Acid Sulfate Soils. (Eds.) DL Dent and MEF Van Mensvoort. ILRI (International Land Reclamation and Improvement) Publication no. 53, 1993; pp. 299–320.

[43] Van Breemen N. Environmental aspects of acid sulfate soils. In Proceedings of 4th International Symposium on Acid Sulfate Soils, ILRI (International Land Reclamation and Improvement), Wageningen, Publication no. 53, 1993; pp. 391-402.

[44] Van Breemen N, and Pons LJ. Acid sulfate soils and rice. In Soil and Rice. The International Rice Research Institute (IRRI), Los Banos, The Philippines, 1978; pp. 739-761.

[45] Van Breemen N. Genesis and solution chemistry of acid sulfate soils in Thailand. Centre for Agricultural Publishing and Documentation, Wageningen, The Netherlands, 1976.

[46] Van Breemen N. Calculation of ionic activities in natural water. Geochemistry Cosmochim , Acta 1973; 37: 101-107.

[47] Van Mensvoort MEF, Dent DL. Acid sulfate soils. Methods for assessment of soil degradation. R. Lal, et al. (eds.). Advances in Soil Science. CRC press LLC, Boca Raton, Flo. 1998; pp. 301-335.

[48] Zaman SMH, Rahman K, Howlader, M. Simple lessons from biometry. Publication no. 54, Bangladesh Rice Research Institute (BRRI), Gazipur, Bangladesh. 1982.

ISSN: 1545-1003

The Journal of American Science

Normal paper structure for the Journal of American Science:

Each manuscript is suggested to include the following components but authors can do their own ways:

(1) The complete article title.
(2) Each author's full name; institution(s) with which each author is affiliated, with city, state/province, zip code, and country; and the name, complete mailing address, telephone number, facsimile number (if available), and email address for all correspondence.
(3) **You must put at least one email address under the authors' address.**
(4) Abstract: including Background, Materials and Methods, Results, and Discussions, 100-300 words preferred.
(5) Key Words.
(6) Introduction.
(7) Materials and Methods.
(8) Results.
(9) Discussions.
(10) Acknowledgments.
(11) Correspondence to.
(12) References.

Description of Manuscript Preparation and Format:

(1) Software: Microsoft Word file.
(2) Font: Normal, Times New Roman, 10 pt, single space.
(3) Indent: 8 spaces in the beginning of each new paragraph.
(4) Manuscript: Don't use "Footnote" or "Header and Footer".
(5) Spelling check: Do spelling check when you finish.
(6) Color: Email and website addresses are blue, and all other contents are black.
(7) Abstract: 100-300 words are preferred, and remember to add "[The Journal of American Science. 2009;x(x):xx-xx]. (ISSN 1545-1003)" in the end of abstract.
(8) Page setup: Margins: top 72 pt, bottom 72 pt. left 72 pt, right 72 pt.
(9) Paper size: Letter, width 612 pt, height 792 pt.
(10) Layout: Header 36 pt, Foot 36 pt.
(11) Title: Use Title Case in the title and subtitles, e.g. "Debt and Agency Costs".
(12) Figures and Tables: Use full word of figure and table, e.g. "Figure 1. Annul Income of Different Groups", Table 1. Annual Increase of Investment".
(13) References: Cite 10-20 references preferred, by "last name, year", e.g. "(Smith, 2003)". References should include all the authors' last names and initials, title, journal, year, volume, issue, and pages etc.
(14) *Reference Examples*: Journal Article: Hacker J, Hentschel U, Dobrindt U. Prokaryotic chromosomes and disease. Science 2003;301(34):790-3.
(15) Book: Berkowitz BA, Katzung BG. Basic and clinical evaluation of new drugs. In: Katzung BG, ed. Basic and clinical pharmacology. Appleton & Lance Publisher. Norwalk, Connecticut, USA. 1995:60-9.
(16) Insert page number by bottom / center.
(17) Header for odd: Marsland Press Journal of American Science 2009;x(x):xx-xx.
(18) Header for even: short title Family name of the first author, et al.
(19) Footer: http://www.americanscience.org americansciencej@gmail.com.
(20) Submission Address: sciencepub@gmail.com, editor@sciencepub.net, Marsland Press, P.O. Box 21126, Lansing, Michigan 48909, The United States, 347-321-7172.

Design and Implementation of Efficient Information Retrieval Algorithm for Chest X-Ray Images

M. Shoaib,Usamn Ghani, Shazia,Kalsoom k. & Syed Khaldoon K.
Department of Computer Science & Engineering
University of Engineering and Technology
Lahore, Pakistan 54890.

shoaibuet@yahoo.com

Abstract: Separating the rib cages and lungs from other irrelevant structures in a given chest x-ray image is a major problem for the professionals of medical domain involved in chest x-rays. To provide an algorithm and automation solution for separating chest x-ray structures especially rib cages and lungs are the main focus of this thesis. An algorithm has been proposed using object recognition and template matching techniques of image processing domain. The results of the proposed solution have been verified for different chest x-ray images and it works with complete accuracy and efficiency. The proposed algorithm can be enhanced to accommodate the study of structures in chest x-ray image and report any inconsistencies. The Journal of American Science. 2009;5(4):43-48]. (ISSN 1545-1003)

Keywords: Image Processing, Computer vision, Gray Scale conversion, Threshold, Segmentation

1. Introduction

Medical related systems have been developed in industry to facilitate humans. In the early days of computer systems, the development of such systems was confined to research laboratories. Since then many systems have been developed in the industry. Many of them have been very successful, which has created a demand for development of such systems. However, many others have been less successful, and have never been taken into operation. An important reason for this is that the art of developing the Medical was not well understood and the other factor is of cost effectiveness.

The chest X-rays in the medical science for investigation and diagnoses of disease is very important. The medical doctors are being misled due to irrelevant structures present in the X-rays.
The focus of the thesis is to process chest x-ray images and differentiate its different parts. Main idea is separating the rib cages as they are of utmost importance. Rib cages are differentiated from lungs and any other data that may occur due to noise effectively and efficiently.
An algorithm has been proposed which separate the rib cages from other structures in four steps. The final structure produced by the algorithm is more readable and understandable for not only the doctors but also for the common man.

The rest of the paper is organized as follows; related work is discussed in section 2, section 3 describes our proposed methodology, section 4 is about results and discussions, then comes conclusion and at the end future recommendations and references are provided.

2. Related Work

An algorithm for the automatic detection of rib borders in chest radiographs is presented (Zhanjun Yue et al., 1995). According to the algorithm it first determines the thoracic cage boundary to restrict the area of search for the ribs. It then finds approximate rib borders using knowledge-based Hough transform. Finally, the algorithm localizes the rib borders using an active contour mode
Automatic detection of abnormalities in chest radiographs using local texture analysis is also presented (Bram Van Ginneken et al., 2002). This is a fully automatic method to detect abnormalities in frontal chest radiographs which are aggregated into an overall abnormality score.
Another algorithm for lung field segmentation in digital postero-anterio chest radiographs has been devised (Paola Campadelli and Elena Casiraghi). This is a lung field segmentation method, working on digital Postero-Anterior chest radiographs. The lung border is detected by

integrating the results obtained by two simple and classical edge detectors, thus exploiting their complementary advantages. The method makes no assumption regarding the chest position, size and orientation; it has been tested on a non-trivial set of real life cases, composed of 412 radiographs belonging to two different databases. An automatic segmentation of lung areas based on SNAKES and extraction of abnormal areas is also discussed (Yoshinori Itai1 et., al). It is a segmentation method for lung areas based on SNAKES without considering any manual operations. Furthermore, abnormal area including ground-glass opacity or lung cancer is classified by voxel density on the CT slice set. Experiment is performed employing nine thorax CT image sets and satisfactory results are obtained.

3. Proposed Methodology

3.1 Conversion of Image to gray-scale

The first step was to convert the image to gray scale. That's because, for the purposes of our processing, we only need to separate the solid regions of the rib cage from all other regions. For doing that, gray scale image is good enough. So by converting the image to gray scale, the processing time is reduced and a faster algorithm is produced. The proposed algorithm with reference to its implementation in MatLab works as under.

1:- The proposed algorithm will be given an image as input.

```
I =  imread (image path);
```

2:- As this image is expected to be present in colored form. So it is necessary to convert it into gray scale for low memory consumption and efficient processing

```
I = rgb2gray(I);
```

3.2 Histogram equalization

The second step performs histogram equalization.This is performed in order to spread the gray scale intensities in the image over the whole possible range of gray scale intensities. This helps the solid regions in the ribs become more prominent than the rest of the image and hence be detected easily. The process is performed in the following steps

1:- Peform histogram equalization

This process differentiate intensities of structures those are present in the image

```
I = histeq(I);
imshow(I);
pixval on;
```

2:- Getting the size of Image:

```
[y x]=size(I);
```

3.3 Threshold

Threshold is performed to separate the region spanned by the boundary of the ribs from the outer region. The process is carried out in the following steps.

1:- Getting the size of Image:

```
[y x]= size(I);
```

2:- Finding threshold and extracting boundaries of rib cages

```
for r=1:y
  for c=1:x
      if I(r,c) > 150
      I(r,c) = 0;
    end
    end
end
imshow(I);
pixval on;
```

3.4 Edge Dection:

If the pixel values change abruptly, consider it as a transition from lung to rib and vice versa. Now we have lugs and rig canes structures and they are not interconnected .The edges of images of lungs and rib cages are detected in this step. Then follows the most important step i.e. detecting the edges of the ribs. Since the intensity of the data at the edges changes frequently, use of a simple threshold function sufficed. If intensity of image changed abruptly from a lower gray scale value to a higher gray scale value, the algorithm recognizes it as the start of the rib-cage region and includes all the following pixels as the rib-cage, until the intensity changes abruptly from higher to lower gray scale value, which is recognized as the end of the rib region

```
max= 4;
min=-4;
maxflag=0;
IA=I;
IA=double(IA);
for c=1:x
  for r=1:y-1
((IA(r+1,c)-IA(r,c))>max &  maxflag ~= 1 )
      I(r,c)=0;
      maxflag=1;
```

```
          continue;
       end
if ( (IA(r+1,c)-IA(r,c))
 < min  & maxflag ~= 0 )
          maxflag=0;
          continue;
       end
    if maxflag==0
         IA(r,c)=0;
       end
                  end
end
IA=uint8(IA);
imshow(IA);
pixval on;
```

3.5 Local averages

It was recognized that gray scale intensity that represented solid region at one point in image represented a non solid region at some other point in the image. Hence the use of all previous techniques left some errors in the output. Finally, a step was used known as use of local averages. In this step, square blocks of some suitable size are used and moved over the whole image. In each block, average is taken

```
for ro=1:40:y-40
   for co=1:40:x-40
          for ri=ro:ro+39
         for ci=co:co+39
         sum=sum+I(ri,ci);
          end
       end
       average=sum / 1600;
       average =average + ( .6 * average );

       for ri=ro:ro+39
          for ci=co:co+39
          if I(ri,ci) == 0
                continue;
             end
        if  I(ri,ci) < average
                I(ri,ci)=0;
                else
                I(ri,ci)=255;
             end
         end
       end
sum = 0;
   end
end
I=uint8(I);
figure;
imshow(I);
pixval on;
```

over intensities of all pixels. This average represents the threshold. In this block, all the pixels below this threshold are set to zero, and ones above it are recognized as solid ribcage data.

```
for r=1:y
   for c=1:x
            if ( IA(r,c) > 0 & IB(r,c) > 0)
         I(r,c)=I(r,c);
        else
         I(r,c)=0;
    end
end
end
figure;
imshow(I);
pixval on;
```

3.6 Finding rib cages:

Move square blocks of empirical size over the image take average gray level in these block the ribs should be ones above the gray level

```
I=double(I);
sum=0;
average=0;
```

3.7 Removing noise pixels:

Check the neighbors of a white pixel if any of them is black, then the current pixel is one of the noise pixels

```
IC=I;

for r=2:y-1
   for c=2:x-1

      if IC(r,c)==255

         if ( IC(r,c+1)==0 | IC(r,c-1)==0 )
               I(r,c)=0;
         end

     end
    end
end
imshow(I);
pixval on;
```

3.8 Making Regions clearer:

Grow regions and delete those who are smaller than 4

```
 counter=0;
```

```
for r=1:y
  for c=1:x
      if ( I(r,c) == 254 )
         continue;
      end
     if ( I(r,c) > 0)
         [I counter]=mark4(I, r, c, counter);
      end
      if ( counter > 0 && counter < 4)
         counter=0;
         [I counter]=mark_black4(I, r, c, counter);
      end
       counter=0; end
end
figure; imshow(I); pixval on;
```

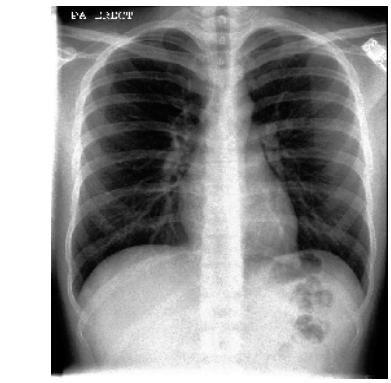

Figure 1: Original Image

This is the image on which I will apply my algorithm to find out rib cages from this image. It can be easily downloaded from Internet or can be obtained by scanning the real chest x-ray image. This image has rib cages, lungs and other structures due to noise. My algorithm will separate lung cages from this image. My ribs become more prominent than the rest of the image and hence are detected easily.

4. Results and Discussions

The above-mentioned procedure produces results that work for 80% images. The benefit of using this procedure is that its very simple and fast to implement and execute. It does not involve any complicated mathematical analysis etc. which are very typical in image processing applications. Hence, this algorithm is better than many others that perform the same job, because of its simplicity and low complexity and fast execution. Our proposed algorithm is explained using figures below.

Figure 2: Performing Histogram Equalization

The gray scale intensities in the image are spread over the whole possible range of gray scale intensities. This helps the solid regions in the ribs become more prominent than the rest of the image and hence be detected easily

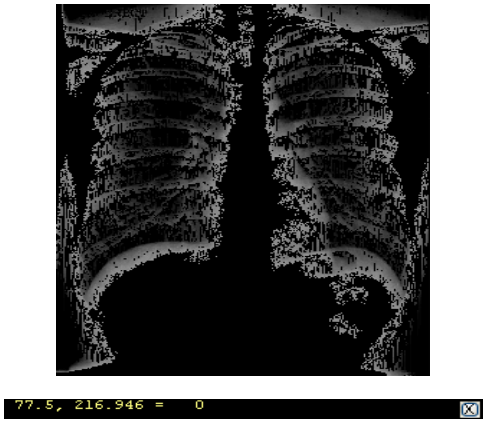

Figure 3: Applying Threshold

Threshold is performed to separate the region spanned by the boundary of the ribs from the outer region.

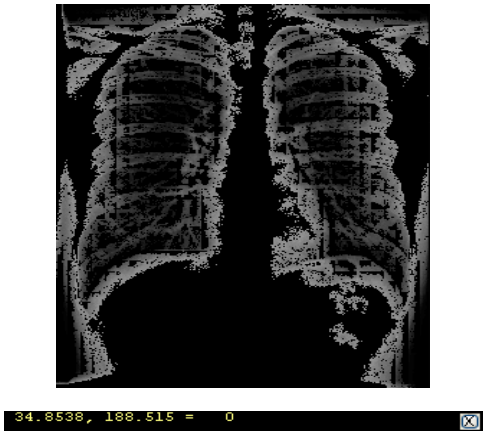

Figure 4: Getting transitions from lung to rib & vice versa

Detecting the edges of the ribs. If intensity of image changed abruptly from a lower gray scale value to a higher gray scale value, the algorithm recognizes it as the start of the rib-cage region and includes all the following pixels as the rib-cage, until the intensity changes abruptly from higher to lower gray scale value, which is recognized as the end of the rib region.

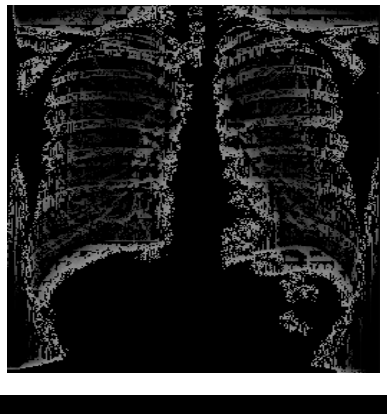

Figure 5: Getting the rib cages

Square blocks of some suitable size are used and moved over the whole image. In each block, average is taken over intensities of all pixels. This average represents the threshold. In this block, all the pixels below this threshold are set to zero, and ones above it are recognized as solid ribcage data.

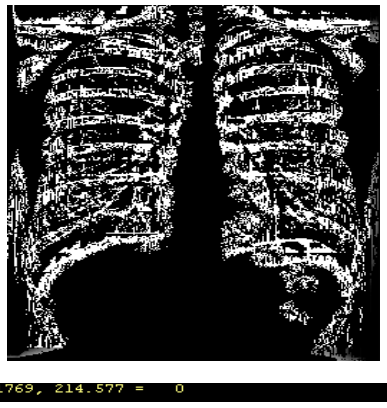

Figure 6: Change color of pixels to white

The color of rib cages is set to white to enhance vision. It is clearer now as it can be seen in the figure.

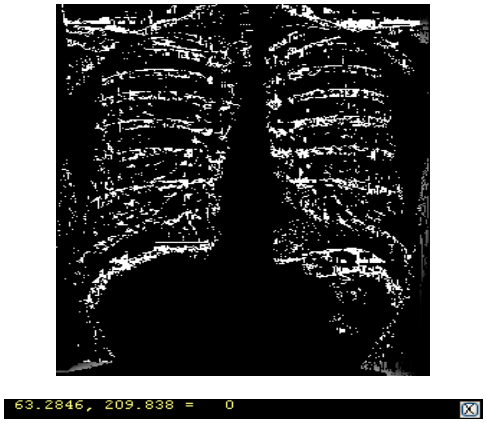

Figure 7: Finally finding the rib cages

The final shape of rib cages is much clearer now as can be seen in the figure. The final image depicts clearly the structure of rib cages and any inconsistencies that may be present in the rib cage structure.

5. Conclusion

Refined information retrieval in Chest x-ray images is the main focus of our research. We have developed a simple and efficient algorithm, which separates rib cages and lungs from other structures in chest, x-rays. The algorithm is based on much simpler concepts of image processing naming grey scale conversion, histogram equalization, finding threshold, edge detection, finding local averages, finding rib cages and finally removing irrelevant data.

6. Future Recommendations

The presented algorithm can be indulged to develop an online expert system for diagnosis of chest x-ray diseases. The system can be used to study structures in chest x-rays and report any inconsistencies. Expert system can study the structures and devise proper diagnosis for diseases and inconsistencies.

Correspondence to:

Dr. Muhammad Shoaib, Associate Professor
Department of Computer Science & Engineering
University of Engineering and Technology
Lahore, Pakistan 54890.
Email: shoaibuet@yahoo.com

References

[1]Zhanjun Yue, Ardeshir Goshtasby, "Automatic Detection of Rib Borders in Chest Radiographs", IEEE Transactions on Medical Imaging, VOL. 14, NO. 3, September 1995, Pp 525.

[2]IEEE Transactions On Medical Imaging, Vol. 21, No. 2, February 2002 139Automatic Detection of Abnormalities in Chest Radiographs Using Local Texture Analysis

[3]Paola Campadelli and Elena Casiraghi, Lung Field Segmentation in Digital Postero Anterior Chest Radiographs Universit`a degli Studi di Milano,Computer Science Department, LAIV Laboratory

[4]Yoshinori Itai1, Hyoungseop Kim1, Katsuragawa2, MemberAkiyoshi Yamamoto4 Kyushu Institute of Technology, Department of Control Eng., 1-1, Sensui-cho Tobata,Kitakyushu 804-8550, Japan

[5]G. A. Johnson and C. E. Ravin, "A survey of digital chest radiography," Radiol. Clin. North Amer., vol. 21, pp. 655-665, 1983.

[6]G. Revesz and H. L. Kundel, "Psychophysical studies of detection errors in chest radiology," Radiol., vol. 123, pp. 559-562, 1977.

[7]H. L. Kundel and G. Revesz, "Conspicuity effects in chest radiography," in Proc. Symp. Optimiz. Chest Radiog., 1979, pp. 16-21.

[8]H. L. Kundel, G. Revesz, and L. Toto, "Contrast gradient and the detection of lung nodules," Invest. Radiol., vol. 14, pp. 18-22, 1979.

[9]G. A. Johnson, N. Danieley, and C. E. Ravin, "Processing alternatives for digital chest imaging," Radiol. Clin. North Amer., vol. 23.

[10]R. H. Sherrier and G. A. Johnson, "Regionally adaptive histogram equalization of the chest," IEEE Trans. Med. Imaging, vol. MI-6,pp. 1-7, 1987.

[11]L. Sider, Ed., Introduction to Diagnostic Imaging. New York: Churchill Livingstone, 1986.C. B. Rabin and M. G. Baron, Radiology of the Chest. Baltimore, MD: Waverly, 1980.

[12]D. H. Ballard, Hierarchic Recognition of Tumors in Chest Radiographs with Computer. New York: Birkhauser Verlag, 1976.

Model for Predicting the Concentration of Sulphur Removed During Temperature Enhanced Oxidation of Iron Oxide Ore

Chukwuka Ikechukwu Nwoye*[1], Stanley Ofoegbu[2], Uchenna Nwoye[3], Stanley Inyama[4], Hilary Eke[1]
Cajetan Nlebedim[5]

1 Department of Materials and Metallurgical Engineering Federal University of Technology, P.M.B 1526 Owerri, Nigeria.
2 Department of Materials Science, AveiroUniversity Portugal.
3 Data Processing, Modelling and Simulation Unit, Weatherford Nig. Ltd. Port-Harcourt Nigeria.
4 Department of Industrial Mathematics, Federal University of Technology, P.M.B 1526 Owerri, Nigeria
5 Department of Materials Science, University of Cadiff, Wales, United Kingdom.
chikeyn@yahoo.com

Abstract: Model for predicting the concentration of sulphur removed during temperature enhanced oxidation of iron oxide ore has been derived. The model;

$$\%S = \left(\frac{0.1011}{\text{LogT}}\right)$$

was found to predict the concentration of sulphur removed, very close to the corresponding %S values obtained from the actual experimental process. It was found that the model is dependent on the values of the treatment temperature used during the desulphurization process. The validity of the model is believed to be rooted in the expression $[(T)^{\gamma\%S}] = \alpha/k_n$ where both sides of the relationship are correspondingly almost equal. The positive or negative deviation of each of the model-predicted values of %S from those of the corresponding experimental values was found to be less than 37% which is quite within the range of acceptable deviation limit of experimental results, hence showing the validity and usefulness of the model for predictive analysis.
[Journal of American Science 2009;5(4):49-54]. (ISSN: 1545-1003).

Keywords: Model, Prediction, Sulphur Removed, Oxidation, Temperature, Iron Oxide Ore.

1. Introduction

Agbaja iron ore deposit is the largest known Nigerian iron ore deposit estimated at 1250 metric tonnes of ore reserve. It consists of oolitic and pisolitic structures rich in iron oxides, in a matrix that is predominantly clay.The principal constituent mineral is goethite, with minor hematite, maghemite, siderite, quartz, kaolinite pyrite and an average of 0.09%S (Uwadiele,1984).

An intensive and selective oil agglomeration of Agbaja iron ore has been carried out (Uwadiele, 1990). The researcher, starting from the crude ore Fe content (45.6%), concentrated the ore by oil agglomeration technique to 90% Fe recovery and 65% Fe assay. He stated that the ore require grinding to minus 5µm to effect adequate liberation. These results were obtained at optimum pH 9. Successful studies on the effect of temperature on magnetizing reduction of Agbaja iron ore have been carried out (Uwadiele and Whewell, 1988). The results of the investigation showed that the fine-grained oolitic Agbaja iron ore, which is not responsive to conventional processing techniques, can be upgraded by the magnetizing reduction method with an Fe recovery of 87.3% and Fe assay of 60% at 600^0C.

Attempt has been made to enhance concentrate Fe recovery (Kulkarni and Somasundaran, 1980). The researchers stated that concentrate Fe recovery decreases progressively below pH 8. In this pH region, oleate used is present as dispersion of oleic acid, and its adsorption on the surface of the iron oxides is similar to the process of hetero-coagulation involving positively charged iron oxide particles and negatively charged oleic acid droplet.

Agbaja oolitic iron ore, which has not been responsive to so many upgrading processes, has been upgraded to 73.4% Fe assay (starting from as-received concentrate assaying 56.2%Fe) by under taking a process referred to as pyrometallurgical-oxidation method (Nwoye,2008). Main parameters investigated were the effects of treatment temperature and oxidant ($KClO_3$) on the upgrading process. It was established that 800^0C is the optimum temperature for the upgrading step considering the range of temperature used (500-800^0C). It was observed from results of the investigation that both oxidant and temperature increase (up to 12g per 50g of iron ore and maximum of 800^0C respectively) during the process are vital conditions for improving on the grade of the ore concentrate.

Nwoye et al (2009) derived a model for computational analysis of the concentration of iron upgraded during dry beneficiation of iron oxide ore.

The model;

$$\%Fe = 2.25[(\ln (T/\mu))^{2.58}] \quad (1)$$

shows that the concentration of upgraded iron is dependent on the treatment temperature T, used when the mass of iron oxide ore μ, added is constant.

Nwoye (2008) carried out desulphurization of Agbaja iron oxide ore concentrate using solid potassium trioxochlorate (V) ($KClO_3$) as oxidant. The concentrate was treated at a temperature range 500 – 800^0C. The results of the investigation revealed that simultaneous increase in both the percentage of the oxidant added (up to 15g per 50g of ore) and treatment temperature (maximum 800^0C) used give the ideal conditions for increased desulphurization efficiency. This translates into high desulphurization efficiency when both oxidant concentration (up to 15g per 50g of ore) and treatment temperature (maximum 800^0C) are high.

The mechanism and process analysis of desulphurization of Agbaja iron ore concentrate using powdered potassium trioxochlorate (v) ($KClO_3$) as oxidant has been reported (Nwoye, 2009). Concentrates were treated at a temperature range 500 – 800^0C. Results of the process analysis indicate that oxygen required for the desulphurization process was produced following decomposition of $KClO_3$ within a temperature range 375-502^{o}C. It was observed that this temperature range is the Gas Evolution Temperature Range (GETR) for sulphur present in Agbaja iron ore. Sulphur vapour and oxygen gas produced at this temperature range were believed to have reacted to form and liberate SO_2. The process analysis suggests that the mechanism of the desulphurization process involves gaseous state interaction between oxygen and sulphur through molecular combination. The results for the extent of desulphurization reveal that simultaneous increase in both the percentage of the oxidant added and treatment temperature used (up to 15g $KClO_3$ per 50g of ore and maximum of 800^0C respectively) are the ideal conditions for the best desulphurization efficiency.

Investigations made by Bardenheuer and Geller (1934) indicated that the sulphur transfer from metal to slag or slag to gas during desulphurization involves oxygen transfer in the opposite direction. They posited that the mechanism of such desulphurization involves oxidation of sulphur resident in the metal or slag by oxygen from the slag through ionic exchange between the oxygen and sulphur, since the whole system is made up of liquid/molten condition during this process.They maintained that oxygen in the slag comes from CaO, which is one of the products of decomposition of $CaCO_3$ deposited into the slag as a slag forming agent.

St Pierre and Chipman (1956), on studying gas-slag system during iron making discovered that at oxygen partial pressure below about 10^{-5} atm., sulphur dissolves in the melt as sulphide ions; at oxygen partial pressure higher than 10^{-3} atm., sulphur enters the melt as sulphate ions. In both cases, they stated that both the sulphide and sulphate ions leave the furnace through the slag. They therefore concluded that the mechanism of such desulphurization process is oxidation of sulphur by oxygen from the slag through ionic exchange between the two participating elements.

It was found by Turkdogan and Darken (1961) that at a temperature well below about 1600^0C, the pyrosulphate reaction also occurs. They found that this reaction was an enhancement to the desulphurization process actually taking place in the furnace. Also oxygen for this process was found to come from the slag, engaging sulphur in ionic exchange; being the mechanism of such process.

It was discovered that one of the most important factors influencing the desulphurization process during iron making is the state of oxidation of the bath (Pehlke et.al 1975) .

Nwoye et al. (2009) derived a model for the predictive analysis of the concentration of sulphur removed as result of the molecular-oxygen-induced desulphurization of iron oxide ore (potassium chlorate being the oxidant). The model;

$$\%S = \left(\frac{0.0415}{\text{Log } \gamma}\right) \quad (2)$$

was found to predict the concentration of sulphur removed, very close to the corresponding %S values obtained from the actual experimental process. It was found that the model is dependent on the values of the weight-input of the oxidant γ, ($KClO_3$) during the desulphurization process. The validity of the model is believed to be rooted in the expression $k_n[(\gamma)^{\mu\%S}] = T/\alpha$ where both sides of the expression are correspondingly almost equal. The positive or negative deviation of each of the model-predicted values of %S from those of the corresponding experimental values was found to be less than 33% which is quite within the range of acceptable deviation limit of experimental results.

Nwoye et al (2009) derived a model for computational analysis of the concentration of sulphur removed during oxidation of iron oxide ore by powdered potassium chlorate. The model;

$$\%S = \left(\frac{0.0357}{\text{Log } \alpha}\right) \quad (3)$$

indicates that the predicted %S is dependent on the weight-input of $KClO_3$ α, added during the desulphurization process. The maximum deviation of the model-predicted values of %S from those of the corresponding experimental values was found to be less than 37%

Model for predicting the concentration of sulphur removed during gaseous desulphurization of iron oxide ore has been derived by Nwoye et al. (2009). The model;

$$\%S = \left(\frac{0.0745}{\text{LogT}} \right) \quad (4)$$

shows that the predicted %S is dependent on the treatment temperature T, used during the desulphurization process.

The aim of this work is to derive a model for predicting the concentration of sulphur removed during temperature enhanced oxidation of Agbaja (Nigerian) iron oxide ore

2. Model

The solid phase (ore) is assumed to be stationary, contains some unreduced iron remaining in the ore. It was found (Nwoye, 2008) that oxygen gas from the decomposition of $KClO_3$ attacked the ore in a gas-solid reaction, hence removing (through oxidation) the sulphur present in the ore in the form of SO_2 .Equations (5) and (6) show this.

$$2KClO_{3\,(s)} \longrightarrow 2KCl_{\,(s)} + 3O_{2\,(g)} \quad (5)$$

$$S_{(s)} \xrightarrow{\text{Heat}} S_{(g)} + O_{2\,(g)} \longrightarrow SO_{2\,(g)} \quad (6)$$

2.1 Model Formulation

Experimental data obtained from research work (Nwoye,2007) carried out at SynchroWell Research Laboratory, Enugu were used for this work. Results of the experiment as presented in report (Nwoye, 2007) and used for the model formulation are as shown in Table 1.

Computational analysis of the experimental data shown in Table 1, gave rise to Table 2 which indicate that;

$$[(T)^{\gamma\%S}] = \alpha/k_n \quad \text{(approximately)} \quad (7)$$

$$k_n [(T)^{\gamma\%S}] = \alpha \quad (8)$$

Taking logarithim of both sides

$$\text{Log}\,(k_n[(T)^{\gamma\%S}]) = \text{Log}\,\alpha \quad (9)$$

$$\text{Log}k_n + \text{Log}\,[(T)^{\gamma\%S}]) = \text{Log}\,\alpha \quad (10)$$

$$\text{Log}k_n + \gamma\,\%S\text{LogT} = \text{Log}\,\alpha \quad (11)$$

$$\gamma\%S\text{LogT} = \text{Log}\alpha - \text{Log}\,k_n \quad (12)$$

$$\%S = \frac{\text{Log}\alpha - \text{Log}k_n}{\gamma\,\text{LogT}} \quad (13)$$

Introducing the values of α , k_n and γ into equation (13) (since the are constants) and evaluating further, reduces it to;

$$\%S = \frac{0.1011}{\text{LogT}} \quad (14)$$

Therefore

$$\%S = \frac{D_f}{\text{LogT}} \quad (15)$$

Where

%S = Concentration of sulphur removed during the pyrometallurgical-oxidation process.

k_n = 8.30 (Decomposition coefficient of $KClO_3$ relative to its weight input (10g per 50g of the iron ore) determined in the experiment (Nwoye,2007)

(γ)= 0.8 (Temperature coefficient relative to weight-input of $KClO_3$) determined in the experiment (Nwoye,2007)

(α) = Weight of $KClO_3$ added as oxidant (g)

T = Treatment temperature used for the process (^{0}C)

D_f =0.1011 (Assumed desulphurization enhancement factor)

Table 1: Variation of concentration of sulphur removed with treatment temperature (Nwoye,2007)

T (^{0}C)	M	%S
500	50	0.030
550	50	0.035
600	50	0.040
650	50	0.043
700	50	0.050
750	50	0.055

Table 2: Variation of α/k_n with $T^{\gamma\%S}$

α/k_n	$T^{\gamma\%S}$
1.2048	1.1608
1.2048	1.1932
1.2048	1.2272
1.2048	1.2496
1.2048	1.2996
1.2048	1.3381

3. Boundary and Initial Condition

Consider iron ore (in a furnace) mixed with potassium chlorate (oxidant). The furnace atmosphere is not contaminated i.e (free of unwanted gases and dusts). Initially, atmospheric levels of oxygen are assumed just before the decomposition of $KClO_3$ (due to air in the furnace).Weight, M of iron oxide ore used; (50g), and treatment time; 360secs. were used. Treatment temperature range; 500-750^{o}C, ore grain size; 150µm, and weight of $KClO_3$ (oxidant); 10g were also used. These and other process conditions are as stated in the experimental technique (Nwoye, 2007).

The boundary conditions are: furnace oxygen atmosphere due to decomposition of $KClO_3$ (since the furnace was air-tight closed) at the top and bottom of the ore particles interacting with the gas phase. At the bottom of the particles, a zero gradient for the gas scalar are assumed and also for the gas phase at the top of the particles. The reduced iron is stationary. The sides of the particles are taken to be symmetries.

4. Model Validation

The formulated model was validated by direct analysis and comparison of %S values predicted by the model and those obtained from the experiment for equality or near equality.

Analysis and comparison between these %S values reveal deviations of model-predicted %S values from those of the experiment. This is attributed to the fact that the surface properties of the ore and the

physiochemical interactions between the ore and the oxidant (under the influence of the treatment temperature) which were found to have played vital roles during the oxidation process (Nwoye, 2007) were not considered during the model formulation. This necessitated the introduction of correction factor, to bring the model-predicted %S values to those of the experimental %S values (Table 3).

Deviation (Dv) (%) of model-predicted %S values from experimental %S values is given by

$$Dv = \left(\frac{Dp - DE}{DE}\right) \times 100 \qquad (16)$$

Where Dp = Predicted %S values from model
DE = Experimental %S values

Correction factor (Cf) is the negative of the deviation i.e

$$Cf = -Dv \qquad (17)$$

Therefore

$$Cf = -\left(\frac{Dp - DE}{DE}\right) \times 100 \qquad (18)$$

Introduction of the corresponding values of Cf from equation (18) into the model gives exactly the corresponding experimental %S values (Nwoye, 2007).

5. Results and Discussion

The derived model is equation (14) or (15). A comparison of the values of %S from the experiment and those from the model shows minimum positive and negative deviations less than 37% which is quite within the acceptable deviation limit of experimental results hence depicting the reliability and validity of the model. This is shown in Table 3.

The validity of the model is believed to be rooted in equation (7) where both sides of the equation are correspondingly almost equal.

Table 2 also agrees with equation (7) following the values α/k_n and $T^{\gamma\%S}$ evaluated from Table 1 as a result of corresponding computational analysis. The value 0.1011 has a direct relationship with the value of %S as shown in equation (14). This indicates that the constant contributes directly (as a multiplying factor) to the predicted concentration of sulphur removed from the ore. Based on the foregoing, the constant is denoted as desulphurization enhancement factor D_f

Table 3: Comparison between %S removed as predicted by model and as obtained from experiment. (Nwoye ,2007)

$\%S_{exp}$	$\%S_M$	Dv (%)	Cf (%)
0.030	0.0375	+25.00	-25.00
0.035	0.0369	+5.43	-5.43
0.040	0.0364	-9.00	+9.00
0.043	0.0360	-16.28	+16.28
0.050	0.0355	-29.00	+29.00
0.055	0.0352	-36.00	+36.00

Where
$\%S_{exp}$ = %S values from experiment (Nwoye,2007)
$\%S_M$ = %S values predicted by model

6. Conclusion

The model predicts the concentration of sulphur removed during temperature enhanced oxidation of Agbaja iron oxide ore. The validity of the model is believed to be rooted in equation (7) where both sides of the equation are correspondingly almost equal. The deviation of the model-predicted %S values from those of the experiment is less than 37% which is quite within the acceptable deviation limit of experimental results.

Further works should incorporate more process parameters into the model with the aim of reducing the deviations of the model-predicted %S values from those of the experiment

Acknowledgement

The authors thank Dr. Ekeme Udoh, a modelling expert at Linkwell Modelling Centre Calabar for his technical inputs. The management of SynchroWell Nig. Ltd. Enugu is also appreciated for permitting and providing the experimental data used in this work.

Correspondence to:
Chukwuka Ikechukwu Nwoye
Department of Materials and Metallurgical Engineering, Federal University of Technology,
P.M.B 1526 Owerri. Imo State, Nigeria.
Cellular phone: 0803 800 6092
Email: chikeyn@yahoo.com

References

[1]Uwadiele GGOO. Beneficiation Studies of Agbaja Iron Ore. Ph.D Thesis,Univerity of Strathdyde 1984.
[2]Uwadiele GGOO. Selective Oil Agglomeration of Agbaja Iron Ore. Metallurgical Transaction B 1990: 20a: 23.
[3]Uwadiele GGOO, Whewell RJ. (1988) Effect of Temperature on magnetizing Reduction of Agbaja Iron ore; Metallurgical Transaction B 1988: 19b: 3.
[4]Kulkarni KE, Somasundaran DU. Effect of pH on the Concentrate Iron Recovery Using Oleate Solution ,Metallurgical Transaction B 1980: 18b:30.
[5]Nwoye CI. Upgrading of Agbaja Iron Oxide Ore Concentrate by Pyrox Method. JMME 2008: 3(1): 14-16.
[6]Nwoye CI, Mbuka IE, Menkiti M, Nwoye CC, Nnuka E, Onyemaobi OO. Model for Computational Analysis of the Concentration of Iron Upgraded during Dry Beneficiation of Iron Oxide Ore, Journal of Advances in Science and Technology (in press)

[7]Nwoye CI. Gaseous Desulphrization of Agbaja Iron Ore Concentrate. Journal of Engineering and Applied Sciences 2008:3(1,2): 72-75.
[8]Nwoye CI. Process Analysis and Mechanism of Desulphurization of Agbaja Iron Oxide Ore. JMME 2009: 8: 27-32.
[9]Bardenheuer P, Geller, W. Kais. Wilh. Inst., Eisenforsch 1934: 16:77- 91.
[10]St.Pierre GR, Chipman J. Trans. AIME 1956: 206:1474-83.
[11]Turkdogan ET, Darken LS. Trans. Met. Soc. AIME 1961: 221:464-74.
[12]Pehlke RD, Porter WF, Urban RF, Gaines JM. BOF, Steel Making, Iron &Steel Soc. AIME 1975: 2:142- 153.
[13] Nwoye CI, Anyakwo CN, Nwoye CU, Inyama S, Ejimofor R, Nwakwuo CC. Model for Predictive Analysis of the Concentration of Sulphur Removed by Molecular-Oxygen-Induced Desulphurization of Iron Oxide Ore, Journal of Nature and Science 2009: 7(3):36-40.
[14]Nwoye CI, Lee SO, Nwoye CU, Obi MC, Onuoha E, Trans T. Model for Computational Analysis of the Concentration of Sulphur Removed during Oxidation of Iron Oxide Ore by Powdered Potassium Chlorate, Journal of Advances in Science and Technology 2009: 3(1):45-49.
[15] Nwoye CI, Nwakwuo CC, Nwoye CU, Onugha E, Obiji S, Mbuka IE, Obasi GC. Model for Predicting the Concentration of Sulphur Removed during Gaseous State Desulphurization of Iron Oxide Ore, Journal of Engineering and Earth Sciences (in press)
[16]Nwoye CI. SynchroWell Research Work Report, DFM Unit,No 2007146, 2007: 35-45.

ISSN: 1545-1003

The Journal of American Science

Normal paper structure for the Journal of American Science:

Each manuscript is suggested to include the following components but authors can do their own ways:

(1) The complete article title.
(2) Each author's full name; institution(s) with which each author is affiliated, with city, state/province, zip code, and country; and the name, complete mailing address, telephone number, facsimile number (if available), and email address for all correspondence.
(3) **You must put at least one email address under the authors' address.**
(4) Abstract: including Background, Materials and Methods, Results, and Discussions, 100-300 words preferred.
(5) Key Words.
(6) Introduction.
(7) Materials and Methods.
(8) Results.
(9) Discussions.
(10) Acknowledgments.
(11) Correspondence to.
(12) References.

Description of Manuscript Preparation and Format:

(1) Software: Microsoft Word file.
(2) Font: Normal, Times New Roman, 10 pt, single space.
(3) Indent: 8 spaces in the beginning of each new paragraph.
(4) Manuscript: Don't use "Footnote" or "Header and Footer".
(5) Spelling check: Do spelling check when you finish.
(6) Color: Email and website addresses are blue, and all other contents are black.
(7) Abstract: 100-300 words are preferred, and remember to add "[The Journal of American Science. 2009;x(x):xx-xx]. (ISSN 1545-1003)" in the end of abstract.
(8) Page setup: Margins: top 72 pt, bottom 72 pt. left 72 pt, right 72 pt.
(9) Paper size: Letter, width 612 pt, height 792 pt.
(10) Layout: Header 36 pt, Foot 36 pt.
(11) Title: Use Title Case in the title and subtitles, e.g. "Debt and Agency Costs".
(12) Figures and Tables: Use full word of figure and table, e.g. "Figure 1. Annul Income of Different Groups", Table 1. Annual Increase of Investment".
(13) References: Cite 10-20 references preferred, by "last name, year", e.g. "(Smith, 2003)". References should include all the authors' last names and initials, title, journal, year, volume, issue, and pages etc.
(14) *Reference Examples*: Journal Article: Hacker J, Hentschel U, Dobrindt U. Prokaryotic chromosomes and disease. Science 2003;301(34):790-3.
(15) Book: Berkowitz BA, Katzung BG. Basic and clinical evaluation of new drugs. In: Katzung BG, ed. Basic and clinical pharmacology. Appleton & Lance Publisher. Norwalk, Connecticut, USA. 1995:60-9.
(16) Insert page number by bottom / center.
(17) Header for odd: Marsland Press Journal of American Science 2009;x(x):xx-xx.
(18) Header for even: short title Family name of the first author, et al.
(19) Footer: http://www.americanscience.org americansciencej@gmail.com.
(20) Submission Address: sciencepub@gmail.com, editor@sciencepub.net, Marsland Press, P.O. Box 21126, Lansing, Michigan 48909, The United States, 347-321-7172.

6/2/2009

Epidemiology of Chlamydia Bacteria Infections - A Review

Adetunde, I.A. [1,*], Koduah, M. [1], Amporful, J.K [1], Dwummoh – Sarpong, A. [1], Nyarko, P.K. [1], Ennin, C.C. [1], Appiah, S.T. [1], Oladejo, N. [2]

1. University of Mines and Technology, Dept. of Mathematics, P. O. Box 237, Tarkwa, Ghana.
2. University for Development Studies, Dept. of Mathematics and Computer Science, P. O. Box 24, Navrongo, Ghana

adetunde@gmail.com,mkoduah@umat.edu.gh,stappiah@umat.edu.gh, iadetunde@umat.edu.gh,jkampoful@umat.edu.gh,adwummoh-sarpong@umat.edu.gh,ccennin@umat.edu.gh, pknyarko@umat.edu.gh, oladejonath@yahoo.com

Abstract: In this paper we study the Chlamydia Bacteria Infections. The authors especially try to find the effect of these bacteria infections in human beings. We reviewed the existing models and outlined what Chlamydia causes. [Journal of American Science 2009; 5(4):55-64]. (ISSN: 1545-1003).

Keywords: Chlamydia, *Chlamydia trachomatis*, Sexually transmitted diseases (STDs), *pelvic inflammatory disease* (PID), epididymitis, lymphogranuloma venereum, proctitis

1. Introduction

A lot of work has been reported dealing with Chlamydia. Relevant publications are Thylefors et al., (1995); Ward (1995); Aldous et al., (1992); Campbell and Kuo, (2003); Mathews et al.,(1999); Shaw et al., (2000); Hsia et al., (1997); Fields and Hackstadt (2000); Fields et al.,(2003); Rockey and Matsumoto,(1999); Beagley and Timms, (200); Wilson et al., (2003); (2004); Yang and Brunham, (1998); Dreses – Werringloer et al., (2001) and Magee et al.,(1995) to mention but a few .

Chlamydia is a sexually transmitted disease caused by an organism called *Chlamydia trachomatis*, which is considered to be a type of bacteria. The National Institute of Allergy and Infectious Diseases estimate that the cost of Chlamydia infections and subsequent complications exceeds $2 billion annually.

Sexually transmitted diseases (STDs) are among the most common infectious diseases in the United States today, affecting more than 13 million men and women annually. Among the more than 20 STDs that have now been identified, chlamydia is the most frequently reported, with an estimated 4 million new cases each year. In Illinois, there were 50,559 cases of chlamydia reported in 2005. Most of these cases--71 percent--occurred among persons 15- to 24-years-old.

Chlamydia is known as a "silent" disease because 75 percent of infected women and at least half of infected men have no symptoms. If symptoms do occur, they usually appear within 1 to 3 weeks of exposure. Symptoms, if any, might include an abnormal vaginal discharge or a burning sensation when urinating. The infection is often not diagnosed or treated until there are complications.

The infection first attacks the cervix and urethra. The infection spreads from the cells of cervix to the uterus, to fallopian tubes, ovaries and cause *pelvic inflammatory disease* (PID). Some women may still have no signs or symptoms, which is why it is often transmitted from one sexual partner to another without either knowing. However, if they do have symptoms, they might have lower abdominal pain, pain in the lower pelvic region, low back pain, nausea, fever, pain during sex, pain on passing urine, frequency passing urine, bleeding between menstrual periods and an examination may show a yellowish pussy inflammation of the cervix. Women are often reinfected, meaning they get the STD again, if their sex partners are not treated. Reinfections place women at higher risk for serious reproductive health complications, including infertility. If untreated, chlamydia infection can cause serious reproductive and other health problems. Like the disease itself, the damage that chlamydia causes is often "silent", that is *pelvic inflammatory disease* (PID). This happens in up to 40 percent of women with untreated chlamydia. PID can cause:

- **Infertility.** This is the inability to get pregnant. The infection scars the fallopian tubes, keeping eggs from being fertilized.
- **An ectopic or tubal pregnancy.** This means that a fertilized egg starts developing in the fallopian tube instead of moving into the uterus. This is a dangerous condition that can be deadly to the woman.
- **Chronic pelvic pain.** Pain that is ongoing, usually from scar tissue.

Women who have chlamydia may also be more likely to get HIV, the virus that causes AIDS, from a person who is infected with HIV. Because of the symptoms associated with chlamydia, infected individuals have a three- to five-fold increase in the risk of acquiring HIV (the virus that causes AIDS) if exposed to the virus during sexual intercourse. In people having anal sex with a partner who has chlamydia, the bacteria can cause proctitis, which is an infection of the lining of the rectum. The bacteria causing chlamydia infections can also be found in the throats of people who have oral sex.

In pregnant women, chlamydia infections may lead to premature delivery. Babies born to infected mothers can get infections in their eyes, called conjunctivitis or pinkeye, as well as pneumonia. Symptoms of conjunctivitis include discharge from the eyes and swollen eyelids, usually showing up within the first 10 days of life. Symptoms of pneumonia are a cough that steadily gets worse and congestion, usually showing up within three to six weeks of birth.

Men with symptoms might have a discharge from the penis and a burning sensation when urinating which may range from clear to pussy. Men might also have burning and itching around the opening of the penis or pain and swelling in the testicles/scrotum, or both.This can be a sign of epididymitis, an inflammation of a part of the male reproductive system located in the testicles. Both PID and epididymitis can result in infertility.

Untreated chlamydia in men typically causes infection of the urethra, the tube that carries urine from the body. Infection sometimes spreads to the tube that carries sperm from the testis. This may cause pain, fever, and even infertility.

Other complications include proctitis (inflamed rectum) and conjunctivitis (inflammation of the lining of the eye). A particular strain of chlamydia causes another STD called lymphogranuloma venereum, which is characterized by prominent swelling and inflammation of the lymph nodes in the groin.

Despite the availability of publications on the subject matter, very little had been done on the Chlamydia in developing Countries. Most recently Walraven et al., (2001) emphasized on the burden of reproductive - organ disease in rural women in The Gambia, West Africa. It was recently that Jorn et al., (2008) worked on Chlamydia trachomatis infection as a risk factor for infertility among women in Ghana, this is the first study that investigated the association between C. trachomatis infection and infertility among women in Ghana. In developing countries, data about the prevalence of Chlamydia bacterial infections and their complication, such as infertility, is very scarce because of the fact that reliability test assays are too expensive and too complex for routine use in resource – limited settings.

2 Classification of Chlamydia

Chlamydia is small Gram-negative cocci and is intracellular parasites. All three species; psittaci, pneumoniae, and trachomatis can cause respiratory tract infections. C psittaci and pneumoniae infections are more frequently found in older children and adults. C trachomatis is usually associated with ocular and genital infection as well as neonatal pneumonia. It rarely causes respiratory tract infections in normal healthy adults. The genus chlamydia comprises of 3 species - C psittaci, C trachomatis and the TWAR agent. C trachomatis is the most common member of the chlamydia genus known to infect man and is most common transmitted by the sexual route; an animal reservoir is not recognized. C psittaci is a zoonotic infection where avian species are the main natural hosts and man becomes incidentally infected. The TWAR agents were considered to be more closely related to C psittaci but now appear to be a single distinct species with no recognized animal reservoir.

- **Chlamydia_Psittaci**

Human C psittaci infection acquired from psittacine birds (parrots) is termed psittacosis. It is called ornithosis when contracted from other sources. These terms can be unhelpful, particularly when patients with proven C psittaci infection have no known bird or animal contact. C psittaci infection can be acquired from pet birds and also turkeys and ducks. There had been outbreaks associated with duck processing plants.

The incubation period is usually 7 to 10 days. Patients present with a rapid onset of headache, chills, fever and non- productive cough. All patients with community acquired pneumonia should therefore be questioned about recent foreign travel and bird contact. Respiratory symptoms can be absent and these patients may often present with CNS features. Infection may also be associated with other extrapulmonary manifestations such as abdominal pain, vomiting, headache, myalgia, fever, hepatitis, endocarditis and Stevens-Johnson syndrome.

- **Chlamydia_Pneumoniae**

Previously known as TWAR agents (Taiwan acute respiratory). Serological studies indicate that all C pneumoniae strains are very closely related and genetic studies have shown that they have more than 94% DNA homology with each other but less than 10% homology with the two other chlamydial species. The REA patterns of C pneumoniae isolates are similar to each other, but distinct from other chlamydial species. C pneumoniae infections are distributed worldwide and 20 to 70% of adults have serological evidence of previous infection. Infection is usually acquired by the respiratory route. C pneumoniae is rare in children less than 5 years of age and is most frequently found in

schoolchildren and adults. Epidemics occur every few years. 70 to 90% of C pneumoniae infections are subclinical and reinfection may occur. C pneumoniae produces similar clinical symptoms to mycoplasma pneumoniae and respiratory viruses. There are reports linking C pneumoniae to myocardial and endocardial disease.

2.1 Methods of Diagnosing Chlamydia

- **Serology** - the CFT is the most widely used method for diagnosing chlamydial infections in the UK. A result of 256 or more is consistent with are recent infection. The micro-immunofluorescence test can be used to distinguish between C psittaci and C pneumoniae species, as is the whole cell-inclusion immunofluorescence test.
- **Culture** - all chlamydial species can be grown in cell culture. Extreme care must be exercised with respiratory samples as C psittaci is a category 3 pathogen. C pneumoniae is the most difficult species to grow.
- **Antigen detection** - antigen detection techniques have been widely used to diagnose adult genital and ocular infections and neonatal C trachomatis infection. At present, sputum samples are not routinely submitted for chlamydial diagnosis. Some commercial assays can be used to detect chlamydia in sputum samples.
- **PCR** - increasing importance is being placed on molecular techniques to diagnose respiratory chlamydial infections accurately, because of difficulties in interpreting serological results and the problems associated with culture of C pneumoniae.
- **Antibody Detection** - Many methods have been employed for the detecting M pneumoniae antibodies in human serum. Methods used for the detection of rising titres of IgG are suitable for patients of all ages. However, methods used for detecting IgM are more suitable for use in younger patients, since IgM is found less frequently in patients experiencing re-infection (hence older patients).
- CFT is the mainstay of routine laboratory diagnosis of M pneumoniae infections. However, antibodies may not be detected by this method 7-10 days after the onset of symptoms and not all culture-positive patients develop CF antibody or a significant rise in titre. It is also very difficult to determine the significance of CFT titres obtained with single samples of serum, unless they are very high. Such high titres can be found many months after infection and so particularly in the months following periods of high incidence of M pneumoniae infection. Demonstration of a fourfold or greater rise in antibody titre is required to be reasonably sure of the diagnosis

2.2 Infections of Chylamydia with the Complications

Chlamydia_Trachomatis

The chlamydia genus is antigenically diverse, possessing species, subspecies and type-specific antigens but share a common genus-specific lipopolysaccaride antigen (LPS). Within the C trachomatis species, numerous serotypes are recognized.

C trachomatis (D-K) cause occulogenital infection and primarily infect the epithelium of the male urethra and the female cervix and urethra. Symptomatic genital infection, presenting as a urethritis, is common in males. Asymptomatic infection in females is much higher, with a reported incidence of approximately 60% in some groups.

A._Genital_Infection_in_Men

Genital C trachomatis infection in men usually presents as an urethritis which may occur concomittantly with a gonococcal infection.

Non-gonococcal_Urethritis_(NGU)

Non-gonococcal urethritis accounts for more than 100,000 cases reported each year by GUM clinics in England and Wales. It is estimated that 30 - 58% of these NGU cases are attributable to C trachomatis infection.

Post-gonococcal_Urethritis_(PGU)

This syndrome occurs in patients who have been infected with both N gonorrhoeae and C trachomatis. As antimicrobial therapy for N gonorrhoeae does not eradicate C trachomatis, post-gonococcal urethritis results from the replication of C trachomatis in the urethra. Isolation of C trachomatis in patients with N gonorrhoeae treatment ranges from 17.5 to 32%. In contrast, the detection rate of C trachomatis in patients treated for N gonorrhoeae infection with urethritis ranges from 38 to 88%.

Serotypes	Disease	Complications
A -C **1 - 3**	Trachoma	-
	Lymphogranuloma venerum	-
A –K Male	Non-gonococcal urethritis (NGU)	Epididymitis
	Post-gonococcal urethritis (PGU)	Reiter's
	Conjunctivitis	Sexually acquired
	Proctitis	Arthritis (SARA)
Female	Mucopurulent cervicites	Salpingitis
	Urethritis	Perihepatitis
	Conjunctivitis	Endometritis
	Proctitis	Infertility
		Ectopic Pregnancy
Neonates	Conjunctivitis	Pneumonia

Complications

A number of complications can arise following infection with C trachomatis. These include epididymitis, Reiter's syndrome, sexually acquired reactive arthritis (SARA), and possibly endocarditis.

There is convincing evidence that epidymitis in younger men (<35) is associated with C trachomatis infection and the organism has been demonstrated in epididymal aspirates. Approximately 50% of the estimated 500,000 annual cases of acute epididymitis in the United States are caused by C trachomatis infection.

The classical triad of Reiter's syndrome comprises of urethritis, conjunctivitis and arthritis. In Asia and Africa, it is primarily related to GI infections but whereas in North America and Europe, it is recognized as a sexually-acquired syndrome following C trachomatis infection. This syndrome is more common in males than females.

B._Genital_Infection_in_Women

In contrast to C. trachomatis infections in males, infection in the female is commonly asymptomatic. However, the consequences of female infection are far more serious. The organism infects and replicates within the epithelium of the cervix and urethra. An ascending infection with involvement of the upper genital tract can result in clinical or subclinical pelvic inflammatory disease (PID), presenting as endometritis, salpingitis or a perihepatitis (Fitz-Hugh Curtis Syndrome). Tubal damage may occur which may lead to infertility and ectopic pregnancy. C. trachomatis is the most important cause of PID in the developed world accounting for 25% - 50% of the one million cases in the U.S.A

C. trachomatis is recovered from the cervix in 12% - 31% of women attending GUM clinics in the UK. The majority of infections are asymptomatic but C trachomatis has an important role in mucopurulent cervicitis. The recovery of C trachomatis from the cervix of pregnant women attending family planning clinics in the UK is much lower (3%), but is epidemiologically important in the light of the neonatal infections which occur at delivery. C trachomatis has been recovered from the cervix in 10% - 16% of women undergoing termination of pregnancy. This indicates the need to screen women prior to termination of pregnancy if PID following termination is to be avoided.

In addition to cervical infection in women, C trachomatis has also been isolated simultaneously from the urethra. In some cases, C trachomatis can also be isolated from the urethra only. The "acute urethral syndrome" presents as dysuria and frequency and occurs most commonly in young sexually active females.

Pelvic_inflammatory_Disease

C. trachomatis is the most important cause of PID in the Western world and the organism has been recovered from the cervix in 31% of cases. Canicular spread of C trachomatis from the lower genital tract gives rise to symptomatic or subclinical salpingitis. Definitive evidence for the role of C trachomatis in salpingitis has been demonstrated by the direct isolation of the organism from the fallopian tubes in 5% to 30% of women but not from the fallopian tubes of women without salpingitis. Risk factors for PID include the use of an IUD as well as termination of pregnancy in sexually active young women.

Infertility

The consequence of tubal damage may be infertility and the role of C trachomatis is now well recognized. Attempts to demonstrate C trachomatis in the endocervix of infertile women are usually

unsuccessful because tubal damage has often occurred years earlier but serological tests are thought to be useful.

Perihepatitis

N gonorrhoeae is well established as a cause of acute perihepatitis (Curtis-Fitz-Hugh Syndrome). Women present with right sided upper abdominal pain. There is now good evidence that C trachomatis is also involved. The precise incidence of this syndrome is unknown. The recovery of C trachomatis from endocervical swab is suggestive but not conclusive evidence of perihepatitis and treatment should nonetheless be instigated.

C._Conjunctivitis

Ocular infections caused by C trachomatis are common in sexually active individuals. Usually infection presents, after an incubation period of 1-2 weeks, as a follicular conjunctivitis which may be clinically indistinguishable from a viral infection. Laboratory diagnosis is essential to identify the causative agent.

D._Neonatal_Infection

The risk of neonatal infection at delivery may be more than 50% for pregnant women with active cervical infection. The most common clinical manifestation is neonatal conjunctivitis, which usually presents between the third and thirteenth day of life. The severity of the conjunctivitis may range from a mild "sticky eye" to severe inflammation and discharge and closure of the eye. Chlamydial opthalmia neonatorum is considered to be 3 to 5 times more common than gonococcal opthalmia neonatorum in the U.K. An untreated neonatal infection may lead to a severe pneumonitis between the fourth and twelve weeks of life.

Mathematical Model Formulation

According to Wilson (2004), we use the following notations and/or definitions for the human populations.

$C(t)$: The number of concentration of free extracellular Chlamydia particles.

$E(t)$: The number of non-infected individual mucosal epithelial cells (main host cell for Chlamydia).

$I(t)$: The number of Chlamydia- infected epithelial cells.

Assuming in the given population at time say t; $C(t)$, $E(t)$ and $I(t)$ denote what had been defined above.

We define the following parameters as follows:

P: is the number of chlamydial particles released from infected cells at a rate of k_2,

k_2: is the rate infected cells burst,

μ: is the rate of clearance by macrophages,

k_1: is the rate of epithelial cell infection, which may reduce the antibodies.

P_E: is the rate at which epithelial are produced.

δ_E: is the rate of epithelial cell natural death, and

γ: is the rate of clearance of infected cells due to cell-mediated immunity.

In view of the above, we have the following system of differential equations:

$$\frac{dc}{dt} = Pk_2 I(t) - \mu C(t) - k_1 C(t)E(t) \quad \text{.....(1)}$$

$$\frac{dE}{dt} = P_E - \delta_E E(t) - k_1 C(t)E(t) \quad \text{.....(2)}$$

$$\frac{dI}{dt} = k_1 C(t)E(t) - \gamma I(t) - k_2 I(t) \quad \text{.....(3)}$$

Equilibrium Analysis: The governing system of equations of the model [(i.e. equation (1) to (3) demands that we investigate whether the diseases could attain a pandemic level or it could be wipe out. The equilibrium analysis helps to achieve this, thus we shall have two non – negative equilibrium points namely: the disease – free equilibrium which can also be refers to as the trivial steady state and the endemic equilibrium which can equally been refers to as non – trivial state.

Continuity of the right hand side of the system of equations (1) to (3) and its derivatives imply that the model is well posed. However, the system of equation (1) to (3) has trivial steady state when

$$\frac{dC}{dt} = 0, \quad \frac{dE}{dt} = \frac{P_E}{\delta_E}, \quad \frac{dI}{dt} = 0,$$

and a non-trivial steady state is achieved when

$$\frac{dC}{dt} = \frac{P_E[(P-1)k_2 - \gamma]}{\mu(\gamma + k_2)} - \frac{\delta_E}{k_1} \quad \text{.....(4)}$$

$$\frac{dE}{dt} = \frac{\mu(\gamma + k_2)}{K_1[(P-1)k_2 - \gamma]} \quad \text{.....(5)}$$

$$\frac{dI}{dt} = \frac{P_E}{\gamma + k_2} - \frac{\delta_E \mu}{k_1[(P-1)k_2 - \gamma]} \quad \text{.....(6)}$$

corresponding to clearance of infection and active disease respectively.

The basic reproduction ratio

$$R_0 = \frac{P}{(1+\gamma/k_2)(1+\mu/(k_1 E_0))} \quad \text{.....(7)}$$

where $E_0 = P_E/\delta_E$.

The trivial steady state is asymptotically stable provided $R_0 \langle 1$ *and the non – trivial steady state is stable when* $R_0 \rangle 1$.

With these conditions we can minimize / clear the infection if and only if the following cases /conditions are satisfied according to Wilson. We shall now briefly emphasize on the three cases as discussed by Wilson.

Case i: the macrophage engulfment of the Chlamydial particles occurs prior to host cell infection (μ/k_1). This has to do with tracking the distribution of antibiotics aggregating on Chlamydia particles based on the large number of binding sites and high antibody concentration for its neutralization.

Case ii: the cytotoxic immune response clears cell prior to lysis of the infected cell (γ/k_2). Here chlamydiae have a complex replicative cycle complicating the tracking of intracellular chlamydial particles. The response of chlamydial changes as the number of Cytotoxic T cells increases with time due to immune responsiveness. The assumption here is that the magnitude of the cell- mediated immune response t proportional to the number of replicating forms of Chlamydia particles within a host cell.

Case iii: the number of infectious Chlamydia particles released by an infected cell is reduced (P). Here the Chlamydia's life cycle is initiated when the infectious, extracellular transmission cell, termed the elementary body (EB), attached to a susceptible host cell. The host cell internalized the EB, where, the EB undergoes morphological changes, reorganizing to the larger reticulate body (RB), the replicative form as Chlamydia. According to Wilson, at this stage, the RBs multiply 200-300 fold by binary fission. At 20 - 25 hours after infection, infectious EBs appears as the EB to RB conversion process is reversed. Some RBs continue to divide whilst others reorganize into EBs, resulting in asynchronous growth, until the host cell cannot support the multiplication any longer. The host cell burst, releasing the EBs, thereby initiating new cycles of infection. Depending on the strain of Chlamydia, the developmental cycle takes between 40 and 72 hours. The metamorphosis of EB to RB includes passage via an intermediate body. Under this case the chlamydial particle that has been induced into abnormal state by either pathway is refer to as an aberrant body. (AB). This case lead to modeling of the developmental cycle.

According to Wilson (2004) the developmental model cycle is given as:

$$\frac{dI_{B0}}{dt} = -\frac{\partial}{\partial r}\{k_f(r,t) I_{B0}(r,t) \quad \text{.....(8)}$$

$$\frac{dA_B}{dt} = -\frac{\partial}{\partial s}\{\left(k_{af}(s,t) - k_{ar}(s,t)\right) A_B(s,t)\} + \rho(s,t) A_B(s,t) \quad \text{.....(9)}$$

$$\frac{dI_B}{dt} = \frac{\partial}{\partial r}\{k_r(r,t) I_B(r,t)\} \quad \text{.....(10)}$$

$$\frac{dE_B}{dt} = k_r(r_0,t) I_B(r_0,t) \quad \text{.....(11)}$$

In this model, he used
$R_B(t)$ *and* $E_B(t)$ *to be the numbers of RBs and EBs in the host cell at time t and* $I_{B0}(r,t)$ *and* $I_B(r,t)$ *to be the number of IBs that are in the process of transfor* min *g from an EB to RB , andfrom a RB to an EB respectively at time t, where r is the* deg *ree of maturation along the transformation process,* sin *ce there is a spectrum of IBs between the EB and RB forms* (*there is also a spectrum of ABs*). *Here,* $r_0 \le r \le r_1$, *where* r_0 *and* r_1 *denote an EB and RB respectively. We also let* $A_B(s,t)$ *be the number of ABs at time t with* deg *ree of aberratiohere sn measured by the parameter s,* $s_0 \le s \le s_1$ *and* $s = s_0$ *denotes a normal RB.*

k_f *is the rate of maturing of an IB towards the RB and* k_r *is the rate of reverse maturation of an IB towards the RB and* k_r *is the rate of reverse maturation of an IB towards an EB.The rate an AB progresses in its* deg *ree of aberration to / from an RB is given by* $k_a = k_{af} - k_{ar}$ *and depends on the concentration of antimicrobial agent in the system. We let c be the rate of RB commitment to transform to EBs and* ρ *be the rate of replication of RBs and aberrant RBs* (*ABs*).

Numerical Analysis

The system of equations (1) to (3) was solved numerically using maple mathematical package. We give numerical simulation of the equilibrium and stability conditions of the governing equations of the model following Wilson (2004), below are some of the hypothetical parameters values used:

$$P = 200-500,\ k_1 = 0.02\,mm^3/day/cell,$$
$$k_2 = 0.33-0.6\,days^{-1},$$
:
$$P_E = 40\,cells/mm^3/day,\ \delta_E = 2\,days^{-1},$$
$$\gamma = 2-10\,days^{-1}\ and\ \mu = 2-10\,days^{-1}$$

The results of the numerical simulation are shown graphically in fig. (1) – fig. (6) below:

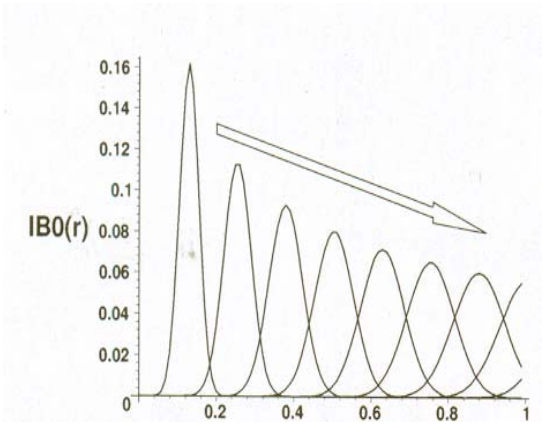

Fig. 1: The Normal growth of I_{BO} for various times

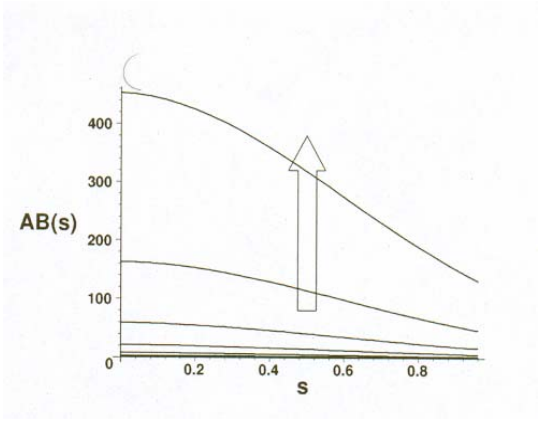

Fig. 2: The development of A_B for various times

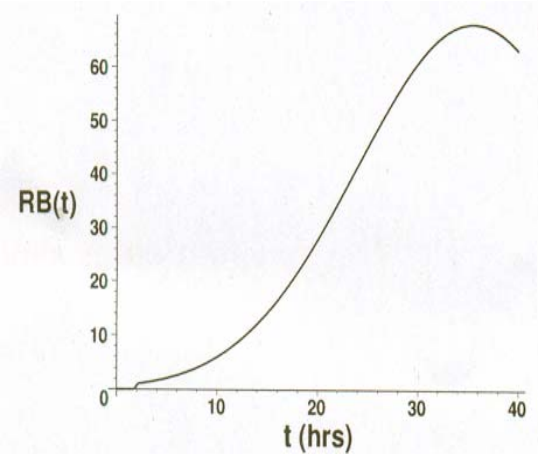

Fig. 3: The time courses of the number of RB

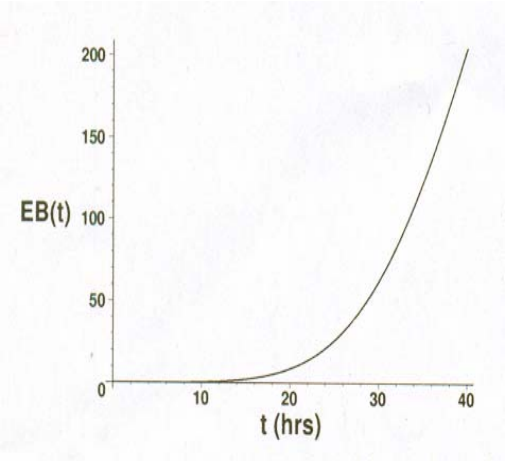

Fig. 4: The time-courses development of the numbers of RB

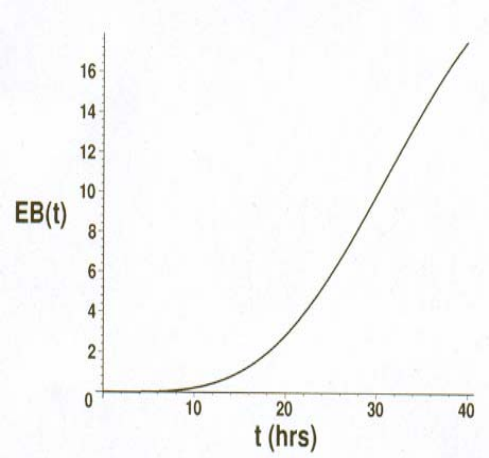

Fig. 5: The Normal growth of EB per host cell with respect to time

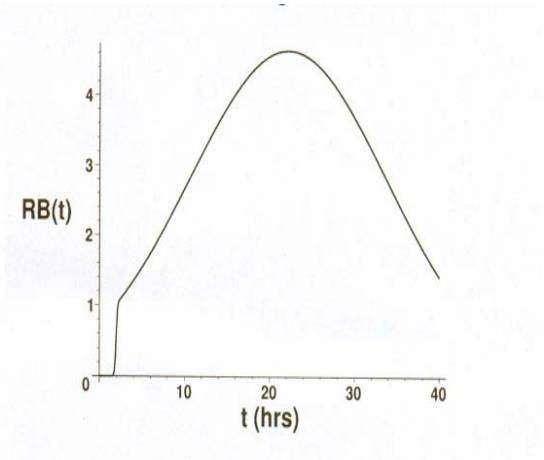

Fig. 6: The Development of EB per host cell

Results

First of all the mathematical model described in the previous section(i.e equations (1) to (3) and particularly equations (8) to (11) that were arrived at by Wilson through his developmental Cycle models have been used to simulate the results shown in figures 1 to 6, by setting the initial conditions

$$I_{Bo}(r,0)=1,\ I_{Bo}(r\neq r_o,0)=R_B(0)=0$$

$$A_B(s,0)=I_B(r,0)=E_B(0)=0,$$

and the boundary conditions

$$\left.\frac{dI_{BO}}{dt}\right|_{(r_0,t)}=0,\quad \left.\frac{dI_B}{dt}\right|_{(r_1,t)}=c(t)R_B(t).$$

$$\left.\frac{dA_B}{dt}\right|_{(s_0,t)}=k_{af}(s_0,t)R_B(t),$$

Using the Central – difference formulars for the derivatives in solving the system of equations (8) to (11). It was observed according to (Wilson, Beagley and Timms) that figure 1 illustrate normal Chlamydial development (persistent AB_s been not induced) and persistent chlamydial development (where AB_s *are induced*).

Discussions

Epidemiology of Chlamydia bacteria infections – A Review was presented to look into the mathematics models developed by Wilson to investigate the three cases stated in previous section, i.e humoral immunity, cell – mediated immunity and within host dynamics. Evidence shown, that most of the recorded chlamydial infection occurs as a result of long term inflammation which leads to fibrosis and scarring. With most of the research work conducted on the subject matter, very little application of it is found in African Countries, as the disease and other related problems of Chlamydial infections are now common around the world.

Discussions

Epidemiology of Chlamydia bacteria infections – A Review was presented to look into the mathematics models developed by Wilson to investigate the three cases stated in previous section, i.e humoral immunity, cell – mediated immunity and within host dynamics. Evidence shown, that most of the recorded chlamydial infection occurs as a result of long term inflammation which leads to fibrosis and scarring. With most of the research work conducted on the subject matter, very little application of it is found in African Countries, as the disease and other related problems of Chlamydial infections are now common around the world.

Correspondence to:
Adetunde, I. A.
University of Mines and Technology, Dept. of Mathematics, P. O. Box 237, Tarkwa, Ghana.
Telephone: +233-243151871, +233208264591
Emails: adetunde@gmail.com, iadetunde@umat.edu.gh

References

[1] Ward, M.E (1995): The Chlamydia developmental Cycle in Pictures. http:/www.chlamydiae.com/docs/biology/boil_devcycle.htm C207

[2] Wilson, D.P; Mathews.C;Wan and D.L.S.McElwain (2004): Use of a quantitative gene expression assay based on micro-array techniques and a mathematical model for the investigation of chlamydial generation time and inclusion size, Bulletin of Mathematical Biology, Vol.66Issue 3 Pp 523- 537.

[3] Aldous, M.B; Grayston,J.T; Wang, S.P and Foy. H.M (1992): Seroepidemiology of Chlamydia pneumoniae TWAR infection in Seattle families, 1966 – 1979. Infect.Dis 166, 646

[4] Campell, L.A and Kuo,C.C.(2003): Chlamydia pneumoniae and therosclerosis.Semin.Respir.Infect.18, 48

[5] Mathew, S.A; Volp,K.M and Timms, P. (1999): Development of a quantitative gene expression of σ factors. FEBS Lett. 458,354.

[6] Hasia, R.C; Pannekoek, Y; Ingerowski,E; and Bavoil, P.M (1997): Type III Secretion genes identify a putative virulence locus of Chlamydia, Mol. Microbiol.25, 351.

[7] Rockey, D.D; Matsumoto, A. (1999): The Chlamydia development al cycle. In: Brun, Y.V.,Shimkets, L.J. (Eds), Prokaryotic Development. ASM Press, Washington,DC, Pp 403- 425.

[8] Fields, K.A; Mead, D.J; Dooley,C.A and Hackstadt, T. (2003): Chlamydia trachomatis type III secretion: evidence for a functional apparatus during early – cycle development, Mol. Microbiol.48,671

[9] Fields, K.A and Mead, Hackstadt, T. (2003): Evidence for Chlamydia trachomatis CopN by a type III secretion mechanism, Mol. Microbiol.38,1048.

[10] Beagley, K.W. and Timms, P (2000): Chlamydia trachomatis infection: incidence, health cost and prospects for vaccine development, J. of Reproductive Immunology. 48: 47- 68, C209

[11] Dreses – Werringloer, U, Padubrin, I and Kohler, L (2001): Effects of Azithromycin and Rifampin on Chlamydia trachomatis Infection in Vitro,

Antimicrob. Agents Chemother; 45: 30001 – 30008, C208.

[12] Magee, D.M; Williams, D.M; Smith, J.G ; Bleicker , C.A; Grubbs, B.G; Schacter, J and Rank, R.G (1995): Role of CD8 T Cells in Primary Chlamydia Infection,. Infect. Immun., 63: 516 – 521, C203.

[13] Wilson, D.P; Timms, P; and D.L.S.McElwain (2003): A mathematical model for the investigation of the Th1 immune response to Chlamydia trachomatis. Math. Biosci., 182: 27 – 44. C206.

[14] Yang, X and Brunham, R.C (1998) T lymphocyte immunity in host defence against Chlamydia trachomatis and its implication for vaccine development. Canadian J. Infect. Dis., 9: 99 - 108. C203

[15] Shaw, E.I; Dooley, C.A; Fischer, E.R; Scidmore, M.A; Fields, K.A and Hackstadt, T (2000): Three temporal classes of gene expression during the Chlamydia trachomatis developmental Cycle. Mol. Microbiol. 37, 913.

Time and Matter

John Linus OôSullivan

Independent Researcher, Connecticut 06824, USA
johnlosullivan@att.net

Abstract: Photons travel at the speed of light in a vacuum. Electrons travel at the speed of light in a quantum cone. When mass is more than the speed of light relative to infinity, mass will become nonexistent or having no energy at the nodes of standing half waves. On this note, there does not have to be a beginning of anything just because we exist, the energy from which we came from always existed and if it did not always exist, then how can we ask the question where did the energy come from ?, unless it was always there. This report will show the relation between mass and infinity where the speed of light is common to both giving an understanding of time and matter in the electromagnetic field. This brief report can be printed out in color or black and white. [Journal of American Science 2009; 5(4):65-70]. (ISSN: 1545-1003).

Key words: Photon, Electron, Quantum Gravity, Spacetime, Electromagnetic Field.

1. Introduction

The electromagnetic field is comprised of standing waves in the opposite direction where direction is relative to the source of energy. The wave duality of the standing waves provides for the electromagnetic and gravitational forces. A photon is a unit (packet) of energy from standing half waves at the antinodes where the speed of light is relative to infinity and mass is part of infinity. Energy is equal to frequency of the photons based on Planckôs constant, $E = hf$.

2. Report

From the illustration Figure 1a, energy is formed into half wavelengths at ultra high frequency standing waves. The half wavelengths become transverse waves because of the expansion process forming electro half waves perpendicular to the magnetic half waves. The half waves have two free ends where the antinodes are at the ends and nodes are in the middle such that each half wave keep multiplying indefinitely to complete whole wavelengths where $C = f \lambda$. As the wavelengths multiply from energy displacement, the expansion of the transverse waves become three dimensional as a cone resulting in an endless unit without a boundary in time. Each photon (half wave) in the field cone has its own independent cone state in the expansion process. Each photon (half wave) in the cone is equivalent to two smaller half waves as a spiral within the photon to complete a whole wavelength where $C = f \lambda$.

From the field illustration Figure 1b, the black-red (dark) are the electro waves perpendicular (at right angles) to the page and brown-green (light) magnetic waves are on the same plane as the page. The transverse waves in the figure need to be visualized in three dimensions and the expansion of the waves visualized in a cone or spiral. The page figure 1b is a spectrum of different size wavelengths increasing in size moving outwardly (not just one wavelength as shown). As the field expands outwardly into multiple wavelengths in a cone, the atom is depicted at center when electro field couplings become nuclei from expansion. The e coupling constant, about 137.03597 is the amplitude for a real electron to emit or absorb a real photon (Feynman, 1988). Due to the expansion of the standing waves in a spiral cone (energy displacement of standing waves into larger waves), the base or space between the circles give the necessary amplitude for the photons and electron(s) to interact as a coupling and the apex or dead center between the circles in the cone is the nuclei fused in time at much shorter wavelengths.

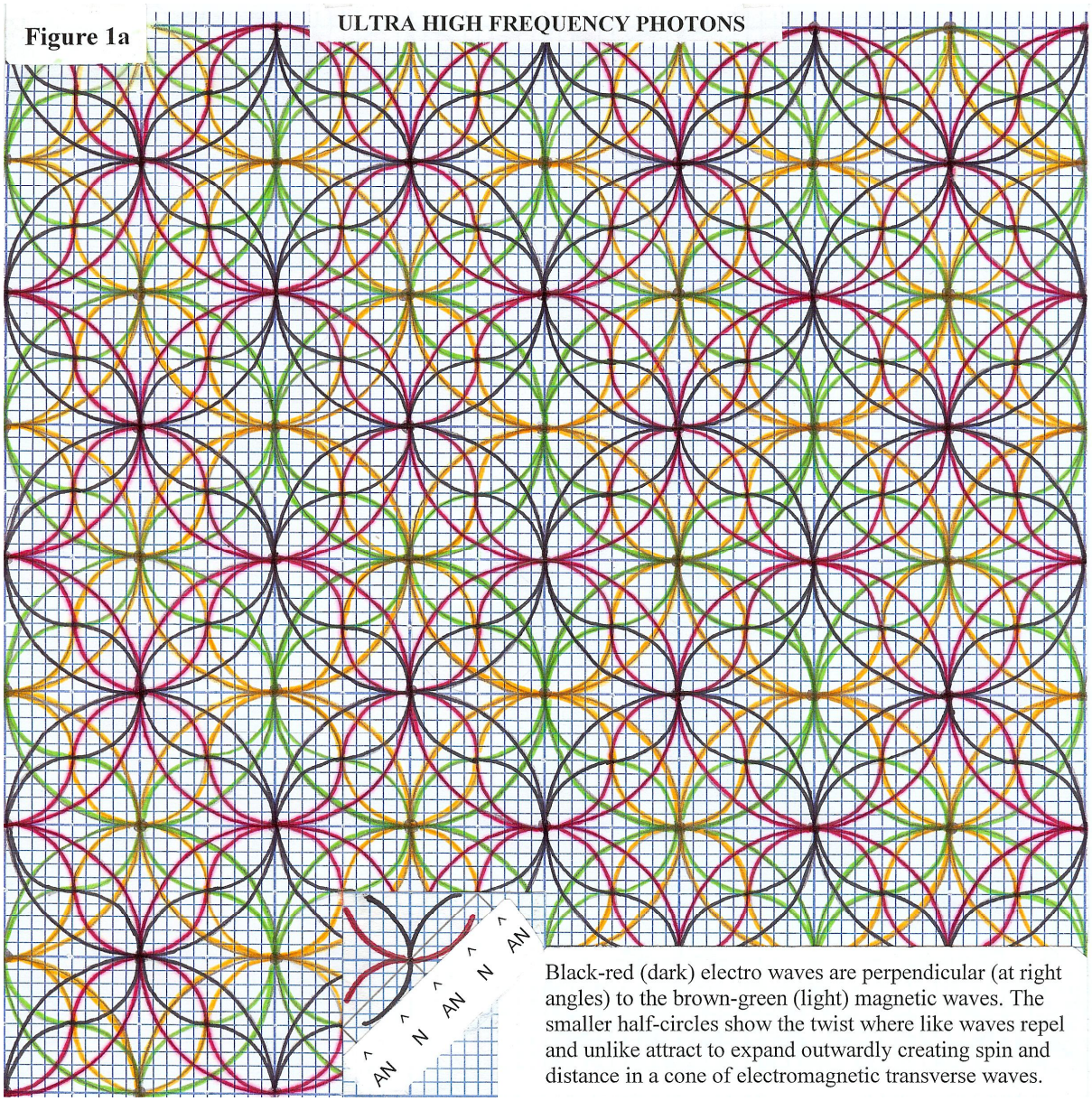

Black-red (dark) electro waves are perpendicular (at right angles) to the brown-green (light) magnetic waves. The smaller half-circles show the twist where like waves repel and unlike attract to expand outwardly creating spin and distance in a cone of electromagnetic transverse waves.

It is important to visualize a quantum cone in Figure 1b from a spectrum of different size wave-lengths moving outwardly. Electro and magnetic waves expand into larger waves from the antinodes (displacement) energy of standing waves at twice the wave amplitude of the smaller wave giving distance to the field. The waves increase in amplitude forming atom cones in the field where the apex of each atom cone from an infinite singularity have a strong nuclear force as nuclei. Electron(s) as photon(s) of mass continue outwardly to interact with real photons at the base of the quantum cone which is the amplitude of the e coupling constant. The electron as a wave particle makes quantum jumps on the different size waves that form the atom cone.

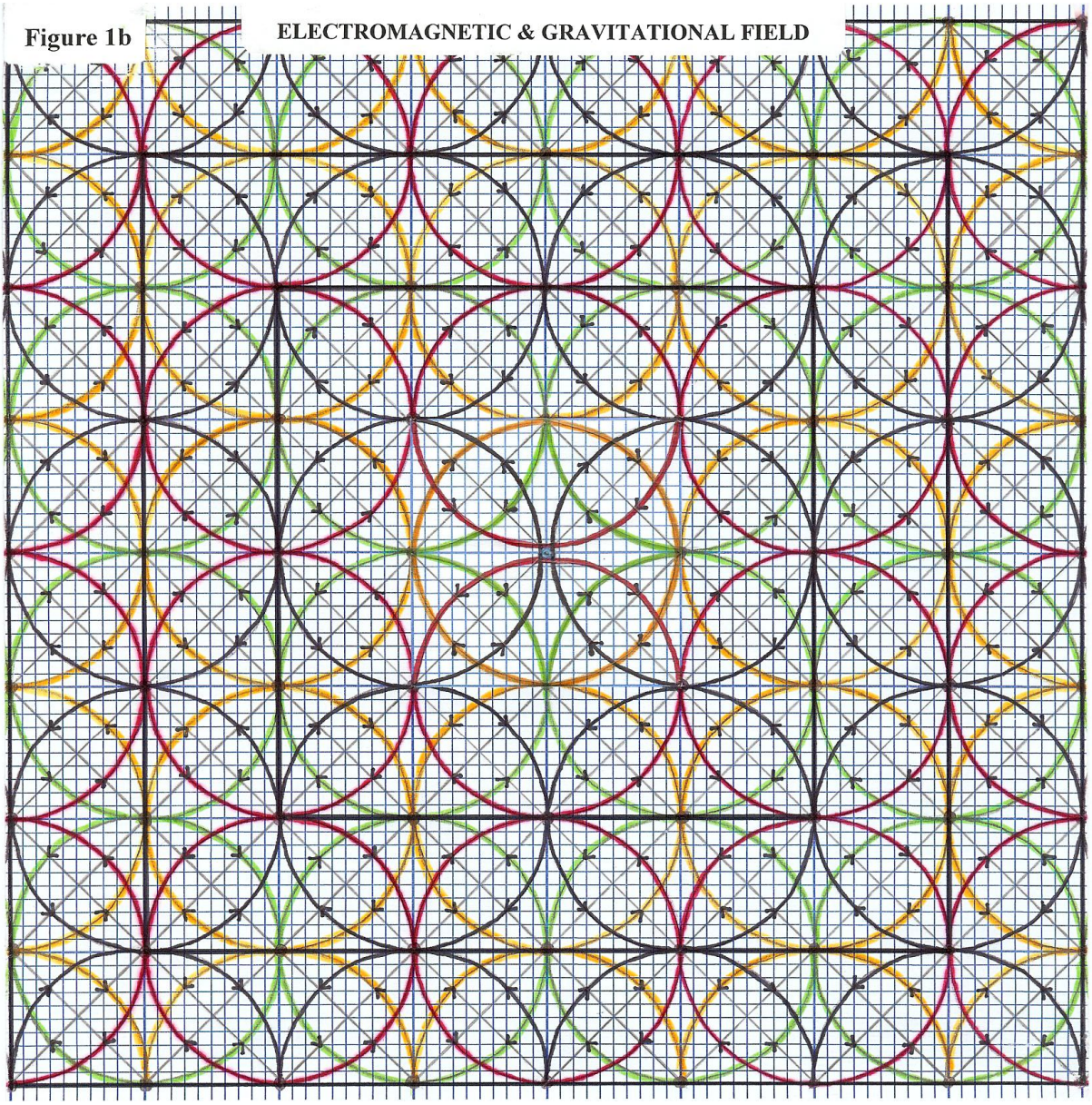

The electro field wave is perpendicular (at right angles) to the inside magnetic field wave, therefore, the electro will become nuclei as the preference of the two from energy expansion. Atom identity is determined by the life cycle duration of the electro couplings that became mass. Like the life cycle of a star, the electro couplings having a longer duration to expand will nuclei as a lighter atom such as a hydrogen atom. A star is formed when a large amount of gas (mostly hydrogen) starts to collapse in on itself due to its gravitational attraction (Hawking, 1996). The field expands into larger waves from the displacement energy of standing waves and the energy from mass propagates on the waves. The field waves are endless in time; hence the waves are open regardless of the size of the spiral waves in the wavelength spectrum.

Moving two steps from center in Figure 1b and squaring, there are four complete green (light) circles in the square. On three steps from center and squaring, there are nine complete brown (light) circles in the square and so on in the inverse square distance of the magnetic field. Moving diagonally from the center in Figure 1b, (Pythagorean Theorem), the photon half waves alternate between the electro and magnetic waves as photon energy in a vacuum which is the way light travels. Holding the page up diagonally at eye level show how the transverse waves oscillate as photon energy in a vacuum.

Gravity forces come from the magnetic waves around the atom Figure 1b (center) which is an inward attraction force at the nodes that help conserve the energy Figure 1a. The electro is an outward expanding wave from the source of energy while the magnetic is an inward contracting wave to conserve the energy. Gravity will adjust inward forces to conserve energy in any kind of atom right down to the nuclei apex within the cone. The atom and gravity are united and comply with the inverse square distance and constant G. It follows that the accumulation of mass includes the accumulation of gravity as the photon waves interact with other field electrons.

In Figure 1b, energy forms matter from electro couplings giving a point center to the magnetic circle of photons where the ratio of the diameter in the magnetic circle to its circumference is infinite. This ratio is pi and infinite from the open ended waves with pi having the same value regardless of the size of the circle. Mass is the center for a diameter in the field as a ratio to the open circumference.

In summary, mass is created from open ended electro half waves at the apex of cone expansion in the electromagnetic field. Gravity inward forces from the magnetic half waves are the result of mass given that there can be no mass without gravity; hence, pi is the result of gravity forces on mass regardless of mass size.

3. Conclusion

Left Side *Right Side*

Expanded Equation: $E = C = \infty$ = Open Cir. $= MC^2$

Infinity is on the left side of the equation above. Mathematics has little application on the left side of the equation because there is nothing to measure or count. Photons are counted on the right side of the equation with mass because C is finite (general relativity). Photons are not counted on the left side of the equation because C is infinite (no relativity). In essence, the speed of light is relative to infinity and mass is part of infinity because the speed of light is from the same energy.

Velocity is distance divided by time; therefore any time frame relative to infinity will have a value of C or less. Distance is the inverse square expansion of the magnetic field that contracts inward to offset time (mass) in the form of gravity. C^2 is the offset to the inverse square distance of the magnetic field where mass is equal to energy divided by C^2. Mass and C^2 cancel out leaving energy to equal C and infinity.

Time is relative only when mass is created where C is finite. Time includes the three spatial dimensions in the form of ñmass as finite energyò on the right side of the equation. The classical three spatial dimensions plus time is equal to ñmass as finite energyò where mass is the three dimensions and finite energy is the time. Time is finite on the right side of $E = MC^2$, where time has a beginning and an end. Time is infinite on the left side of the equation having no beginning or end. An observer is part of time and part of infinity from the same source of energy where the speed of light is the same for all observers. General relativity indicates that space-time is not flat but curved or warped by the distribution of mass and energy in it (Hawking, 1996). This energy is finite where time has a beginning and an end. Energy at the square root of C^2 as an outward force is synonymous with velocity, time, mass and finite C while the square root of C^2 as an inward opposing force is synonymous with gravity, antimatter and conservation of energy.

Mass is regulated by gravity as an opposing force at the speed of light. The satellites orbiting the earth are subject to gravity of the earth and the earth in turn is subject to gravity of the sun. All mass in the universe is receding in the electromagnetic field due to the different gravity levels in the field. Thus, $E = C = MC^2$ where mass is not the multiplicative of C^2 but the multiplicative inverse of C^2. Energy is the same as mass and conversely mass is the same as energy when C is finite as in the square root of C^2 because E is equal to the square root of C^2 both on the right side and left side of the equation above.

Photons in the form of energy are infinitely small just as they are infinitely large; matter as finite energy is an intermediary and part of infinite energy. Matter is projected as energy at each half cycle; hence, there is no energy or matter at the nodes where $C = f \lambda$. The bridge between E and MC^2 is C, therefore $C = MC^2$ and mass is the reciprocal of C^2. C^2 divided by mass is equal to infinite C on the left side of the equation because the wavelengths are open ended at the antinodes. $C = MC^2$ can also be seen as a static universe. The electromagnetic field is fixed or static from standing half waves and the mass in it is receding to look like expansion as a result of the different gravity levels in the field evidenced by the redshift and distance. Mass is receding in the field of a static universe that give finite time on the right side of the equation.

4. Supplemental Data

Left Side *Right Side*

- $E = C = \infty$ = Open Cir. = MC^2

The square root of C^2 (gravity) offset mass on the right side of the equation above and is infinite on the left side of the equation.

- $M = \frac{E = C = \infty}{C^2}$

Distance is the inverse square expansion of the magnetic field and contracts inward to offset time (mass) in the form of gravity.

- Velocity = $\frac{\text{Distance } (C^2)}{\text{Time } (M)} = \infty$

Time includes the three spatial dimensions in the form of "mass as finite energy" on the right side of the equation.

- $C = MC^2 = \frac{C^2 \text{ (Magnetic Field)}}{\text{M (Electro Field)}} = \infty$

- $\frac{\text{Inward Magnetic (-) B to A} = C^2}{\text{Outward Electro (+) A to B} = M} = \infty$

- $C = \frac{C^2}{M} = \infty$ Where $C = f\lambda$, $\lambda = \infty$

The standing wavelengths are open ended at the antinodes for each photon.

References

[1] Feynman, R.P. QED The Strange Theory of Light and Matter, Princeton University Press, 1988: p129.
[2] Hawking, S. The Illustrated A Brief History of Time, Bantam Books, 1996: p105.
[3] Ibid, pp40-42.

Spectroscopic Characterization of Olivine [$(Fe, Mg)_2 SiO_4$] in Madadevpur H4/5 ordinary chondrite

[1,3] **Bhaskar J. Saikia,** [2]**G. Parthasarathy and** [3]**N.C. Sarmah**

[1] G. B. Pant Institute of Himalayan Environment and Development, Almora - 263 643, India
[2] National Geophysical Research Institute (CSIR), Hyderabad -500 007, India
[3] Department of Physics, Dibrugarh University, Dibrugarh -786 004, India

e-mail:vaskar_r@rediffmail.com

Abstract
This study demonstrates for the first time, the spectroscopic characterization of Mahadevpur H4/5 chondrite that fell at Mahadevpur near Namsai town (Lat.27°40′N, Long. 95°47′E, Auranachal Pradesh, India) on 21 February 2007. The olivine group [$(Mg, Fe)_2SiO_4$] in Mahadevpur is characterized by the Fourier transform infrared (FT-IR), X-ray fluorescence (XRF) and Laser-Raman spectroscopic (RS) method. A comparison of results with Dergaon H5 chondrite is presented. Particular emphasis is given to the 10μm (1000cm^{-1}) and 20μm (500 cm^{-1}) region of infrared and Raman bands, which is originated from tetrahedral vibrations of silicates. [The Journal of American Science 2009; 5(4): 71-78]. (ISSN: 1545-1003)

Key words: Mahadevpur meteorite; olivine; spectroscopic characterization

1. Introduction

Meteorites are fragments of rocks which originated from outer planetary bodies and fell on the surface of the earth. Meteorites can be divided into two major types, primitive and differentiated. Differentiated meteorites are igneous rocks that were crystallized from magmas generated at the interiors of their parent bodies. The primitive ones have not experienced the melting in their parent bodies, thus their bulk compositions, except for volatiles, are considered to represent those of the solar nebula where and when the meteorites formed. Since the majority of primitive meteorites have chondrules, they are commonly called chondrites. Chondritic meteorites are the oldest and most primitive rocks in the solar system. The primary divisions of chondrite classification are the carbonaceous, ordinary, and enstatite classes (Parthasarathy and Sarma, 2004). The chondrites are the most numerous meteorite group, accounting for 87% of all meteorites observed to fall. The largest group of chondritic meteorites is known as the ordinary chondrites, account for 80% of all known meteorites (Philip et al 2000). Three subgroups of ordinary chondrites are identified, H group (high iron), L group (low iron), and LL group (low total iron, low metal). Chondrites contain small round masses of olivine or pyroxene. The silicates in meteorites predominantly consist of olivine and pyroxenes or non-crystalline silicates of intermediate compositions (Freund and Freund 2006).

On 21 February 2007, a meteorite fell Mahadevpur near Namsai town (Lat.27°40′N, Long. 95°47′E, Auranachal Pradesh, India) at 09:10 hrs Indian standard time (GMT+5:30hrs) (Weisberg et al 2008). The Mahadevpur meteorite is the forth documented meteorite from the north-eastern region of India. The last one was reported to fell on 2 March, 2001, at Dergaon and is classified as H5 chondrite (Grossman et al 2001). The other two are 'Assam' (1846) of type L5 and 'Goalpara' (1868) of type ureilite. The Mahadevpur meteorite has been documented as type H4/5 ordinary chondrite (Weisberg et al 2008). The present study represents the nature of olivine [$(Mg,Fe)_2SiO_4$] in Mahadevpur meteorite by comparing with Dergaon H5 chondrite.

The olivine of Dergaon meteorite has reported by Gohainbarua (2003); Bhattacharyya (2004) (Gohainbarua et al 2003; Bhattacharyya et al 2004). The comparative study of Mahadevpur is performed using X-ray fluorescence (XRF), Fourier transform infrared (FTIR) and Laser-Raman spectroscopy (RS). Particular interest is directed toward the 10μm (1000cm^{-1}) and 20μm (500cm^{-1}) region which exhibits the characteristics of olivine group.

2. Materials and Methods

A part of the meteorite samples (Figure 1) was crushed into fine powder by using agate mortar for analysis. The X-ray fluorescence (XRF) data on the Dergaon and Mahadevpur meteorite were collected by using powdered homogenous sample in pellet form. For XRF studies a Philip Magix XRF spectrometer PRO model PW 2440 has been used in wavelength dispersive mode. Typical uncertainty involved is +/- 0.02 wt %. The thin sections of the sample have been characterized by electron microprobe analyzer. The experimental details were similar to that described elsewhere (Bhandari et al. 2005; Dhingra et al. 2004). We tried to minimize the grinding time to avoid the deformation of the crystal structure, the ion exchange and the water absorption from atmosphere. The powdered sample was homogenized in spectrophotometric grade KBr (1:20) in an agate mortar and was pressed 3mm pellets with a hand press. The infrared spectra was acquired using Perkin-Elmer system 2000 FTIR spectrophotometer with helium-neon laser as the source reference, at a resolution of 4 cm^{-1}. The spectra were taken in transmission mode in the region 400-4000 cm^{-1}. The room temperature was 27°C during the experiment.

Raman spectrum is recorded using a Perkin-Elmer System 2000 FT-Raman spectrometer. For Raman microscopy a 50x objective was used and the spectra were excited by the 633 nm line of a He-Ne laser operating at 8 mW at the sample. The excitation laser for the FT-Raman spectra was a Nd:YAG laser of 1064nm wavelength, which could be operated at powers up to 500mW, but 150-250 mW for the high-pressure phases to avoid overheating the samples. Depending on fluorescence of the sample and acquisition times were between 120 and 180s. Slit widths were near 2 cm^{-1}.

(a) (b)

Figure 1: The photograph of the studied meteorite samples. (a) Dergaon H5 chondrite (b) Mahadevpur H4/5 chondrite.

3. Results

The elemental composition of Dergaon and Mahadevpur chondrite by X-ray fluorescence (XRF) using the Dhajala (H3) meteorite as a standard. The classification, petrological and chemical characteristics of the Dergaon has been reported by Shukla et al 2005 (Shukla et al 2005). The elemental composition of Mahadevpur is compared with standard literature of Mason (1962) and Dergaon H5 chondrite which is listed in Table1. The elements of Mahadevpur are well agreement with the Mason (1962) and Dergaon results. The elemental ratio is compared with results of Aderson (2007) and Dergaon (Table 2). Olivine is the most abundant mineral in chondrites, followed by hypersthene, feldspar, nickel-iron, troilite and diopside

with minor apatite, chromite and ilmenite. The composition of the olivine varies widely, from 0 to 30 wt% Fe_2SiO_4 (Fa) (Mason 1962; Anderson 2007). Generally chondrites are distinguished by Mg/Si ratios. The Mg/Si ratio of Mahadevpur is indicative to the type-H (Table 2). The olivine compositions of the two meteorites are presented in Table 3. The mineralogical phases of olivine in Mahadevpur meteorite is: olivine ($Fo_{80.8}$ $Fa_{19.3}$), orthopyroxene (En_{81} Fs_{17} Wo_1), and clinopyroxene (En_{58} Fs_8 Wo_{35}).

Table1: Major elements observed in Dergaon and Mahadevpur meteorite. The elements of the studied meteorites are compared with the data obtain by Mason (1962) for H chondrite.

Sample	Element (wt%)											
	Si	**Mg**	**Ca**	**Al**	**Fe**	**Ni**	**Co**	**Cr**	**K**	**P**	**Na**	**Ti**
H chondrite *	17.08	14.10	1.26	1.22	27.81	1.64	0.09	0.29	0.08	0.15	0.64	0.06
Dergaon	17.30	14.26	1.19	1.20	27.73	1.75	--	0.03	0.067	0.15	0.670	0.04
Mahadevpur	16.90	14.10	1.19	1.32	28.40	1.67	0.07	0.20	0.075	0.12	0.052	0.04

Table 2: Comparison of elemental ratio of Dergaon, and Mahadevpur with the data of Aderson (2007) for a standard H chondrite.

Sample	Elemental ratio (wt%)			
	Al/Si	**Mg/Si**	**Ca/Al**	**Cr/Mg**
H chondrite (standard) *	0.063	0.800	1.110	0.025
Dergaon	0.069	0.824	0.992	0.002
Mahadevpur	0.078	0.834	0.084	0.014

Table 3: Olivine composition of Dergaon and Mahadevpur meteorite.

Oxides (wt%)	**Dergaon-1**	**Dergaon-2**	**Dergaon-3**	**Mahadevpur-1**	**Mahadevpur-2**	**Mahadevpur-3**
SiO_2	39.030	38.900	39.297	37.500	36.300	36.230
Cr_2O_3	0.047	0.047	--	0.026	0.026	0.026
FeO	18.400	18.734	18.999	18.650	18.650	18.470
MnO	0.455	0.475	0.465	0.100	--	--
MgO	41.372	41.512	41.774	43.600	44.320	44.800
NiO	--	--	0.063	0.070	0.010	--
CaO	0.294	--	0.261	--	0.150	--
Total	**99.568**	**99.668**	**100.859**	**99.946**	**99.456**	**99.526**

The silicates in primitive meteorites carry important information about cosmic silicates and their modification in the solar system. Strong emission and absorption features found around 9.7μm and 18 μm, produced by Si-O stretching and O-Si-O bending modes, respectively. The 18 μm band is additionally broadened due to the coupling of the bending mode to the metal-oxygen stretching vibration located in this spectral region.

The position of the Si-O stretching vibration depends on the level of SiO_4 polymerization. Generally, the spectrum can be divided into three main spectral regions. The bands between 1100 and 800 cm^{-1} correspond to different asymmetric and symmetric stretching vibrations of the SiO_4 tetrahedra. The various features between 700 and 470 cm^{-1} are caused by bending vibrations of the SiO_4 tetrahedra.

The far-infrared bands in the low-frequency region beyond 470 cm^{-1} can be attributed to translational motions of the metal cations within the oxygen cage and complex translations involving metal and Si atoms.

The comparison of olivine group (Gadsden 1975) with Dergaon and Mahadevpur meteorite is presented in the Table 2. Generally free SiO_4 ion has exhibit four fundamental vibrational modes: a symmetric stretch (v1); a symmetric bend (v2); an asymmetric stretch (v3 and an asymmetric bend (v4). The infrared spectra o Dergaon and Mahadevpur meteorite in the 10µm an 20µm region are shown in the Figure 2. The stron bands in the 10µm (800-1150cm^{-1}) region is identifie as Si-O stretching and the bands present in the 20µn (400-700cm^{-1}) region is assigned as Si-O-Si bendin vibrations. The decreasing intensities in the Si-(stretching and Si-O-Si bending region are observed a 1053, 1012, 935, 920, and 504 cm^{-1} and 1059, 1002 944, 927, and 506 cm^{-1} for Dergaon and Mahadevpu meteorite respectively, which are identical to the band of fayalite (Fe_2SiO_4), the bands found at 407, 467, 506 601, 839, 988 and 1002 cm^{-1} in Mahadevpur infrare spectra and 467, 504, and 1012 cm^{-1} in Dergaor infrared spectra are identical to the bands of forsterit (Mg_2SiO_4) and the infrared bands 410, 506, 537, 694 725, 927, 973, 1059, 1121 cm^{-1} and 504, 537, 724, 920 976, 1012, 1053, 1122 cm^{-1} observed at Mahadevpu and Dergaon infrared spectra respectively are identica to the bands of enstatite (Mg_2SiO_3) (Gadsden1975). Th band found at 506.0 cm^{-1} can be interpreted as Si-O an Mg-O vibrational modes in enstatite ($MgSiO_3$) wit slight shifts in the matrix (Nakamoto 1978). Th petrologic type-5 chondrites have two strong peaks a 973 cm^{-1} and 535 cm^{-1} which may be related to Fe-(and Mg-O stretching modes (Nyquist et al 1971). Th existence of these two peaks is found in Mahadevpu infrared spectra in weak and medium intensities.

The Figure 2 displaying clear Raman lines attribut to olivine in the meteorites. Generally olivine has 8 numbers of optic modes, out of which 36 numbers ar Raman-active (Chopelas 1991; Hofmeister 1987). Th Raman spectra (Figure 2) are divided into three region as: below 400 cm^{-1}; 400– 800 cm^{-1} (20µm); and 800- 1100 cm^{-1}(10µm). It may be noted that 20µm Rama bands are relatively weak as compare to their infrare counterparts. The peaks between 800 and 1100 cm^{-1} are attributed to SiO_4 internal stretching vibrational modes; the dominant feature in this region is a doublet with peaks near 818 and 852 cm^{-1}. The relative heights of these peaks are a function of crystal orientation (Ishii 1978). These peaks result from coupled symmetric (v_1) and asymmetric (v_3) vibrations of SiO_4 tetrahedra (Piriou and McMillan 1983; Chopelas 1991; Hofmeister 1987; Paques-Ledent and Tarte 1973; Lam et al 1990). The peaks in the 400–800 cm^{-1} region are the SiO_4 internal bending vibrational mode.

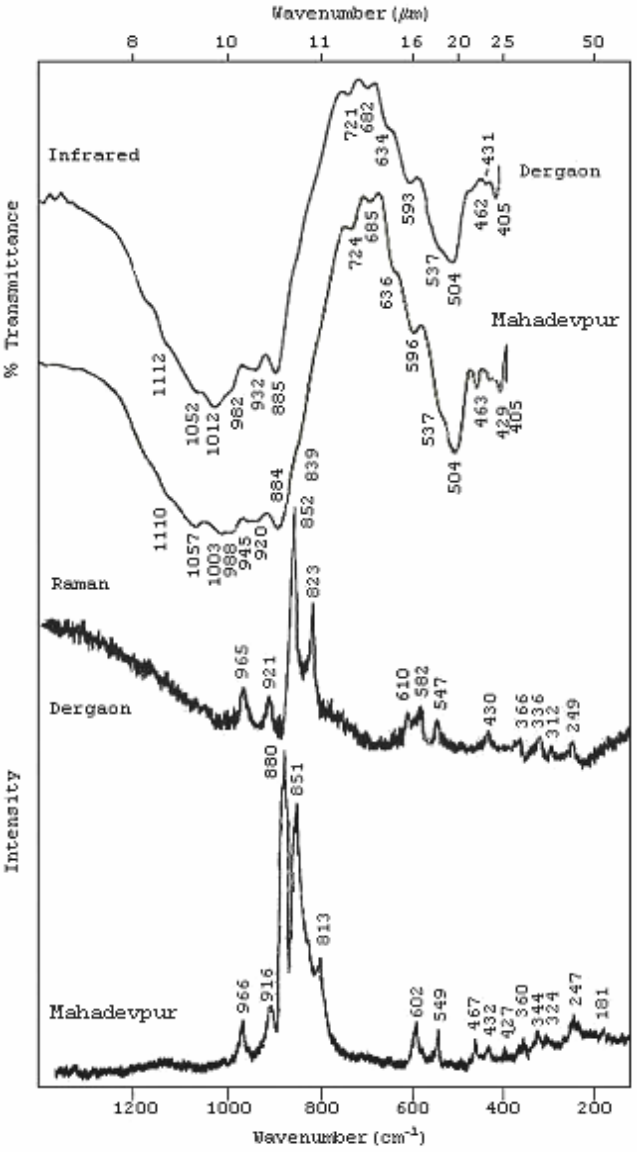

Figure 2: Infrared and Raman spectra of Dergaon and Mahadevpur meteorite in 10µm (800-1150cm^{-1}), 20µm (400-700cm^{-1}), and below 400 cm^{-1} region.

The peaks below 400 cm^{-1} are mostly contributed by lattice modes: rotations and translations of SiO_4 units and translations of octahedral cations in the crystal lattice (Chopelas 1991). These are weaker peaks, not often resolved in multi-phase spectra so only the doublet in the 800 –1100 cm^{-1} region is used in the calibration. In the studied meteorite samples, weak olivine bands are observed at 916-921 and 965-966 cm^{-1}. The other bands at 249, 312-324, 336-344, 366 and 602-610, cm^{-1} correspond to pyroxene.

In the infrared spectrum the Si-O asymmetric stretching vibration (TO2-T2O5) is observed in between the peaks 1112-1003 cm^{-1}. In between the peak position 920-988 cm^{-1} and 885-884 cm^{-1} the meteorites exhibits Si-O asymmetric vibration (TO3) and (T2O7--TO4) respectively. In the bending vibration region, the symmetrical bending vibration of O-Si(Al)-O is observed at the peak position 685-682 cm^{-1}. Another peak is observed at 463-462 cm^{-1} which is due to Si-O-Si bending vibration. In the Raman spectrum strong Si-O symmetric stretching bands appear at 813-823 and at 852-852 cm^{-1}, and a medium-intensity antisymmetric Si-O stretching band appears at 965-966 cm^{-1} due to fosterite (Fo). The peaks of the 813-852 cm^{-1} doublet is assigned to a mixed contribution of the symmetric (v1) and asymmetric (v3) stretching modes of Si-O_{nb} bonds (Non-Bridge Oxygen, NBO) in SiO_4 tetrahedra (Lam et al 1990). This peak position may shift upwards as the values of F_o increase (Chopelas1991). The value F_o= Mg/(Mg+Fe) of an olivine can be determined from the XRF results. The peak 811-823 cm^{-1} has a higher contribution of v3 (asymmetric mode) than the 852 cm^{-1} peak. This mode is more easily affected by variations

Table 4: Comparative spectral positions of the Dergaon and Mahadevpur meteorite with fayalite, forsterite and enstatite in 10µm and 20µm region of infrared and Raman spectrum. The infrared data of Gadsden (1975) and Raman data of Griffith (1975), White (1975) is taken as standard for fayalite, forsterite and enstatite spectral position analysis.

Fayalite (Fe_2SiO_4)		**Forsterite (Mg_2SiO_4)**		**Enstatite (Mg_2SiO_3)**		**Dergaon**		**Mahadevpur**	
IR (cm^{-1})	**Raman** (cm^{-1})	**IR** (cm^{-1})	**Raman** (cm^{-1})	**IR** (cm^{-1})	**Raman** (cm^{-1})	**IR** (cm^{-1})	**Raman** (cm^{-1})	**IR** (cm^{-1})	**Raman** (cm^{-1})
--	--	--	--	1128-04	--	1112	--	1110	--
1060	--	--	--	1070-56	--	1052	--	1057	--
--	--	1000-990	--	1020-10	--	1012	--	1003	--
--	--	--	964	--	--	--	--	--	--
965-55	--	965-58	--	980-70	--	982	963	988	966
950-47	--	--	--	942-28	938	932	--	945	--
920-15	--	--	919	908-02	--	--	919	920	916
880-73	--	890	--	877-52	--	885	--	884	880
--	838	840	855	--	863	--	852	839	852
828	815	--	824	--	758	--	818	--	813
--	--	--	--	728-19	715	721	--	724	--
--	--	--	--	695-93	681	682	--	685	--
--	608	620-02	608	--	650	634	610	636	602
--	--	--	589	--	--	593	582	596	--
566-58	550	545	--	--	545	--	--	--	--
--	--	524	544	535	523	537	547	537	549
510-02	--	512-01	--	505	--	504	--	504	--
482-80	--	473-63	--	460	--	462	--	463	467
--	--	430-28	434	--	--	431	430	429	432
--	--	409-05	--	410	--	409	--	405	427
--	--	--	--	397	--	366	--	360	--
380	--	374	--	375	--	336	--	344	--
--	--	317	--	340	--	312	--	324	--
--	--	--	234	249	--	247	--	--	--
--	--	--	--	--	--	--	181	--	--

in the Si-O_{nb} force constant, and is also affected by the breakdown of SiO_4 during polymerization (Lam et al 1990). The medium intensity peak in the region 547-610 cm^{-1} occurs due to the bridging oxygen (BO). The medium intensity peak at 916-921 cm^{-1} is indicative of the polymerization. The relative peak height is a function of crystal orientation (Ishii 1978). Therefore, the systematic variations of the high-frequency Si-O bands are attributed to decreased distortion of SiO_4 tetrahedra.

4. Discussions

This is the first spectroscopic characterization of Mahadevpur H4/5 chondrite. The olivine group is identified from the compositional analysis, and is identical to the infrared and Raman results. The olivine composition of both meteorites is almost similar to each other. The strong IR and Raman absorption bands are due to olivine. It may be noted that in 20μm region Raman bands are relatively weak as compare to their infrared counterparts which is due to pyroxene.

Acknowledgements

We thank Directors, National Geophysical Research Institute, Hyderabad, and Indian Institute of Chemical Technology, Hyderabad for providing analytical facilities for characterization of the meteorites. One of us (GP) is grateful to ISRO, Department of space, Government of India, for partial financial support under PLANEX program. The authors are thankful to Prof. S. V. S. Murty, Physical Research Laboratory, Ahmedabad for his valuable discussions. Dr. P. K. Baruah, Gauhati University, Guwahati is thanked for his assistance with the infrared analysis. Special thanks to Dr. N. K. Gogoi, NGRI-Project Office, Tezpur for his cooperation in sample collection and Mr. P.K. Bhuyan, Superintendent of Police, Tinsukia, Assam for supplying the Mahadevpur meteorite specimen for study.

Correspondence to:
Bhaskar J. Saikia , e-mail: vaskar_r@rediffmail.com

References

1. Anderson, D. L., *New Theory of Earth*, Cambridge University Press, United Kingdom, 2007; 23-24
2. Bhandari, N., Murthy, S.V.S., Shukla, P.N., Mahajan, R.R., Shukla, A.D., Suthar, K.M., Parthasarathy, G., and Paliwal, B.S., Bhawad, LL6 chondrite : Chemistry, Petrology, noble gases, nuclear tracks, and cosmogenic radionuclides, *Meteoritics and Planetray Sciences* 2005, **40**: 1015-21
3. Bhattacharyya, S., Gohainbarua, A., Knowar, R., Changmai, R., Baruah, G. D., Nature of the emission band of Dergaon meteorite in the region 5700-6700Å, *Pramana*, 2004; **62**: 1299-01
4. Chopelas, A., Single crystal Raman spectra of forsterite, fayalite, and monticellite. *American Mineralogist* 1991; **76**: 1101–09
5. Dhingra, D., Bhandrai, N., Shukla, P.N., Murty, S.V.S., Mahajan, R.R., Ballabh, G.M., Lashkari, G., Shukla, A.D., Parthasarathy, G., Spectacular fall of the Kendrapara H5 chondrite, *Meteoritics and Planetary Sciences* 2004; **39**: A121-32
6. Freund, M. M., Freund, F. T., Solid solution model for I interstellar dust gains and their organics. *The Astrophy. J.* 2006; **639**: 210-26
7. Gadsden, J. A., *Infrared spectra of Mineral and related Inorganic Compounds*. USA: Butterworths. 1975; 165-90
8. Gohainbarua, A. Barua, B. P., Bhattachyya, S., Baruah, G. D., Spectroscopic investigation of Dergaon meteorite with reference to 10μm and 20μm bands., *Pramana* 2003; **60**: 47-52
9. Griffith, W.P., *Raman spectroscopy of Terrestrial minerals in Infrared and Raman Spectroscopy of Lunar and Terrestrial Minerals*, Clarence Karr, Jr.(Ed), Acadimic Press, New York, 1975: 299-23
10. Grossman, J.N., Zipfel, J. ,The Meteoritical Bulletin, No.85, 2001, Sept. *Meteritics & Planetary Science* 2001;**36**: A293-22
11. Hofmeister, A.M., Single-crystal absorption and reflection infrared spectroscopy of forsterite and fayalite. *Physics and Chemistry of Minerals*, 1987; **14**: 499–13
12. Iishi, K., Lattice dynamics of forsterite. *American Mineralogist* 1978; **63**: 1198-08
13. Lam, P.K., Yu, R., Lee, M W., and Sharma, S K., Relationship between crystal structure and vibrational mode in Mg_2SiO_4. *American Mineralogist* 1990; **75**: 109-19
14. Mason, B., *Meteorites*, Jhon Wiley and Sons, New York, 1962: 65
15. Nakamoto K., *Infrared and Raman Spectra of Inorganic and Coordination Compounds*, New York, John Wiley & Sons, 1978: 105-39
16. Nyquist, R. A. & Kagel, R. O., *Infrared Spectra of Inorganic Compounds, 3800-45cm^{-1}* , Academic Press: New York, 1971: 16
17. Paques-Ledent, M, .Th., and Tarte, P., Vibrational studies of olivine- type compounds. I. The i.r and Raman spectra of the isotopic species of Mg_2SiO_4. *Spectrochimica Acta* 1973; 29 A: 1007-16

18. Parthasarathy, G and Sarma, S. R., High-temperature electrical and thermal properties of Burdett, Dalhart, Faucet and Wellman ordinary chondrites, *Curr. Sci*. 2004; 86(10): 1366-68
19. Philip, A.B., Alex W.R. B., Tim Jull, A. J., Ancient Meteorite Finds and the Earth's Surface Environment, *Quaternary Research* 2000; **53**: 131–42
20. Piriou, B., and McMillan, P., The high frequency vibrational spectra of vitreous and crystalline orthosilicates. *American Mineralogist*, 1983; **68**: 426-43
21. Shukla, P.N., Shukla, A.D., Rai,V.K., Murthy, S.V.S., Bhandari, N., Goswami, J.N.,Mazumder,A.C., Phukon, K., Duorah, K.,Greenwood,R.E.,and Franchi,I.A., The Dergaon (H5) chondrite: Fall, classification, petrological and chemical characteristics, cosmogenic effects, and noble gas records, *Meteoritics & Planetary Science*, 2005; **40**: 627–37
22. White, W.B., *Structural interpretation of Lunar and Terrestrial minerals by Raman spectroscopy, in Infrared and Raman Spectroscopy of Lunar and Terrestrial Minerals*, Clarence Karr, Jr.(Ed),Academic Press, New York, 1975; 325-58
23. Weisberg, M. K., Smith, C., Benedix. G., Foloco. L., Righter, K., Zipfel, J., Yamaguchi, A., and Chennaouiaoudjehane, H., The Meteoritical Bulletin, No. 94. September 2008, *Meteoritics & Planetary Science* 2008; **43**(9): 1551–1588

ISSN: 1545-1003

The journal of American Science

Normal paper structure for the Journal of American Science:

Each manuscript is suggested to include the following components but authors can do their own ways:

(1) The complete article title.
(2) Each author's full name; institution(s) with which each author is affiliated, with city, state/province, zip code, and country; and the name, complete mailing address, telephone number, facsimile number (if available), and email address for all correspondence.
(3) **You must put at least one email address under the authors' address.**
(4) Abstract: including Background, Materials and Methods, Results, and Discussions, 100-300 words preferred.
(5) Key Words.
(6) Introduction.
(7) Materials and Methods.
(8) Results.
(9) Discussions.
(10) Acknowledgments.
(11) Correspondence to.
(12) References.

Description of Manuscript Preparation and Format:

(1) Software: Microsoft Word file.
(2) Font: Normal, Times New Roman, 10 pt, single space.
(3) Indent: 8 spaces in the beginning of each new paragraph.
(4) Manuscript: Don't use "Footnote" or "Header and Footer".
(5) Spelling check: Do spelling check when you finish.
(6) Color: Email and website addresses are blue, and all other contents are black.
(7) Abstract: 100-300 words are preferred, and remember to add "[The Journal of American Science. 2009;x(x):xx-xx]. (ISSN 1545-1003)" in the end of abstract.
(8) Page setup: Margins: top 72 pt, bottom 72 pt. left 72 pt, right 72 pt.
(9) Paper size: Letter, width 612 pt, height 792 pt.
(10) Layout: Header 36 pt, Foot 36 pt.
(11) Title: Use Title Case in the title and subtitles, e.g. "Debt and Agency Costs".
(12) Figures and Tables: Use full word of figure and table, e.g. "Figure 1. Annul Income of Different Groups", Table 1. Annual Increase of Investment".
(13) References: Cite 10-20 references preferred, by "last name, year", e.g. "(Smith, 2003)". References should include all the authors' last names and initials, title, journal, year, volume, issue, and pages etc.
(14) *Reference Examples*: Journal Article: Hacker J, Hentschel U, Dobrindt U. Prokaryotic chromosomes and disease. Science 2003;301(34):790-3.
(15) Book: Berkowitz BA, Katzung BG. Basic and clinical evaluation of new drugs. In: Katzung BG, ed. Basic and clinical pharmacology. Appleton & Lance Publisher. Norwalk, Connecticut, USA. 1995:60-9.
(16) Insert page number by bottom / center.
(17) Header for odd: Marsland Press, Journal of American Science 2009;x(x):xx-xx.
(18) Header for even: short title, Family name of the first author, et al.
(19) Footer: http://www.americanscience.org americansciencej@gmail.com.
(20) Submission Address: sciencepub@gmail.com, editor@sciencepub.net, Marsland Press, P.O. Box 21126, Lansing, Michigan 48909, The United States, 347-321-7172.
(21)

Comparison of Theoretical and Experimental Power output of a Small 3-bladed Horizontal-axis Wind Turbine

K.R. Ajao
Department of Mechanical Engineering, University of Ilorin, Ilorin, Nigeria
E-mail: ajaomech@unilorin.edu.ng
&
J.S.O. Adeniyi
Formerly of the Department of Mechanical Engineering, University of Ilorin, Ilorin, Nigeria
E-mail: adeniyijso@yahoo.com

Abstract

A small three-bladed horizontal axis wind turbine was parameterized, modelled, developed and tested for power performance. The turbine blades were fabricated from *Mansonia Altissima* wood with a rotor swept area of 3.65 sq. metres and a blade pitch angle of 7^0. The turbine was installed on the roof top of University of Ilorin, Faculty of Engineering Central Workshop Building at a hub height of 14.9 metres from the ground level while the turbine generator was sourced locally. The direct current (d.c.) power output of the test turbine measured at the battery bank terminal by a "Feigao" Power Analyzer. Installed at about 8.4m from the test turbine is a meteorological tower (MET) carrying an "APRS" anemometer with a data logger and measured the wind speed and direction over the test period. The cut-in wind speed, that is, the speed at which the wind turbine starts to produce power was determined to be 3.5 m/s. One minutes averages of wind speed and power output have been used to determine the power curve for the wind turbine in accordance with IEC(International Electrotechnical Commission) 61400-12-1 guideline for small wind turbines. Measured power increase consistently with increased wind speed and the power curve obtained compared fairly well with other standard power curves. [Journal of American Science 2009;5(4):79-90]. (ISSN: 1545-1003).

Keywords: Pitch angle, hub height, meteorological tower, anemometer, power curve.

1. Introduction

The precise date when man first used a machine to assist him in his daily work would be virtually impossible to determine. However, it seems clear that the earliest machines were based on the principle of rotation as a means of providing continuous motion for routine tasks such as grinding corn or pumping water. Thus, there were the mills, driven by animal or man-power, in which the rotating shaft was vertical and driven by a long horizontal beam, fixed to it, and pulled or pushed around by the animal walking round in a circular path (Golding, 1976).

Wind energy has been used for a long time. The first field of application was to propel boats along the river Nile around 5000B.C. By comparison wind

turbines technology is a fairly recent invention. The first simple windmills were used in Persia as early as the 7th century for irrigation purposes and for milling grains.

The aerodynamic research for wind turbines has contributed significantly to the success of modern way of harnessing wind energy. For most unsolved problems engineering rules have been developed and verified. All of these rules have limited applicability, and the need to replace these rules by physical understanding and modeling is increasing.

Simplified analyses of horizontal-axis wind turbine flows aimed at overall aerodynamic performance prediction developed for modern rotor theories are available in literature. There have, however, been few thorough tests of the adequacy of such analyses by direct comparison with actual measurements over a wide range of configurations and conditions.

The conversion of wind energy to useful energy involves two processes: the primary process of extracting kinetic

energy at the rotor axis, and the secondary process of the conversion of such mechanical energy into useful electrical energy depicted in Figure 1.

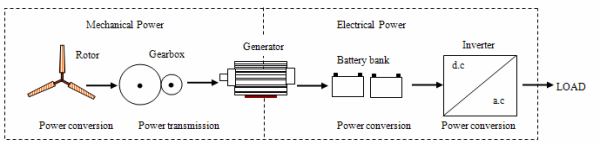

Figure 1: Conversion from wind power to electrical power in a wind turbine

1.1 Energy in the wind

Wind is merely air in motion. It is produced by the uneven heating of the Earth's surface by energy from the Sun. Since the Earth's surface is made of different types of land and water, it absorbs the Sun's radiant energy at different rates. Much of this energy is converted into heat as it is absorbed by land areas, bodies of water and the air over the Earth surface (Ajao et al., 2009). The air has mass, though its density is low, and when this mass has velocity, the resulting wind has kinetic energy which is proportional to 1/2[mass x (velocity)^2]. The mass of air passing in unit time is ρAV and the kinetic energy passing through the area in unit time (power available in the wind) is:

$$P_w = \frac{1}{2}\rho AV.V^2 = \frac{1}{2}\rho AV^3 \qquad (1)$$

ρ = Air density (approx.1.225 kg/m^3 at sea level)

V = Velocity of wind (m/s)

A = Area through which the wind passes normally (m^2).

This is the total power available in the wind (approx. $3.6x10^{12}kW$) obviously, only a fraction of this power can actually be extracted.

The power extracted by a wind turbine can therefore be given as:

$$P = k.\frac{1}{2}\rho AV^3 \qquad (2)$$

$$k = C_p.N_g.N_b$$

C_p = coefficient of performance or power coefficient (approx. 0.593)

N_g = Generator efficiency

N_b = Gearbox/bearing efficiency

The torque generated by the wind turbine is:

$$T_s = \frac{P}{\omega_s} \qquad (3)$$

T_s = mechanical torque at the turbine side

P = power output of the turbine

ω_s = rotor's speed of the wind turbine

The power coefficient C_p is the percentage of power in the wind that can be converted into mechanical power and the ratio of the blade tip speed to the wind speed is referred to as the tip-speed ratio (TSR).

$$TSR = \frac{\omega_s R}{V} \quad (4)$$

R is radius of the wind turbine rotor.

2. Small Wind Turbines

All wind turbines can be characterized as either Horizontal Axis Wind Turbines (HAWT) or Vertical Axis Wind Turbines (VAWT). In HAWT, the rotor spins about an axis horizontal to the earth's surface. The rotor of a VAWT spins about an axis perpendicular to the Earth's surface.

Vertical axis wind turbines are typically developed only for built environment. Changes in wind direction have fewer negative effects on this type of turbine because it does not need to be positioned into the wind direction. However, the overall efficiency of these turbines in producing electricity is lower than HAWT. VAWTs are categorized as Savonius or Darrieus types, according to the principle used to capture the wind flow. For the Savonius type, the wind pushes the blades, which implies that the rotation speed is always lower than the wind speed. Contrary to that, the shape of the rotor of the Darrieus type makes it possible for the rotor to spin faster than the wind speed.

Rotors of HAWT are placed on towers to position them where the wind speed is fastest and exhibits most power (Jonkman, 2003). A nacelle typically resides atop the tower and contains the support structure for the rotor, the rotor shaft, a gearbox and the electric generator (alternator). The gearbox is used to transform the low-speed high-torque power of the rotor to high-speed, low-torque power that can run the electric generator.

Rotor can be positioned upwind or downwind of the tower. Downwind rotor configurations can track the wind automatically as wind direction changes. However, the wind must flow around the tower to reach the rotor of a downwind turbine. This results in complex flow patterns and periodic fluctuations in aerodynamic loads, which have important dynamic effects on the turbine structure. Flow passing through the rotor plane is unobstructed by the tower for upwind rotor configurations.

The hub structure connects the blades to the drive shaft. Hubs are generally characterized as either rigid or teetering. In rigid hub designs, the hub is rigidly attached to the drive shaft. In contrast teetered hubs are connected to the drive shaft by means of a teeter pin, a bearing that permits the rotor to rock into and out of the plane of rotation. Teetered hubs have the benefit that bending moments brought about by thrust forces acting on the blades are not transferred to the nacelle and tower structure. Consequently, the nacelle and tower structures of turbines with rigid hub must be designed more robustly than those with teetered hub.

Small wind turbine need to be reliable, affordable and almost maintenance free. To meet these criteria, optimal turbine performance is sometimes sacrificed for simplicity in design and operation (Andrew, 2005). Thus, rather than using the generator as a motor to start and accelerate the rotor when the wind is strong enough to begin producing power, small

wind turbines rely solely on the torque produced by the wind acting on the blades.

Furthermore, small wind turbines are often located where the generated power is required, which is not necessarily where the wind resource is best. In low or unsteady wind conditions slow starting potentially reduces the total energy generated. Also, a stationary wind turbine fuels the perception of wind energy as an unreliable energy source.

The main technical challenge in the design of a small wind turbine is to come up with a system configuration and control algorithm that maximizes wind energy production from the turbine and also provide favourable charging conditions for batteries. This task is complex because of the variability of the wind, which results in varying wind turbine power output. Ideally, the system configuration and its control should optimize the match between the wind turbine rotor and load, thereby allowing the maximum available power from the wind to be used, while at the same time charging the batteries with an optimum charge profile (Corbus et al., 1999).

The generators of small turbines often cause a significant resistive torque that must be overcome aerodynamically before the blades will start turning. Furthermore, pitch control is rarely used on small wind turbine because of cost. Thus, it is not possible to adjust the turbine blade's angle of attack to the prevailing wind conditions. This problem is particularly acute during starting.

A further major difference is that small turbines usually operate with varying shaft speed in an attempt to maintain maximum performance as the wind speed varies. Many large turbines run at constant speed as this allows the generator to maintain synchronicity with the utility grid.

The IEC 61400-2 (International Electrotechnical Commission) defines a small turbine as having a swept area less than 200m^2, which correspond to a power output of about 120kW. In addition, there is a further subdivision in that turbine of swept area less than 2m^2 (about 1.2kW) do not need to have their tower included in the certification process (Introduction to Wind Turbine Technology: accessed at http:// www.wind.newcastle.edu.au/notes.html , on 12th February, 2007). Clausen & Wood (1999) have made a further subdivision as shown Table1.1.

Table 1. Operating parameters of small wind turbines

Category	Power (kW)	Turbine blade radius(m)	Maximum rotor speed (rpm)	Generator type(s)
Micro	≤1.2	1.5	700	Permanent magnet (PM)
Mid-range	1-5	2.5	400	Permanent magnet or induction
Mini	20-100	5.0	200	Permanent magnet or induction

2.1 Wind Turbine Blades

All forms of wind turbine are designed to extract power from a moving air stream. The blades have an airfoil cross-section and extract wind by a lift force caused by a pressure difference between blade sides. When air passes over an airfoil section; it travels faster over the top of the blade than it does below it. This makes the air pressure above the blade lower than it is below. Due to the unequal pressures the blade experiences a lifting force (BWEA). For maximum efficiency, the blades often incorporate twist and taper.

The mechanical power produced by a rotor is purely a function of the blade geometry and the incident velocity. The design parameters that affect

aerodynamic performance include blade pitch (angle of attack), taper, and twist distribution. For a given blade, its geometric shape is usually fixed, i.e. the aerodynamic shape, taper and twist distribution do not change.

The torque produced by the rotor can be controlled in two ways: changing the geometry by varying the blade pitch angle, or by changing the rotor's rotational speed so that the rotor operates at the optimal blade tip speed ratio.

In the beginning most wind turbine blades were adaptations of airfoil developed for aircraft and were optimized for wind turbine uses. In recent years development of improved airfoil sections for wind turbines has been on going. The prevailing tendency is to use NACA 63 (National Advisory Council on Aeronautics) and NREL S809 (National Renewable Energy Laboratory) (Ajao, 2008) airfoil cross-section that may have modifications in order to improve performance for special applications and wind conditions.

2.2 The Gearbox

The gearbox is required to speed up the slow rotational speed of the low speed shaft before connection to the generator. The speed of the blade is limited by efficiency and also by limitations in the mechanical properties of the turbine and supporting structure. The gearbox ratio depends on the number of poles and the type of generator. A direct driven generator (without gearbox) would require a generator with 600 poles to generate electricity at 50Hz.

2.3 Turbine generator

The generator used in geared wind turbines are more or less standard off-the-shelf electrical machines, so that major development steps were not necessary. There are different types of generators depending on their configuration and areas of application.

The wind turbine generator converts mechanical energy to electrical energy. The efficiency of an electrical generator usually falls off rapidly below its rated output. The phenomenon of inducing a current by changing the magnetic field in a coil of wire is known as electromagnetic induction which underpins the design of most electric generators (Cotrell, 2002). With the important exception of electrostatic generators such as the Van de Graf machine, all important schemes for converting mechanical motion into electrical energy depends on Faraday's Law of electromagnetic induction .

3. Aerodynamic theory of wind turbines

Accurate models of the aerodynamic aspects of wind turbines are essential to successfully design and analyze wind energy systems. Wind turbine aerodynamic models are used to relate wind inflow conditions to loads applied to the turbine (Jonkman, 2003).

The true fluid flow passing around and through a wind turbine is governed by the Navier-Stokes equations. Unfortunately, these equations are so complex that analytical solutions have been found for only a few simple cases.

The subsequent analysis develops the most common aerodynamic theory employed in the wind turbine design and analysis environment, the blade element and momentum theory (BEM). To aid the understanding of combined blade element and momentum theory it is useful initially to consider the rotor as an actuator disc. Although this model is very

simple, it does provide valuable insight into the aerodynamics of the rotor (Bossanyi, 2001).

3.1 Actuator Disc Theory and the Betz limit

In the one-dimensional Rankine-Froude actuator disc model, the rotor is represented by an 'actuator disc' through which the static pressure has a jump discontinuity (Jonkman, 2003). Consider a control volume fixed in space whose external boundary is the surface of a stream tube. The fluid passes through the rotor disc, a cross-section of the stream tube upwind of the rotor, and a cross-section of the stream tube downwind of the rotor as shown in Figure 2.

The following assumptions are made in the actuator disc model:

(1) Purely One-dimensional analysis

(2) Infinitely thin disc which offer no resistance to air passing through it.

(3) Wind is steady, homogenous and fixed in direction.

(4) Air is incompressible, inviscid and irrotational.

(5) Both the flow and the thrust are uniform across the disc. The flow is uniform at the upwind (station 0) and downwind (station 3) boundaries of the control volume.

(6) The upwind and downwind boundaries are far enough removed from the rotor that the static pressure at these points is equal to the unobstructed ambient static pressure. The static pressure on the stream tube portion of the boundary is also equal to the unobstructed ambient static pressure.

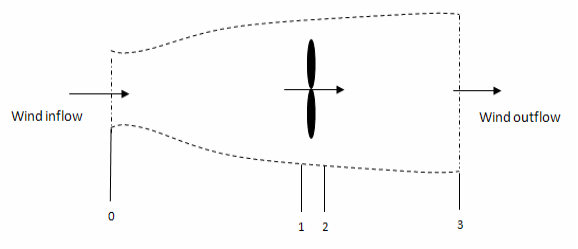

Figure 2. Control volume of actuator disc model (source: Jonkman, 2003)

For a wind turbine rotor to act as an actuator disc, the rotor would have to be composed of an infinite number of very thin, dragless blades that rotate with a tip speed much higher than that of the incoming wind. Also, station 1 designated to be slightly upwind and station 2 slightly downwind of the rotor. Since air does not pass through the stream tube porting of the control volume boundary by definition of a stream tube, applying the conservation of mass (which asserts that the instantaneous rate of change of mass within a control volume must equal the net flux of mass out of the control volume) to the control volume gives:

$$V_0 A_0 = V_1 A_1 = V_2 A_2 = V_3 A_3 \qquad (5)$$

V_i is the wind speed at station i and A_i is the cross-section area of station i. Since V_1 is equal to V_2 according to assumption (5) and since A_1 equal A_2 by necessity, the component of the wind speed and cross sectional area of the plane of the disc are designated without subscripts for the rest of this analysis (i.e. $V = V_1 = V_2 \quad and \quad A = A_1 = A_2$).

The thrust at the rotor disc, T, can be found by applying the conservation of linear momentum to the control volume in the axial direction.

This results in:

$$T = \rho A_0 V_0^2 - \rho A_3 V_3^2 \quad (6)$$

Substituting equation (3.1) into equation (3.2) gives

$$T = \rho A V (V_0 - V_3) \quad (7)$$

ρ is the density of the air. The thrust at the rotor disc T is also the differential pressure between station 1 and 2 multiplied by the disc area.

$$T = (P_1 - P_2) A \quad (8)$$

Since no work is done on either side of the turbine rotor, Bernoulli's equation can be applied to obtain the pressure incorporated into equation (3.4)

$$P_0 + \frac{1}{2}\rho V_0^2 = P_1 + \frac{1}{2}\rho V^2 \quad (9)$$

and,

$$P_3 + \frac{1}{2}\rho V_3^2 = P_2 + \frac{1}{2}\rho V^2 \quad (10)$$

Pressure P_o *and* P_3 are identical by assumption (6) so pressure P_1 and P_2 can be eliminated from equation (3.4) with the help of equations (3.5) and (3.6) to obtain,

$$T = \frac{1}{2}\rho A (V_0^2 - V_3^2) \quad (11)$$

By equating equations (3.3) and (3.7), the velocity of the flow through the rotor disc is the average of the upwind and downwind velocities

$$V = \frac{V_0 + V_3}{2} \quad (12)$$

An axial induction (sometimes called interference) factor a is defined as the fractional decrease in wind velocity between the freestream (upwind) and the rotor plane:

$$a = \frac{V_0 - V}{V_0} \quad (13)$$

or,

$$V = V_0 (1 - a) \quad (14)$$

Using equation (3.8)

$$V_3 = V_0 (1 - 2a) \quad (15)$$

The velocity lost at the rotor plane, $V_0 - V$ is known as the induced velocity.

As a increases from zero, the downwind flow speed steadily decreases until, a = ½, meaning that the rotor has completely stopped and the simple theory is no longer applicable.

By substituting for V_3 from equation (3.11), equation (3.7) can be re-written as:

$$T = \frac{1}{2}\rho A V_0^2 4a(1 - a) \quad (16)$$

The power extracted from the wind by the rotor, P, is the product of the thrust, T, and the wind velocity at the rotor plane, V, from equation (3.10)

$$P = \frac{1}{2}\rho A V_0^3 4a(1 - a)^2 \quad (17)$$

The non-dimensional power coefficient C_p representing the fraction of available power in the wind that is extracted by the turbine, is defined as:

$$C_P = \frac{P}{\frac{1}{2}\rho A V_0^3} \quad (18)$$

Substituting equation (3.13) into equation (3.14) yields;

$$C_P = 4a(1 - a)^2 \quad (19)$$

The dimensionless thrust coefficient C_T is therefore given as,

$$C_T = \frac{T}{\frac{1}{2}\rho A V_0^2} = 4a(1 - a) \quad (20)$$

The maximum power coefficient C_p occurs when a is 1/3.

Substituting for a in equation (3.15) gives:

$$C_p = \frac{16}{27} \approx 0.593 \qquad (21)$$

This is known as Betz limit.

The thrust coefficient C_T has a maximum value of 1 when a = ½

Therefore the maximum possible efficiency for an idealized wind turbine is roughly 59.3%.

4. Model Turbine

Capturing the characteristics and nuances of three-dimensional flow separation in a stochastic inflow environment on a large piece of rotating machinery poses as significant a challenge as understanding the underlying fluid mechanics.

A number of design codes have been used over the last decade to model the wind turbine's dynamic behaviour. They carry out design calculations or develop dynamic and steady state models for all components within a wind turbine. In a longer term, they can be used in a complete optimization of a wind turbine system including models for mechanical part (wind, drive train, stall and variable pitch control),model for generators (induction generator, synchronous generator, permanent magnet generator), and models for power converters, transformers, and the grid (Florin et al., 2004).

The Visual Basic program was written because of its flexibility and ease of its accessibility in formulating the design to suit the desired objective. Standard shaft and gears equations in conjunction with wind energy equations were used to develop the Visual Basic program hereby referred to as WINMECH. The input parameters to the program and the output results at the rated wind speed of 10 m/s and operating time of six (6) hours per day, gives a power output of about 590 Watts and 3.56 kW/hr of energy

4.1 Weibull Distribution and Annual Energy Production (AEP)

The expected annual energy production (AEP) for the model turbine can be estimated at rated wind speed and this will later be compared with that of the test wind turbine. The Visual Basic-modelling program is run at different wind speed and the expected power output is serves as input data to the WINMECH turbine performance model program.

In the WINMECH program, shown in Figure 5, the wind speed probability is calculated as a Weibull curve defined by the average wind speed and a shape factor k. For each wind speed, instantaneous wind turbine power (W) is multiplied by the Weibull wind speed probability (f). This cross product (net W) is the contribution of wind speeds to average turbine power output. The sum of these contributions is the average power output of the turbine on a continuous 24 hours basis. Air density factor is the reduction from sea level performance.

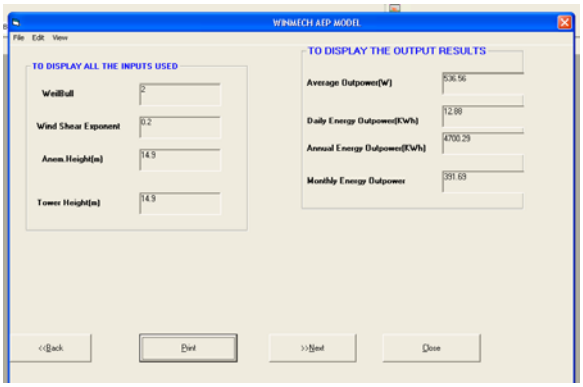

Figure 3. Model turbine annual energy output estimation using WINNMECH

5. The Test Turbine

The wind turbine under test is installed on the roof top of University of Ilorin, Faculty of Engineering Central Workshop at about 14.9m from the ground. Ilorin, Nigeria is on latitude 8.5^0N and the site average temperature and air density are 27^0C and 1.21kg/m^3 respectively (Lasode, 2004).

The test turbine shown in Figure 4, has a rotor diameter of 2.15m and a rated power of 110watts at 10m/s. It is a three-bladed, upwind variable speed, horizontal axis having blade pitch angle (angle of attack) of 7^0. It is permanent wind facing at 285^0 of compass North. The turbine uses an automobile alternator (generator) modified to higher rating to produce d.c. power output measured by a FEIGAO Power Analyzer .The output power is stored in two 12V d.c. batteries connected in parallel.

Installed at about 8.4m from the test turbine is a meteorological tower (MET). This is more than three rotor diameters from the test turbine in the measurement sector as required by the IEC standard. The MET tower carries an APRS anemometer at hub height transmitting wind data to a data logger housed inside the Data Centre. The data logger supports Secure Digital (SD^{TM}) card up to 128MB where all the wind data are logged and later transferred to a compatible personal computer (PC) for analysis.

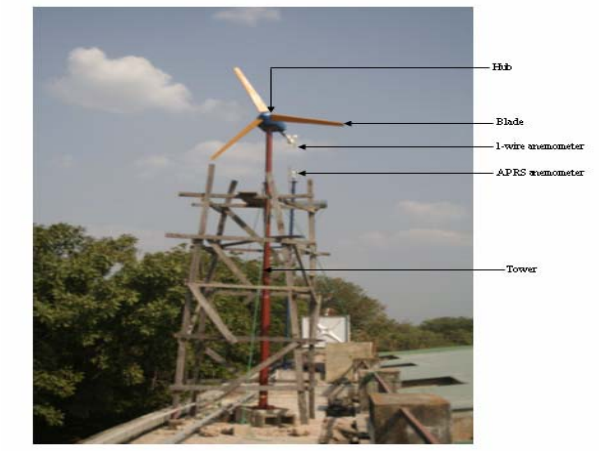

Figure 4. Test Turbine showing anemometers and Meteorological Tower (MET)

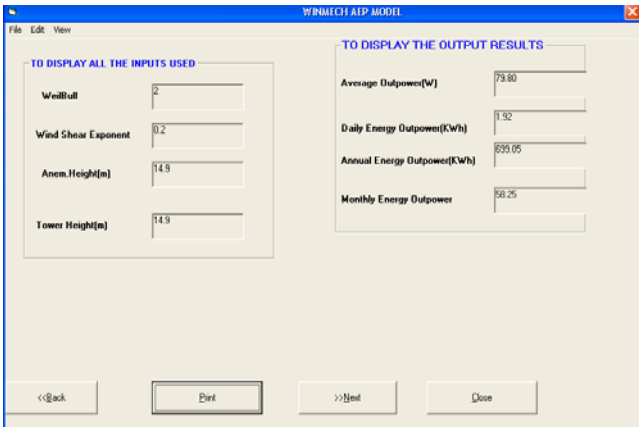

Figure 5. Test turbine annual energy output determination using WINMECH

6. Power Curves Analysis

The amount of power that a wind turbine produces depends on the wind speed at the time. The power curve describes the relationship between the wind speed and the power that the turbine generates.

6.1 Measured (d.c.) Power

Table 2 below shows the measured direct current (d.c.) power at site average air density (1.21 kg/m^3) and normalized to the power at sea level air density

(1.225 kg/m^3). Normalization to sea level air density is done by multiplying measured power by the ratio of sea level air density to site average air density. Measured wind speed is also binned and normalized. The IEC standard requires at least three one-minute points per bin. This condition was met except for normalized wind speed of 18 m/s, 19 m/s and 20 m/s.

Table 2. Direct current (d.c.) power at site average air density and normalized to sea level air density.

Wind Speed (m/s)	Normalized Wind Speed (m/s)	Measured Power (d.c.) at site average air density (W)	Power (d.c.) normalized to sea level air density (W)
1	1.4	0	0
2	2.3	1.33	1.35
3	3.2	2.57	2.61
4	4.3	8.80	8.92
5	5.8	14.54	14.74
6	6.7	23.20	23.53
7	7.4	32.20	32.65
8	8.2	63.00	63.89
9	9.3	97.20	98.57
10	10.1	110.20	111.75
11	11.7	159.00	161.23
12	12.4	166.10	168.43
13	13.5	170.80	173.20
14	14.2	209.94	212.89
15	15.4	275.25	279.12
16	16.2	282.62	286.59
17	17.4	284.19	288.18
18	18.1	285.00	289.00
19	19.8	289.53	293.60
20	20.9	381.10	386.45

The power curves for the measured d.c. power at site average air density and normalized to sea level air density are shown in Figure 6 and Figure 7.

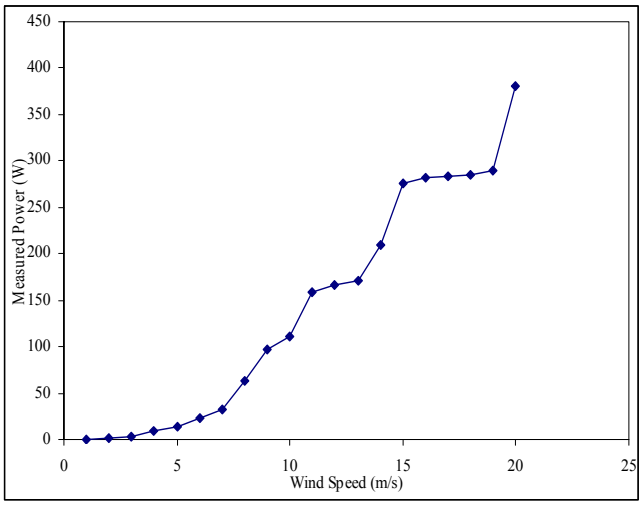

Figure 6. Direct current (d.c.) Power Curve at site average air density, 1.21kg/m^3

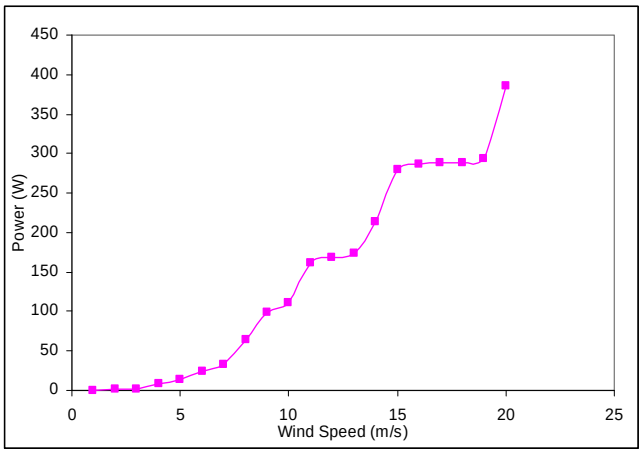

Figure 7. Direct current (d.c.) Power Curve at sea level air density, 1.225kg/m^3

6.2 Measured Versus Model Power Curve

To determine the performance of the test turbine, measured power output i.e. the actual power produced by the turbine in operation is compared to the power of the modelled turbine. Figure 8 below shows the comparison of the modeled turbine and the test turbine power.

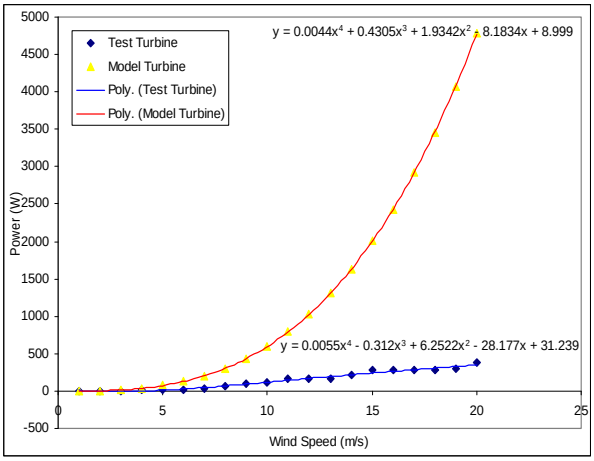

Figure 8. Model vs. Measured power curve.

7. Discussion

The result of the wind speed measurements indicated that the daily average wind speed is lower than the cut-in wind speed and for most part of the day the wind turbine is idling. Normalization to sea level air density has no significant effect on the result.

Measured power increases consistently with increased wind speed. The resulting power curve showed some discrepancies at certain wind speed but compared favourably with standard power curves. The curve fit of the test turbine and that of the model turbine indicated that the projected power output of the test turbine at the cut-out wind speed of 25m/s is approximately 507.8W.

Using the WINMECH modeling program, the average output power of the test turbine is 80W and the annual energy output is 698kW.These results when compared to the average output power of 536W and annual energy output of 4698kWh of the model turbine yields a capacity factor of approximately fifteen percent (15%).

8. References

1. Ajao K.R, Mahamood M.R and Iyanda M.O (May, 2009). Interface for modeling the power output of a small wind turbine**.** Indian Journal of Science and Technology Vol.2 No 5
2. Andrew K.W (September, 2005). Aspects of the Aerodynamics and Operation of a Small Horizontal Axis Wind Turbine. Ph.D. Thesis, Department of Mechanical Engineering, University of Newcastle, Australia
3. Bossanyi E (2001). Bladed for Windows Theory Manual, 282/BR/009 ISSUE: 010 Garrad Hassan and Partners Limited
4. Bossanyi E (2001). Bladed for Windows Theory Manual, 282/BR/009 ISSUE: 010 Garrad Hassan and Partners Limited
5. Clausen P.D and Wood D.H (1999). Research and Development issues for Small Wind Turbines. Renewable Energy 16, pp.922-927
6. Corbus D, Baring-Gould I, Drouilhet S, Gervorgian V, Jimenez T, Newcomb C and Flower L (1999). Small Wind Turbine Testing and Applications Development. NREL/CP-500-27067
7. Cotrell J (January, 2002). A preliminary Evaluation of a Multiple-Generator Drive train Configuration for Wind Turbines. NREL/CP-500-31178
8. Florin I, Anca D.H, Clemens J, Poul S and Frede B (March, 2004). Advanced Tools for Modelling, Design and Optimization of Wind Turbine System. Conference proceedings, Nordic wind power conference,

Chamlers University of Technology, Finland March, pp. 1-12.

9. Golding E.W (1976). The generation of electricity by wind power. E&F.N SPON Ltd, London
10. Jonkman J.M (2003). Modelling of the UAE wind turbine for refinement of FAST-AD. NREL/TP-500-34755, National Renewable Energy Laboratory, Golden Colorado, U.S.A
11. Lasode O.A (2004). An Improved Solar Cabinet Dryer with Convective heat Transfer. Journal of Applied Science, Engineering and Technology, Vol.4 No.2; pp.32-39
12. www.wind.newcastle.edu.au/notes.html. Introduction to Wind Turbine Technology, Accessed on 12th February, 2007

Residues of Organochlorine Pesticides in Vegetables from Deyang and Yanting Areas of the Chengdu Economic Region, Sichuan Province, China

Odhiambo Joshua Owago[1]*, Shihua Qi*[1], Xing Xinli[1], Zhang Yuan[1] and Muhayimana Annette Sylvie[1]

[1]School of Environmental Studies and MOE Key Laboratory of Biogeology and Environmental Geology, China University of Geosciences, Wuhan, 430074, China

joowago@hotmail.com; shihuaqi@cug.edu.cn

Abstract

Residual levels of organochlorine pesticides (OCPs) were determined in 34 samples of 19 varieties of vegetables collected from selected sites around Deyang city and Yanting County, Southwest China, in June and September 2007. The analytical method included soxhlet extraction with a mixture of dichloromethane and acetone (2:1 vv). Clean-up was done on superposed layers of alumina/silica gel (1:2 v/v) impregnated with concentrated sulfuric acid. The determinations were done using a gas chromatograph with electron capture detector (GC-ECD). The compounds targeted are: isomers of hexachlorocyclohexane or HCHs (α-HCH, β-HCH, γ- HCH or lindane and δ-HCH); isomers/metabolites of dichloro-diphenyl-trichloroethane (DDTs) namely p,p^1-dichloro-diphenyl-dichloroethylene (p,p^1-DDE), p,p^1-dichloro-diphenyl-dichloroethane (p,p^1-DDD), p,p^1- and o,p^1-dichloro-diphenyl-trichloroethane (p,p^1-DDT and o,p^1-DDT). The results indicated that all the vegetable samples had some levels of one or more OCPs in them. Residues of DDTs were found in 94.12% while HCHs were in 91.18% of all the samples analyzed indicating high incidence of these xenobiotics in the vegetables from the areas investigated. Among the HCH isomers, γ- HCH was the most prevalent but β-HCH was the most abundant indicating both old and fresh inputs of HCHs. DDT metabolites p,p-DDE and p,p'-DDD were more prevalent than the parent material, p,p-DDT suggesting minimal fresh inputs of DDT. The OCPs residue levels in the vegetables were generally low (≤ 1.3 ng/ g wet weight) except in one sample of green pepper (*Capsicum annum L*) in which the concentrations (ng/g wet weight) of o,p'-DDT (82.59), p,p'-DDE (61.41) and total DDT (148.44), all exceeded the Chinese Extraneous Maximum Residue Limit of 50 ng/ g for DDTs in vegetables according to the guidelines of the Chinese quality standard for food (GB 2763-2005). Considering the industrial and agricultural growth around the areas investigated, a deeper investigation and regular ecological and foodstuff monitoring is recommended.
[Journal of American Science 2009; 5(4):91-100]. (ISSN: 1545-1003).

Key words: Vegetables, Organochlorine pesticides, Deyang, Yanting

1.0 Introduction

Oraganochlorine pesticides (OCPs) are among the xenobiotics that have become constituents of the biosphere due to their great use all over the world, stability in several natural conditions and mobility in the environment. In china, large quantities of OCPs, particularly hexachlorocyclohexane (HCH) and dichlorodiphenyltrichloroethane (DDT) were produced and used in agriculture and public health until 1983. Therefore, the occurrence of excessive OCPs residues in Chinese environments is believed to be serious and widespread and has over the years sustained considerable research interests in elucidating environmental contamination status and human exposure in the country. Sichuan province is one of the leading agricultural regions in China and it is an important Southern China vegetable production base (Chen et al, undated). To keep the pest effects at economical levels, obviously, Sichuan province has been a major consumer of pesticides including OCPs. It was estimated that between 10,000 and 20,000 metric tons (MT) of technical HCH and 16 000 MT of DDT were used in Sichuan during the period 1951-1984 and these were among the highest usages in China (Li et al, 1998; Liu et al, 2006). The extent of usage suggests that environmental contamination could also be widespread; however, the magnitude and distribution of this is only just beginning to be accurately characterized.

A survey recently undertaken in the Chengdu Economical Region (CER) which is the main agricultural and industrial region in Sichuan, found out that OCPs were still detectable in all surface soils

despite having been forbidden more than 20 years in China (Xing et al, 2009). The study also revealed that the DDT residual contents of agricultural soils in some areas including Deyang and Yanting, were in excess of 50 ng/g, which is maximum permissible level in agricultural soils in China, according to the Chinese environmental quality standard for soils (GB15618-1995). This called for explanations about the possible occurrence of OCPs in food crops grown in these soils since several crops are known to accumulate OCP in edible parts up to critical levels, which may contribute to dietary intake of the contaminants. In addition, a national dietary intake survey of 1992 showed that Sichuan was one of the regions in China with high dietary intakes of DDT (Chen and Gao, 1993). Already, Li et al (2006) have reported a high prevalence of β-HCH (91.2%), p,p'-DDE (92.1%) and p,p'-DDT (91.2%) as well as positive correlation between high levels of these compounds in the subjects' sera on one hand and breast cancer on the other, particularly among premenopausal women in the province. Therefore, information on OCPs residue levels is of paramount importance to the consumers of agricultural produce from CER, Sichuan province. This paper presents the results of a preliminary survey carried out on the residue levels of orgnochlorine pesticides (DDTs and HCHs) in vegetables produced in Deyang and Yanting areas of the agricultural and industrial CER. Vegetables are important components of the Chinese diet both in terms of quantities consumed and nutritional value. Also, vegetables are consumed directly without much processing or storage. Therefore, even low residual levels of toxic contaminants in vegetables spell high danger to the consumers. These make information on residue levels of xenebiotics (such as DDT and HCHs) in vegetables very important for the protection of human health. Vegetables were also selected for this survey because, at the time of the survey, they were the most widely distributed food plants in the study area.

2.0 Materials and Methods

2.1 Description of the Study Areas

The sampling spots are located within two areas, Deyang and Yanting in the CER, Sichuan Province. The names of the areas were for the purposes of this report and are not restricted to administrative boundaries with same names.

Deyang sampling area is located at the central part of the CER, western edge of Sichuan Basin between the latitudes: 30^0 57' 56 N and 31^0 21' 00" N and between longitudes 104^0 05' 40" E and 104^0 15' 32"E. It includes selected sites in Pengzhou County of Chengdu City prefecture; Shifang, Mianzhu and Guanghan counties in Deyang City. This is typically a hilly area that falls within a subtropical humid climate zone with a continental monsoon climate. The average annual temperature is about 15.7^0C (which means no extreme temperatures in summer and winter) while annual precipitation average here is about 1053mm. The soil types are varied but the main ones are paddy soil, purple soil, and yellow earth. The soils are acidic to neutral (pH: 5.5-7.5) with organic matter content 0.6-4.0%. (Xing et al, 2009). Arable land forest and non-arable land evenly share the total land area. The Deyang area is an important vegetable production area in Sichuan. The main vegetables grown are: Pepper, celery, eggplant, tomato, lettuce, four season beans, cowpea, Chinese leaf, cucumber, bitter gourd, rape shoots (Chen et al., undated).

Yanting area in Yanting County of the Mianyang City prefecture falls within the Northeastern part of the CER, in central Sichuan Basin or northern part of Sichuan Province between the latitudes 31^0 13' 04" N and 31^0 19' 58"N and longitudes 105^0 19' 53"E and 105^0 57' 56"E. The annual average temperature in Yanting is 17-18^0C and precipitation 800 -1000 mm, with most of the precipitation occurring during the rainy season from May through August. The soil is classified as purple soil- a lithologic soil (Regosols in FAO Taxonomy) (CERN, 2003). The soil organic matter contents are low (0.6-2.0%) but pH high (8.0-8.6) (Xing et al., 2009). Steeper hills are forested, flat or gentle slopes are used for crops and lowlands used for irrigated paddy. The main crops are rice, wheat, corn, rape and sweet potato.

2.2 Site Selection and Sampling

The sampling sites were selected following the results of our soil OCPs survey (Xing et al, 2009) that covered the entire Chengdu economic region. Crop samples were taken from the farmlands whose soils had been found with relatively elevated levels of OCPs (≥ 10 ng g^{-1} dry weights). A global positioning system (GPS) instrument was used to locate sampling locations. Vegetables found growing on the sites or within the immediate vicinity were eligible for sampling. More samples were collected from the Deyang area (N=24) than from the Yanting area (N=10), since during the soil survey, a larger area in Deyang than in Yanting had been found to contain relatively elevated soil OCP residue levels (≥ 10 ng g^{-1} dry weight). Vegetables were collected directly from the fields to ensure that they originated within the study areas. The samples were collected on June 11-12 (spring vegetables) and September 22-26 (autumn vegetables) in the year 2007. Each

sample was sealed in a clean polythene sampling bag, and immediately transported to the laboratory where they were kept refrigerated at 4^0C until analysis.

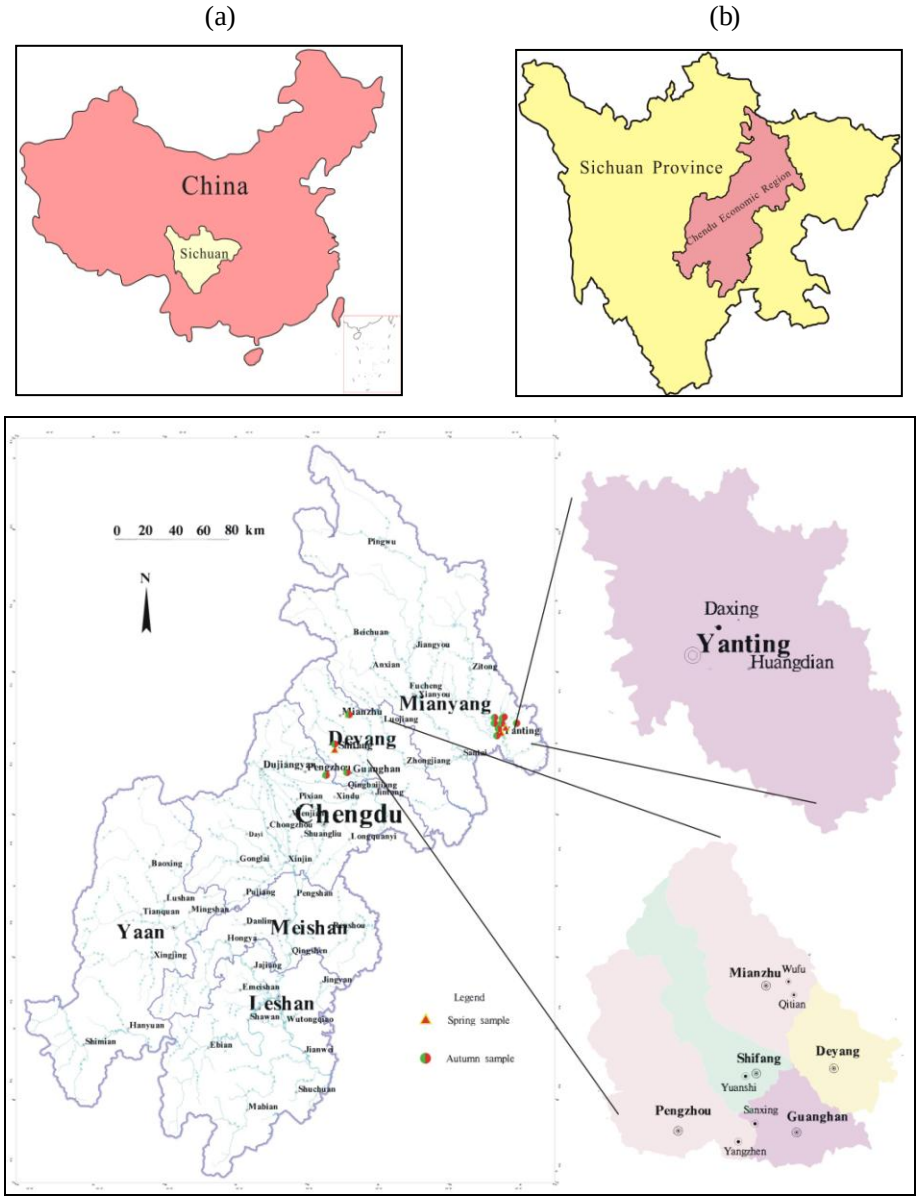

(c)

Figure 1. Sampling locations in Deyang and Yanting areas of the Chengdu Economic Region, Sichuan Province, China; (a) Location of Sichuan Province in china (b) Location of Chengdu Economic Region in Sichuan and (c) the location of sampling spots

2.3 Experimental Procedures

2.3.1 Extraction and Clean Up

About 50g of thawed edible portion of each vegetable sample was chopped (where possible) and blended for 3-5 minutes. Ten grams (10 g) of the homogenate was carefully weighed and transferred into a well tucked filter paper containing about 20 g of anhydrous sodium sulfate. The sealed mixture was spiked with 20ng of 2,4,5,6- tetrachloro-m-xylene (TCMX) and decachlorobiphenyl (PCB 209) as recovery surrogates. The mixture was then soxhlet extracted for 48 hours with 120 mL of dichloromethane and acetone mixture (2:1 vv). The extract was then concentrated to about 2 mL using a rotary evaporator at 40^0C, solvent-exchanged to n-hexane and transferred into a separatory funnel where about 3 mL of concentrated sulfuric acid (98%) was added with shaking (to remove lipids). The mixture was allowed to stand until two distinct layers were observed. The lower turbid layer (lipids in acid) was then removed and discarded. The procedure was repeated three times or until the lower acid layer appeared clear. The remaining organic layer (containing OCP extracts) was passed through alumina/silica gel (1:2 v/v) clean-up column (8 mm i.d.). The sample extract was eluted three times with 30mL dichloromethane/hexane (2:3) mixture to yield the OCPs fraction. The eluate was concentrated to about 0.5 mL before being transferred (using n-hexane) into a 2 ml screw cap cell bottle (Agilent Technologies USA) where it was concentrated further to 0.2ml under gentle stream of purified nitrogen gas at 40-45^0C. The extracts were stored at -20^0C, prior to GC-ECD analyses. Pentachloronitrobenzene (PCNB) was added as an internal standard before the analyses.

2.3.2 Instrumental Analysis

Concentrations of organochlorine pesticide residues were determined with HP 6890 gas Chromatograph (GC) system equipped with a micro-cell ^{63}Ni electron capture detector (ECD). The sample volume injected was 2 µl. The separation was performed on a fused silica capillary column (HP-5, 30 m x 0.32 mm i.d. and film thickness of 0.25µm). The carrier gas was nitrogen at a flow rate of 2.5 mL/min in a constant flow mode. Injector and the electron capture detector temperatures were set at 290^0C and 300 ^{0}C respectively. The oven temperature was programmed as follows: Initial temperature 100^0C held for 4 minutes; increased to 200^0C at a rate of 4^0C/min then increased to 230^0C at a rate of 2 ^{0}C/min followed by 8 ^{0}C/min till the final temperature of 280^0C at which it was held for 15 minutes. A six points response factor calibration was established to quantify the target analytes. System control was by HP-3365 Chem-station software.

2.3.3 Quality Assurance and Control

All analytical procedures were monitored using strict quality assurance and control measures. Chemicals used in the sample preparation and analyses were of high grade analytical standards obtained from Tedia Company, USA and J.T Baker, USA. Before use, neutral alumina, neutral silica gel and anhydrous sodium sulfate were soxhlet-extracted for 48 hours with dichloromethane and then baked for 12 hours in 250 ^{0}C, 180 ^{0}C and 450^0C respectively. Laboratory glassware were washed with concentrated sulfuric acid/potassium dichromate mixture, rinsed with distilled water and n-hexane then dried in the oven at 110^0C overnight prior to use. With each set of samples analyzed, field and procedural blanks were also analyzed to check for cross contamination and interferences. None of the target compounds were detected in the blank samples. The method of detection limits (MDLs) of OCPs ranged from 0.005-0.01 ng/g. The recovery rates of the surrogates; TMCX and PCB209 were 65±4% and 74±5% respectively. Each sample was analysed in duplicate and the average pesticides residue levels in the duplicates recorded as the residue level in the candidate sample. The relative standard deviation (RSD) for duplicate samples averaged 4%. Results of the analysis are reported in ng/g on wet-weight (wet wt) basis. A reporting limit of >0.01 ng/g wet wt was taken for calculation purposes since some duplicate averages were below the MDLs. Levels below the reporting limit or below MDL were taken as zero (0) in the calculations.

3. Results and Discussion

3.1 Occurrence and Levels of OCPs in Vegetables

A total of 34 samples of different species of vegetables (leafy, fruiting, root/bulbs and beans) were analysed for OCPs. The monitored OCPs are α-HCH, β-HCH, γ-HCH and δ-HCH (HCHs); p,p'-DDE , p,p'-DDD, o,p'-DDT and p,p'-DDT (DDTs). Concentration and detection rates of detected OCPs residues are given in Table 1. Quantifiable residues of DDTs were found in virtually all the vegetable samples from Deyang and in all but two samples from Yanting, indicating a widespread contamination of vegetables by OCPs in the study areas. The DDT metabolites (p,p'-DDE and p,p'-DDD) were in general more prevalent than the parent materials (o,p'-DDT and p,p'-DDT) suggesting either efficient biotransformation of the parent materials in the plant systems or old sources of

DDT contamination. Among the HCH isomers, lindane was the most frequently quantified both in the Deyang and Yanting vegetable samples (Table 1).

Without the single sample of green pepper (*Capsicum annuum* L.), the average residue level of total HCH (∑HCH) was slightly higher than that of total DDT (∑DDTs) in both Deyang (0.25 vs 0.24 ng/g) and Yanting (0.17 vs 0.11 ng/g). The pepper was not included in the calculations because DDT residue levels in it (totaling 148.44 ng/g wet wt.) appeared anomalous and since there was no other pepper sample to compare, the results were considered as outlier. Previous surveys had also reported ∑HCHs dominance over ∑DDTs but with higher concentrations than found in the present study, which indicates the use limitations of the chemicals are effective. For example, a national dietary survey undertaken in 1992 found average residue levels of ∑HCHs and ∑DDTs in vegetables to be 7.1 and 1.00 ng/g respectively (Liu et al, 1995) while in Shanghai (in the year 2000) the average concentrations were 4.9 and 2.9 respectively (Nakata et al, 2002). The slightly higher concentrations of ∑HCHs than ∑DDTs is probably because more technical HCH (approximately 4.9 million tons) than technical DDTs (0.4 million tons) were produced and used in China before the agricultural uses of these insecticides were banned in 1983 (Hua and Shan, 1996). Moreover, lindane replaced technical HCH in 1991 and about 3200 tons were used between 1991 and 2000 (Li et al, 2001). It should however, be noted that in a soil survey of the present study areas, Xing et al (2009) reported much higher mean residue levels of DDT (31.00 ng/g) than HCH (1.96 ng/g) in the agricultural soils. The discrepancy between the residue levels of DDT and HCHs in soil and their accumulative levels in the edible portions of vegetables could be because DDT is more hydrophobic than HCH. Hydrophobic compounds are strongly bound to root and soil organic colloid surfaces resulting in less absorption and/or translocation (Pereira et al, 2006).

Average HCH residue levels in the vegetables from Deyang were in the range, 0.06 -0.56 ng/g wet wt with bean (*Phaseolus vulgaris*) as the least contaminated vegetables and radish (*Raphanus sativus*) as the most, respectively. The range in Yanting was from <0.01 ng/g wet wt in spinach (*Spinacia oleracea*) to 0.30 ng/g wet wt in Pumpkin (*Cucurbita spp*). As for the ∑DDTs the average residue concentrations ranged from 0.03 ng/g to 0.64 ng/g in Deyang and from <0.01 to 148.44 ng/g in Yanting. Bean (*Phaseolus vulgari*) was again the least contaminated crop in Deyang where potato (*Solanum tuberosum*) had the highest mean ∑DDTs value. In addition to the pepper, residue levels of DDT in Deyang vegetables were notable for cabbages (*Brassica spp.*; 0.39 ng/g) and radish (*Raphanus sativus*; 0.33). However, apart from the pepper sample, vegetables in this study had residue levels far much below the recommended extraneous maximum residue limits (EMRLs) of 50 ng/ g wet wt (for lindane, ∑HCH and DDT), as set forth by the Chinese ministry of public health (Chinese food standard, GB 2763-2005), indicating minimal risk to the consumers.

Our results are not easy to compare with those of many other studies, because the differences in sampled species, analytical method employed and to some extent, differences in expression of analytical results (wet weight vs lipid content basis). However, it can be seen in Table 2 that our results for ∑DDTs and ∑HCHs or lindaneare in agreement with those reported in Shanghai (Nakata et al, 2002) but in most cases much lower than reported in Tianjin, China where the ∑DDT residue level in spinach (102 ng/g) exceeded the EMRL of 50 ng/g for vegetables as recommended by the Chinese laws (Tao et al, 2005). In comparison with results obtained in other countries (Table 2), the residue levels of ∑DDT and ∑HCH in vegetables found in this study were comparable to found in vegetables from Gambia and Senegal (Manirakiza et al., 2003) but lower than found in Agra, India (Bhanti and Taneja, 2005), Debrecen, Hungary (Hovánszki et al, 2007) and Nigerian markets (Adeyeye and Osibanjo, 1999). A much more serious vegetable contamination was found in the urban markets of Ghana (Amoah et al, 2006) where residue levels of lindane and ∑DDTs upto 300 ng/g wet wt and 400 wet wt respectively, were found.

Table 1. Edible tissue concentration (ng/g wet wt) of organochlorine residues in vegetables from Deyang and Yanting, Sichuan

Vegetable (N)	α-HCH	β-HCH	γ-HCH	δ-HCH	∑HCHs	p,p'-DDE	p,p'-DDD	o,p'-DDT	p,p'-DDT	∑DDTs
Samples from Deyang										
Amaranth (1)	0.07	0.10	0.05	<0.01	0.22	0.06	0.02	<0.01	<0.01	0.08
Beans (3)	0.04 (0.10)a	<0.01	0.02 (0.05)	<0.01	0.06 (0.16)	0.03 (0.04)	<0.01	<0.01	<0.01	0.03 (0.04)
Cabbages (4)	0.01 (0.02)	0.12 (0.37)	0.05 (0.10)	<0.01	0.17 (0.46)	0.25 (0.92)	0.02	0.04 (0.15)	0.07 (0.29)	0.3 9 (1.27)
Celery (1)	0.01	0.09	0.06	0.01	0.17	0.03	<0.01	0.03	<0.01	0.06
Eggplant (1)	0.40	0.08	<0.01	<0.01	0.48	0.14	<0.01	<0.01	<0.01	0.14
Lettuce (6)	0.04 (0.09)	0.10 (0.26)	0.03 (0.08)	0.18 (0.47)	0.35 (0.57)	0.08 (0.31)	0.01 (0.05)	<0.01	0.09 (0.30)	0.24 (0.85)
Onion (1)	<0.01	0.14	0.02	<0.01	0.16	0.05	0.01	<0.01	<0.01	0.06
Potato (2)	<0.01	0.02 (0.03)	0.04 (0.08)	<0.01	0.06 (0.11)	0.52 (1.02)	0.01 (0.02)	<0.01	0.10 (0.21)	0.64 (1.22)
Pumpkin (1)	0.12	<0.01	0.08	<0.01	0.20	0.01	<0.01	<0.01	0.19	0.20
Radish (2)	0.05 (0.09)	0.36 (0.62)	0.11 (0.19)	0.04 (0.08)	0.56 (0.98)	0.12 (0.22)	0.04 (0.09)	<0.01	0.17 (0.34)	0.33 (0.64)
Spinach (2)	0.01 (0.01)	0.09 (0.12)	0.08 (0.09)	0.06 (0.08)	0.24 (0.26)	0.04 (0.05)	0.03 (0.04)	0.03 (0.04)	0.03 (0.05)	0.12 (0.15)
All Samples (24)	**0.05 (0.40)**	**0.09 (0.62)**	**0.05 (0.19)**	**0.05 (0.47)**	**0.25 (0.98)**	**0.13 (1.02)**	**0.01 (0.09)**	**0.03 (0.19)**	**0.06 (0.34)**	**0.24 (1.27)**
Positive samples (%)	**62.50**	**66.67**	**70.83**	**37.50**	**91.67**	**91.67**	**45.83**	**29.17**	**33.33**	**100.0**
Samples from Yanting										
Cabbages (1)	0.02	0.23	0.02	<0.01	0.29	0.04	<0.01	0.11	<0.01	0.15
Pepper (1)	0.13	0.12	0.02	<0.01	0.27	61.41	0.41	82.59	4.04	148.44
Eggplant (1)	0.02	0.00	0.00	<0.01	0.02	<0.01	<0.01	<0.01	<0.01	<0.01
Lettuce (2)	<0.01	0.07 (0.07)	0.00 (0.02)	<0.01	0.09 (0.09)	0.01 (0.01)	<0.01	<0.01	<0.01	0.01 (0.01)
Pumpkin (2)	0.03 (0.06)	0.07 (0.15)	0.02 (0.04)	0.17 (0.29)	0.30 (0.48)	0.05 (0.10)	<0.01	<0.01	<0.01	0.05 (0.10)
Spinach (1)	<0.01	<0.01	<0.01	<0.01	<0.01	0.07	0.02	0.08	0.17	0.34
Rape stalk (2)	0.08 (0.15)	0.05 (0.10)	<0.01	<0.01	0.21 (0.23)	0.02 (0.03)	<0.01	<0.01	0.06 (0.11)	0.19 (0.34)
All samples (9)[b]	**0.03 (0.15)**	**0.07 (0.23)**	**0.03 (0.08)**	**0.04 (0.29)**	**0.17 (0.48)**	**0.03 (0.10)**	**0.00 (0.02)**	**0.03 (0.11)**	**0.04 (0.23)**	**0.11 (0.34)**
Positive samples (%)	**50.00**	**60.00**	**70.00**	**20.00**	**90.00**	**70.00**	**20.00**	**40.00**	**30.00**	**80.00**
EMRL[c]			**50**		**50**					**50**

Note: [a] Maximum residue value
[b] Residues in pepper (*Capsicum annuum* L.) not included in the calculations but included in frequency counts.
ΣHCHs= α-HCH + *β*-HCH + *δ*-HCH + *γ*-HCH; ΣDDTs = *p, p'*-DDE + *p, p'*-DDD + *o, p'*-DDT + *p, p'*-DDT
[c] The Chinese statutory Extraneous Maximum Residue Limit according to food standard (GB 2763-2005)
N= number of samples analysed

3.2 Compositional Analysis for Possible Sources of OCPs

Relative abundances of the HCH congeners to he total HCHs (∑HCHs) were quite similar in all crops samples and when all samples were considered together the order β-HCH >α-HCH ≈γ-HCH>δ-HCH (in Deyang samples) and β-HCH >δ-HCH > α-HCH ≈γ-HCH (in Yanting samples). The predominance of β-HCH was probably due to its high stability, low water solubility and resistance to microbial degradation and because α-HCH can be converted to β-HCH in the environment (Willet et al, 1998). Surprisingly, the most prevalent isomer in the vegetables of this study, γ-HCH (lindane), was not the overall most abundant HCH isomer. This is attributable to the instability of γ-HCH, which may be converted to α-HCH in the presence of solar radiation (Willet et al, 1998).

The composition pattern in terms of the ratio of α -HCH to γ -HCH (lindane) can be used to monitor whether the source was technical HCHs or lindane The ratio α –HCH/γ-HCH should be 4–7 for technical HCH, and nearly zero (0) for technical lindane (Iwata et al., 1995). In the present study, the ratio α –HCH/γ-HCH varied from 0.00 to 0.00-0.70 in vegetables from Deyang and from 0.00-1.88 in vegetables from Yanting. It is important to note that the soils from the CER, Sichuan (including the present study areas) were also found with predominantly lower α-HCH/γ–HCH ratio than in technical HCH with 95% of the ratios being in the range 0.00 – 0.14 (Xing et al, 2009). Accordingly, it can be concluded that lindane was still being used in the areas studied.

The average concentration levels of DDT isomers/metabolites in the vegetables were observed in the following order: p,p'-DDE > p,p'-DDT > o,p'-DDT > p,p'-DDD in Deyang and p,p'-DDT > p,p'-DDE >o,p'-DDT >p,p'-DDD in Yanting. DDT is known to biodegrade to DDE under aerobic and to DDD in anaerobic conditions. The predominance of p,p-DDE and low levels of p,p-DDD in Deyang show that either the DDT compounds were from the historical sources or that the biotransformation of DDT in the vegetables is very efficacious. Conversely, the fact that p,p-DDT was the main contributor in vegetables from Yanting, indicates recent inputs of DDT in the area. Furthermore, ratios of (DDD + DDE)/ DDTs of >0.5 shows DDTs have been subjected to long term weathering (Doong et al, 2007). In the present study, 58.33% of the samples from Deyang and 40.00% of samples from Yanting had the ratio (DDD + DDE)/ DDTs >0.5 showing that both weathered and fresh DDT could be contaminating crops in the areas.

Table 2 Global comparison of Organochlorine pesticide residue levels in some vegetables (ng/g wet wt)

Vegetable	Location	n	Year	∑HCHs	∑DDTs	Reference
Cabbage	Deyang, China	4	2007	0.17	0.39	Present study
	Yanting, China	1	2007	0.29	0.15	Present study
	Tianjin, China	-	2002	38.00	34.00	Tao, et.al. (2005)
	Debrecen, Hungary	-	-	-	19.30	Hovánszki et al. (2007)
	Agra, India	-	2002-03	2.49 [a]	2.33	Bhanti & Taneja (2005)
	Gambia/Senegal	-	2002	1.10	0.12	Manirakiza et al. (2003)
Celery	Deyang, China	1	2007	0.17	0.06	Present study
	Tianjin, China	-	2002	40.00	32.00	Tao et al. (2005)
	Shanghai, China	1	2000	1.70	2.50	Nakata et al., 2002
	Debrecen, Hungary	-	2004	-	10.60[b]	Hovánszki et al. (2007)
Lettuce	Deyang, China	6	2007	0.35	0.24	Present study
	Yanting , China	2	2007	0.09	0.01	Present study
	Urban markets, Ghana	60	2002	300 [a]	400	Amoah et al (2006)
	Gambia/Senegal	-	2002	0.30	0.45	Manirakiza et al. (2003)
Amaranth	Deyang, China	1	2007	0.22	0.08	Present study
	Nigeria	11	1991-92	5.40	22.60	Adeyeye & Osibanjo (1999)
Spinach	Deyang, China	2	2007	0.24	0.15	Present study
	Yanting , China	1	2007	<0.01	0.34	Present study
	Tianjin, China	-	2002	43.00	102.00	Tao, et al (2005)
	Shanghai, China	1	2000	<0.03	0.14	Nakata et al. (2002)
	Agra, India	-	2002-03	14.17	6.61	Bhanti & Taneja (2005)
Eggplant	Deyang, China	1	2007	0.49	0.14	Present study
	Yanting , China	1	2007	0.02	<0.01	Present study
	Shanghai, China	1	2000	0.09	<0.03	Nakata et al.(2002)
	Agra, India	-	2002-03	6.40 [a]	8.44	Bhanti & Taneja (2005)
	Gambia/Senegal	-	2002	0.30	5.10	Manirakiza et al. (2003)
	Nigeria	11	1991-92	3.40	21.50	Adeyeye & Osibanjo (1999)
Pumpkin	Deyang, China	1	2007	0.20	0.20	Present study
	Yanting	2	2007	0.30	0.05	Present study
	Agra, India	-	2002-03	0.04 [a]	ND	Bhanti & Taneja (2005)
	Debrecen, Hungary	-	2004	-	19.3 [b]	Hovánszki et al. (2007)
Radish	Deyang, China	2	2007	0.56	0.33	Present study
	Agra, India	-	2002-03	6.15	8.44	Bhanti & Taneja (2005)
	Gambia/Senegal	-	2002	0.30	1.44	Manirakiza et al. (2003)
Onion	Deyang, China	1	2007	0.16	0.06	Present study
	Shanghai, China	1	2000	0.15	0.07	Nakata et al (2002)

Note: Where more than one site was sampled, the site with highest level was taken for this comparison.
[*] ng/g dw
[a] mean level of γ-YCH; [b] mean value for DDE; [c] composite samples; ND=not detected; - Not available

3.3 Seasonal Variation

The residue levels and the detection rates of the OCPs are given in Table 3. The autumn vegetables had higher OCPs levels than spring vegetables. This may be because more pests were active during summer when the vegetables were growing – a situation which might have necessitated the illegal use of some of the OCPs. It is also possible that the high temperatures in summer volatilized the OCPs from their reservoirs such as soil or vegetation and that the edible parts of the crops may have trapped some of the evaporating pesticides.

It can also be seen in Table 3 that residues of β-HCH, γ-HCH (lindane) and hence ∑HCHs were more prevalent in spring samples than in autumn ones. In particular, the insecticide lindane was quantifiable in all the spring vegetables, which suggests that the vegetables might have been contaminated at the beginning of spring or earlier when they were planted. In the southern China region, lindane was mainly used in summer as a seed dressing or a general insecticide (Yang et. al., 2007).

The distribution of the DDTs was similar in both seasons, with degradation products p,p'-DDE and p,p'-DDD leading in prevalence especially in the winter crops. This further suggests historical rather than current sources of DDTs in the areas studied.

Table 3 Residue levels (ng/g wet wt) and incidence (%) of organochlorine pesticides in vegetables from Deyang and Yanting , Sichuan

Compound	Spring Vegetables (N=18)		Autumn Vegetables (N=16)	
	Incidence (%)	Average (min-max)[a]	Incidence (%)	Average (min-max)[a]
α-HCH	50.00	0.02 (<0.01-0.15)	75.00	0.07 (<0.01-0.40)
β-HCH	94.44	0.13 (0.01-0.37)	25.00	0.06 (<0.01-0.62)
γ-HCH	100.00	0.06 (0.02-0.10)	50.00	0.03 (<0.01-0.19)
δ-HCH	27.77	0.01 (<0.01-0.0.08)	41.67	0.08 (0.06-0.47)
∑HCHs	100	0.19 (0.02-0.46)	81.25	0.24 (<0.01-0.98)
p,p'-DDE	88.89	0.03 (<0.01-0.06)	87.5	0.20* (<0.01-61.41)
p,p'-DDD	38.89	0.01 (<0.01-0.04)	31.25	0.01* (<0.01-0.41)
o,p'-DDT	38.89	0.05 (<0.01-0.18)	18.75	0.02*(<0.01-82.59)
p,p'-DDT	11.11	0.02 (<0.01-0.23)	50.00	0.11* (<0.01-4.04)
∑DDTs	100.00	0.09 (0.01-0.34)	87.50	0.34* (<0.01-148.44)

∑DDTs = p,p'-DDT + o,p'-DDT + p,p'-DDD + p,p'-DDE; ∑HCHs= α- + β- + γ- + δ-HCH
* DDT values for one sample, pepper not included in the calculation of the mean

4.0 Conclusions

This survey revealed high occurrence rates but low residue levels of OCPs in vegetables produced in Deyang and Yanting farmlands Southwest China. Since most of the determined residue levels are far below the prescribed national and international residue limits, it can be concluded that there was a good observance of limitations in agricultural application of the chlorinated pesticides. However, the high prevalence of contamination was worrisome considering the cumulative nature, level of persistence of these pesticides and, especially, the high amounts of vegetables in the Chinese diets. Consumption of pesticide free vegetables and elimination of the vegetable OCP contamination are recommended.

Acknowledgement

This study was part of the project financed by the Natural Science Foundation of China under Grant No. 40473043 and Geological Survey of Sichuan Province, People's Republic of China. We thank Su Qiuke and the environmental organic Chemistry post graduate students of China University of Geosciences (Wuhan), who helped with the collection and /or extraction of the samples.

Correspondence to:
Shihua Qi,
MOE Key Laboratory of Biogeology and Environmental Geology
School of Environmental Studies
China University of Geosciences, Lumo Road 388, Wuhan, Hubei, 430074, P.R. China
Email: shihuaqi@cug.edu.cn

References

Adeyeye A and Osibanjo O. 1999. Residues of organochlorine pesticides in fruits, vegetables and tubers from Nigerian markets, Science of the Total Environment, 231: 227-233.

Amoah P. Drechsel P, Abaidoo RC, and Ntow WJ 2006. Pesticide and Pathogen Contamination of Vegetables in Ghana's Urban Markets. Arch. Environmental Contamination and Toxicology, 50: 1–6.

Bhanti M. and Taneja A. 2005. Monitoring of organochlorine pesticide residues in summer and winter vegetables from Agra, India – a Case Study. Environmental Monitoring and Assessment, 10: 341–346.

Chen J and Gao J. 1993. The Chinese total diet study in 1990 Part I. Chemical contaminants AOAC International,.76: 1193–1205.

Chen Y, van Wijk MS, Hong FX, Zhang,X. (undated): An overview of vegetable production in Sichuan province, China. VEGSYS Research project no. PRO1 www.VEGSYS.nl

Chinese Ecosystem Research Network (CERN), 2003.Yanting Agro-Ecological Experimental Purple Soil. CERN. Available onlin: http://www.cern.ac.cn:8080/stations/second.jsp?id=432 (Accessed: May 20, 2009)

Doong RA, Peng CK, Sun YC, Liao PL. 2002. Composition and distribution of organochlorine pesticide residues in surface sediments from the Wu-Shi River estuary Taiwan. Marine Pollution Bulletin, 45:246-253

Hováanszki D, Prokisch J, and Gyōri, Z. 2007. Case study: Testing of organochlorine pesticide contamination in a backyard garden. Cereal Research Communications, 35 (2): 493-496.

Hua XM and Shan ZJ. 1996. The production and application of pesticides and factor analysis of their pollution in environment in China. Advances in Environmental Sciences, 4: 33–45.

Iwata H, Tanabe S, Ueda K and Tatsukawa R 1995. Persistent organochlorine residues in air, water, sediments, and soils from the Lake Baikal Region, Russia. Environmental Science Technology, 29:792–801

Li JY, Li H, Tao P, and Lei, FM. 2006. Serum organochlorine pesticide level of non occupational Women exposure and risk of Breast cancer: a case-control study. *Wei Sheng Yan-Jiu*, 35(4): 391-416 (in Chinese).

Li YF, Cai DJ, and Singh, A. 1998. Technical hexachlorocyclohexane use trends in China and their impact on the environment. Archives of Environmental Contamination and Toxicology, 35: 688-697.

Li YF, Cai, DJ, Shan, ZJ, and Zhu, ZL. 2001. Gridded Usage Inventories of Technical Hexachlorocyclohexane and Lindane for China with 1/6° Latitude by 1/4° Longitude Resolution Archives of Environmental Contamination and Toxicology, 41: 261–266.

Liu HZ, Chen HJ, and Wang XQ, 1995. Chinese total diet study in 1992-pesticide residues. Journal of Hygiene Research. 24:356-360 (in Chinese).

Liu L, Jian A, Ren N, Jiang G, and Li Y. 2006. Gridded inventories of historical usage for selected organochlorine pesticides in Heilongjiang River Basin, China. Journal of Environmental Science, 18(4):822-826.

Manirakiza P, Akinbamijo O, Covaci A, Pitonzo R, Schepens P. 2003. Assessment of Organochlorine Pesticide Residues in West African City Farms: Banjul and Dakar Case Study. Archives of Environmental Contamination Toxicology, 44:171–179.

Nakata H, Kawazoe M, Arizono K, Abe S, Kitano T, Shimada H, Li W. and Ding, X. 2002. Organochlorine Pesticides and Polychlorinated Biphenyl Residues in Foodstuffs and Human Tissues from China: Status of Contamination, Historical Trend, and Human Dietary Exposure. Archives of Environmental Contamination and Toxicology, 43: 473–480.

Pereira RCM, Camps-Arbestain B, Garrido R, Macı´as F, Monterroso C. 2006. Behaviour of α-,β-, γ-, and δ-hexachlorocyclohexane in the soil-plant system of a contaminated site. Environmental Pollution, 44: 210-217

Tao S, Xu F L. Wang X J, Liu W X, Gong Z M, Fang JY, Zhu YM. and Luo J. 2005. Organochlorine Pesticides in Agricultural Soil and Vegetables from Tianjin, China Environmental Science and Technology, 39 (8): 2494 -2499.

Willett KL, Ulrich EM, and Hites RA. 1998. Differential toxicity and environmental fates of hexachlorocyclohexane isomers. Environmental Science and Technology, 32(15): 2197– 2207.

Xing X, Qi S, Odhiambo JO, Zhang Y. and Liu, Y. 2009. Influence of Environmental Variables on spatial distribution of organochlorine pesticides in Sichuan, West China. Environmental and Earth Sciences, 59(1): 215-222.

Yang Y., Li, D., Mu, D, (2007). Levels, seasonal variations and sources of organochlorine pesticides in ambient air of Guangzhou, China. Atmospheric Environment, 42(4): 677-687

Pravastatin Preserves Vasomotor Response in Atherosclerotic Arteries after Balloon Angioplasty

Ma Hongbao*, **, Yang Yan **, Cherng Shen ***

* Bioengineering Department, Zhengzhou University, Zhengzhou, Henan 450001, China, mahongbao@zzu.edu.cn; hongbao@gmail.com; 01186-137-8342-5354
** Brookdale University Hospital and Medical Center, Brooklyn, New York 11212, USA, youngjenny2008@yahoo.com
*** Department of Electrical Engineering, Chengshiu University, Niaosong, Taiwan 833, China, cherngs@csu.edu.tw; 011886-7731-0606 ext 3423

Abstract: Vasodilation response to pharmacological challenge is inhibited following balloon angioplasty. Pravastatin, a 3-hydroxy-3-methylglutaryl coenzyme A reductase inhibitor, has been demonstrated to enhance endothelial cell production of nitric oxide and reduce low-density lipoprotein cholesterol. This study was conducted to evaluate the effect of pravastatin on vasodilation following balloon angioplasty in normal and atherosclerotic arteries. Three normal and 3 atherosclerotic New Zealand White rabbits were used. Atherosclerosis was induced by feeding a high cholesterol diet. Rabbits were sacrificed and carotid arteries were isolated and placed in a dual perfusion chamber. Both arteries from each rabbit were perfused with oxygenated physiologic buffered solution at 37^{o}C and 60 mmHg. One artery was exposed to pravastatin (100 μM) and the other served as control. Balloon angioplasty (BA) was performed in both arteries using a 2.5×15 mm balloon catheter inflated to 10 atm at 3 different sites for one minute each. Pharmacological challenge was given using acetylcholine (2×10^{-5} M) and sodium nitroprusside (2×10^{-5} M) in norepinephrine (2×10^{-6} M) preconstricted arteries. Vessel diameter was measured by a computer planimetry system. After BA in normal rabbit arteries, acetylcholine did not demonstrate significant difference in percent lumen dilation between control and pravastatin (25.5±10.4 vs 16.6±7.5, p=ns) while atherosclerotic arteries had significantly preserved vasomotor response with pravastatin (16.9±7.2 vs 33.6±18.2, $p<0.005$). Similar results were noted with nitroprusside in normal arteries (29.0±14.5 vs 18.0±10.5, p=ns) and atherosclerotic arteries (18.6±7.4 vs 38.4±19.8, $p<0.003$). Pravastatin preserved vasomotor response in atherosclerotic arteries following BA when compared to normal arteries. This effect may be due to an enhanced production of nitric oxide in atherosclerotic arteries. However, pravastatin also appears to influence vasomotor response by either non-endothelial dependent or a combination of endothelial and non-endothelial dependent mechanism. [Journal of American Science 2009;5(4):101-106]. (ISSN: 1545-1003).

Keywords: artery; atherosclerosis; pravastatin; rabbit

Abbreviation: Ach: Acetylcholine; EDTA: Ethylenediamine-tetraacetic acid; G-6-Pase: Glucose 6-phosphatase; HDL: High-density lipoprotein; HMG-CoA: Inhibiting 3-hydroxy-3-methylglutaryl-coenzyme A; LDL: Low-density lipoproteins; NE: Norepinephrine; PBS: Physiologic buffered saline solution; SN: Sodium nitroprusside

1. Introduction

Atherosclerosis is a major reason resulted in cardiovascular disease and stroke (Zhu and Zhang, 2008). Hypercholesterolemia is a recognized independent risk factor for coronary heart disease, and the lack of physical activity in the general population is a public health problem and is recognized as an independent risk factor for the development of coronary disease (Boraita Perez, 2008). Epidemiological studies have shown that hypertriglyceridemia and low HDL-cholesterol were both associated with an increased risk of coronary heart disease (Fruchart and Duriez, 2006). Drug therapy is recommended for patients whose low-density lipoprotein (LDL) cholesterol concentrations are not adequately lowered by dietary modifications. Statins (atorvastatin, cerivastatin, fluvastatin, lovastatin, pravastatin and simvastatin) are the most effective agents currently available for lowering plasma levels of LDL cholesterol by inhibiting 3-hydroxy-3-methylglutaryl-coenzyme A (HMG-CoA) reductase, a key enzyme in the synthesis of cholesterol (Blumenthal, 2000; Gbelcova et al., 2008; Neuvonen et al., 2006). HMG-CoA reductase is a rate-controlling microsomal enzyme that converts HMG-CoA to mevalonic acid, a precursor of cholesterol (Shitara and Sugiyama, 2006). HMG-CoA reductase inhibitors are the primary

hypolipidemic drug treatment in most countries and statins are the mainstay of therapy for hyperlipidemia (Illingworth and Tobert, 1994). Pharmacological lowering of LDL cholesterol concentration has been shown in several primary and secondary intervention trials to decrease the occurrence of coronary heart disease and to prevent or delay coronary heart disease progression and the regression of atherosclerotic lesions has been demonstrated in some patients (Levy, 1984). Pravastatin is a new HMG-CoA reductase inhibitor for the treatment of hypercholesterolemia, which reduces LDL cholesterol and increases high-density lipoprotein (HDL) cholesterol (Jungnickel et al., 1992).

Pravastatin is formed by microbial transformation by the *microorganism Nocardia autotrophica*. The structural formaula of pravastatin is shown in Figure 1 along with those of lovastatin and simvastatin. The dihydroxyheptanoic acid moiety is the substrate analogue that interacts with the active site of HMG-CoA reductase. The decalin ring interacts with the binding site. Pravastatin sodium is chemically designed as [1S-[1α (βS*, δS*), 2α, 6α, 8β(R*), 8α]]-1,2,6,7,8,8a-hexahydro-β,δ,6-trihydroxy-20methyl-8-(2-methyl-1-oxobutoxy)-1-naphthaleneheptanoic acid, monosodium salt. Its empirical formula is $C_{23}H_{35}NaO_7$ and its molecular weight is 446.52 (Watanabe et al., 1988). Pravastatin is a hygroscopic, crystalline powder that is freely soluble in water (>300 mg/ml) and methanol, slightly soluble in isopropanol, and practically insoluble in acetone, acetonitrile, chloroform and ether (Watanabe et al., 1988). Atherosclerotic plaque disruptions with subsequent arterial thrombosis are critical causes for acute coronary ischemic syndromes (Bentzon et al., 2007; Libby, 2006). Pharmacological protections of artery are under searching. We suppose that pravastatin will preserve the vasoactivity of the atherosclerotic artery by its affectation of lowering LDL cholesterol levels.

The effects of statin drug therapy on the cardiovascular system extend beyond their anti-hyperlipidemic properties. Many studies showed that statins have a pronounced antioxidant effect as well as well documented endothelial protective effect (Namazi, 2004). Statins are 3-hydroxy-3-methylglutaryl-coenzyme A (HMG-CoA) reductase inhibitors, a key enzyme in the synthesis of cholesterol. They have been shown to decrease significantly risk of cardiac events in the setting of primary prevention, secondary prevention or during acute coronary syndrome (MIRACL trial). Since the effect of statin therapy is so diversified we selected to study effect of pravastatin on vasoreactivity of the endothelium following acute physical injury mimicking the current intravascular interventions.

3-Hydroxy-3-methylglutaryl-coenzyme A reductase (HMGR) catalyzes the formation of mevalonate - converts HMG-CoA to mevalonic acid (Zhang, Wan et al. 2007). In many classes of organisms, this is the committed step leading to the synthesis of essential compounds, such as cholesterol. However, a high level of cholesterol is an important risk factor for coronary heart disease, for which an effective clinical treatment is to block HMGR using inhibitors like statins. Recently the structures of catalytic portion of human HMGR complexed with six different statins have been determined by a delicate crystallography study (Ma et al, 2008).

2. Materials and Methods

Six, male, New Zealand White rabbits (Harlan-Sprague Dawley, Inc., Indianapolis, IN, USA) weighing between 2.8 and 3.2 kg were used in this study. The control group consisted of 3 normal rabbits that were fed a regular diet (Harlan-Sprague Dawley, Inc., Indianapolis, IN, USA) for six months. To induce atherosclerosis, another 3 rabbits underwent balloon-induced arterial injury, then were maintained on a 1% cholesterol diet (Harlan-Sprague Dawley, Inc., Indianapolis, IN, USA) for one month followed by another month of alternated regular diet and the two months diet cycle was repeated for three times to keep the rabbits for total of six months. Balloon-induced arterial wall injury of the aorta was performed with a 4F Fogarty Arterial Embolectomy catheter (0.9 × 40 cm, Baxter Healthcare Corporation, Irvine, CA, USA) introduced through the right femoral artery cutdown. The catheter was advanced in a retrograde fashion to the aortic valve and then withdrawn 3 cm. The balloon was inflated with 1.5 cm^3 of air, and the catheter was retracted down to the iliofemoral artery. This was repeated three times in each rabbit. Rabbits were anesthetized with ketamine (50 mg/kg, IM, Fort Dodge Animal Health, Fort Dodge, Iowa, USA) and xylazine (20 mg/kg, IM, The Butler Company, Columbus, Ohio, USA) in this surgery process.

After intravenous administration of heparin sulfate (1000 IU/rabbit) (Elkins-Sinn, Inc, Cherry Hill, NJ, USA) to prevent postmortem clotting, rabbits were anesthetized by injecting nembutal sodium solution (pentobarbital 50 mg/ml, 1 ml/kg rabbit) (Abbot Laboratories, North Chicago, IL, USA) through a marginal ear vein. Both carotid arteries from each rabbit were removed immediately after rabbits were sacrificed and were immersed in oxygenated physiologic buffered saline solution (NaCl 119 mM, KCl 4.7 mM, $CaCl_2$ 2 mM, NaH_2PO_4 1.2 mM, $MgSO_4$ 1.2 mM, $NaHCO_3$ 22.6 mM,

glucose 5.5 mM, Na_2EDTA 0.03 mM) (PBS). Arteries were perfused in a dual organ chamber under 60 mmHg flow pressure and 2.5 ml/min flow rate at 37°C and artery diameter vasodilation was measured. Balloon angioplasty was performed in both arteries using a 2.5×15 mm balloon catheter inflated to 10 atm at 3 different sites for 1 minute. One artery was served as non-pravastatin control and the other one was exposed to pravastatin (100 μM). After norepinephrine (NE, 2×10^{-6} M, Sigma Chemical Co, St Louis, MO, USA) preconstriction, pharmacological challenge was done with acetylcholine (Ach, 1×10^{-5} M, Sigma, St. Louis, MO, USA) and sodium nitroprusside (SN, 1×10^{-5} M, Sigma, St. Louis, MO, USA) (Table 1).

Data were calculated according to the formulas: (PBS-NE) (%)=(PBS-NE)/NE×100, (Ach-NE) (%)= (Ach-NE)/NE×100 and SN-NE (%)=(SN-NE)/ NE×100 separately, where Ach, NE, PBS and SN represented average diameter (mm) of arteries that were perfused by PBS containing a corresponding chemical. Balloon angioplasty was performed in both arteries using a 2.5×15 mm balloon catheter inflated to 10 atm at 3 different sites for 1 minute. The Vessel diameter was measured by a computer planimetry system (Figure 1). Procedures were performed according to NIH Animal Care.

Table 1. Artery Perfusion Step for Diameter Measurement

Treatments	Perfusion Steps	Perfusion Steps - Abbreviation in Figures	Perfusion Time (min)
Cycle 1: Before balloon injury Without pravastatin	Buffer 1	B1	10
	NE 1	N1	10
	Ach 1	A1	10
	SN 1	S1	10
	Buffer 2	B2	10
Cycle 2: Before balloon injury Half of arteries with pravastatin (100 μM)	Buffer 3	B3	10
	NE 2	N2	10
	Ach 2	A2	10
	SN 2	S2	10
	Buffer 4	B4	10
Cycle 3: After balloon injury Half* of arteries with pravastatin (100 μM)	Buffer 5	B5	10
	NE 3	N3	10
	Ach 3	A3	10
	SN 3	S3	10
	Buffer 6	B6	10

* Same arteries as in cycle 2

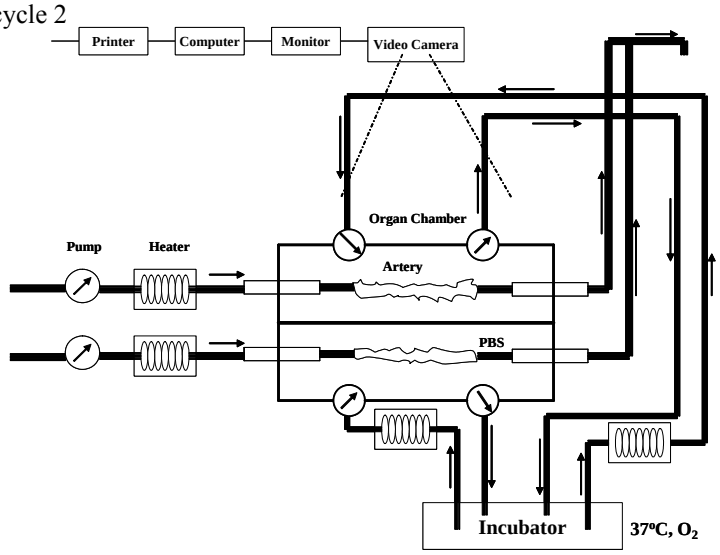

Figure 1. Dual organ chamber with separate perfusion using oxygenated physiological buffered solution at 37°C. Vessel diameter was measured by a computer planimetry system.

Statistical analysis:

With Jandel Scientific program, SigmaStat (Sigma Chemical Co., St. Louis, MO, USA) was used for data statistical analysis. $P<0.05$ was considered statistically significant difference. Measured data were reported as mean±SD. The student t-test was used for different studies.

3. Results

From the observation of aorta arteries, all the rabbits were atherosclerosis with the balloon-induced injury and maintained on a 1% cholesterol diet for one month alternatively up to 6 month feeding.

Myocardial infarction in human cases a triggering activity such as physical exertion precipitates the acute onset of the disorder (Mittleman et al., 2005; Muller et al., 1989; Tofler et al., 1990), but it is difficult to be studied in human. Therefore, a suitable animal model is important for the research in this field. This study demonstrated that atherosclerotic rabbit can be induced with balloon induced arterial injury surgery combined with 6 months of alternative 1% cholesterol diet. The rabbits which were balloon induced arterial injury and then were maintained in an alternative 1% cholesterol diet for a total of 6 months clearly caught atherosclerosis. This model is a useful method to get atherosclerotic animal for the related scientific research purpose.

In this experiment, the vasoactivity of both normal and atherosclerotic rabbit carotid arteries was measured using NE preconstriction and pharmacological challenge with Ach and SN (Figure 2, 3, 4). The measurements were performed with the steps of a perfusion cycle as showed in Table 1.

For normal rabbit arteries under PBS perfusion and pharmacological challenged by Ach and SN to NE, there was no significant difference in percent vasodilation between control and pravastatin in both before balloon injury and after balloon injury cycle (25.5±10.4 vs 16.6±7.5 for Ach, p=ns; 4.5 vs 18.0±10.5 for SN, p = ns). However, compared to control, pravastatin demonstrated a significantly greater percent vasodilation on atherosclerotic arteries after balloon angioplasty (16.9±7.2 vs 33.6±18.2 for Ach, $p<0.005$; 18.6±7.4 vs 38.4±19.8 for SN, $p<0.003$) (Figure 2, 3, 4).

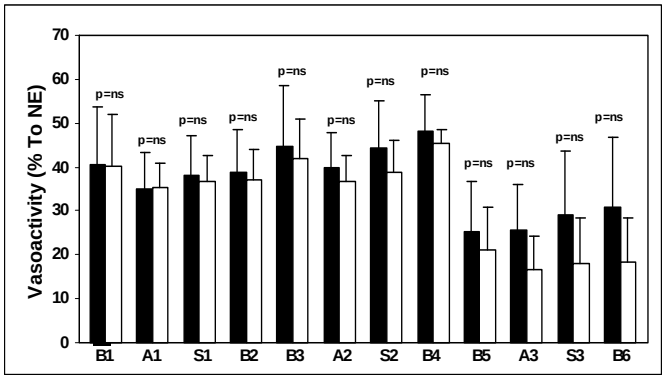

Figure 2. Vasoactivity (% to norepinephrine) of control rabbit.
▬: Control; ▭ : Pravastatin. Letter meanings are shown in Table 1.

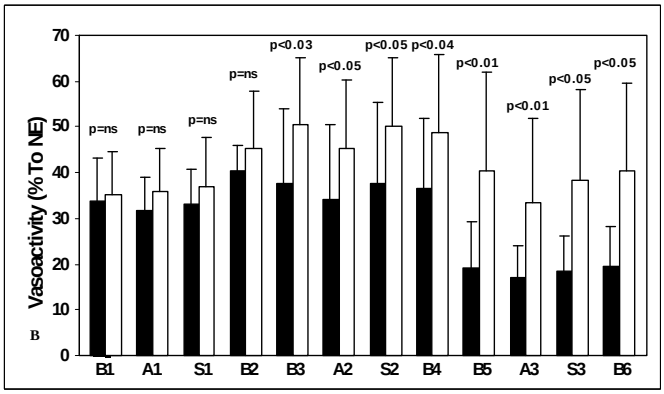

Figure 3. Vasoactivity (% to norepinephrine) of atherosclerotic rabbit.
▬: Control; ▭ : Pravastatin. Letter meanings are shown in Table 1.

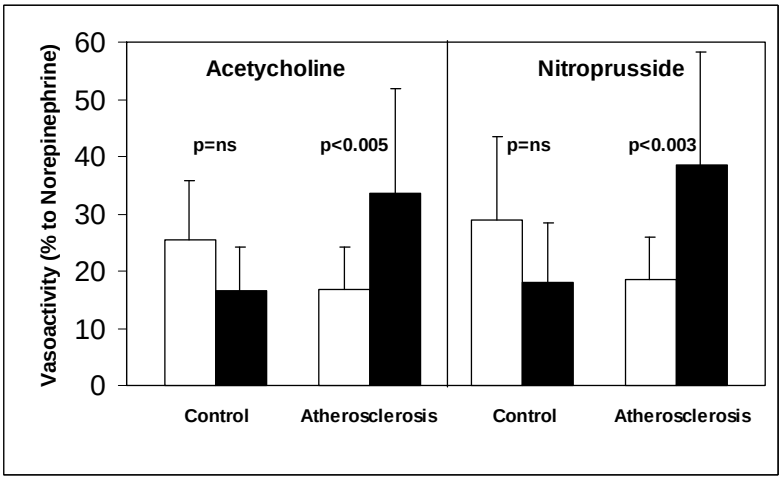

Figure 4. Vasoactivity (% to Norepinephrine) of rabbit carotid balloon injured. ☐ Perfused by buffer; ■ Perfused by buffer plus pravastatin.

Aasodilatation range of ratio to NE of PBS and pharmacological challenge with Ach and SN was 30-50% for before balloon injury and 20-40% for after balloon injury. Pravastatin enhances the vasodilation response in atherosclerotic arteries following balloon angioplasty. Pravastatin may influence vasodilation by a combination of endothelial and non-endothelial dependent mechanism.

Pravastatin enhances both endothelium dependant and independent vasoreactivity of carotid arteries in setting of acute balloon injury. This was true in presence of atherosclerosis. Mechanism of this effect is unlikely to be due to the lipid lowering property of pravachol. This might be due to its antioxidant effect or to some other unidentified process through a direct endothelial process, or the activation of some receptors or the induction of some signal that ultimately relates to the genomic makeup of endothelium. Its effect on the NO system is being established and might be part of the puzzle.

4. Discussions

Atherosclerosis, or "hardening of the arteries", is the process that causes heart attacks and most strokes (Rahmani et al., 2006). It is currently believed that cholesterol, especially the LDL, must be modified or oxidized before they can be taken up to cause foam cells. When cells use oxygen for energy, they produce by-products called free radicals. Free radicals damage cells and tissues during a process called oxidation - a factor in many chronic illnesses, including some forms of cancer, cataracts, arthritis and cardiovascular disease. LDL, known as the "bad cholesterol", is actually a protein that carries cholesterol throughout the body. The cholesterol carried by LDL deserves its bad reputation, however. It often ends up in our arteries, causing clots that can lead to heart attacks. Oxidation of LDL-cholesterol contributes to the plaque build-up in arteries, a process called atherosclerosis that can cause blockages and reduced blood flow. The process also plays a role in the loss of elasticity in arteries.

Antioxidants help neutralize free radicals and prevent them from causing cellular damage (McDaniel et al., 2003). Once oxidized, cholesterol is less apt to be expelled by body's cleaning mechanisms and more likely to be stored in arteries.

One problem for atherosclerotic rabbits is that their free radical and oxidation condition are changed under disease. Free radical modification of serum that is not the solely increased level of lipoprotein oxidation products in blood lipoproteins is an important cause for cholesterol accumulation in cells, and apparently for their transformation into foam cells during atherosclerosis (Panasenko et al., 1991).

Once altered by free radical oxidation, plasma lipoproteins undergo dramatic change, both in the manner in which they can interact with cells and in the ways in which they influence cell functions (Chisolm, 1991). Pravastatin preserved vasomotor response in atherosclerotic arteries following BA when compared to normal arteries. This effect may be due to an enhanced production of nitric oxide in atherosclerotic arteries. However, pravastatin also appears to influence vasomotor response by either non-endothelial dependent or a combination of endothelial and non-endothelial dependent mechanism. Pravastatin play protection function on vascular activity may through anti-oxidation.

Correspondence to:
Ma Hongbao, PhD, Professor
Bioengineering Department, Zhengzhou University
Zhengzhou, Henan 450001, China
hongbao@gmail.com; 01186-137-331-67674

References

1. Bentzon JF, Sondergaard CS, Kassem M, Falk E. Smooth muscle cells healing atherosclerotic plaque disruptions are of local, not blood, origin in apolipoprotein E knockout mice. Circulation. 2007;116(18):2053-61.
2. Blumenthal RS. Statins: effective antiatherosclerotic therapy. Am Heart J. 2000;139(4):577-83.
3. Boraita Perez A. Exercise as the cornerstone of cardiovascular prevention. Rev Esp Cardiol. 2008;61(5):514-28.
4. Chisolm GM, 3rd. Antioxidants and atherosclerosis: a current assessment. Clin Cardiol. 1991;14(2 Suppl 1):I25-30.
5. Fruchart JC, Duriez P. Mode of action of fibrates in the regulation of triglyceride and HDL-cholesterol metabolism. Drugs Today (Barc). 2006;42(1):39-64.
6. Gbelcova H, Lenicek M, Zelenka J, Knejzlik Z, Dvorakova G, Zadinova M, Pouckova P, Kudla M, Balaz P, Ruml T, Vitek L. Differences in antitumor effects of various statins on human pancreatic cancer. Int J Cancer. 2008;122(6):1214-21.
7. Illingworth DR, Tobert JA. A review of clinical trials comparing HMG-CoA reductase inhibitors. Clin Ther. 1994;16(3):366-85; discussion 365.
8. Jungnickel PW, Cantral KA, Maloley PA. Pravastatin: a new drug for the treatment of hypercholesterolemia. Clin Pharm. 1992;11(8):677-89.
9. Levy RI. Causes of the decrease in cardiovascular mortality. Am J Cardiol. 1984;54(5):7C-13C.
10. Libby P. Atherosclerosis: disease biology affecting the coronary vasculature. Am J Cardiol. 2006;98(12A):3Q-9Q.
11. Ma H, Jenny Y, Cherng S. HMG-CoA reductase (3-hydroxy-3-methyl-glutaryl-CoA reductase) (HMGR). Journal of American Science. 2008;4(3):62-4.
12. McDaniel MA, Maier SF, Einstein GO. "Brain-specific" nutrients: a memory cure? Nutrition. 2003;19(11-12):957-75.
13. Mittleman MA, Maclure M, Glasser DB. Evaluation of acute risk for myocardial infarction in men treated with sildenafil citrate. Am J Cardiol. 2005;96(3):443-6.
14. Muller JE, Tofler GH, Stone PH. Circadian variation and triggers of onset of acute cardiovascular disease. Circulation. 1989;79(4):733-43.
15. Namazi MR. Statins: novel additions to the dermatologic arsenal? Exp Dermatol. 2004;13(6):337-9.
16. Neuvonen PJ, Niemi M, Backman JT. Drug interactions with lipid-lowering drugs: mechanisms and clinical relevance. Clin Pharmacol Ther. 2006;80(6):565-81.
17. Panasenko OM, Vol'nova TV, Azizova OA, Vladimirov YA. Free radical modification of lipoproteins and cholesterol accumulation in cells upon atherosclerosis. Free Radic Biol Med. 1991;10(2):137-48.
18. Rahmani M, Cruz RP, Granville DJ, McManus BM. Allograft vasculopathy versus atherosclerosis. Circ Res. 2006;99(8):801-15.
19. Shitara Y, Sugiyama Y. Pharmacokinetic and pharmacodynamic alterations of 3-hydroxy-3-methylglutaryl coenzyme A (HMG-CoA) reductase inhibitors: drug-drug interactions and interindividual differences in transporter and metabolic enzyme functions. Pharmacol Ther. 2006;112(1):71-105.
20. Tofler GH, Stone PH, Maclure M, Edelman E, Davis VG, Robertson T, Antman EM, Muller JE. Analysis of possible triggers of acute myocardial infarction (the MILIS study). Am J Cardiol. 1990;66(1):22-7.
21. Watanabe Y, Ito T, Shiomi M, Tsujita Y, Kuroda M, Arai M, Fukami M, Tamura A. Preventive effect of pravastatin sodium, a potent inhibitor of 3-hydroxy-3-methylglutaryl coenzyme A reductase, on coronary atherosclerosis and xanthoma in WHHL rabbits. Biochim Biophys Acta. 1988;960(3):294-302.
22. Zhang QY, J Wan, et al. Structure-based rational quest for potential novel inhibitors of human HMG-CoA reductase by combining CoMFA 3D QSAR modeling and virtual screening. J Comb Chem. 2007;9(1):131-8.
23. Zhu Y, Zhang W. Cloning and analyzing of the cDNA sequence of N-terminal region and C-terminal region of zinc finger protein (ZFP580) gene. Life Science Journal. 2008; 5(1): 11 – 6.

Assessment of Lichen Species in a Temperate Region of Garhwal Himalaya, India

Balwant Kumar

Department of Botany, Kumaun University,
Nainital- 263002 (Uttarakhand), India
drbalwantkumararya@gmail.com

ABSTRACT: An enumeration of 106 lichen species belonging to 47 genera and 28 families from Baniyakund-Chopta areas of Garhwal is provided. The area is dominated by macrolichens (foliose to fruticose form). The area exhibit the luxuriant growth of corticolous lichens represented by the occurrence of 64% of corticolous (bark inhabiting) lichens followed by 30% of saxicolous (rock inhabiting) and 4% of terricolous (soil inhabiting) lichens. A single species growing on leaves (foliicolous) is also recorded from the area. If we compare the lichen diversity of the study area vis-à-vis other regions, it is about 30% of the Garhwal Himalayas, 20% of the Uttarakhand and 10% of the Himalayas and less than 0.5% of Indian lichen diversity. [The Journal of American Science. 2009; 5(4):107-112]. (ISSN 1545-1003).

Key words: Lichen diversity, phorophytes, substratum, growth forms

INTRODUCTION

Lichens comprise a unique group of plant that consists of two unrelated organism, a fungus and an alga, growing together in a close symbiotic association. The study of lichen remains quite neglected throughout the world, through they together with mosses form dominant organisms in ecosystem covering over 10% of the earth terrestrial habitats, particularly at higher elevations (Nash and Egan 1988). Lichens with cynobacterial blue green symbionts, contribute significantly for forest nitrogen fixation (Slack 1988). Besides many other uses, lichens are also used as pollution monitors. They are the plants that occur in most adverse conditions of climate and substrate. Thus the importance of this group in an ecosystem is very high in its own way. Lichens are just like little sponges that take up everything that comes their way, including air pollution (Fleishner 1994).

Lichens are universally distributed organisms occurring in varied climatic conditions ranging from the poles to the tropics in earth. They may look like crust, spreading rapidly over the surface (crustose lichens) or leafy and loosely attached to the surface (foliose lichens) and branched and shrubby, hanging from tree twigs or branches, with a single attachment (fruticose lichens). The collections were made along the way from Dalkuri to Bhujgali (Chopta) via Chpota and at different localities of the region. Negi (2000) recorded the occurrence of 85 macrolichens in the area. The micro lichens from the area were not listed so far.

MATERIALS AND METHODS

Site Description

The study site Baniyakund-Chopta is situated between 2500m to 3500m (asl) in the Rudraprayag district of Uttarakhand along with Akashkamini valley at 79^0-79^0 30'E and 30^0 30' – 30^0 42' N. The local human population settled in the low land fringe areas comprises semi pastoralists with livestock grazing and agriculture as their dominant land use activities. While low elevation woodlands such as *Quercus* forests are open for fodder and fuel wood collection throughout the year, grazing in the higher elevation forests and grasslands starts in early June, reaching a maximum in July, August and stop in early October. The maximum monthly temperature in the area varies from around 19ºC to 37ºC from the higher altitude grasslands to the lower elevation *Quercus* forests respectively during the snow free months of May to October, while the minimum temperature drops as low as -15ºC in the alpine grasslands during the months of December to February.

In general the climate of the Chopta region is less severe summer, more or less higher precipitation and colder or more prolonged winter. The climatic factors i.e. precipitation, temperature, relative humidity and wind, in association with elevation (valley or mountain ranges from foot hills to mountain zones), proximity to Great Himalaya, slope aspect and vegetation type etc, cause variation in climates at local or even micro levels (Gaur 1999). Major output of precipitation is in
the form of rainfall besides occasional occurrence of due hailstorms, fog, frost, snow fall etc. The south east monsoon commences towards the end of June and bursts until the mid of September.

Methodology

The lichen specimens were collected with the help of Chisel and Hammer along with their ecological notes. The type of forest vegetation, host tree type, location of the lichens thallus (on trunk, branch, twigs or leaves, soil and rock substratum); together with altitudes and other ecological notes were recorded. The collected specimens were investigated morphologically, anatomically and chemically at Lichenology laboratory of the National Botanical Research Institute, Lucknow. The collected samples were packed on hard card sheets inside a lichen herbarium packet (17cmX10mm) with details of the locality and are preserved at museum Center for Ecological Studies, Appropriate Technology India Ukhimath (Rudraprayag), Uttarakhand and also preserved at Botany Department, Hemwati Nandan Bahuguna Garhwal University Sirinagar (Garhwal) Uttarakhand. A voucher specimen of each species was also preserved at Herbarium of National Botanical Research Institue, Lucknow (LWG).

Identification of lichen species

The external morphology was studied under dissecting binocular microscope. The anatomy of the thallus and apothecia were studied under compound microscope. The external morphology was examined generally in dry condition but dark brown to bluish specimens of *Leptogium* were studied in wet condition. The anatomical structures were studied after cutting the section of dry material by microtome and with the help of safety razor blade. The thin dry sections of the thallus and ascocarp were immersed in 90% ethyl alcohol to drive off the intercellular or inter-hyphal air bubbles and the sections were mounted in water or in cotton blue in lactophenol. The colour of medulla, epithecium, hypohtecium, and ascus were recorded. The shape and size of the asci, ascospores and conidia were measured in the sections mounted in water. The measurements of the thallus, medulla, epithecium, and hymenium were generally taken in the sections mounted in cotton blue. The thallus size was measured in centimeter, lobe size and ascocarps in millimeter and thallus medulla, epithecium, hymenium thickness, asci and ascospores size in milimicron. Chemistry of the specimens was included colour spot tests and Thin Layer Chromatography (TLC).

RESULTS

A total of 106 species of lichen specimens from the study area Chopta forest (a purely *Q. semecarpifolia* forest) between 2500m to 3500m altitudes were recorded (Table 1). The specimens were collected in the month of May to October 2006.

Table 1: List of 28 families with 47 genera and 106 species of lichens recorded on different substrates in the Baniyakund-Chopta.

S. No.	Lichen Taxa	Family	Growth Form	Substratum
1	*Acarospora chlorophana* (Wahlenb, in Ach.) Massal.	Acarosporaceae	Crustose	On rock
2	*Acarospora saxicola* Fink ex Hedrick	Acarosporaceae	Crustose	On rock
3	*Allocetraria stracheyi* (Bab.) Kurok. & Lai	Parmeliaceae	Foliose	On rock
4	*Aspicilia dwaliensis* Rasanen	Hymeneliaceae	Crustose	On rock
5	*Buellia leptocline*(Flotow) Massal.	Physciaceae	Crustose	On bark
6	*Buellia stigmea* Tuck.	Physciaceae	Crustose	On rock
7	*Bulbothrix bulbochaeta* (Hale.) Hale.	Parmeliaceae	Foliose	On bark
8	*Bulbothrix meizospora* (Nyl.) Hale.	Parmeliaceae	Foliose	On bark
9	*Caloplaca pelodella* (Nyl.) Hasse	Teloschistaceae	Crustose	On bark
10	*Caloplaca* sp1	Teloschistaceae	Crustose	On rock
11	*Caloplaca* sp2	Teloschistaceae	Crustose	On rock
12	*Canoparmelia aptata* (Krempedh) Elix & Hale	Parmeliaceae	Foliose	On bark
13	*Cetrariopsis wallichiana* (Taylor) Kurokawa	Parmeliaceae	Foliose	On bark
14	*Cetrelia braunsiana* (Muell. Arg.) Culb & C. Club	Parmeliaceae	Foliose	On bark
15	*Cetrelia cerarioides* (Delise ex Duby) Culb & C. Culb	Parmeliaceae	Foliose	On bark
16	*Cetrelia pseudolivetorum* (Asah) Club & C. Club	Parmeliaceae	Foliose	On bark
17	*Cetrelia sanguinea* (Schaerer) Club & C. Club	Parmeliaceae	Foliose	On bark
18	*Cetrelia sanguinea* (Schaerer) Club. & C. Club.	Parmeliaceae	Foliose	On bark
19	*Chrysothrix candelaris* (L.) Laundon	Chrysothricaceae	Crustose	On bark/rock
20	*Chrysothrix chlorina* (Ach.) Laundon	Chrysothricaceae	Crustose	On bark
21	*Cladonia corymbescens* Nyl.	Cladoniaceae	Squamules	On soil
22	*Cladonia furcata* (Huds) Schrader	Cladoniaceae	Squamules	On bark/rock with moss
23	*Cladonia* sp.	Cladoniaceae	Squamules	On rock
24	*Cladonia squamosa* (Scop) Hoffm	Cladoniaceae	Squamules	On bark
25	*Dermatocarpon vellereum* Zschacke	Dermatocarpaceae	Foliose	On rock
26	*Everniastrum cirrhatum* (E Fries) Hale ex Sipman	Parmeliaceae	Foliose	On bark
27	*Everniastrum nepalense* (Taylor) Hale ex Sipman	Parmeliaceae	Foliose	On bark
28	*Graphis aicatricosa* Nyl.	Graphidiaceae	Crustose	On bark
29	*Graphis chlorotica*	Graphidiaceae	Crustose	On bark
30	*Graphis proserpens* Vainio	Graphidiaceae	Crustose	On bark
31	*Graphis scripta* (L.) Ach.	Graphidiaceae	Crustose	On bark
32	*Graphis sikkimensis* (Nagarkar & Patw.)	Graphidiaceae	Crustose	On bark
33	*Heterodermia diademata* (Taylor) D. Awasthi	Phyasciaceae	Foliose	On bark
34	*Heterodermia hypocaesia* (Yasuda) Awasthi	Phyasciaceae	Foliose	On rock
35	*Heterodermia incana* (Stirton) D. Awasthi	Phyasciaceae	Foliose	On bark
36	*Heterodermia isidiophora* (Vainio) Awasthi	Phyasciaceae	Foliose	On bark
37	*Heterodermia japonica* (Sato.) Swinsc. & Krog.	Phyasciaceae	Foliose	On soil with moss
38	*Heterodermia leucomela* (L.) Poelt	Phyasciaceae	Foliose	On bark
39	*Heterodermia pseudospeciosa* (Kurokawa) Culb	Phyasciaceae	Foliose	On bark with moss
40	*Heterodermia speciosa* (Wulfen) Trevisan	Phyasciaceae	Foliose	On rock
41	*Hymenelia* sp.	Hymeneliaceae	Foliose	On bark

42	*Hypotrachyna awasthi*Hale & Patw.	Parmeliaceae	Foliose	On rock with moss
43	*Hypotrachyna crenata* (Kurok) Hale	Parmeliaceae	Foliose	On rock
44	*Hypotrachyna exsecta* (Taylor) Hale	Parmeliaceae	Foliose	On bark
45	*Hypotrachyna scytophylla* (Kurok.) Hale	Parmeliaceae	Foliose	On rock
46	*Ioplaca pindarensis* (Rasanen) Poelt & Hintergger	Teloschistaceae	Crustose	On rock
47	*Lecanora achroa* (Nyl.) Crombie	Lecanoraceae	Crustose	On bark
48	*Lecanora* sp	Lecnoraceae	Crustose	On rock
49	*Lecidea* sp.	Lecideaceae	Crustose	On bark
50	*Lepraria lobificans* Nyl.	Lichen imperfecti	Crustose	On bark
51	*Lepraria* sp1	Lichen imperfecti	Crustose	On bark
52	*Lepraria* sp2	Lichen imperfecti	Crustose	On bark
53	*Leprocaulon pseudoarbuscula* (Asah.) Lamb & Ward	Lichen imperfecti	Crustose	On rock
54	*Leptogium askotense* D. Awasthi	Collemataceae	Foliose	On bark
55	*Leptogium papillosum* B. de Lesd Dodge	Collemataceae	Foliose	On bark
56	*Leptogium pedicelatum* M. P. Jorg	Collemataceae	Foliose	On bark
57	*Leptogium trichophorum* (Muell.) Arg.	Collemataceae	Foliose	On bark
58	*Lobaria retigera*(Bory) Trevisan	Lobariaceae	Foliose	On bark
59	*Lobaria* sp	Lobariaceae	Foliose	On bark
60	*Myelochora aurulenta* (Tuck) Elix & Hale	Parmeliaceae	Foliose	On bark
61	*Myelochora irrugans* (Nyl.) Exil & Hale	Parmeliaceae	Foliose	On bark
62	*Myelochora xantholepsis* (Mont & Bosch) Elix & Hale	Parmeliaceae	Foliose	On bark
63	*Ochrolechia rosella* (Muell. Arg.) Vers.	Pertusariaceae	Crustose	On bark
64	*Opegrapha* sp.	Opegraphaceae	Crustose	On Leaf
65	*Parmelia squarrosa*Hale	Parmeliaceae	Foliose	On bark
66	*Parmelinella wallichiana* (Taylor) Elix & Hale	Parmeliaceae	Foliose	On soil with moss
67	*Parmotrema mesotropum* (Muell. Arg.) Hale	Parmeliaceae	Foliose	On bark
68	*Parmotrema nilgherrense* (Nyl.) Hale	Parmeliaceae	Foliose	On bark
69	*Parmotrema saccatilobum*(Taylor) Hale	Parmeliaceae	Foliose	On bark
70	*Peltigera polydactyla* (Neck) Hoffm	Peltigeraceae	Foliose	On bark/Soil with moss
71	*Peltigera rufescens* (Weiss) Humb	Peltigeraceae	Foliose	On soil with moss
72	*Pertusaria aqussiae* Fe	Pertusariaceae	Crustose	On bark
73	*Pertusaria leucosorodes* Nyl.	Pertusariaceae	Crustose	On bark
74	*Phaeophyscia hispidula* (Ach.) Moberg	Phyasciaceae	Foliose	On bark
75	*Phyllopsora albicans* Muell. Arg.	Lecideaceae	Crustose	On bark
76	*Physcia dimidiata* (Ach.) Nyl.	Physciaceae	Foliose	On bark
77	*Porpidia albocoerulescens (*Wulfen) Hertel & Knoph in Hertel	Porpidiaceae	Crustose	On rock
78	*Porpidia crustulata*(Ach.) Hertel & Knoph in Hertel	Porpidiaceae	Crustose	On rock
79	*Porpidia macrocarpa*(DC) Hertel & Knoph in Hertel	Porpidiaceae	Crustose	On rock
80	*Punctelia borreri* (Sm) Krog.	Parmeliaceae	Foliose	On bark
81	*Punctelia neutralis* (Hale) Korg.	Parmeliaceae	Foliose	On rock
82	*Punctelia subrudecta* (Nyl.) Krog.	Parmeliaceae	Foliose	On rock
83	*Pyrenula immersa* Muell. Arg.	Pyrenulaceae	Crustose	On bark
84	*Pyrenula immissa* (Stirton) Zahlbr	Pyrenulaceae	Crustose	On bark
85	*Pyxine berteriana* var *himalaica* D. Awasthi	Phyasciaceae	Foliose	On bark
86	*Pyxine subcinerea*Stirton	Physciaceae	Foliose	On bark
87	*Ramalina conduplicans* Vainio	Ramalinaceae	Fruticose	On bark

88	*Ramalina himalensis*Rasanen	Ramalinaceae	Fruticose	On rock
89	*Ramalina roesleri* (Hochst) Hue	Ramalinaceae	Fruticose	On bark
90	*Ramalina sinensis* Jatta	Ramalinaceae	Fruticose	On bark
91	*Rimelia reticulata* (Taylor) Hale & Fletcher	Parmeliaceae	Foliose	On rock
92	*Stereocaulon foliolosum* Nyl.	Stereocaulaceae	Foliose	On rock
93	*Stereocaulon pomiferum* Duvign.	Stereocaulaceae	Foliose	On rock
94	*Sticta nylanderiana*Zahlbr.	Stictaceae	Foliose	On bark
95	*Sulcaria sulcata*(Lev) Bystr. Ex Brodo & D. Hawkow	Alectoriaceae	Foliose	On bark
96	*Umbilicaria badia* Frey	Umbilicariaceae	Foliose	On rock
97	*Umbilicaria indica* Frey	Umbilicariaceae	Foliose	On rock
98	*Umbilicaria virginis* Schaerer	Umbilicariaceae	Foliose	On rock
99	*Usnea aciculifera*Vainio	Usneaceae	Fruticose	On bark
100	*Usnea eumitrioides* Mot.	Usneaceae	Fruticose	On bark
101	*Usnea indica* Mot.	Usneaceae	Fruticose	On rock
102	*Usnea longissima* Ach.	Usneaceae	Fruticose	On bark
103	*Usnea orientalis* Mot.	Usneaceae	Fruticose	On bark
104	*Usnea pectinata* (Taylor)	Usneaceae	Fruticose	On bark
105	*Usnea subfloridana* (Stirton)	Usneaceae	Fruticose	On bark
106	*Verrucaria acrotella* Ach.	Verrucariaceae	Crustose	On rock

DISCUSSION

The most common lichen species growing on different phorophytes belongs to the genera *Chrysothrix*, Parmelioid, Usnioid and Graphidiaceous lichens while *Acarospora, Aspicilia, Umblicaria, Dermatocarpon, Porpidia, Buellia* and *Caloplaca* mostly prefers to grow on rocks. Species of lichen genera *Peltigera, Lobaria* and *Sticta* prefers soil for their growth. The lichen flora in the study area exhibits greatest abundance in variety and luxuriance of growth. The lichens in the study area seem to prefer the bark of trees or rock as their substratum. Lichens also occur on soil, decaying wood, mosses and humus. The corticolous lichens are greatly influenced by the physical characters of the bark. Corticolous lichens may be epiphloedal or endophoedal based on their growth above or within the substratum. In epiphloedal lichens or the lichen tissue (especially the algal layer) develops above the outermost corky layer of bark, although few layers of cork are incorporated into the lower portion of the thallus. In endophloedal lichens the thallus crust lies entirely below the cork of periderm. Section of endophloedal crustose lichens together with their bark substrate generally show that the lichen thallus remains to the corky outer periderm by one or many layers of suberised impermeable cork cells. The nature of bark (smooth or rough) and moisture retaining capacity of bark also plays vital role in determining the type of lichen species. *Quercus, Rhododendron, Acer* spp. and many other trees, as well as species of shrub and ringal act as favorable substrate for the luxuriant growth of lichens. Together with trees some shrubs of *Berberis* and *Cotoneaster* also provide a suitable substrate for growth of many lichen taxa.

The growth of lichens on rock is based on the physical and chemical characters of the rocks. The hard, permanent, and moist rock preferred by most of the lichen than the rocks which weather soon and allowing less time to the lichen to produce reproductive organs. Proximity of water to substratum also exerts great influence in determination of the type of lichen growth.

The lichen on the rock depends upon whether the rocks are acidic or basic. The exposure and moisture relationship strongly influence the lichen cover on rocks. The boulders along the stream and in open fields and fell fields are suitable habitats for lichens. In the open boulder fields the foliose lichen *Heterodermia* and *Phaeophyscia* occupies the exposed rocks and boulders while humus and soil containing pebbles at the base of boulders in moist places provide a habitat for lichen species *Cladonia* and *Peltigera*. The exposed dry boulders received sunrays throughout the day remains more or less dry and hot and only few dark black *Buellia* and *Acarospora* species able to grow.

The common epiphytic foliose and fruticose genera are *Everniastrum, Parmoterma, Heterodermia, Bulbothix, Hypotrachyna, Leptogium, Parmelia, Parmellinella, Lobaria,*

Ramalina, *Rimelia*, and *Usnea.* These genera colonize on trunk, branches, minor branches and twigs.

The moist shady location in the study area provide suitable habitat for growth of terricolous (soil inhabiting) and muscicolous (moss inhabiting) lichen species of *Peltigera* and *Cladonia*. Vertical face of roads covered with moss and small herbaceous plant provide a moist shady habitat for growth of terricolous and muscicolous lichens. Among different lichen forms the foliose forms dominated the area by 57 species followed by crustose 34 and 11 fruticose and 4 squamules species. Among the different lichen families, the Parmeliaceae exhibit its dominance in the area represented by 15 genera (31.9%) out of the 74 genera of lichens known from the area.

ACKNOWLEDGEMENT

I thankful to Dr. D. K. Upreti, N.B.R.I. Lucknow (UP) for the identification of lichen species and also thankful to Executive Director, Center for Ecological Studies, Appropriate Technology India (A.T. India) Guptakashi, Uttarakhand for providing necessary facilities.

REFERENCES

Fleishner T L. Ecological costs of livestock grazing in Western North America. Conservation Biology 1994; **8**(3): 633.

Gaur R D. Flora of district Garhwal Himaya (with ethnobotanical notes). 1999; 3-4.

Kumar B. Lichen species distribution, cover and fall in a *Quercus semecarpifolia* (J E Smith) forest of Garhwal Himalaya (Ph. D. Thesis), HNB Garhwal University, Srinagar (Garhwal), India. 2008.

Nash T H. & Egan R S. The biodiversity of lichens and bryophytes. In: Lichen, Bryophytes and air quality eds. Thomas Nash III & Vilkmar Wirth. Bibl. Carmer in der Gebr. Borntra. Verlag. Berlin, Stuttgart. Lichenol.1988; 30: 11-22.

Negi, H R. On the pattern of abundance and diversity of macrolichens of Chopta-Tunganath in the Garhwal Himalaya.

Indian Academy of Sciences 2000; 25 (4): 375-77.

Slack N G. The Ecological Importance of lichen and Bryophyte. Bib. Lichenol. 1988; 30: 23-53.

Assessment of fault-zone materials and their impact on hydrocarbon accumulation using integrated Exploration techniques.

Oyedele, K. F. and Adeyemi, A.S.
Department of Physics (Geophysics Programme)
University of Lagos, Lagos, Nigeria.
kayodeunilag@yahoo.com

Abstract

This paper presents the findings of an integrated exploration methods conducted on rock exposures in Enugu, Anambra basin, southeastern Nigeria. The methods employed include geological, geophysical and borehole geophysics to study the properties of fault-zone materials as the sealing mechanisms. Results from this study revealed that outcrop data alongside geophysical and borehole data could be useful in the optimal evaluation of fault-zone materials with respect to their potentials in hydrocarbon accumulation. It is also concluded that both the nature of materials juxtaposed across a fault and the character of materials in the fault zones could play significant and complimentary roles in fluid control across a fault. "[The Journal of American Science. 2009;5(4):113-122]. (ISSN 1545-1003)"

Keywords: Fault-zone, hydrocarbon, fault gouge, siliciclastic sequence.

Introduction

In hydrocarbon exploration, faults play a crucial role in the distribution of hydrocarbon because of their capacity to act as seals (Bouvier et al, 1989).Several oil and gas companies have studied this impact extensively with emphasis on juxtaposition of materials of different hydraulic properties across a fault, rather than on the materials inside the core of the fault zone.

Fault zone can act as either as barrier or preferential flow paths to fluid (knipe et al, 1997, Bense et al, 2003). Fault zones are usually the sites of large discontinuous changes in mechanical and transport properties that are controlled by the composition and structures of the fault gouge. The early development of the fault gouges starting from the initial discontinuities is less well known. The early researchers such as Antonelli and Aydin, 1995, Fulljames et al, 1997 and knipe et al, 1997 have so far mainly concentrated on faults in thick layers and thus single phase materials. In such cases, dependent on lithology and environmental parameters (effective stress, temperature, etc) and a range of gain-scale processes have been documented.

Bouvier et al, 1989, presented a qualitative method of predicting "static" fault seal in siliciclastic sequence from the Num river field in the Niger delta, Nigeria using subsurface data. Since then the method has been developed and applied to faults in many hydrocarbon provinces worldwide, such as the North Sea Gulf of Mexico (Davis et al, 2003). There are several outcrop-based studies of the Anambra basin (Hogue, 1997, Nwajide, 1980 and Ladipo, 1988), yet the basin is not as well understood as the adjourning Niger delta in a totally comprehensive manner.

To this end, this study aims at contributing to the scarce information and limited understanding of fault zone materials in Anambra basin and its potential in hydrocarbon accumulation.

Materials and methods

Geology of the Study area.

The study area is located within the Anambra basin, in the central portion of Southeastern Nigeria (figure1), extending from Longitude 5^{o}E to 6^{o}E and Latitude 5^{o}N to $5^{o}30^{o}$N, and covering an area of about 700 square kilometers. The Anambra basin with over 600m of both pre-santonian and post-santonian sediments is documented to have estimated reserves of 1 billion barrels of oil and 30 trillion cubic feet of gas (Akande, S.O et al, 2005). However, the expolaration history of the basin has been an unsuccessful one, with only six out of over fourty well drilled so far encountering gas and / or oil. This low success rate has greatly reduced the interest of explorationists who considered the besin a more difficuit and less rewarding than the adjacent Niger delta.

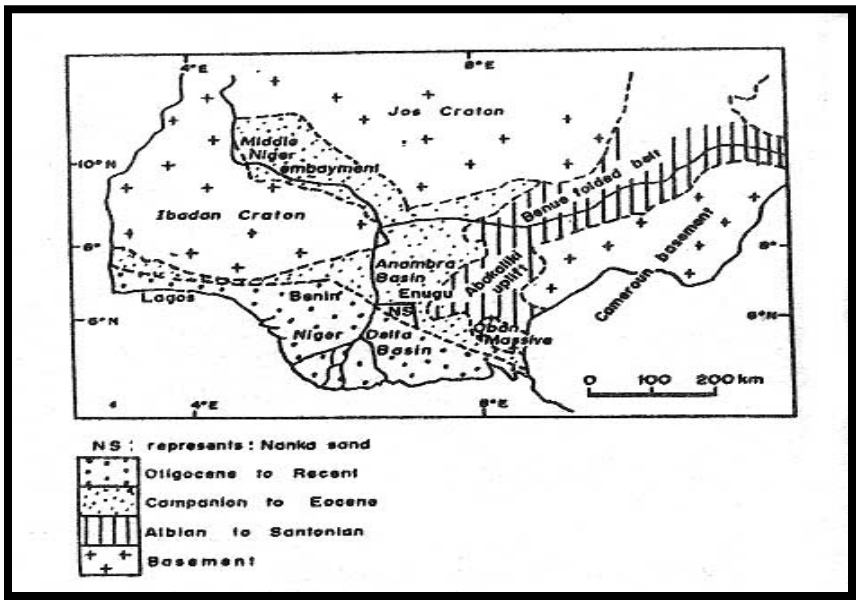

Figure.1: Generalized map of Nigeria showing the Anambra Basin. (Modified from Murat, 1972)

Tectonic Setting and Geological evolution.

The tectonic setting and geological evolution of Anambra basin (figure 2) can be traced back to the mesozoic (late Jurassic) when the splitting of the gondwanaland super continent took place along rift zones of different orientations that met at a triple junction. This triple junction is now the site at which the present day Nigeria delta is located. In this region, rifting started in the late Jurassic and persisted into the middle cretaceous (Murat, 1972).

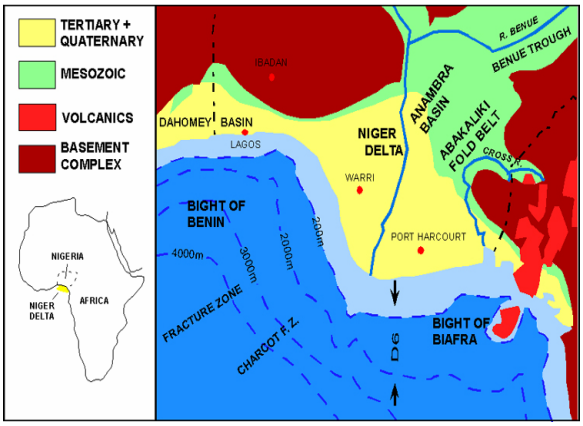

Figure 2: Tectonic map of southern Nigeria, modified after Whiteman; 1962.

The fracture zone ridges subdivided the margin into individual basins, and form the boundary fault of the cretaceous Benin-Abakaliki trough, which cuts far into the West African shield. The trough represent a failed arm of a rift triple junction associated with opening, of the South Atlantic, and gave rise to the Benue aulacogen, a NE-SW trending, folded aborted rift basin that runs obliquely across Nigeria.

The Anambra Basin proper formed after the Santonian tectonic pulse, dating back to 84million years, following the deformation and uplift of the Abakaliki sector of Benue trough. During the Santonian tectonism, the (proto-Anambra platform) are bordering the Benue trough to the West (Anambra platform) and to the East (Afikpo platform) became downwarped to form the Anambra basin and Afikpo respectively (Petter and Ekweozor 1982, Ojoh, 1992). The emergent Abakaliki anticlinorium became a positive area that supplied detritus to these new basins. Sediments were also derived from the uplands beyond the Benin hinge line and the Benue fold belt. Subsequently, the basins were filled with sediments ranging from late to early cretaceous.

Field procedures.

The process of data gathering involved the use of flowchart technique in order to ensure repeatability of process and consistency of results of sampling done in different locations (figure 3). The search for outcrops was aided by literature research of previous work done in the area. Fault identification on outcrops was also aided by the use of some fault recognition criteria, such as offset rock body and topographic features, juxtaposition of different rock bodies, presence of fault gouge or breccia, slickensides and slickenlines and presence of faceted spurs and sag pond.

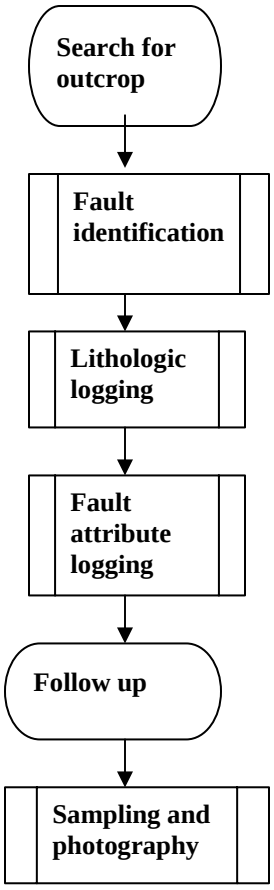

Figure.3: Flowchart for field program

At each location where faults have been identified, the lithologies of the fault planes were logged from bottom to top. Typical thickness of strata at an outcrop was recorded in the field notebook where the layers are drawn to scale and described as rock type, grain size, fossil content, colour, bed dip, sedimentary structures and other attributes. Thickness of strata was measured using the tape rule. In addition to logging the offset strata, the zone within the fault surface in the vicinity of the fault plane were also logged. Some of the measured attributes include fault throw, fault length, strike of the fault, fault slip, dip heave and fault gap. Also measured and described were deformation bands, joints, microfolds, clay smear and fault profile roughness.

Samples were taken at three lecatious: (1) road cut along the expressway to Onitsha from Enugu, close to the flyover) (2) West of Enugu city by the river channel, Ekulu river (3) Road cut at Agbogugu, south of Enugu along Enugu Port-harcourt road) to capture information on different rock types encountered. Similarly, pictures were taken at the various lecatious to detail the fault gouge materials (figures. 4 to 7). The follow-up survey involved input of data into the computer and further literature research.This was done in order to get a full understanding of the cause, process and product of the features being examined. It was also done to correct for any error of oversight that could mar the results of the data collection exercise. The pictures on figures 4 to 7 was used for up-scaling the sampled faults to seismic-scale faults (figures 8 and 9).

Data processing and analysis.

The numeric values obtained from fault surface and lithologic logging were input into a pre-formatted table in MS Excel spreadsheet (Tables 1 to 3). The parameters obtained from field mapping and data acquisition were also input into structural geology software called (GXII), (figure 10) for the purpose of validation of manual interpretation. The measurements and detailed description were done at each of the locations for attributes such as fault throw, fault slip, orientation, deformation bands, fault profile, roughness and fault heave.

The Algorithms that were employed in data analysis and development of fault seal potentials are industry known and accepted. These algorithms include the following:

Clay Smear potentials (CSP): This is the relative amount of clay that has been smeared from individual shale source beds at a certain point along a fault plane.

Shale Smear factor (SSF): This is a ratio of the fault throw to the thickness of the shale bed that provides smear along the fault surface.

Shale Gouge Ratio (SGR): This is the percentage of shale or clay in slipped interval.

The empirical relationships of the algorithms are summarized below:

CSP = (Shale bed interval) ^{2} / Distance from the source bed

SSF = Fault throw / Shale layer thickness

SGR = $\sum$(thickness of shale bed / fault throw) X 100%

Results and Discussion.

Results

The data set obtained for the various measured elements were interpreted as follows:

Pressure data: pressure data from drilling mud weight were obtained from the wells in the area. From the analysis, it was obtained that there is a lateral variation in pressure across the fields in the area. Also two pressure gradients were obtained in well 2, thus showing that there is a vertical variation in the pressure gradient as well.

Fault geometry: In the outcrop, bedding is horizontal to sub-horizontal, with no dip larger than 6^o The faults strike perpendicular to the main outcrops faces (Figures.4 to7). The average fault strike was 090^o-300^o. The fault plane orientations show that the faults were mainly dipping south.

Deformation bands: In dataset from the study area, deformation bands were quite common, particularly in locations 2 and 3, and show evidence for cataclasis. They usually have displacements of a few millimeters, sometimes up to

Figure 4: Studied fault system at location 1; Road cut along the Expressway to Onitsha

Figure 5: Studied fault system at location 2, West of Enugu city by the river channel (Ekulu river)

Figure 6: Studied fault system at Location 3, Road cut at Agbogugu.

Figure 7: Zoomed in section from one of the fault splay at location 3.

Figure.8:A 3-D Seismic section taken close to the Study Area in Anambra Basin.

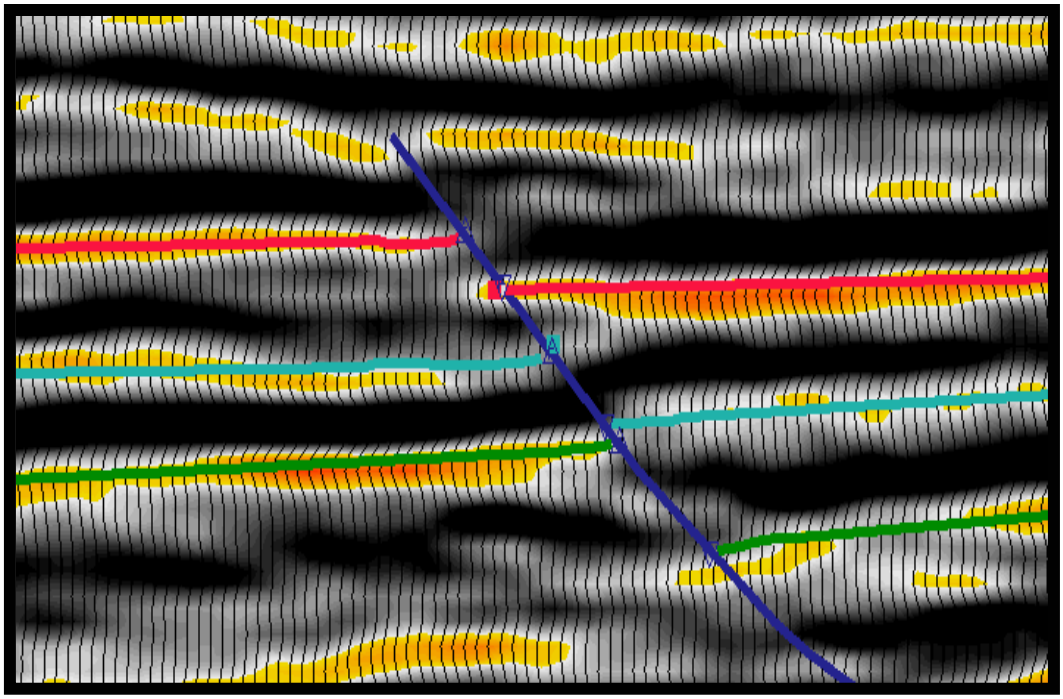

Figure 9: A Zoomed in section of the seismic line in Fig.8 showing the targeted sandstones juxtaposed against shales.

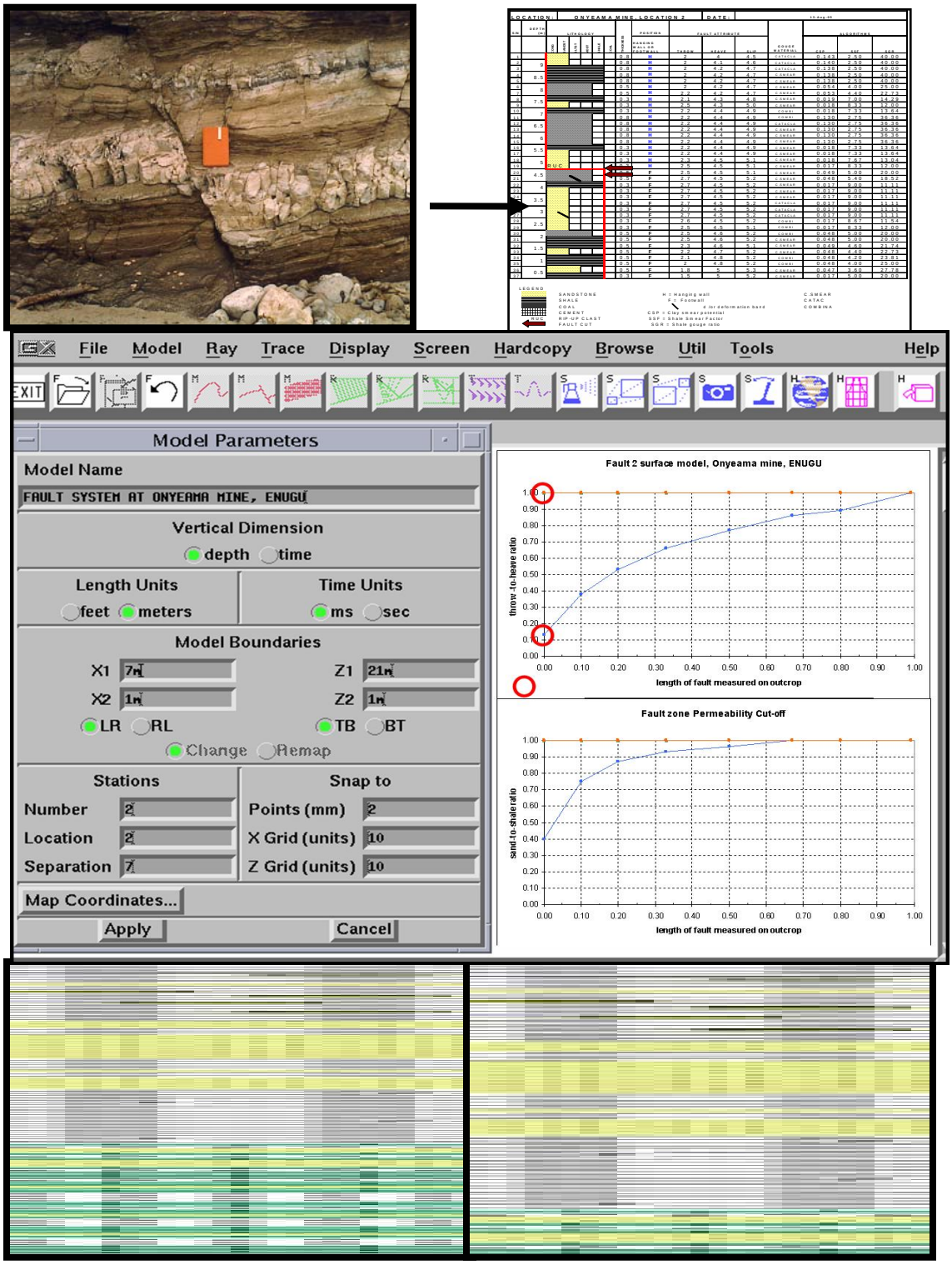

Figure10: Computer modelling workflow

one centimeter. Movement direction is down-dip, with rarely a strike-slip competent. Figure 11 shows a typical pressure data and plots from wells 1 and 2 drilled in the study areas.

Joints: In the Agbogugu outcrops, some beds have a well-developed joint pattern. The average strike of these joints is 035^0, forming obliquely to the fault strike. The large majority of these joints do not show any movement along the joint surface.
These joints were interprepted as late features, absent during the main phase of deformation; hence do not aggregate enough to evolve into fault surfaces in the study area.

Segmented fault planes: Almost all of the faults obtained from the studied areas were segmented. These segments do not necessarily have the same plane.This causes structures such as soft-linkage and splay faults which is observed clearly at Agbogugu and Onyeama mines.

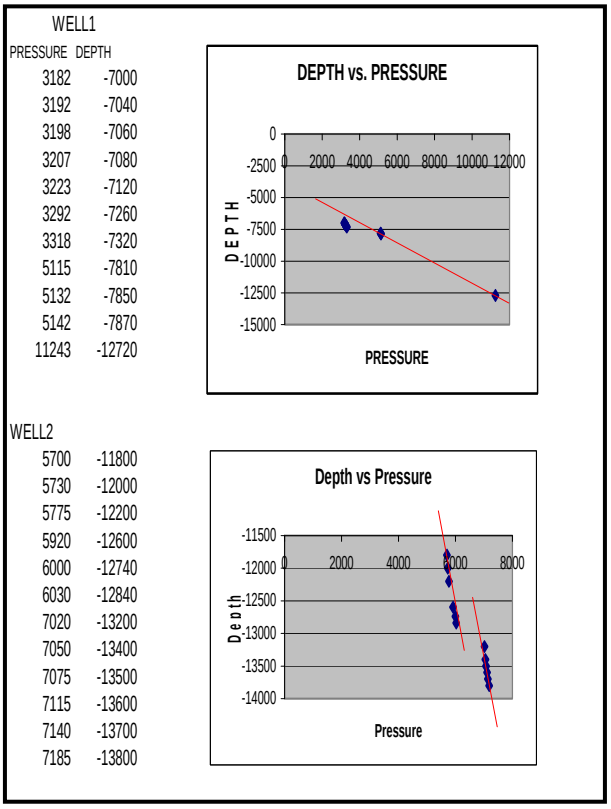

Figure 11: Pressure data and plots from well 1 and well 2 drilled in the Area.

(the negative depth values indicate sub-surface depths).

Multiple slip planes: Faults containing multiple parallel planes were identified in Agbogugu area, forming different slip angles and varying throw along the main fault surfaces from over 10m in some places to 2m or less in others. Such structures are described as zones of segment linkage, and near restraining bends.

Sealing Mechanisms: Several workers in sandstone-shale sequence of Anambra basin have documented the various sealing mechanisms observable from outcrops samples and geophysical data. The types include clay smear, cataclasis, fault cementation, pressure solution, crystal plasticity, and a combination of mechanism. This present study has shown that more than one of these mechanisms are present at the fault zones in Enugu area of Anambra basin. The study has also produced set of cross plots; which are comparable to similar plots from previous studies using different approaches (figures 12 & 13).

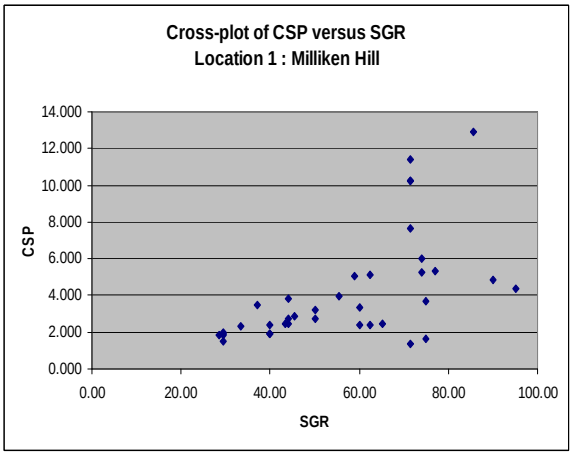

Figure 12a: Cross-plot of Clay Smear Potential and Shale Gouge Ratio at Location 1.

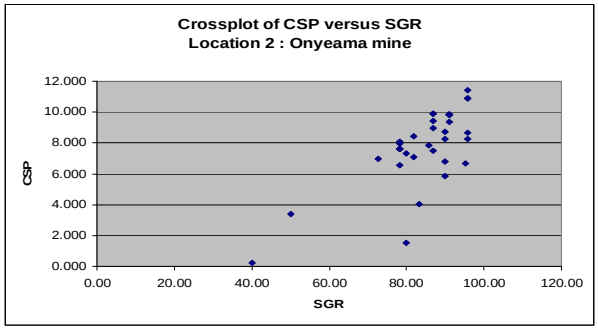

Figure 12b: Cross-plot of Clay Smear Potential and Shale Gouge Ratio at Location 2.

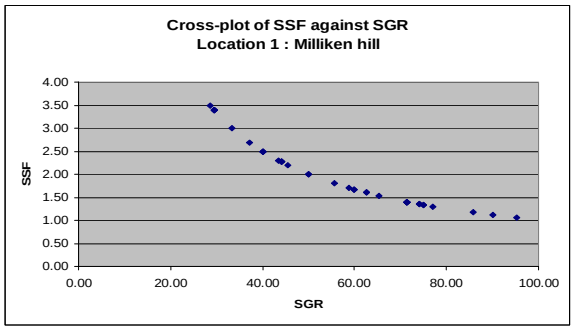

Figure13a:Cross-plot of shale smear factor against Shale gouge ratio at location 1

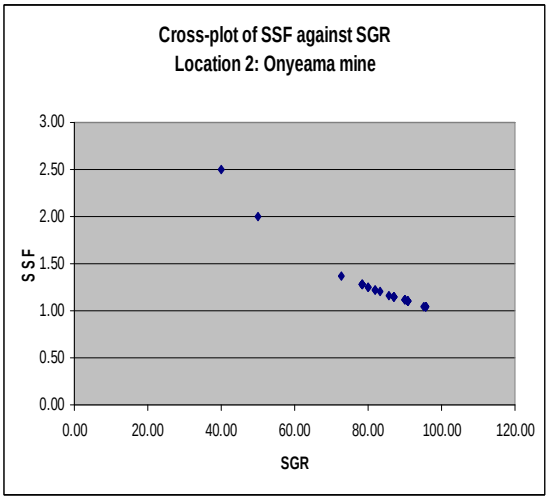

Figure 13b: Cross-plot of shale smear factor against Shale gouge ratio at location 2

Discussion of results

A number of mechanisms have been recognized where by fault planes can act as seals. This includes juxtaposition, clay smear, cataclasis, digenesis and pressure solution.

Using the cross-plot studies, it has shown that more than one of these mechanisms are present at the fault zones in Enugu area of Anambra basin. For instance in figure 12, a cross plot of shale smear factor (SSF) and shale Gouge Ratio (SGR) clearly shows a curvilinear relationship between the two algorithms. this implies that a high SGR is equivalent to a low SSF value. This is quite a good match to the plots obtained by Bouvier et al, 1989 and Yielding et al, 1997 for fault K. Num River field, Niger Delta. An SGR value of bout 15-20% is widely considered to represent the threshold between non-sealing and sealing bahaviour of faults in siliciclclastic sequences such as the Niger Delta (Fristad et al 1997).

Figures 12 and 13 show that this documented SGR values of 15-20% correspond respectively to SSF of 3.5 to 10 and CPS of 0.1 TO 3.0. The obtained vales for the CSP are somewhat similar to the values obtained by Bretan et al,(2004) for work done in Niger Delta using different methods. Jev et al, (1993) used the same technique of CSP calculations on the Akaso field in the Niger Delta and quoted a CSP of less than 15 as non-seating and CSP of more than 30 as sealing for faults bounding unsealed prospects.

Similarly, from a study of 80 faults, Lindsay et al, (1993) opined that smaller values of SSF are more likely to correspond to continuous smears and therefore to a sealing layer, than larger values. He therefore concluded that shale smear may be and incomplete for a SSF value greater than 7. Comparing this to figure 13, this actually correlates very well to the SGR values of less than 40% (within threshold).

In the nutshell, a deduction from these analyses is that the results obtained from using integrated approach in the study area, are quite comparable to those from other methods. One can therefore use the results to locally calibrate any future work in Anambra basin using same or different techniques.

This study has shown that outcrop data alongside seismic and well log data could be useful in the delineation and examination of faults sealing mechanisms with respect to their hydrocarbon potentials. From the results obtained from the study area, the following submissions could be drawned:

a. The estimated plots agree reasonably well with the measures obtained from similar work, using different techniques and dataset.

b. The pressure plots show that both vertical and lateral variations exist in Anambra basin and these variations could be due to processes other than fault sealing.
c. The results of seismic interpretaition show the fault throw in the range of 20 meters, which have been classified as sealing.

Although the study has not provided answers to all the questions on fault gouge materials and their impact on hydrocarbon accumulation, but it has provoked some thoughts about possible clues why hydrocarbon may not be trapped against faults in Anambra basin.

Correspondent to:
Oyedele, K.F
Department of physics, University of Lagos, Lagos, Nigeria.
Telephone: +2340833357439
kayodeunilag@yahoo.com.

References.

1. Akande, S.O, Viczian, I. and Erdtmann, B.D: Prediction of petroleum generation intervals in the Southern Nigeria rift basins by means of clay transformation, vitrinite reflectance and fluid inclusions studies. NAPE Bulletin, 2005;Vol. 18 (1). p38 – 51.

2. Antoneli, M. and Aydin, A: Effect of faulting on fluid flow in porous sandstones: Geometry and spatial distribution. Bulletin of the American Association of petroleum Geologists 1995; 79(5) p642-671.

3. Bense V.F., Van Balen, R.T. de Vries, J.J: The impact of faults on the hydrogeological conditions in the Roer Valley Rift Sytem: an overview. Netherlands Journal of Geosciences.2003; 82(1) p41 – 45.

4. Bouvier, J.D., Kaars–Sijpesteijn, C.H. Kluesner, D.F., Onyejekwe, C.C., Vander Pal, R.C. Three-dimensional siesmic interpretations and fault sealing investigations, Num River Field, Nigeria. AAPG Bulletin 1989; 73.

5. Fristed, T. Groth, A., Yeilding, G. Freeman, B. Quantitative fault seal prediction: a case study from Oseberg Sydney. 1997; In: P. Moller-Pedersen, and A.G.

6. Fulljames, J.R., Zijerveld, L.J.J., Franssen, R. C.M.W., Ingram, G.M and Richard, P.D. Fault seal processes, in Norwergian Petroleum Society, eds. Hydrocarbon seal-importance from petroleum exploration and production 9th conference abstract.1996; Oslo, NPS p5.

7. Hogue, M**.** Petrographic differentiation of tectonically controlled cretaceous sedimentary cycles, Southeastern Nigeria sed. Geol.1997; Vol.17 p235 – 245.

8. Knipe, R.J., Fisher, Q.J., Jones, G. Clennell, M.R. Farmer, A.B., Harrison, A., White, E. A. Fault seal analysis: Successful methothologies, application and future directions. In: p. Moller-pederson, and A.G. Koesther (Eds.). Hydrocarbon Seals, NPF Special publication 7,1997, p15-38.

9. Ladipo, K.O. Paleogeography, sedimentation and tectonic of the upper cretaceous Anambra basin, Southeastern Nigeria. Journ. Of Afr. Earth. Scs. 1988; vol.7p81- 821.

10. Lindsay, N.G., Murphy, F.C., Walsh, J.J., Watterson,J. Outcrop studies of shale smears on fault surfaces special publication of International Association of Sedimentology.1993; 15, p113 – 123.

11. Murat, R.C. Stratigraphy and paleogeography of the cretaceous and lower tertiary in the southern Nigeria.1972; p45-60.

12. Nwajide, C.S. Eocene tidal sedimentation in the Anambra basin, southeastern Nigeria. Nigerian Journ. of min. Geol. 1987; vol.16 p 103-109.

13. Ojoy, K.A. The Southern part of the Benue trough (Nigeria) cretanceous stratigraphy basin analysis, paleo–oceanography and geodynamic evolution of the equatorial domain of the South Atlantic. NAPE Bull. 1992; vol.7 p 131–152.

14. Yielding, G., Freeman, B., Needham, D.T. Quatitative fault seal prediction: AAPG Bull.1997; 81(6) p 897–917.

Effect of Water uptake on Germinability in Seeds of Some Medicinal Plants, Uttarakhand, India

Anoop Badoni*, Mayank Nautiyal, Kiran Gusain, Manpreet Kaur, Rakhi Dhiman, Chetna Bisht[+] and J. S. Chauhan

Seed Physiology Laboratory
Department of Seed Science and Technology
([+]High Altitude Plant Physiology Research Center)
H. N. B. Garhwal Central University Srinagar- 246 174, Uttarakhand, India
*For Correspondence: annabadoni@yahoo.co.in

Abstract

Three important medicinal plants of Uttarakhand, India were used in the present study. The effect of different imbibitions time and percentage were first time reported on seed germination and early seedling growth in *Withenia somnifera, Pyracantha crinulata and Andographis paniculata.* The initial weight of 800 seeds from each species were taken and dipped in water for imbibition. In every 3rd hr. 100 seeds were taken out and after weighing kept in seed germinator at 25^0C temperature and 16/8 hr. photoperiod for germination test, the process was done till to 24 hr. In *Withenia somnifera* maximum germination (38%) was reported after 24 hr. imbibition while in *Pyracantha crinulata* maximum germination (94%) was reported after 12 hr imbibition and in *Andographis paniculata* 15 hr and 24 hr imbibition showed maximum germination (80%). [The Journal of American Science. 2009;5(4):123-128] (ISSN 1545-1003).

Introduction

Each living organism has its own set of environmental conditions under which it grows most efficiently. Plant and environment interaction primarily regulates the survival of all living being on the earth. Water is one of the most remarkable and essential components for all life. It comprises approximately 85 to 95% of the initial fresh weight in physiological active herbaceous plants. If the water contents in most of the species falls much below this level many of the physiological activities of plants are impaired. Water is an important necessity for germination (Purohit, 2008). There is a great irregularity in the rate of water absorption by plant materials, including cotyledons of pea, corn, grains and seeds of *Xanthium, Gossypium,* and *Hibiscus*, and tissue of *Auricularia.* It was determined that the rate of intake is rapid at first, gradually falling off as more water is taken up until it approaches zero as the tissue becomes nearly saturated. Finally absorption ceases, due to complete saturation or to the balance of outward diffusion of soluble substances from the tissues with inward diffusion from the surrounding solution. Seed priming is a pre-sowing strategy for infuencing seedling development by modulating pre-germination metabolic activity prior to emergence of the radicle and generally enhances germination rate and plant performance (Bradford, 1986; Taylor and Harman, 1990). During priming, seeds are partially hydrated so that pre-germinative metabolic ac-tivities proceed, while radicle protrusion is prevented, then are dried back to the original moisture level (McDonald, 2000).

Material and Method

The present study was carried out with the objective to evaluate the effect of different imbibition time on germinability in seed of *Withenia somnifera, Pyracantha crinulata and Andographis paniculata.* This is first time reported, about every 3rd hr. imbibition percentage till to 24 hr. and its effect on germination in above three important medicinal plants. In the present investigation the initial weight of 800 seeds from each species were taken and dipped in water for imbibition. In every 3rd hr. 100 seeds were taken out and after weighing kept in seed germinator at 25^0C temperature and 16/8 hr. photoperiod for germination test, this process was done till to 24 hr. Data were observed daily for radical emergence and early seed germination.

Result and Discussion

Germination and seedling establishment are critical stages in the plant life cycle. In crop production, stand establishment determines plant density, uniformity and management options (Cheng and Bradford, 1999). In arid and semi-arid environments, the water needed for germination is available for only a short period, and consequently, successful crop establishment depends not only on the rapid and uniform germination of the seed, but also on the ability of the seed to germinate under low water availability (fischer and Turner, 1978). However, if the stress efect can be alleviated at the germination stage, chances for attaining a good crop with economic yield production would be high (Ashraf and Rauf, 2001).

In the present study Imbibition percentage directly affected the germination percentage, in all three plants (Table-1). In *Withenia somnifera* maximum germination (38%) was reported after 24 hr. imbibition (Fig.1 and 2-a) while in *Pyracantha crinulata* maximum germination (94%) was reported after 12 hr imbibition (Fig.1 and 2-b) and in *Andographis paniculata* 15 hr and 24 hr imbibition (Fig.1 and 2-a) showed maximum germination (80%). The early seed germination in all three species were recorded in 24 hr imbibition, in *Withenia somnifera* germination was start after 7th day while in *Pyracantha crinulata* and *Andographis paniculata* germination was start after 6th and 4th days respectively. Similarly Some researchers have indicated that the main reason for germination failure was the inhibition of seed water uptake due to a high salt concentration (Coons et al., 1990; Mansour, 1994), whereas others have suggested that germination was affected by salt toxicity (Leopold and Willing, 1986; Khajeh-Hosseini et al., 2003).

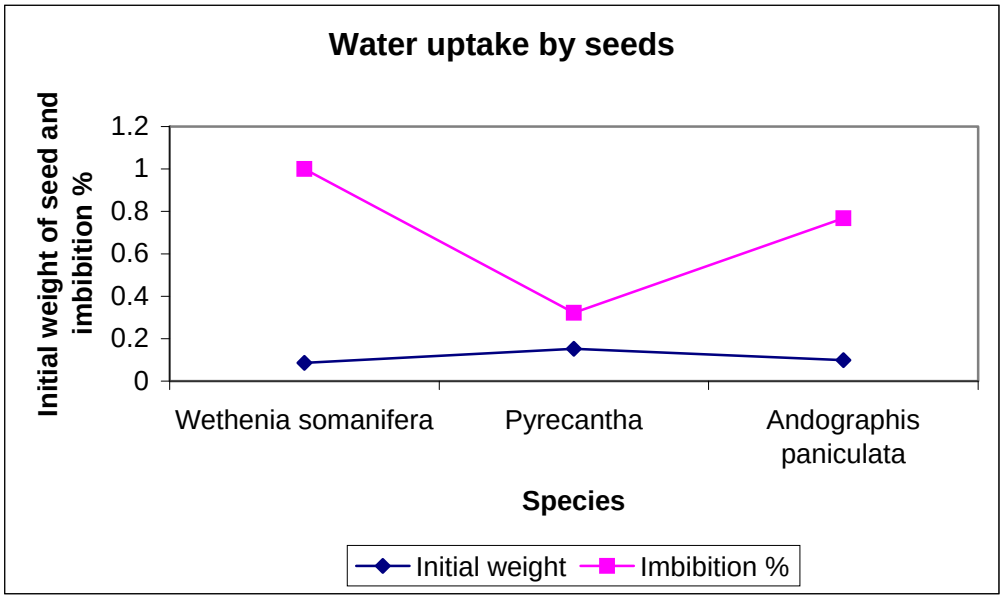

Fig. 1 Initial weight and total water uptake by seeds of medicinal plants

Table-1 Effect of Imbibition on Germination behavior of *Withenia somnifera*

Imbibition hr.	Imbibition%	Germination%	Days required for onset of germination	Days required for completion of grmination
3	18.6	18	10	28
6	22	8	12	30
9	33.7	26	9	26
12	38.8	16	14	34
15	40.6	12	14	34
18	54.6	20	10	28
21	80.2	18	12	30
24	100	38	7	22

Table-2 Effect of Imbibition on Germination behavior of *Pyrecantha crinulata*

Imbibition hr.	Imbibition%	Germination%	Days required for onset of germination	Days required for completion of grmination
3	13.8	72	12	15
6	14.4	70	10	12
9	21.7	82	12	10
12	26.3	94	8	10
15	28.2	72	14	15
18	32.2	84	10	12
21	41.4	76	10	12
24	42.2	78	6	9

Table-3 Effect of Imbibition on Germination behavior of *Andographis paniculata*

Imbibition hr.	Imbibition%	Germination%	Days required for onset of germination	Days required for completion of grmination
3	16.1	76	10	12
6	19.1	70	9	12
9	22.2	42	10	14
12	42.4	66	10	14
15	45.4	80	6	10
18	69.6	48	9	12
21	70.7	72	9	12
24	76.7	80	4	8

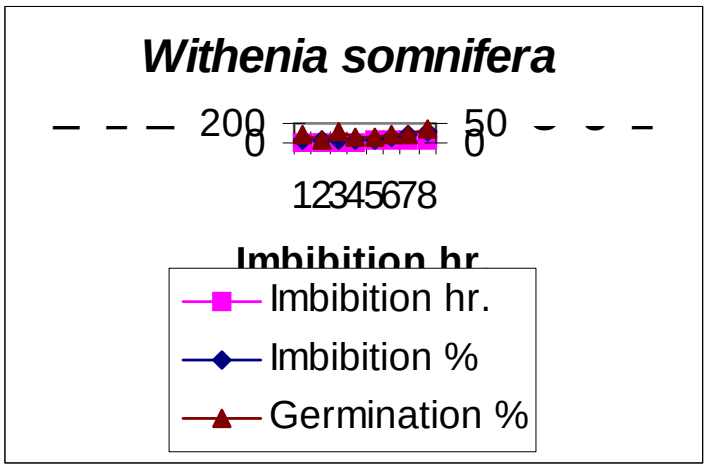

(a)

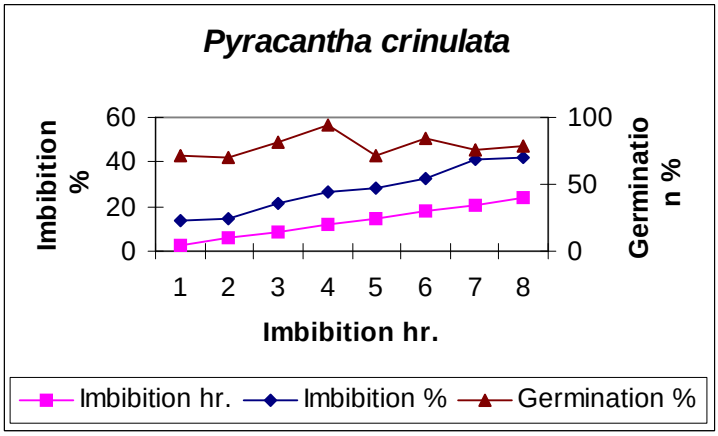

(b)

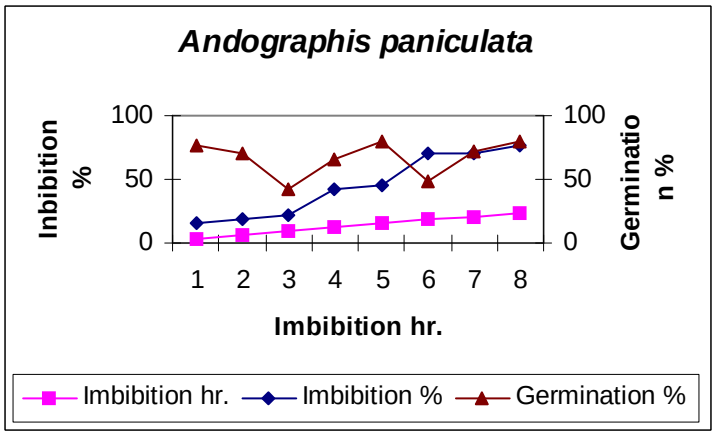

(c)

Fig. 2 Effect of Imbibition percentage on seed germination behavior of **(a)** *Withenia somnifera* **(b)** *Pyracantha crinulata and* **(c)** *Andographis paniculata*

References

1. Ashraf, M., H. Rauf (2001) Inducing salt tolerance in maize (Zea mays L.) through seed priming with chloride salts, growth and ion transport at early growth stages. Acta Physiol. Plant. 23: 407-414.
2. Bradford, K. J (1986) Manipulation of seed water relations via osmotic priming to improve germination under stress conditions. Hurt. Sci. 21: 1105–1112.
3. Cheng, Z., K. J. Bradford (1999) Hydrothermal time analysis of tomato seed germination responses to priming treatments. Journal of Experimental Botany 33: 89-99.
4. Coons, J. M., R.O. Kuehl and N.R. Simons (1990) Tolerance of ten lettuce cultivars to high temperature combined with NaCl during germination. J. Amer. Soc. Hort. Sci. 115: 1004-1007.
5. Fischer, R. A., N. C. Turner (1978) Plant productivity in the arid and semiarid zones. Ann. Rev. Plant Physiol. 29: 277-317.
6. Khajeh-Hosseini, M., A.A. Powell and I.J. Bingham (2003) The interaction between salinity stress and seed vigour during germination of soybean seeds. Seed Sci. & Technol. 31: 715-725.
7. Leopold, A.C. and R.P. Willing (1984) Evidence of toxicity effects of salt on membranes. In: Salinity Tolerance in Plants, (eds. R.C. Staples and G.H. Toenniessen), pp. 67-76. John Wiley and Sons, New York.
8. Mansour, M.M.F (1994) Changes in growth, osmotic potential and cell permeability of wheat cultivars under salt stress. Biologia Plantarum, 36: 429-434.
9. McDonald, M. B. (2000) Seed priming, Black, M., J. D. Bewley, (Eds.), Seed Technology and Its Biological Basis, Shefeld Academic Press, Shefeld, UK, 287–325.
10. Purohit, Mamta (2008) Effect of water stress on seed germination and metabolism in *Albizia chinensis* (Osbeck) Merril, M. Phil. Thesis, to H. N. B. Garhwal University, Srinagar, Uttarakhand, India
11. Taylor, A. G., G. E. Harman (1990) Concepts and technologies of selected seed treatments. Ann. Rev. Phytopathol. 28:321–339.

3/17/2009

Correspondence to:

Anoop Badoni
Researcher and Young Scientist (UCOST)
Department of Seed Science and Technology
H. N. B. Garhwal Central University Srinagar-246 174,
Uttarakhand, India
annabadoni@yahoo.co.in

The Journal of American Science

The ***Journal of American Science*** is an international journal with a purpose to enhance our natural and scientific knowledge dissemination in the world under the free publication principle. Any valuable paper that describes natural phenomena and existence or any reports that convey scientific research and pursuit is welcome. Papers submitted could be reviews, objective descriptions, research reports, opinions/debates, news, letters, and other types of writings that are nature and science related. All the manuscripts will be processed in a professional peer review. After the peer review, the journal will make the best efforts to publish all the valuable works as soon as possible.

Introductions to Authors

1. General Information

(1) Goals: As an international journal published both in print and on internet, *The Journal of American Science* is dedicated to the dissemination of fundamental knowledge in all areas of nature and science. The main purpose of *The Journal of American Science* is to enhance our knowledge spreading in the world under the free publication principle. It publishes full-length papers (original contributions), reviews, rapid communications, and any debates and opinions in all the fields of nature and science.

(2) What to Do: *The Journal of American Science* provides a place for discussion of scientific news, research, theory, philosophy, profession and technology - that will drive scientific progress. Research reports and regular manuscripts that contain new and significant information of general interest are welcome.

(3) Who: All people are welcome to submit manuscripts in any fields of nature and science.

(4) Distributions: Web version of the journal is freely opened to the world, without any payment or registration. The journal will be distributed to the selected libraries and institutions for free. For the subscription of other readers please contact with: editor@americanscience.org or americansciencej@gmail.com or editor@sciencepub.net

(5) Cost: This journal will be no charge for the manuscript contributors. If the author needs hard copy of the journal, it will be charged for US$100/issue to cover the printing and mailing fee.

(5) Advertisements: The price will be calculated as US$400/page, i.e. US$200/a half page, US$100/a quarter page, etc. Any size of the advertisement is welcome.

2. Manuscripts Submission

(1) Submission Methods: Electronic submission through email is encouraged and hard copies plus an IBM formatted computer diskette would also be accepted.

(2) Software: The Microsoft Word file will be preferred.

(3) Font: Normal, Times New Roman, 10 pt, single space.

(4) Indent: Type 4 spaces in the beginning of each new paragraph.

(5) Manuscript: Don't use "Footnote" or "Header and Footer".

(6) Cover Page: Put detail information of authors and a short title in the cover page.

(7) Title: Use Title Case in the title and subtitles, e.g. "**Debt and Agency Costs".**

(8) Figures and Tables: Use full word of figure and table, e.g. **"Figure 1.** Annul Income of Different Groups**", Table 1. Annual Increase of Investment".**

(9) References: Cite references by "last name, year", e.g. "(Smith, 2003)". References should include all the authors' last names and initials, title, journal, year, volume, issue, and pages etc.

Reference Examples:

Journal Article: Hacker J, Hentschel U, Dobrindt U. Prokaryotic chromosomes and disease. Science 2003;301(34):790-3.

Book: Berkowitz BA, Katzung BG. Basic and clinical evaluation of new drugs. In: Katzung BG, ed. Basic and clinical pharmacology. Appleton & Lance Publisher. Norwalk, Connecticut, USA. 1995:60-9.

(10) Submission Address: editor@sciencepub.net, Marsland Company, P.O. Box 21126, Lansing, Michigan 48909, The United States, 517-980-4106.

(11) Reviewers: Authors are encouraged to suggest 2-8 competent reviewers with their name and email.

2. Manuscript Preparation

Each manuscript is suggested to include the following components but authors can do their own ways:

(1) Title page: including the complete article title; each author's full name; institution(s) with which each author is affiliated, with city, state/province, zip code, and country; and the name, complete mailing address, telephone number, facsimile number (if available), and e-mail address for all correspondence.

(2) Abstract: including Background, Materials and Methods, Results, and Discussions.

(3) Key Words.

(4) Introduction.

(**5) Materials and Methods**.

(**6) Results**.

(**7) Discussions**.

(**8) References**.

(**9) Acknowledgments**.

Journal Address:
Marsland Press
2158 Butternut Drive
Okemos, MI 48864
The United States
Telephones: 347-321-7172; 718-404-5362; 517-349-2362
Emails: editor@americanscience.org; americansciencej@gmail.com; sciencepub@gmail.com
Websites: http://www.americanscience.org; http://www.sciencepub.net; http://www.sciencepub.org

Pathogens Associated with Citrus Fruit Rots in Imo State of Nigeria

Ezeibekwe I. O and Unamba C.I.N.
Department of Plant Science and Biotechnology, Imo State University, Owerri, Nigeria
cinu2010@yahoo.com, innocent_ezeibekwe@yahoo.co.in

Abstract: The Study of pathogens associated with the rot of citrus fruits in some parts of South Eastern Nigeria presented four pathogens identified as *Phytophthora citrophthora (Butler), Fusarium oxysporum schlecht, Fusarium equiseti (Corda)* Sacc, *Botryodiplodia theobromae* (pat). The study showed that the rot caused by *B. theobromae* was more severe, followed by *P. citrophthora* rot, *F. oxysporum* rot and *F. equiseti* rot. Some disease control measures were recommended. [Journal of American Science 2009;5(4):129-132]. (ISSN: 1545-1003).

Key words: Pathogens, Citrus, Fruits, Rots, Imo State, Nigeria.

1. Introduction

Citrus is a tropical plant cultivated extensively in the sub-tropics with a Mediterranean climate (Mary *et al*,2003). Its fruits have been reported by Jim (2003) as very economically valued fruits among the. According to Nicole (2000), the fruits are used in making fruit salad and fruit juice. Mumoz (2003) recorded that their juice are palatable and can be taken as mild laxatives in constipation. Their essential oils are used in the cosmetic and pharmaceutical industries (Frazier and Westhote, 1978).

In the whole world, the post-harvest rots of these fruits have been extensively studied. (Fatemi (1972) reported *Citrus* fruits decline in Iran due to fruit rot incited by *Pythium aphanidermatum* (edson) fitz; and *Phytophthora citrophthora* (Butler) Leonian favaloro and Somma (1971) described *Phytophthora syringae* Kleb, *P. citricola* Sawada and *P. citrophthora* as the most widespread citrus fruit rot pathogens in Italy. Graham and Tummer (1994) also described *Phytophthora nicotianae* and *P. citrophthora* as the most common causal organisms of brown rot of *Citrus* fruits in Florida. Timmer and Menge (2000) implicated *P. citricola* Sawada, *P. citriophthora* (R.E. Sm & E.H. Sm) Leonian, *P. hibernalis* Carne, nad *P. nicotianae* Breda de Haan var. parasitica (Dastur) as causal agents of brown rot of fruits. They also described *Botryodiplodia theobromae* (Pat.) Griffon and Maubl as stem end rot pathogen. *Fusarium oxysporum* Schlechtend Fr. F. sp. citri was also described by them as a causal organism of dry fruit rot of *Citrus.*

In Nigeia, Adisa and Fajola (1982) implicated *Penicillum digitalum* and *P. citrinum* as pathogens of *Citrus fruit rots* in South Western Nigeria. They also considered *B. theobromae* as the most important fruit pathogen in South Western Nigeria. Nzekwe (1996) found out that *Fusarium spp, Curvularia spp, Aspergillus spp* and *Penicillum spp* cause *Citrus fruit* rots in Abia State of Nigeria. Dim (2004) isolated and recorded *Aspergillus spp, B. theobromae, Botrytis cinerea Pers. Fr., Fusarium spp, Phytophthora spp, Rhizopus stolonifer (Ehrenh fr)* Vuill, *Syncephalastrum racemoses, Gloesporium nervisequum and Mucor racemosus* in some harvested *Citrus* fruits in Imo State of Nigeria.

From the look of things and available materials, it seems that no investigation appears to have been carried out on the extent of fruit rots or the epidemiology of fruit rots in South Eastern Nigeria. This paper therefore looked into the incidence and severity and extent of citrus rots in some parts of South Eastern Nigeria with a view to suggesting some control measures.

2. Materials and Methods

Rotted fruits were collected from the plantations and markets between September and October, 2008 in clean and labeled polyethylene bags to the laboratory where isolations were carried out by swabbing diseased fruits with 0.01 percent $HgCl_2$ and rinsed with sterile distilled water. Discs (3mm thick) of rotted tissues were then cut under aseptic conditions and plated on Sabourands Dextrose Agar (SDA) and incubated at 30^0c. Isolates were identified using Barnet and Hunter (1987), Paul *et al* (1983).

In the pathogenicity tests, pure isolates of each type of rot were inoculated into healthy fruits at the same stage of ripening. The healthy fruits were surface sterilized with 0.01 percent $HgCl_2$ and washed in changes of sterile distilled water. A cork borer (5mm in diameter) was driven to a depth of 4mm into the fruits making sure that the bored tissues were not removed after withdrawing the cork borer.

Two drops of a spore suspension ($5x10^4$/ml) of each isolate were deposited around the wound outline made on the healthy fruits. In the controls, two drops of sterile distilled water were used. For each isolate, ten treatments and ten controls were set up. Each inoculated fruit was vaselined at the point of inoculation and

placed in a micro-humidity chamber at 25^0c for the first seven days. Regular observations were made and re-isolation of any pathogenic fungi was done for comparism with the original isolate.

During this period, the extent of rot caused by each isolate was measured at interval with ruler (in cm) and also recorded. The data obtained was subjected to analysis using Analysis of Variance at 5% level of significance between the extent of rots caused by the four isolates.

$$F = \frac{MSB}{MSW}$$

Results

Table 1: **Characterization and Identification of Isolates**

ISOLATES	COLONY FEATURES	MICROSCOPIC FEATURE	REMARK
1st Isolate	Isolate/organism was seen in a culture growth rate was slow. Mycelium was in a white colony, delicate with purple tinge, sparse and sometimes abundant (plate 1)	Uder the microscope, the organism was seen to have conidia of varied sizes. Micro conidia borne on simple conidiosphore arising laterally on the hyphae. Microconidia generally abundant, variable, oval, ellipsoid, cylindrical, straight to curved structure. Macroconidia sparse and thin walled, generally 3-5 septate and pointed at both ends. There was presence of chlamydospores (Plate 1)	Isolate identified as *Fusarium schlecht*
2nd Isolate	Colony growth wa rapid with dense aerial growth. Mycelium white but turned tan to brown colour with age. Underneath surface brownish.	Move of macroconidia strongly septate present, sickle shaped with distinctive curvature. Apical cell move elongated in curvature and basal cell footshaped. Chlamydospores abundant and thickwalled (plate 2)	Isolate identified as *Fusarium equisett* (Corda) Sacc.
3rd Isolate	Isolate seen as white dense fast growing culture, extensive in growth but gradually formed dirty white to black (plate 3)	Short simple conidiosphore was seen, conidia dark, ovoid to elongate. Mature conidia 2-celled, intercalary chlamydospores seen (plate 3)	Identified as *Botryodiplodia theobromae* Pat.
4th Isolate	Colony whitish culture, gradually spreading, not profuse but flat and depressed. Underneath colour is milk to yellowish. Aerial mycelium abundant, colony rapid growth (plate 4)	Mycelium highly branched, and non-septate when young, but an old cultures mycelium became septate bearing reproductive bodies (sporangia). The sporangium lemon shaped was borne symbolically on short sporangiosphores. Sporangium ovoid narrow at base produced singly. Sporangia production is sparse, few chlamydosphores	Isolate identified as *Phytophthora palmivora (*Butler)

Table 2: The extent of rots caused by the four fungi isolates (0.05)

Isolates	3rd Day (cm)	4th Day (cm)	5th Day (cm)	Average (cm)
P. citrophthora	2.90	5.10	8.00	5.33
B. theobraomae	3.00	4.90	9.20	5.70
F. oxysporium	0.50	1.10	2.70	1.43
F. equiseti	0.10	0.20	0.60	0.30

Data on average of three determinations from isolations

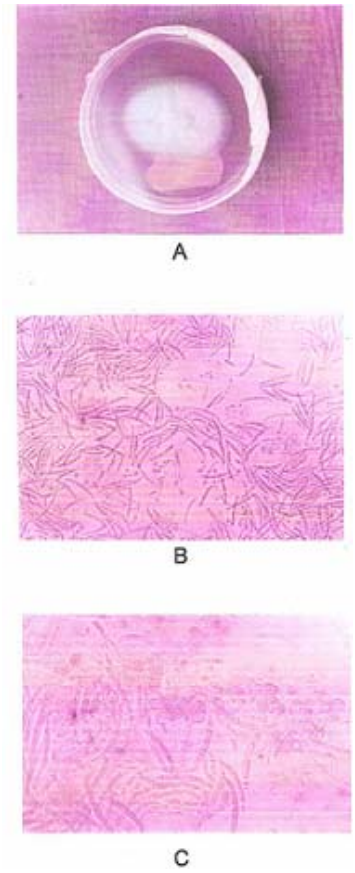

Plate 1: (a) culture (b) Conidia and (c) chlamydospores of *Fusarium oxysporum*

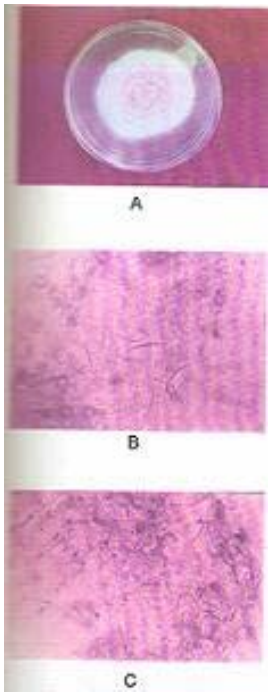

Fig 2: (a) Culture (b and c) hyphae, conidia and chlamydospores of *Fusarum equiseti*

Plate 3: (a) Hyphae (b) Conidium and chlamydospores of *B. theobromae*

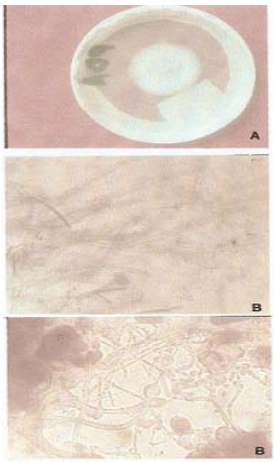

Plate 4: Culture (a) Hyphae (b) Sprangia of *P. citrphthora.*

3. Discussion

During the study, four organisms (pathogens) were isolated, characterized (Table 1), identified as *Fusarium oxysporium* Schlecht, *Phytophthora citrophthora* Butler, *Botryodiplodia theobromae* Pat and *Fusarium equiseti* (Corda*)* (plates 1,2,3 and 4). Pathogenicity studies confirmed them to be responsible for citrus fruit rot.

During the pathogenicity test, *P. citrophthora* was found to be associated with the fruits infected by browb rot, *B. theobromae* associated with those infected with brown leathery rot and stem end rot, and *Fusarium spp* were found in associuation with fruits infected with dry rot. This confirms the works of Graham and Timmer (1994) and Timmer and Menge (2000) that *Phytophthora spp* cause brown rot of *Citrus spp* and also that *B. theobromae* caused stem end rot of *Citrus* fruits. They also implicated *Fusarium spp* as causal organisms of dry fruit rots.

The extent of the rot caused by *B. theobromae* seems to be more severe (table 2). This means that the rot it caused advanced considerably within five days. This confirms the findings of Adisa and Fajola (1982) that *B. theobroamae* is the most important *Citrus* fruit rot in the South Western Nigeria. It was also observed that the extent of rot caused by *P. citrophthora* (5.33cm within 5 days) as well as the incidence and severity of the rot it causes (brown rot) were all high during the study. This finding is in line with the findings of Timmer and Menge (2000) that *P. citrophthora* as the causal agents of brown rot diseases of *Citrus* fruits. It also agrees with the finding of Favoloro and Somma (1971) who described *P. citropphthora* as the most widespread *Citrus* fruits rot pathogens in Italy. The extent of rots caused by the two *Fusarium spp* were moderate and the incidence and severity of the types of rot they cause (dry rot) was also moderate. This agrees with the work of Dim (2004) who mainly isolated and recorded *Fusarium spp* as been associated with diseased *Citrus* fruits in Imo State of Nigeria.

4. Conclusion and Recommendation

The results of this study showed a high incidence and severity of *Citrus* fruit rot caused by fungal pathogens like *B. theobromae, Fusrium species and Phytophthora spp* cause fruit rots in the areas studied.

Care should be taken as a disease control measure to avoid wounds on the citrus fruits especially during harvesting and transportation of citrus fruits since wounds encourage easy entrance of the pathogens. Fruits should not be plucked with sticks but be done by climbing the citrus trees with jute bags hung on the tree which is lowered with rope when full. The harvesting is better done when the fruits are mature green. Harvested fruits should be wrapped in papers in baskets during transportation to avoid wounds on the fruits. Most post harvest diseases of citrus fruits are infections that established before harvest. Therefore, pre-harvest treatment or control of the pathogens with fungicides are necessary.

Correspondence to
Dr. I. O Ezeibekwe
Department of Plant Science and Biotechnology, Imo State University, Owerri, Imo State Nigeria.
innocent_ezeibekwe@yahoo.co.in,
cinu2010@yahoo.com

References

Adisa, V.A and Fajola, A.O (1982). Post harvest fruit rot of three species of *Citrus* in South Western Nigeria. *Indian phytopath*. Department of Botany, University of Ibadan 35(4):595-603.

Bannet, H.L and Hunter, B.B (1987). Illustrated genera of imperfect fungi (4th ed). Macmillan Publishing Company, New York, ISOP

Dim, M.U (2004). A survey of diseases of *Citrus* in Owerri zone of Imo State. Project work, Department of Plant Science and Biotechnology, Imo State University. P vi

Atemi, J (1972). Pythiaceous fungi associated with *Citrus* decline in Iran. *Phytopath. Z 74*:153-160.

Frazier, W.C and Westhofe, D.C (1978). Contamination, preservation and spoilage of vegetables and fruits. *Food Microbiology*. New York. McGraw Hill Book Company, 3rd edition 12:194-214.

Graham, j.M and timmer, L.W (1994). *Phytophythora* diseases of *Citrus. A series of the plant pathology department*. Florida Co-operative Extension Service, Institute of Food and Agricultural Science, University of Florida. Life Science, University of Arizona.

Mumoz, D.J.A (1978). *Intenational Journal of Refrigeration 3*: 279-287.

Micole, R (2000). Use of *Citrus* fruits. Phytopath 3: 180-200.

Nzekwe (1996). Diseases of *Citrus sinensis* fruit. Project work, Department of Botany, Abia State University. Pp 11-31.

Paul, E.N; Toussoun, T.A; Marassas, W.F.O (1983). *Fusarium spp.* Manual for identification. The Pennsylavia State University Press, London, 91pp

Timmer, L.W and Menge, J.A (2000). Common names of plant diseases. Diseases of *Citrus* APS Interactive Careers and Placement. *Journal and News Online Resources.* Kagawa APS Press Bookstore.
cinu2010@yahoo.com
3/22/2009

Comparative Effect of the Foliar Spray and Seed Soaking Application Method of Gibberellic Acid on the Growth of *Abelmoschus Esculentus* (Okra Dwarf)

Unamba C.I.N., Ezeibekwe I.O. and Mbagwu F.N.

Department of Plant Science and Biotechnology, Imo State University, Owerri, Nigeria.
cinu2010@yahoo.com

Abstract: This work was aimed at determining the effect of low concentrations (0,1,5,10,20 and 30 ppm) of gibberellic acid on the growth of *Abelmoschus esculentus* (dwarf) and also compared the efficacy of the spraying and seed soaking method of application of this acid. Several growth parameters were measured which include Number of internode, Length of Internode, Plant height, Number of leaves, Length of petiole, Number of flower buds and Number of fruits after the acid was applied exogenously using the two methods of application. The test of two population means analytical procedure adopted at 5% level of significance showed that gibberellic acid significantly stimulated internode elongation, Plant Height and Number of leaves and caused a reduction in the petiole length in both treatment methods. Gibberellic acid also stimulated earlier flowering , increased bud formation and fruit production. The foliar spray application was found to have a significant effect on the plant height when compared with the seed soaking application technique. Although GA_3 stimulated Internode elongation, it had no effect on the number of Internodes in both the treated plants and the control indicating that dwarfism of this variety of Okra may be due to the absence of adequate endogenous gibberellic acid. [Journal of American Science 2009;5(4):133-140]. (ISSN: 1545-1003).

Key words: Comparative effect, Foliar spray, Seed soaking, Application, Gibberellic acid, *Abelmoschus esculentus*,

1. Introduction

Plant regulators are organic compounds which, in small amounts, somehow modify a given physiological plant process and rarely act alone, as the action of two or more of these compounds is necessary to produce a physiological effect. Gibberellic acid is a simple gibberellin, promoting growth and elongation of cells. It affects decomposition of plants and helps plants grow if used in small amounts, but eventually plants grow a tolerance for it. Gibberellic acid stimulates the cells of germinating seeds to produce mRNA molecules that code for hydrolytic enzymes (Bidwell,1974).

Okra belongs to the family Malvaceae. It is a tropical and semi tropical plant with edible seed pods used as a vegetable. It is cultivated by means of seeds. Okra is an important vegetable crop plant in West Afric where the immature fruits which are good sources of vitamin C are used for the preparation of soup and sauces (Epenhuijsen, 1974). The immature leaves are used for soup preparation. Both the leaves and fruits may be conserved by drying. It can also be used for salad dressings, ice cream and its high protein content makes it a valuable food crop (Akinlade and Adesiyan, 1982).

Gibberellins stimulate extensive growth in intact plants. These enable them to overcome genetic dwarfness in some species if that dwarfness is because of a gene mutation, resulting into blocked gibberellin production.

This compound has now been applied to a large variety of plant organs in several ways and it has been found to greatly enhance stem elongation as its most striking effect. This was observed in many plants after treatment with minute amount of gibberellic acid (Brian and Hemming, 1955). An example of such a response was shown by (Bukovac and Wittwer, 1956) on dwarf bean which was induced to turn to a climbing bean. Gibberellins (GAs) play an essential role in many aspects of plant growth and development, such as seed germination (Haba et al., 1985, Khafagi et al., 1986, Kumar & Neelakandan, 1992; Maske et al., 1997), stem elongation and flower development (Yamaguchi & Kamiya, 2000). Wareing and Phillips (1976), recorded enhanced vegetative growth in plants sprayed with GA3. also when GA# was applied to plants there was similar increase in leaf area, leaf length and width. Also with respect to leaf growth, GA3 generally promoted elongation of graa leaves but had little or no effect on enlargement of broad leaves of dicotyledons.

Although there are many literatures on gibberellic

acid, no attempt has been made to find out the most effective method of application. This work therefore investigated the effect of low exogenous foliar spray and seed soaking application of gibberellic acid on the morphology of dwarf cultivar of Okra and ascertain the method of application of gibberellic acid-Foliar spray and seed soaking that is most effective to use. It also assessed whether the observed dwarfness in the Okra plant is as a result of possible low endogenous content of gibberellic acid.

2. Materials and Methods

60 Dried viable seeds of *Abelmoschus esculentus* were extracted, soaked in distilled water for 24 hours after which they were spread on moist filter paper in Petri-dishes. The Petri-dishes were kept in dark cupboards at room temperature of 37^{O}c . Polybags were filled with sandy loam soil. All the polybags were perforated at the base to enhance effective drainage. 30 of the seeds tested for viability were divided into six groups and soaked in GA_3 concentrations of 0,1,5,10,20 and 30ppm respectively for 12 hours. These were planted in the polybags. The remaining half of the seeds were also divided into six groups and planted without soaking them nor applying any GA_3 concentration. Three seeds were planted in each polybags and later thinned down to one.

Seven (7) days after planting, the seedlings that were not soaked were sprayed with GA_3 concentration of 0,1,5,10,20 and 30ppm respectively using a hand pump. During the spraying, the leaves were completely wet or moistened until droplets of the chemicals started to form. In the control, the plants were soaked and sprayed with distilled water. Each seedling was moistened daily with water. Each treatment was replicated 5 times

Fourteen (14) days after planting, the growth and development of the plants were observed and recorded at weekly intervals for six (6) weeks until the plants started fruiting. The parameters measured were Number of Internode, Length of Internode, Plant Height, Number of Leaves, Length of Petiole, Number of flower buds, Number of fruits. On each sampling occasion, three replicate plants were selected randomly for the above measurements. The results obtained were subjected to statistical analysis using the test of two population mean.

3. Results

The results of this work which adopted two different methods of GA_3 application for its study (foliar and seed soaking) showed a significant increase in the plant's physiological growth after treatment with varying concentrations of the acid. (figs 1 & 2)

The foliar and seed soaking application methods did not have any effect on the number of internodes in the treated plants when compared to the control (Table 1 & 2). There was however an increase in plant height, Number of leaves and length of internode. This increase was continuous throughout the period the experiment was conducted. A decrease in the length of petiole was observed in both treatment methods when compared with the control though a more increase was observed in the soaked seeds. (Tables 3-10)

The foliar spray application technique was found to produce more increase in plant height when compared to the seeds soaked in the GA_3. (Table 5 & 6). It appeared that there were two (2) ranges of linearity (a low and high range) in the increase of the parameters measured in response to the applied Ga_3 in both the foliar and seed soaking application techniques. The low linearity was observed from 0-5 ppm whereas the high range was from 10-30 ppm with 20 ppm having a relatively lower or somewhat inhibitory effect compared to 10 and 30 ppm, although the effect of the concentration of 20 ppm were still stimulatory when compared with the control. The peak increase in the foliar spray was observed at a concentration of 10 ppm while 30 ppm were more effective in the soaked seeds. (fig 1 & 2).

This increase when reviewed statistically at 95% level of confidence that is at 5% level significance was found to be significant.

Table 1: The effect of foliar spray application of GA_3 on Number of Internode of *Abelmoschus esculentus.* cv dwarf

	GA_3 concentration (ppm)					
Plant Age (days)	**0**	**1**	**5**	**10**	**20**	**30**
14	2	2	2	2	2	2
21	3	3	3	3	3	3
28	5	5	5	5	5	5
35	6	6	6	6	6	6
42	7	7	7	7	7	7
49	8	8	8	8	8	8

ΣX	**31**	**31**	**31**	**31**	**31**	**31**
X	**5.17**	**5.17**	**5.17**	**5.17**	**5.17**	**5.17**

Values are mean of three replicates

Table 2: The effect of seed soaking application of GA_3 on Number of Internode of *Abelmoschus esculentus.* cv dwarf

	GA_3 concentration (ppm)					
Plant Age (days)	**0**	**1**	**5**	**10**	**20**	**30**
14	2	2	2	2	2	2
21	3	3	3	3	3	3
28	5	5	5	5	5	5
35	6	6	6	6	6	6
42	7	7	7	7	7	7
49	8	8	8	8	8	8
ΣX	**31**	**31**	**31**	**31**	**31**	**31**
X	**5.17**	**5.17**	**5.17**	**5.17**	**5.17**	**5.17**

Values are mean of three replicates

Table 3: The effect of foliar spray application of GA_3 on Length of Internode (cm) of *Abelmoschus esculentus.* cv dwarf

	GA_3 concentration (ppm)					
Plant Age (days)	**0**	**1**	**5**	**10**	**20**	**30**
14	0.9	1.0	0.9	0.9	0.8	0.9
21	1.3	1.33	1.4	1.43	1.2	1.3
28	2.2	2.6	2.6	3.4	3.0	2.9
35	2.6	3.2	3.3	4.3	3.8	4.0
42	3.1	3.7	3.8	4.3	4.2	4.5
49	4.0	4.4	4.5	4.9	4.7	5.1
ΣX	**14.1**	**16.2**	**16.5**	**19.2**	**17.7**	**18.7**
X	**2.4**	**2.7**	**2.8**	**3.2**	**3.0**	**3.1**

Values are mean of three replicates

Table 4: The effect of seed soaking application of GA_3 on Length of Internode (cm) of *Abelmoschus esculentus.* cv dwarf

	GA_3 concentration (ppm)					
Plant Age (days)	**0**	**1**	**5**	**10**	**20**	**30**
14	0.8	1.0	0.9	0.9	0.8	0.9
21	1.2	1.3	1.4	1.4	1.3	1.4
28	2.2	2.5	2.6	3.1	3.0	3.3
35	2.6	3.2	3.2	3.9	3.7	4.2
42	3.1	3.7	3.8	4.3	4.2	4.5
49	4.0	4.4	4.5	4.9	4.7	5.1
ΣX	**13.9**	**16.1**	**16.4**	**18.5**	**17.7**	**19.4**
X	**2.3**	**2.7**	**2.7**	**3.1**	**2.95**	**3.2**

Values are mean of three replicates

Table 5: The effect of foliar spray application of GA_3 on Plant Height (cm) of *Abelmoschus esculentus.* cv dwarf

	GA_3 concentration (ppm)					
Plant Age (days)	**0**	**1**	**5**	**10**	**20**	**30**
14	6.0	6.4	6.7	7.3	6.7	7.2
21	7.8	9.4	9.8	11.2	10.8	11.2
28	8.7	10.5	10.9	12.8	12.0	12.7
35	10.2	12.5	13.0	14.9	13.7	14.1
42	12.7	15.5	16.0	20.1	16.3	18.9
49	14.6	17.7	18.1	22.4	19.3	21.0
ΣX	**60**	**72**	**74.5**	**88.7**	**78.8**	**85.0**
X	**10.0**	**12.0**	**12.4**	**14.8**	**13.1**	**14.2**

Values are mean of three replicates

Table 6: The effect of seed soaking application of GA_3 on Plant Height (cm) of *Abelmoschus esculentus.* cv dwarf

	GA_3 concentration (ppm)					
Plant Age (days)	**0**	**1**	**5**	**10**	**20**	**30**
14	6.0	6.5	6.8	7.13	6.9	7.2
21	7.7	8.5	8.2	9.8	9.5	9.9
28	8.6	9.6	9.6	11.5	10.7	11.6
35	10.2	11.7	11.2	13.2	12.4	13.6
42	12.7	14.7	14.2	17.7	15.3	18.8
49	14.7	16.8	16.4	20.3	18.3	21.3
ΣX	**59.9**	**67.8**	**66.4**	**76.6**	**73.1**	**82.4**
X	**10.0**	**11.3**	**11.1**	**13.3**	**13.2**	**13.7**

Values are mean of three replicates

Table 7: The effect of foliar spray application of GA_3 on Number of Leaves of *Abelmoschus esculentus.* cv dwarf

	GA_3 concentration (ppm)					
Plant Age (days)	**0**	**1**	**5**	**10**	**20**	**30**
14	4	4	4	4	4	4
21	5	5	5	5	5	5
28	6	7	7	8	7	7
35	7	8	8	9	8	9
42	8	9	9	10	9	10
49	9	10	10	11	10	11
ΣX	**39**	**43**	**43**	**47**	**43**	**46**

X	**6.50**	**7.20**	**7.20**	**7.80**	**7.20**	**7.70**

Values are mean of three replicates

Table 8: The effect of seed soaking application of GA_3 on Plant Height (cm) of *Abelmoschus esculentus.* cv dwarf

	GA_3 concentration (ppm)					
Plant Age (days)	**0**	**1**	**5**	**10**	**20**	**30**
14	4	4	4	4	4	4
21	5	5	5	5	5	5
28	6	7	7	8	7	8
35	7	8	8	9	8	9.3
42	8	9	9	10	9	10.2
49	9	10	10	11	10	11.3
ΣX	**39**	**43**	**43**	**47**	**43**	**47.9**
X	**6.5**	**7.2**	**7.2**	**7.83**	**7.2**	**8.0**

Values are mean of three replicates

Table 9: The effect of foliar spray application of GA_3 on Length of petiole (cm) of *Abelmoschus esculentus.* cv dwarf

	GA_3 concentration (ppm)					
Plant Age (days)	**0**	**1**	**5**	**10**	**20**	**30**
14	2.03	1.73	2.0	2.0	1.9	1.97
21	2.5	2.23	2.43	2.5	2.27	2.5
28	3.0	2.73	3.0	3.0	2.77	3.2
35	3.5	3.23	3.5	3.5	3.30	3.60
42	4.20	3.93	4.03	4.03	3.77	4.0
49	4.73	4.47	4.47	4.57	4.33	4.6
ΣX	**19.96**	**18.32**	**19.43**	**19.63**	**18.34**	**19.87**
X	**3.33**	**3.05**	**3.24**	**3.27**	**3.06**	**3.31**

Values are mean of three replicates

Table 10: The effect of seed soaking application of GA_3 on Length of Petiole (cm) of *Abelmoschus esculentus.* cv dwarf

	GA_3 concentration (ppm)					
Plant Age (days)	**0**	**1**	**5**	**10**	**20**	**30**
14	2.07	1.83	2.1	2.07	1.97	2.1
21	2.57	2.27	2.53	2.60	2.27	2.6
28	3.0	2.80	3.03	3.27	2.83	3.13
35	3.53	3.33	3.53	3.67	3.47	3.49
42	4.33	4.03	4.10	4.0	3.93	4.0
49	4.67	4.53	4.53	4.6	4.37	4.46
ΣX	**20.17**	**18.79**	**19.69**	**20.21**	**18.75**	**19.78**
X	**3.36**	**3.13**	**3.28**	**3.36**	**3.125**	**3.30**

Values are mean of three replicates

Table 11: The effect of foliar spray application of GA_3 on Number of flower buds and number of fruits of *Abelmoschus esculentus.* cv dwarf

Plant Age (days)		GA_3 concentration (ppm) 0	1	5	10	20	30
35	Number of flower buds	-	-	-	1	1	1
	Number of fruits	-	-	-	-	-	-
42	Number of flower buds	1	2	2	3	2	3
	Number of fruits	-	-	-	1	-	1
49	Number of flower buds	2	2	3	4	3	4
	Number of fruits	-	-	-	1	-	1

Table 12: The effect of seed soaking application of GA_3 on Number of flower buds and number of fruits of *Abelmoschus esculentus.* cv dwarf

Plant Age (days)		GA_3 concentration (ppm) 0	1	5	10	20	30
35	Number of flower buds	-	-	-	1	1	1
	Number of fruits	-	-	-	-	-	-
42	Number of flower buds	1	2	2	3	2	3
	Number of fruits	-	-	-	1	-	-
49	Number of flower buds	2	2	3	4	3	4
	Number of fruits	-	-	-	1	-	1

ANALYSIS OF DATA

H_0: There is no difference between the foliar spray application and seed soaking application of GA_3

H1: There is difference between the foliar spray application and seed soaking application of GA_3.

1.96 t_{tab} = 1.96

if t_{cal} < 1.96 (t_{tab}), we accept the null hypothesis and reject the alternative.

Comparism between the effect of foliar spray and seed soaking application of $GA_3$for Length of Internode

	N	Mean	Std. Dev.	T	D.F
S_S	30	2.95	1.46	0.02	8
F_S	30	2.94	1.44		

t_{cal} < 1.96 (t_{tab}), hence we accept the null hypothesis and reject H_1

Comparism of the effect of foliar spray and seed soaking application of GA_3 on Plant Height

	N	Mean	Std. Dev.	T	D.F
F_S	30	13.30	4.51	2.18	57
S_S	30	12.31	4.26		

t_{cal} > 1.96 (t_{tab}), we have therefore rejected H_O thus accepting H_1

Comparism of the effect of foliar spray and seed soaking application of GA_3 on Number of Leaves

	N	Mean	Std. Dev.	T	D.F
F_S	30	7.40	2.36	-0.10	57
S_S	30	7.46	2.39		

t_{cal} > -1.96 (t_{tab}), hence we accept the null hypothesis

Comparism of the effect of foliar spray and seed soaking application of GA_3. on Length of Petiole

	N	Mean	Std. Dev.	T	D.F
F_S	30	3.185	0.903	-2.06	57
S_S	30	3.248	0.881		

t_{cal} < -1.96 (t_{tab}), we accept the null hypothesis .

F_S = Foliar Spray
S_S = Seed Soaking

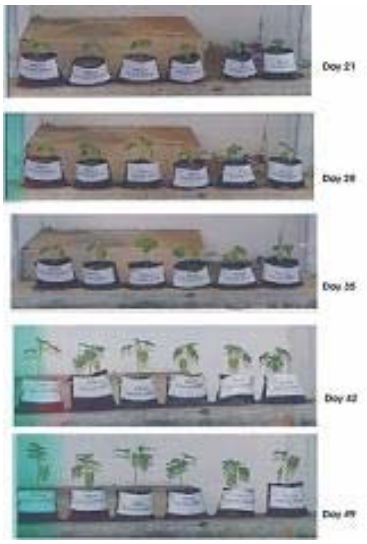

Effect of foliar spray application of GA3 on *A. esculentus*

Effect of foliar spray application of GA3 on *A. esculentus*

5. Discussion

From the observations one would deduce that more increase was observed in the sprayed plants. This is in agreement with the work of Bukovac and Wittwer (1956), when the acid was shown to have a vary remarkable effect on stem elongation of dwarf bean which was induced to turn to a climbing bean. Wareing and Phillips (1976) also recorded enhanced vegetative growth in plants sprayed with GA3. This hypothesis is also sustained by King et al. (2000), who reported greater stem growth in *Fuschia hibrida* and *Pharbitis nil*, resulting in the inhibition of flowering. Kumar & Neelakandan (1992) and Maske et al. (1997), using the same concentrations, and Haba et al. (1985) utilizing 0.1 mg L^{-1} GA_3 and imbibition for three hours, obtained an increase in germination. Since GA translocation occurs mainly through the symplast (Castro & Melotto, 1989), it could be the cause for the difference between responses, because when GA_3 is utilized via foliar application, an increase in hypocotyl length and in the length of the two nodes immediately above it can be verified and, consequently, affect the

height of plants at that stage (Mislevy et al., 1989). Plant hormones will only take effect when and where specific receptors are located. Placing drops of the gibberellin solution on the leaves did not affect the leaves, but mainly caused elongation of the stem. This would tend to indicate that receptors for gibberellins are located in the cells of the stem as opposed to those of the leaf cells. However, application of the gibberellin solution to other locations may hasten it's absorption and travel to the location of activity. For example, if the the gibberellins were applied to the roots - perhaps included while watering - then the hormone may reach the site of action faster, with less being lost or metabolized elsewhere along the way. The roots have a reduced cuticle allowing easy entrance for water and dissolved material, plus little distance need be travelled through the interstitium before vascular tissue is reached. Once the gibberellins have reached the vascular tissue they can rapidly move up to the active region of the stem (Hilton, 1983).

From the above observations, it is inferred that the foliar spray application technique caused an increase in plant height than the seed soaking application. Also both application techniques are effective and can cause desirable effects.

Correspondence to:

Unamba Chibuikem I.N

Department of Plant Science & Biotechnology,

Imo State University, Owerri, Imo State, Nigeria

Email: cinu2010@yahoo.com

References

Akinlade, E.A. and Adesiyan, S.O. (1982). “ Nigerian Journal of Pesticides and Agricultural Chemicals”. Vol. 1. pp22.

Bidwell, R.G.S. (1974). Plant Physiology. Macmillan Publishing Co, New York.

Brian, P.W., Elson, G.W., Hemming, H.G., and Radley, M. (1955). “ The plant growth promoting properties of gibberellic acid, a metabolic product of the fungus *Gibberella fujikuroi”*. J. Sci. food. Agr. 5: 602-612.

Bukovac, M.J and Wittwer S.H. (1956). Gibberellic acid and higher plant general growth responses. Quart. Bull. Agric. Exp. Sta. 39:307-320.

Castro, P.R.C.; Appezzato, B.; Lara, C.W.W.R.; Pelissari, A.; Pereira, M.; Medina, M.J.A.; Bolonhezi, A.C.; Silveira, J.A.G. (1990) Ação de reguladores vegetais no desenvolvimento, aspectos nutricionais, anatômicos e na produtividade do feijoeiro (*Phaseolus vulgaris* cv. Carioca). Anais da ESALQ, v.47, p.11-28

Epehuijsen, C.W. Van (1974). “Cf. Journal of Experimental Botany for Physiology, Biochemistry and Biophysics of Plants”. Dec. 1980. Vol. 31. No 125.

Gianfagna, T.J. (1987) Natural and synthetic growth regulators and their use in horticultural and agronomic crops. In: Plant Hormones and Their Role in Plant Growth and Development, Davies, P. J., ed., pp. 614 - 635. Kluwer, Boston.

Haba, P. De-La; Roldan, J.M.; Jimenez, F. (1985). Antagonistic effect of gibberellic acid and boron on protein and carbohydrate metabolism of soybean germinating seeds. Journal of Plant Nutrition, v.8, p.1061-1073, .

Hilton, J.R. (1983). The influence of phytochrome equilibria on gibberellin-like substances and chlorophyll content of chloroplasts of *Hordeum vulgare*. The New Phytologist. 95: 545-548

Khafagi, O.A.; Khalaf, S.M.; El-Lawendy, W.I. (1986). Effect of GA_3 and CCC on germination and growth of soybean, common bean, cowpea and pigeon pea plants grown under different levels of salinity. Annals of Agricultural Science, v.24, p.1965-1982

Kumar, K.G.A.; Neelakandan, N. (1992) Effect of growth regulators on seedling vigour in soybean (*Glycine max* (L.) Merr.) Legume Research, v.15, p.181-182

King, R.W.; Seto, H.; Sachs, R.M.(2000) Response to gibberellin structural variants shows that ability to inhibit flowering correlates with effectiveness for promoting stem elongation of some plant species. Plant Growth Regulation, v.19, p.8-14

Maske, V.G.; Dotale, R.D.; Sorte, P.N.; Tale, B.D.; Chore, C.N. (1997) Germination, root and shoot studies in soybean as influenced by GA3 and NAA. Journal of Soils and Crops, v.7, p.147-149

Mislevy, P.; Boote, K.J.; Martin, F.G. (1989) Soybean response to gibberellic acid treatments. Journal Plant Growth Regulation, v.8, p.11-18.

Taiz, L., Zeiger, E., (1991) Plant Physiology. Benjamin/Cumming Publishing Company Inc.

Wareing, P.F and Philips, I.D.J. (1976). The control of growth and differentiation in plants. Pergamon press, Oxford, New York, Toronto, Sydney, Braunschweig.

Yamaguchi, S.; Kamiya, Y. (2000) Gibberellin biosynthesis: Its regulation by endogenous and environmental signals. Plant and Cell Physiology, v. 41, p. 251-257

3/21/2009

Optical Absorption Spectra Of Chromium In Cassiterite Single Crystals

Jacob I.D. Adekeye

Department of Geology and Mineral Sciences, University of Ilorin, P.M.B. 1515, Ilorin, Nigeria

E-mail address: adekeye2001@yahoo.com

Abstract: Recently, much interest is being shown in the physical properties of cassiterite because of its insulating and semiconducting properties. Of particular interest is the doped cassiterite crystals which have found good uses in varistor ceramic and colour pigmentation. The addition of chromium and some transition elements into the cassiterite lattice has resulted in the modification of the properties of pure cassiterite. The absorption spectra of cassiterite (SnO_2) single crystals doped with chromium were studied by absorption spectrophotometry in order to investigate colour pigmentation in cassiterite. These crystals are coloured red and it was found that absorption is greater in doped crystals than in undoped ones. Spectral bands due to Cr^{3+} and Cr^{2+} were detected using normal light. The bands compare well with those in other chromium containing materials. Heating the crystals to 700^0C under reducing conditions caused large decreases in the spectral intensity of the Cr^{3+} band at 2.3eV. Gamma irradiation of these crystals also produced similar effects. The results obtained here and published data elsewhere suggest that the reduction in the Cr^{3+} band was caused by the ionizing effects on the Cr^{3+} ion to produce Cr^{2+} and Cr^{4+} ions. There was no change in the colouration of the crystal even after heating under reducing condition or gamma-irradiation. This is interpreted to mean that a lot of the Cr^{3+} ions have entered the substitutional Sn^{4+} site in the crystal lattice where they are tightly bonded and cannot easily change their valence states."[The Journal of American Science 2009; 5(4);141-145]. (ISSN 1545 - 1003)"

Keywords: cassiterite crystal, gamma-irradiation, absorption spectra, chromium-doped cassiterite, crystal lattice

1.0 Introduction

In the past few decades, many research workers have investigated the colour center phenomena in solids (Arkhangelskli et al, 1967,1968). Initially, studies on colour centers were mainly confined to alkali halides. But, after the advent of the different techniques of growing synthetic crystals, these studies were extended to other solids as well. Recently, much interest is being shown in the physical properties of cassiterite because of its insulating and semiconducting properties. Of particular interest is the pigmentation. The addition of chromium and some transition elements into the doped cassiterite crystals which have found good uses in varistor ceramic and colour cassiterite lattice has resulted in the modification of the properties of pure cassiterite (Moreira et al, 2006). The optical absorption of pure crystals has been studied by Reddaway and Wright (1965) and Wright (1968). They observed a band in the region of 3.5 eV which was ascribed to oxygen deficiency or some unknown impurities. However, Cohen et al (1985) were able to clearly identify the band to be due to Sn^{2+}. Hou et al (1967) and Lopez-Navarete et al (2003), have done some work on Cr-doped cassiterite single crystals. It is felt that the level of research work on these materials is rather low and therefore a systematic and correlated study on them is necessary. Also, the effect of chromium impurity on colouration of cassiterite is rather faintly understood. The purpose of the present paper is to report on the changes in the optical absorption spectra of chromium doped $Sn0_2$ single crystals heated under reducing conditions and irradiated with gamma-rays at room temperature.

2.0 Materials and Methods

Two red cassiterite crystals were studied. The paler sample NMNH 136748 was obtained from the Mineralogy Branch of the National Museum of Natural History, Washington, D.C. There is no chemical analysis of this sample. The more intense coloured sample C110k was obtained from J. A. Marley and its preparation was described in Marley and MacAvoy (1961). The chemical analysis of the undoped sample was given in Cohen et al (1985) and this sample has been doped with 250ppm chromium by Hou et al (1967). The Cr^{3+} and Cr^{2+} soda-silicate glasses studied were those prepared by Smith and Cohen (1963).

Methods of sample preparation for optical studies have been described in Cohen et al (1985). However, sample NMNH 136748 was too small to cut in the basal section and only its axial spectrum was measured. Sample C11OK was cut into two, the axial and basal sections, and their spectra were

measured. The axial sections of the crystals are less than 1mm and do not cover the 2mm hole in the sample holder. Therefore, matching small holes that are 0.4mm in diameter were specially made for use in the optical absorption measurements. The smallness of the holes made it impossible to measure the polarized spectra of these crystals.

Heat treatment and gamma-irradiation experiments were done as earlier described by Cohen et al (1985). Optical measurements were made on a Cary Model 14 Spectrophotometer at room temperature. The Gaussian resolution of the bands was done using Dupont Model 301 Curve resolver.

3.0 Results

The optical absorption spectra at room temperature of chromium doped cassiterite crystals are presented in Figure1. The crystals have optical absorption bands due to Cr^{3+} at 1.80, 2.28 and 2.88 eV. These bands increase in intensity with increase in chromium content. This is illustrated by comparing the absorption heights of the two samples in Figure1 with the intensely coloured C11Ok sample having higher absorption coefficients than that of the paler NMNH 136748. The polarized spectra of the as grown cassiterite crystals were taken at room temperature and are shown in Figure 2.

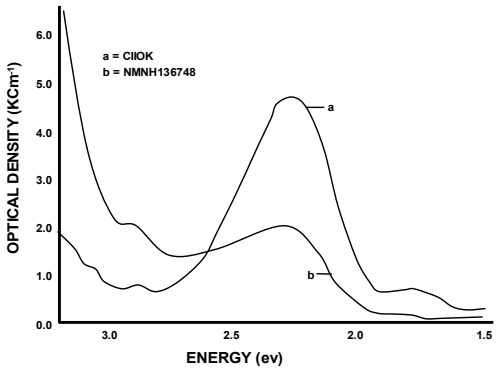

Fig. 1: Absorption spectra of chromium doped cassiterite single crystals using normal light

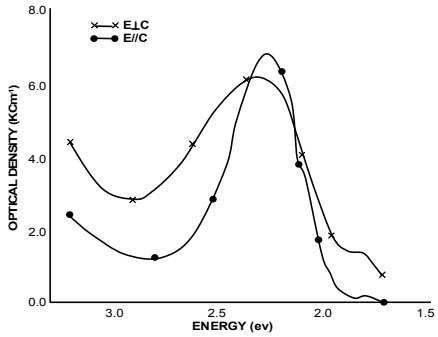

Fig. 2: Polarized spectra of chromium doped cassiterite single crystals

Observed bands for the electric vector (E) of light parallel to c-axis (E//c) are found at 1.78 and 2.25 eV. The band at 2.88eV could not be distinctively resolved. For the electric vector (E) of light perpendicular to c-axis (E1c), the bands are at 1.83 and 2.3eV. Table 1 gives the peak positions of the Cr^{3+} and Cr^{2+} bands compared with those in other chromium containing materials. In Table 2, the details of the polarized spectra of the crystals are given. The absorption spectra of chromium doped cassiterite irradiated with gamma rays at room temperature showing the bands due to Cr^{2+} and Cr^{3+} are presented in Figure3. There was no change in colour but there was a decrease in the absorption coefficient of the broad band in the 2.3eV region. This is an indication that the Cr^{3+} ions causing the band have decreased as a result of gamma-irradiation. New bands at 2.43 and 2.63eV developed.

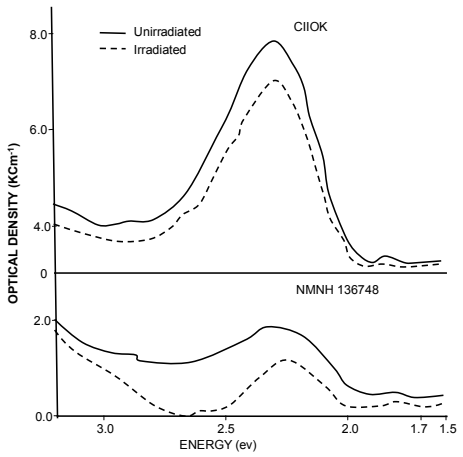

Fig. 3: Absorption spectra of Chromium doped cassiterite showing changes after gamma irradiation

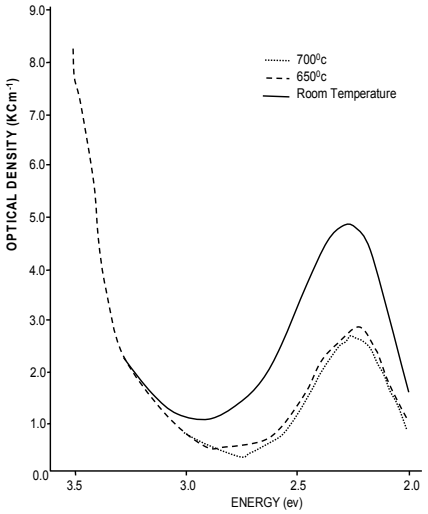

Fig. 4: Changes in spectrum of C11OK on heating from room temperature to 700^0C

Table 1: Peak positions (in eV) of Cr^{2+} and Cr^{3+} absorption bands in soda silicate glass, cassiterite and other materials.

Specimen	Cr^{3+}	Cr^{2+}	Cr^{3+}	Cr^{3+}	Cr^{2+}	Cr^{2+}	Cr^{3+}	Author
Glass: Cr^{2+}		1.90			2.41	2.65		1
Glass: Cr^{3+}	1.80		1.96					1
Ruby	1.78		2.29					2
Cassiterite			2.30					3
NMNH 136748	1.80		2.28				2.88	4
CIIOK (reduced)	1.80		2.29		2.43	2.63	2.89	4

1. Smith and Cohen (1963)
2. Marcfarlane (1963)
3. Hou et al (1967)
4. Present work

Table 2: Peak positions (in eV) of spectra of as grown and reduced crystals of chromium doped cassiterite.

As Grown		Reduced		Author
E//C	E1c	E//c	E1c	
	2.26	2.44	2.65	1
1.78	1.83	2.44	2.49	2
2.25	2.30	2.60	2.65	2

1. Hou et al (1967)
2. Present work

Heating of the samples in a reducing environment produced new bands similar to those developed during gamma-irradiation. There was a marked decrease in the absorption band in the 2.3eV region at 700^0C. Thereafter, no further significant reduction in the band occurred as shown in Figure 4. There was also no change in the colour of the samples. Although Hou et al (1967) reported complete disappearance of the main band at 2.3eV, this has not been recorded in this work. The difference in our results may be due to the types of reducing agents used. While they used a mixture of nitrogen and hydrogen, the reducing agent used in this work was silicon carbide (SiC). It is reasonable to suppose that because at high temperature (>500^0C), ionic diffusion into crystal lattices becomes easy, hydrogen will diffuse into the structure and combine with oxygen to produce OH group. This is why they got the OH stretching vibration absorption band in their spectra. Losos and Beran (2004) also reported the presence of OH defect in cassiterite. The causes of some of these bands have not yet been ascertained.

4.0 Discussion

The phenomena of colouration in ionic crystals such as alkali halides have been well understood and the colouration mechanism has been explained in terms of the trapping of electrons and holes liberated during irradiation process at proper vacancy sites (anion and cation vacancies). These vacancies are either inherently present in the crystal lattice or have been induced by irradiation process. In SnO_2, the lattice energy is considerably higher than in the monovalent alkali halides and as such ionizing radiation would not be very effective in generating new defects as in alkali halides.

Cassiterite has the tetragonal rutile structure in which each tin atom is at the center of six oxygen placed approximately at the corners of a regular octahedron. However, this octahedral site is tetragonally distorted. Three bands corresponding to the transitions:
$^4A_2g \longrightarrow {}^2Eg$ (1.80eV), $^4A_2g \longrightarrow {}^4T_2g$ (2.28eV), $^4A_2g \longrightarrow {}^4T_1g$ (2.88eV) are predicted for Cr^{3+} and similar transition ions like Fe^{3+} and Ti^{4+} in this environment (Marcfarlane, 1963; Wood et al, 1963; Desausoy et al, 1988; Lopez-Navarete et al, 2003). Chromium-doped cassiterite features these bands which compare well with values obtained for Cr^{3+} in glass and other materials.

In the cassiterite lattice, there are vacant cation (Sn^{4+}) and anion (0^{2-}) sites as well as interstitial sites. Cr^{3+} ($0.70A^0$) ions can substitute for Sn^{4+} ($0.77A^0$) as given by Shannon (1976). Cr^{3+} ions can also occupy the interstitial octahedral sites which are larger than the substitutional octahedral sites (Hurlen, 1959). Wittke (1965) worked on the diffusiuon of transition metal ions into the rutile structure and found that at least seventy per cent of the chromium ions are preferentially found in substituttional sites. The EPR work of Hou et al (1967) and Ruck et al (1989) also confirm this for Cr^{3+} in cassiterite. Hence in cassiterite, over seventy per cent of the Cr^{3+} ions enter the substitutional octahedral sites while the remaining thirty percent enters the octahedral interstitial site.

During the incorporation of Cr^{3+} ions into the crystal lattice, it will enter the vacant cation site. The amount entering the Sn^{4+} site will depend on the amount of pre-existing cation vacancies in the crystal. Cr^{3+} is one charge less than Sn^{4+} and there will be need for a charge compensator for charge balance near Cr^{3+} (Brehat et al, 1990). However, a doubly charged cation can compensate for two Cr^{3+} ions. These two situations can be considered as follows:

(a) $Sn^{4+} \longrightarrow Cr^{3+} + A^+$
(where A^+ is a positively charged ion)

(b) $2Sn^{4+} \longrightarrow 2Cr^{3+} + Sn^{2+}$

In (b), Sn^{2+} acts as a compensator between the two Cr^{3+} ions and that is probably why it is difficult for it to change its valence state during heating and gamma irradiation (Cohen et al, 1985).

Upon exposure to gamma rays, the absorption coefficient of Cr^{3+} decreases. This is evidence that some Cr^{3+} ions have changed valence states. Also, oxygen ion would be singly or doubly ionized. The electrons released from the oxygen ions will be trapped at impurity sites or anion vacancies. The change in valence states of Cr^{3+} can occur via one of these mechanisms:

(a) Cr^{3+} (I) + 0^{2-} + γ –ray ⟶ Cr^{2+} (I) + 0^{-} (hole)
(b) Cr^{3+} (I) + 0^{-} + γ -ray ⟶ Cr^{4+} (I) + 0^{2-}
(c) $2Cr^{3+}$ + 0^{2-} + γ -ray ⟶ $2Cr^{2+}$ + 0.

In (a), the oxygen ion loses an electron which is captured by Cr^{3+} to become Cr^{2+}, while it becomes a "hole". A Cr^{3+} ion can capture a hole to become a Cr^{4+} ion as shown in (b). When the two electrons on the oxygen ion are ejected, then the situation depicted in (c) arises whereby neutral oxygen atoms are produced. In this work, no band due to Cr^{4+} has been identified. This is probably because the Cr^{4+} bands are masked by the more intense Cr^{3+} bands. Thus, in the chromium doped cassiterite, there can coexist simultaneously Cr^{2+}, Cr^{3+} and Cr^{4+}(Lopez-Navarete et al, 2003). There is also the Sn^{2+} in octahedral interstitial sites. Gamma irradiation gave rise to new bands at 2.43 and 2.63eV. Maruyama and Matsuda (1964) studied chromium doped ruby single crystals and ascribed the band at 2.43 eV to Cr^{2+}. Govinda (1976) also studied chromium-doped ruby single crystals and ascribed the band at 2.65eV to Cr^{2+}. Thus, the bands at 2.43 and 2.63eV are accordingly ascribed to Cr^{2+}produced by conversion of interstitial Cr^{3+}.

There was no evidence for the formation of additional colour centers by gamma-irradiation as there was no change in the colour of the samples. Additional colour center formation is likely inhibited as a result of high concentration of chromium doping. A possible reason for this is that at high concentrations, the inherent defect concentration becomes considerably reduced. Another possible reason is that the reduction in the concentration of cation vacancies may act as a hinderance to the easy dislodgement of electrons from 0^{2-} ions during gamma-irradiation. The interpretation given by Hou et al (1967) that Cr^{3+} ions exist in different environments in the crystal lattice, i.e. substitutional and interstitial sites is correct. However, they erred by suggesting that Cr^{3+} ions were leaping in and out of the substitutional sites during their reduction experiments. This is unlikely because a lot of bond energy would be required to free the strongly bonded substitutional Cr^{3+} ion. Rather, the thirty per cent Cr^{3+} ions they considered to be leaping out of the substitutional sites are indeed the Cr^{3+} ions that changed valence states during reduction or gamma-irradiation. These are the intersititial Cr^{3+} ions.

5.0 Conclusion

The colour of chromium doped cassiterite is due to the amount of Cr^{3+} ions present in the subsitutional cation sites in the crystal lattice. Gamma-irradiation and heating under reducing conditions led to production of Cr^{2+} and Cr^{4+} ions. Because there is no colour change during production of Cr^{2+} and Cr^{4+}, these ions are not the colour centers causing the observed colour. The Cr^{3+} ions that changed valence states are considered to be interstitially located. Irradiation effects are considered to relate only to the preexisting imperfections.in the crystal lattice (cation and anion vacancies) and to the changes in the valence states of Cr^{3+} ions.

Acknowledgement

The University of Ilorin through the Research Grant Committee is thanked for providing financial assistance for this study.

Correspondence to:
Dr. J.I.D Adekeye
Department of Geology and Mineral Sciences,
University of Ilorin,
P. M. B 1515,
Ilorin, Nigeria.
Cellular Phone: +2348033795444
Email address: adekeye2001@yahoo.com

References

Arkhangelskli, G.E. Morgenshtern, Z.L. &Neustruev, V.B. Colour centers in Ruby crystals. Phys. Stat. Sol. 1967: 22. 289-295.

Arkhangelskli, G.E, Morgenahtern, A.L. & Neustruev, V.B. On the nature of colour centres in ruby. Phys. Stat. Sol. 1968: 29. 831-836.

Brehat, F., Wyncke, B., Lonard, J.M., & Dusausoy, Y. Infrared reflectivity spectra of single crystal cassiterites. Phys Chem Minerals. 1990:17. 191 – 196

Cohen, A.J., Adekeye J.I.D., Hapke, B. & Partlow, D.P. Interstitial Sn (II) in synthetic and natural cassiterite crystals. Phys. Chem. Minerals. 1985:12. 363-369.

Dusausoy, Y., Ruck, R. & Gaite, J.M. Study of the symmetry of Fe^{3+} sites in SnO_2 by electron paramagnetic resonance. Phys. Chem. Minerals. 1988: 15. 300 -303.

Govinda, S. Coloration and Luminescene in pure and chromium-doped AI_20_3 single crystals irradiated with X-ray at room temperature. Phys. Stat. Sol. 1976: (a) 37. 109-117.

Hou, S.L., Summit, R.W. & Tucker, R.F. Electron-Paramagnetic Resonance and optical spectra of Cr^{3+} in $Sn0_2$ single crystals. Phys. Rev. 1967: 154. 258-265.

Hurlen, T. On the defect structure of rutile. Acta. Chem. Scand. 1959: 13. 365-376.

Lopez-Navarete, E., Caballero, A., Orera, V.M., Lazaro, F.J. & Ocana, M. Oxidation states and localization of Cr ions in Cr-doped cassiterite and Cr-doped mayalaite. Acta Materialia. 2003: 51. 2371 – 2381.

Losos, Z. & Beran, A. OH defects in cassiterite. Contr. Mineral Petrol. 2004: 81. 219 – 234.

Marcfariane, R.M. Analysis of the spectrum of d^3 ion in trigonal crystal fields. J. Chem, Phys. 1963:13. 3118-3126.

Marley, J.A. & MacAvoy. T.C. Growth of stannic oxide crystals from the vapor phase. J. Appl. Physc. 1961: 32. 2504-2507.

Maruyama, T. & Matsuda, Y. Colour centers in gamma-irradiated ruby. Japan. J. Phys. Soc. 1964: 19. 1096-1104.

Moreira, M.L., Pianaro, S.A., Andrade, A.V.C. & Zara, A. J. Crystal phase analysis of SnO_2- based varistor ceramic using the Rietveld method. Materials Characterization. 2006: 57. 193-198

Reddaway, S.F. & Wright, D.A. The optical properties of tin oxide crystals. Brit. J. Appl. Phys. 1965: 16. 195-198.

Ruck, R., Dusausoy, Y., Uguyen-Trung, C., Gaite, J.M. & Murciego, A. Powder EPR study of natural cassiterites and synthetic SnO_2 doped with Fe, Ti, Na and Nb. European J. Mineralogy. 1989: 1 (3). 343 – 352.

Shannon, R.D. Revised effective ionic radii and systematic studies of interatomic distance in halides and chalcogenides. Acta. Cryst. A32. 1976: 751-767.

Smith, H.L. & Cohen, A.J. Absorption spectra of cations in alkali-silicate glasses of high ultra-violet transmission. Phys. Chem. Glasses. 1963: 4. 173-187.

Wittke, J.P. Diffusion of transition metal ions in rutile ($Ti0_2$). J. of Electrochemical Society. 1965: 113. 193-194.

Wood, D.L. Ferguson, J. Knox, K. & Dillon, Jr., J.F. Crsstal-field spectra of d^3, d^7 ions III. Spectrum of Cr^{3+} in various octahedral crystal fields. J. Chem. Phys. 1963: 39. 890-898.

Wright, D.A. Electrical and optical properties of tin oxide crystals. Proc. Brit. Ceram. Soc. 1968:10. 103-113.

The Journal of American Science

ISSN: 1545-1003

The international academic journal, "***The Journal of American Science*"** (ISSN: 1545-1003)**,** is registered in the United States, and invites you to publish your papers.

Any valuable papers that describe natural phenomena and existence or any reports that convey scientific research and pursuit are welcome, including both natural and social sciences. Papers submitted could be reviews, objective descriptions, research reports, opinions/debates, news, letters, and other types of writings that are nature and science related. All the manuscripts will be processed in a professional peer review. After the peer review, the journal will make the best efforts to publish all the valuable works as soon as possible.

This journal will be no charge for the manuscript contributors. If the author needs hard copy of the journal, it will be charged for US$100/issue to cover the printing and mailing fee. Here is a new avenue to publish your outstanding reports and ideas. Please also help spread this to your colleagues and friends and invite them to contribute papers to the journal. Let's work together to disseminate our research results and our opinions.

Papers in all fields are welcome, including articles of natural science and social science.

Please send your manuscript to editor@americanscience.org;
sciencepub@gmail.com;
americansciencej@gmail.com

For more information, please visit http://www.americanscience.org;
http://www.sciencepub.net; http://www.sciencepub.org

Marsland Press
2158 Butternut Drive
Okemos, MI 48864
The United States
Telephone: 347-321-7172; 718-404-5362; 517-349-2362
Email: editor@americanscience.org;
sciencepub@gmail.com;
americansciencej@gmail.com
Website: http://www.americanscience.org
http://www.sciencepub.net; http://www.sciencepub.org

Photoperiodic Effect on Seed Germination in Pyrethrum (*Chrysanthemum cinerariaefolium* vis.) under the Influence of Some Growth Regulators

Chetna Bisht[1*], Anoop Badoni[2], R. K. Vashishtha[1] and M. C. Nautiyal

[1]High Altitude Plant Physiology Research Center
[2]Department of Seed Science and Technology
H. N. B. Garhwal Central University, Srinagar- 246 174, Uttarakhand, India
*For Correspondence: bishtchetna@yahoo.com

ABSTRACT: In the present investigation seed germination study of *Pyrethrum* was carried out with the objective to enhance the germination percentage in respect to photoperiodic conditions as well as response of the growth regulators. For germination, seeds were kept under three different photoperiodic conditions i.e. 24 hr. continuous dark, 24 hr. continuous light and 16 hr light/8 hr dark with pre-sowing treatments of IAA-25 and 50 ppm, GA_3-25 and 50 ppm and NaClO- 10 and 20 minutes. Maximum germination (84%) was observed in 16 hr light/8 hr dark condition with IAA-25 ppm. GA_3-50 ppm also showed good germination (60%) in 16/8 hr light condition. Very poor germination was reported in control (4%) of all the light conditions, only 24 hr continuous dark condition showed 13.33% germination in control. [The Journal of American Science. 2009;5 (4):147-150] (ISSN 1545-1003).

INTRODUCTION

Pyrethrum (*Chrysanthemum cinerariaefolium*), regarded as a section of the genus *Chrysanthemum*, family *Asteraceae* is a perennial temperate plant with small white, daisy-like flowers from which natural insecticides, the pyrethrins, are derived. Traditionally, pyrethrum was produced in many African countries where hand-labour was used to plant, harvest, and dry the crop (Davis, 2001; Wandahwa *et al.*, 1996). The First attempt to introduce pyrethrum in India was made by the Forest Department, Jammu and Kashmir as early as in 1931 (Panda, 2005). Besides their ornamental importance, pyrethrum flowers have been widely used as a source material for preparation of insecticides. Being non-poisonous to man pyrethrum is particularly adapted for controlling household insects; however its use for preparing horticultural dusts and sprays, and livestock sprays is no less popular (Gnadinger, 2001). The most valuable property of Pyrethrum in comparison to other insecticides is its very low mammalian toxicity. Because of this quality, pyrethrum is the only insecticide safe for human beings, whereas synthetic insecticides pose a problem of health hazards for human beings, domestic animal and wild life (Panda, 2005).

About 200 years ago someone living in central Asia discovered that dried, crushed flowers of certain chrysanthemums were toxic to insects. During the Napoleonic Wars (1804-1815) this "insect powder" was used to control flea and body lice infestations by French soldiers. Since then, pyrethrum has been used in many forms for effective, low toxicity insect control (Jack, 2009). The increased awareness of the dangers of synthetic insecticides and the rapid building up of residence in the insect population against synthetic insecticides are acting in favour of pyrethrins, which don't show any of these disadvantages. The demand for pyrethrum flowers is therefore, rising rapidly in the word market and India has a very bright future to meet this large increase in demand as pyrethrum can be cultivated successfully in the area like Kashmir valley. Pyrethrum is used as an insecticide in the form of powder, spray, acrosol, coils, cream and ointment (Panda, 2005).

Keeping above points on view the present study is based with the objective to enhance the germinability in pyrethrum (*Chrysanthemum cinerariaefolium*) with respect to different photoperiod and growth regulators.

MATERIAL AND METHOD

For the present study seeds of pyrethrum species were washed with 5% (v/v) T-ween 20 for 15 min. and surface sterilized with 0.1% mercuric chloride (HgCl2) for 3 minutes, followed by a quick rinse in 70% ethanol, and finally 5-6 times washed with sterilized distilled water. After sterilization the seeds were subjected to the following pre-sowing treatments for 24 hr, distilled water was used as control:

T1 Control
T2 IAA-25 ppm
T3 IAA-50 ppm
T4 GA_3-25 ppm
T5 GA_3-50 ppm
T6 NaClO- 10 minute
T7 NaClO- 20 minute

For germination test seeds were sown on moist filter paper in petridishes with three replicates (25 seeds in each replicate) of each treatment and kept in seed germinator at 25 $\pm 1^0$C temperature under three different photoperiodic conditions i.e. 24 hr. continuous dark, 24 hr. continuous light and 16 hr light/8hr dark, watering was done daily or as required. In the course of daily observations, germination was noticed when radical emerged. In the dark condition, the observations on the onset of germination were recorded by using green light.

RESULT AND DISCUSSION

Light, which influences the plant by virtue of its intensity, quality and periodicity, plays the vital role in determining the plant characteristics, distribution and survival. It is unique among the environmental factors as a driving variable and individual organism may be affected by any one of its aspect of intensity, color, duration and direction (Joshi, 2006). Variation in the temperature and light requirement for the germination of various plants has also been reported by various workers (Semwal *et al.,* 1983; Bhatt *et al.,* 1983; Nautiyal *et al.,* 1985). Several workers reported that different hormonal treatments also play an important role to overcome the problem of seed dormancy (Thapliyal and Nautiyal, 1979; Bedawi *et al.,* 1985; Kumar *et al.,* 1996; Rahman *et al.,* 1996).

Published information on photoperiodic effect with growth regulators in Pyrethrum (*Chrysanthemum cinerariaefolium* vis.) was not found so far. This is first report on Pyrethrum species about enhancement of seed germination in relation to photoperiod. In order to find out suitable condition for seed germination in Pyrethrum, seeds were subjected to different pre-sowing treatments viz. IAA, GA_3 and NaClO and different light condition. Data showed in Table-1; Fig.-1 indicates that maximum germination (84%) was observed in 16 hr light/ 8 hr dark (Plate-1-A) condition with T2 treatment (IAA-25 ppm). GA_3-50 ppm also showed good germination (60%) in 16/8 hr light condition. Very poor germination was reported in control (4%) of all the light conditions, only 24 hr continuous dark condition showed 13.33% germination in control. Maithani (2000), have also reported that light some how favored germination in *Rheum emodi* and *R. moorcroftianum* and percentage of germination reduced in dark condition. Semwal and Purohit (1980) have also reported enhanced germination percentage under light condition in various plants.

The conclusion of the present study is that the germination in pyrethrum (*Chrysanthemum cinerariaefolium* Vis.) is very poor in control and 16 hr light and 8 hr dark photoperiodic condition with IAA-25 ppm pre-sowing treatment is best to enhance the seed germination.

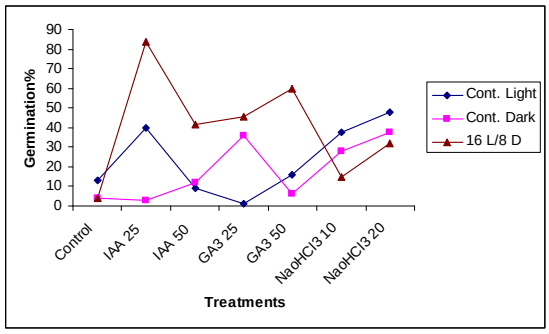

Fig. 1 Seed germination in Pyrethrum using different photoperiod with growth regulators

Plate-1-A-C: **Germination stages in different photoperiodic conditions; (A**) IAA-25 ppm in 16/8 hr, **(B)** NaClO- 20 minute in 24 hr continuous dark and **(C)** NaClO- 20 minute in 24 hr continuous light

Table-1 Photoperiodic effect on seed germination in Pyrethrum

Treatments	Germination Percentage		
	24 hr Continuous Light	24 hr Continuous Dark	16 hr Light/ 8 hr Dark
T1	4 ±0.5	13.33 ±0.3	4 ±0.5
T2	2.67 ±0.4	40 ±1.1	**84** ±1
T3	12 ±1	9 ±0.5	41.33 ±0.3
T4	36 ±1.1	1.33 ±0.3	45.33 ±0.6
T5	6 ±0.5	16 ±0.5	60 ±1.1
T6	28 ±1	37.33 ±0.6	14.67 ±0.1
T7	37.33 ±1	48 ±1.1	32 ±1

Correspondence to:
Chetna Bisht
P. I. (UCOST-Project)
High Altitude Plant Physiology Research Center
H. N. B. Garhwal Central University Srinagar-246 174,
Uttarakhand, India
bishtchetna@yahoo.com

REFERENCES:

Bedawi, F. F. and Mohamad S. M. The pretreatment of seeds of six Sudanese acacias to improve their germination response. Seed Sci. and Tech. 1985; 13: 111-119

Bhatt, R. M., Nautiyal, S. and Purohit, A. N. Seed germination in some Himalayan alpine and sub-alpine composites. 1983; 13: 1-7

Davis, J. M. Study of the flower feasibility of Pyrethrum (*Chrysanthemum cinerariaefolium* Vis.) as a new crop for North Carolina. NCSU Horticulture Science, 2001.

Gnadinger, C.B. Pyrethrum Flowers. Vedams eBooks (P) Ltd New Delhi 110 034, India. 2001;xvi: 380

Joshi, Richa. Physio-Biochemical changes in *Saussurea costus* (Falc.) Lipsch. under varying light regimes. M. Phil. Thesis, H. N. B. Garhwal University, Srinagar, Uttarakhand, India. 2006: 5-11

Kumar, S., Singh P., Katiyar, R. P., Vaish, C. P. and Khan, A. A. Beneficial effect of some plant growth regulators on aged seeds of *Okara* under field condition. 1996; 24(1): 11-14

Maithani, U. C. Ecophysiological and Biochemical variability in *Rheum species* from Garhwal Himalaya. Ph. D. Thesis, H. N. B. Garhwal University, Srinagar, Uttarakhand, India. 2000

Nautiyal, M. C., Rawat, A. S. and Bhadula, S. K. Germination in two *Aconitum species*. Seed Research. 1985; 14(1): 133-139

Panda H. Herbs cultivation and medicinal uses. National Institute of Industrial Research, Delhi. 2005: 1-9

Rahman, M., Farid, A. T. M., Shahidullah, M. and Sultana, W. Improving seed yield quality of Tomato through integrated nutrient management and limiting. Seed Research. 1996; 24(1): 34-37

Semwal, J. K. and Purohit, A. N. Germination of Himalayan alpine and temperate Potentilla. Proc. Nat. Acad. Sci., Pl. Sc. 1980; 89: 61-65

Semwal, J. K., Purohit, A. N. and Gaur, R. D. Seed germination in some Himalayan alpine plants. Seed Research. 1983; 11: 42-46

Thapliyal, P. and Nautiyal, A. R. Inhibition of seed germination by pericarp in *Fraxinus micrantha*. Seed Sci. and Tech. 1979; 17: 125-130

Wandahwa, P., E. Van Ranst and P. Van Damme Pyrethrum (*Chrysanthemum cinerariaefolium* Vis.) cultivation in West Kenya: origin, ecological conditions and management. Industrial Crops and Products. 1996; 5(4): 307-322

3/27/2009

Notes on the existence of an additional lagoon in South-western Nigeria: Apẹsẹ Lagoon

I.C. Onyema

***Department of Marine Sciences**
University of Lagos, Akoka, Lagos
*E-mail: iconyema@gmail.com

ABSTRACT

The existence of an additional lagoon in south-western Nigeria is reported. Hitherto, nine lagoons were known for south-western Nigeria. This account reports information on the tenth lagoon in south-western Nigeria. Apẹsẹ lagoon is a closed lagoon located in Victoria Island, in Lagos, and lies between Latitude 6^{o} 25^{l} 20.83"N, Longitude 3^{o} 27^{l} 15.52"E and Latitude 6^{o} 25^{l} 20.29"N, Longitude 3^{o} 27^{l} 57.19"E. The lagoon is about 32,000m^2 in area, lanceolate in shape and about 1.3km long and 0.16km wide. It is separated from the Atlantic Ocean by less than 100m of sand bar. The maritime condition to which the lagoon and its shore are exposed to presents unique marine situation and ecosystem. Details on this and its relationship with other lagoons in south-western Nigeria are highlighted in this paper. [The Journal of American Science. 2009;5 (4):151-156] (ISSN 1545-1003).

Key words: Apẹsẹ lagoon, Lagos, beach, South-western Nigeria.

INTRODUCTION

According to Kjerfve (1994), a coastal lagoon is an inland body of water, usually oriented parallel to the coast, separated from the ocean by a barrier, connected to the ocean by one or more restricted inlets, and having depths which seldom exceed a couple of meters. A lagoon may or may not be subject to tidal mixing from the sea, and salinity may vary from that of a coastal fresh water lake to a hypersaline lagoon, depending on the hydrologic balance of the area (Kirk and Lauder, 2000, Suzuki *et al*. 2002; Nwankwo, 2004). Kirk and Lauder (2000) are also of the view that lagoons are normally aligned with their largest diameters parallel to the seashore.

Lagoons vary in size and shape in relation to geomorphology and are known to experience forcing from river input, tides, precipitation, wind stress, evaporation and surface heat balance and they respond differently to these forcing functions (Kirk and Lauder, 2000). They are often highly productive habitats for a variety of plants and animals; serve as nurseries for prawns and shrimps and also sites for harbours, wharfs, aquaculture, industries and recreation (Akpata *et al*. 1993). Lagoons are fragile ecosystems susceptible to pollution effects from municipal, industrial and agricultural runoff (Odiete, 1999). Lagoons are important in water transportation, energy generation, exploitation and exploration of some mineral resources including sand; provide natural food resources rich in protein, fish and fisheries farming sites as well as sites for the disposal of both domestic and industrial wastes (FAO, 1969; Kirk and Lauder, 2000; Onyema *et al*. 2003, 2007; Chukwu and Nwankwo, 2004).

Lagoons can be classified as open, closed and semi-closed depending on whether they retain a permanent connection to the sea, an annual or less frequent connection, or a restricted and hence closed connection to the sea (Lawson and John, 1982). Adjoroud (1997) reported that there are essentially two types of lagoons based on their communication with the sea namely closed and open lagoons and they are rather special types of environment for marine organisms. Three interlinked properties greatly influence the physical, chemical and biological diversity of lagoons. These are: salinity, amount of ocean flushing, and the degree of enclosure (Kirk and Lauder, 2000).

Lagoons are common features on the coast of West Africa particularly where the coastline lies approximately 45^{0} to the prevailing South west trade winds (Webb, 1958). According to Webb (1958), Ibe (1988) and Dublin-Green and Tobor (1992) there are four main lagoon systems of the Guinea coast. The fourth and the largest of these systems stretched for 256 km from Cotonou in the Republic of Benin to the

western edge of the Niger Delta in Nigeria. Their formation as reported by Webb (1958) is evidently a result of the movement of sand from the west to the east along a previously notched coast and has taken place since the last glacial period. Furthermore the sands of the beach and the lagoon deposit show signs of wind etching, and it is suggested that they may be derived from the Sahara, being blown into the sea perhaps off the Senegal coast.

Until now, nine lagoons were known in South-western Nigeria (Kusemiju, 1988; Nwankwo, 2004: Onyema, 2008; Onyema and Nwankwo, 2009). They are the Yewa, Badagry, Ologe, Iyagbe, Lagos, Kuramo, Epe, Lekki and Mahin lagoons (Onyema and Nwankwo, 2009; Onyema and Emmanuel, 2009). Little wonder Lagos, Nigeria has been described as the city of aquatic splendor. Iyagbe lagoon until recently was not clearly familiar as a lagoon but referred to in some literature as Badagry creeks (FAO, 1969; Kusemiju, 1988). However, Webb (1958) recognized it as a lagoon and reported explicitly on its probable mode of formation, hydrology and sediment type characteristics. The formation of the Guinea coast lagoons in south-western Nigeria is evidently dependent on the movement of sand along the coast in a west-east direction forming a prograding barrier cum longshore drift (Webb, 1958).

According to Nwankwo (1990), two factors, fresh water discharge from rivers and tidal seawater incursion influence the biological, physical and chemical characteristics of the Lagos lagoon. There is the existence of an environmental gradient linked with rainfall pattern in the Lagos lagoon (Nwankwo and Akinsoji, 1989). Furthermore, gradient of environmental factors in the coastal lagoons have been shown to be more discernable in the dry season than in the wet season (Nwankwo, 1993). With regard to lagoons in the region, the dry season in these lagoons is usually associated with higher light penetration, transparency, conductivity, salinity, pH and sodium values (Olaniyan 1969, Nwankwo and Akinsoji 1992, Nwankwo *et al*., 2003). Furthermore, these lagoons over the years have been increasingly exposed to land based anthropogenic stressors leading to their use as sinks, and their resulting deterioration (Chukwu, 2002; Nwankwo, 2004). Onyema *et al*. (2003) are of the view that pollution of the Nigerian coastal waters has continued unabated through unregulated discharges of a brew of wastes.

The Kuramo lagoon as represented figuratively by Webb, (1958), Hill and Webb (1958), Sandison (1966) and Sandison and Hill (1966) among others extended and tapered further to the East of its current coverage area. Presently, it would seem as if the original dimension of the Kuramo lagoon has now been divided into "two lagoons". This is probably due to coastal sediment transport (Webb, 1958) and or high level habitat modification (Nwankwo, 2004). Whereas the larger half retains the name Kuramo lagoon (waters) and has been scarcely reported (Yoloye and Adegoke, 1977, Edokpayi *et al*., 2004 and Nwankwo *et al*., 2008), the other is unknown (Apẹsẹ lagoon) to the literature of south-western Nigeria. Coastal sediment advance as suggested by Webb (1958) most probably filled in the median of the former and larger Kuramo lagoon as represented by Webb (1958), Hill and Webb (1958), Sandison (1966), Sandison and Hill (1966), hence separating it into two lagoons as currently observed. Consequently giving rise to Kuramo lagoon to the west and Apẹsẹ lagoon to the east. These lagoons exist now as independent entities with distinctive peculiarities. It is quite possible that the end of the effect of the East mole after its increased erosion consequence on the Bar beach caused a build of sand that filled the median and separated the former Kuramo lagoon. Accordingly, it probable that the presence of the east mole lead to the dichotomy that created the "present" Kuramo and Apẹsẹ lagoons from the "former" Kuramo lagoon.

There are presently no reports on any aspect of the physico-chemistry, hydrological characteristics and ecology of the Apẹsẹ lagoon. Furthermore, this is the only completely closed lagoon in the region, as the Kuramo lagoon is semi-closed, in view of the fact that it seasonally opens in the wet season via the Kuramo creek into the Five Cowrie creek to the Lagos lagoon. This usually results from overflow of the Kuramo lagoon from the increased volume associated with storm water inflow during or immediately after rain events. The Apẹsẹ lagoon is located in Apẹsẹ (from where the lagoon derives its name) area of Lagos and it is located eastward of the Kuramo lagoon (1.24km) still in Victoria Island.

The aim of this account was to give some exactitudes on the "new" Apẹsẹ lagoon. This paper is a first of a series on the lagoon. This report therefore will provide first time information on the Apẹsẹ lagoon (the only closed lagoon in Nigeria) which has not previously received attention even in the most general terms, hence the need for this report.

DESCRIPTION OF THE STUDY LAGOON

The Apẹsẹ lagoon (Fig 1) is located in Victoria Island, Lagos state, South-Western Nigeria. The

lagoon is located eastward (1.24km) of the Kuramo lagoon and is about one third of its size. It is the smallest of the ten lagoons in the region. It lies between Latitude 6^{o} 25^{l} 20.83"N, Longitude 3^{o} 27^{l} 15.52"E and Latitude 6^{o} 25^{l} 20.29"N, Longitude 3^{o} 27^{l} 57.19"E. The lagoon is about 32,000m^2 in surface area, lanceolate in shape and approximately 1.3km long and 0.16km across at its widest extreme. It is a narrow lagoon and separated from the proximate sea by a sand bar of less than 100m throughout its length to the south. The popular Kuramo and Oniru beaches in Lagos are also located in the area, a few hundred meters away. The Apẹsẹ lagoon is also about 5 - 6km (crow fly distance) from the Lagos habour.

It is worthy of note that a good number of the exactitudes especially with regard to distances for this 'new' lagoon were obtained by using the Google earth satellite mapping software. More importantly, is the fact that the discovery of the lagoon was due significantly to this software before ground confirmation and pilot / other studies were carried out.

The region experiences a tropical climate with south westerlies which are onshore. The lagoon experiences semi-diurnal tidal regime with two inequalities and is exposed to the wet and dry major seasons in the region. The hamattarn (dust haze) – which is a short season in the dry season, is also recorded in the area. Whereas the wet season stretches most times from May to November, the dry season is usually from December to April. The rains usually come at the middle to end of April in most years.

The vegetation type of the shore of the Apẹsẹ lagoon is similar to the strand of scrubby vegetation colonizing the seashore as described by Akinsoji *et al*., (2002) for the Light house beach (about 9km west) of the Apẹsẹ lagoon. Some identified species occurring at the lagoon shore include sand binders, xerophytic and halophytic species which include *Ipomoea pes-caprae*, *Philoxerus* sp., *Paspalum vaginatum, Schizachryrium pulchellum* and *Remirea maritima*.

.

Sediment type in the area is sandy i.e beach (coarse to medim) sand type common on sandy beaches of littoral states of Nigeria. Water colour of the lagoon was predominantly deep sea blue in February especially towards the center of the lagoon. The occurrence of an array of benthic organisms, shell and fin fish life have been reported by the locals. The lagoon is about 30m deep at its center. During the rain there are increases in the volume of the lagoon water and resulting in the submergence of the riparian zone. However, it retains its brackish / marine characteristics in terms of physico-chemistry all year round. Species directly collected, observed and recorded at the shore and shallow parts of the lagoon include *Ocypoda cursor* and *O. africana, Tilapia* spp., *Callinectes latimanus, Cadmium* sp. a good number of schools of fish juvenile which are commonly seen.

Furthermore seawater at spring tide and during rough sea seasons occasionally overflows the beach berm into the lagoon hence possibly impacting on its water chemistry. The months of April and August are known to be characterized by large swells of plunging waves at sea associated with the development of pressure systems far out in the South Atlantic ocean (Ibe, 1988). These waves are wind generated with intensities generally determined by the wind velocity, duration and fetch. Underground flow through / seepage can also not be ruled out as a source of marine conditions intrusions. At the bank of the lagoon are a few shacks. The locals or inhabitants have constructed make shift houses using dried bamboo and planks for frames, structure and pegging. Furthermore, used nylon, sacks and polythene which are used for covering these frameworks. The total numbers of such shacks on the shore of the beach to the south are between 10 and 15. The chief occupation of the locals is artisanal fishing both in the lagoon and the proximate sea. The sale of shells / cowries as souvenir to tourist is also an additional source of income for the inhabitants. A few modern houses / estates are presently coming up further north of the lagoon area. Most adjacent plots of land to the east and west are currently empty but fenced

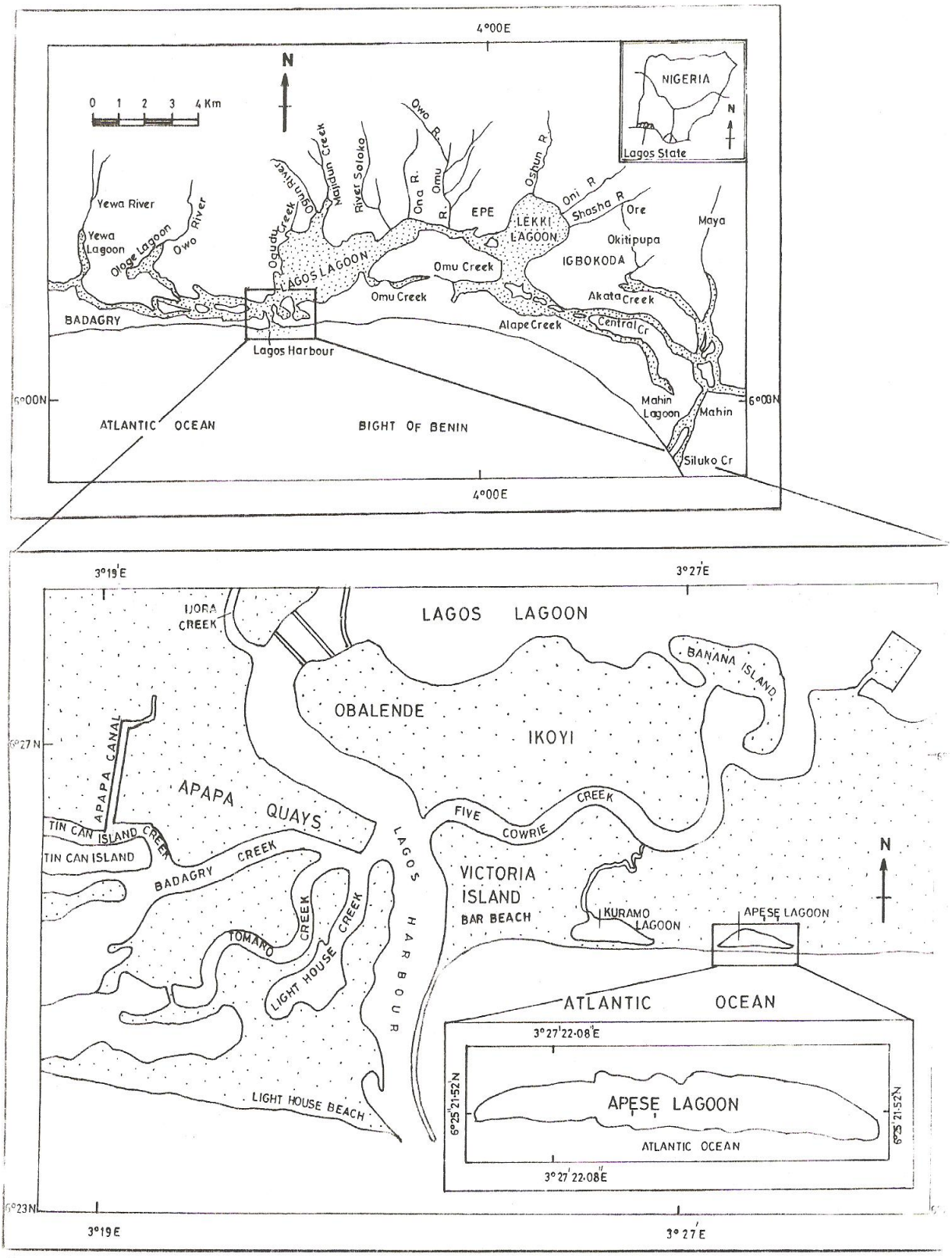

Fig 1: South-western Nigeria lagoons (top) and a map trail to Apesẹ lagoon (bottom left).

RECOMMENDATION.

The Apęsę lagoon is exceptional among the ten lagoons of South-western Nigeria in Lagos since it is the only closed lagoon. There is need for in-depth ecological investigations of this "new" lagoon and to protect it from the effects of high anthropogenic stressors known to plague most of the lagoons in the region. Presently, modicum amount of human activities are observable in the immediate area. The Apęsę lagoon like Tarkwa bay, Lighthouse beach, Kuramo lagoon, vast wetlands and other ecologically sensitive areas in south-western Nigeria that have been suggested as Marine Protected Areas (MPA) (Nwankwo, 2004) must be protected as they are quite vulnerable. There is need for apt coastal management and conservation of the Apęsę lagoon and immediate evnvirons.

ACKNOWLEDGEMENT

I heartily thank Messrs Azeez Abdul Ipaye, Saheed Abimbola Afolabi and Ladega Junaid-Eko for their assistance and help to find and initiate research the Apęsę lagoon. Importantly, thanks also goes to the Management of Google for making the Google earth satellite mapping software available. I am grateful to the department of Marine Sciences, University of Lagos for logistics support and use of its facilities.

References

Adjeroud, M. (1997). Long-term changes of epibenthic macrofauna communities in a closed lagoon (Tairo Atoll, French Polymesia): 1972 – 1994. *Hydrobiologia*. **356**: 11 – 19.

Akpata, T.V.I.; Oyenekan, J.A. and Nwankwo, D.I. (1993). Impact of organic pollution on the Bacterial, Plankton and Benthic Population of Lagos Lagoon, Nigeria. *International Journal of Ecology and Environmental Science.* **19**: 73-82.

Akinsoji, A., Adedoyin, J. and Adekanye, M. (2002). Aquatic macrophytes of three selected sites in Lagos, Southwest Nigeria. *Journal of Science, Technology & Environment*. **2**(1): 9 – 15.

Chukwu, L.O. (2002). Ecological effects of human induced stressors on coastal ecosystems in southwestern Nigeria. PIM 2002 Conference: The ocean in the New economy. Held in Cape Town, South Africa between 8 – 14, December, 2002. 61 – 70.

Chukwu, L. O. and Nwankwo, D. I. (2004). The impact of land based pollution on the hydro-chemistry and macrobenthic community of a tropical West African Creek. *The Ekologia*. **2** (1-2): 1 – 9.

Dublin-Green, C.O. and Tobor, J.G. (1992). Marine Resources and activities in Nigeria. NIOMR Tech Paper No. 84. 25pp.

Edokayi, C.A., Lawal, M.O., Okwok, N.A. and Ogunwemo, C.A. (2004). Physico-chemical and macrobenthic faunal characteristics of the Kuramo water, Lagos, southern Nigeria. *African Journal of Aquatic Sciences*. **29** (2). 235-241.

F.A.O. (1969). Fisheries Survey in the Western and Mid-Western Regions of Nigeria. FAO/Sf: 74/NIR 6. 142pp.

Hill, M.B. and Webb, J.E. (1958). The ecology of Lagos lagoon II. The topography and physical features of the Lagos harbour and Lagos lagoon. *Philosophical Transaction of Royal Society, London.* **241**: 307-417.

Hynes, H.B.N. (1960). *The biology of polluted waters*. Liverpool University Press, Liverpool.202pp.

Ibe, A. C. (1988). *Coastline erosion in Nigeria*. University Press, Ibadan. 217pp.

Kjerfve, B. (Ed.) 1994: *Coastal lagoon processes*. Elsevier Oceanography Series 60. Elsevier, Amsterdam. 577pp.

Kusemiju, K. (1988). Strategies for effective management of water hyacinth in the creeks and lagoons of south-westrn Nigeria. Proceedings of the international on water Hyayacinth, Lagos 7 – 12 August, 1988. 39 – 45.

Kirk, R.M. and Lauder, G.A. (2000). Significant coastal lagoon systems in the South Island, New Zealand. Coastal processes and lagoon mouth closure. *Science for conservation*.**146:** 47 p. Kjerfve, B. (Ed.) 1994: *Coastal lagoon processes*. Elsevier Oceanography Series 60. Elsevier, Amsterdam. 577pp.

Nwankwo, D.I. (1990). Distribution and seasonal variation of dinoflagellates in Lagos lagoon, Nigeria. *Nigerian Journal of Botany.* **3**: 197-207.

Nwankwo, D.I. (2004). The Microalgae: Our indispensable allies in aquatic monitoring and biodiversity sustainability. University of Lagos Press. Inaugural lecture seris. 44pp.

Nwankwo, D.I. and Akinsoji, A. (1989). The Benthic Algal Community of a Sawdust Deposition Site in Lagos Lagoon.

International Journal of Ecology and Environmental Sciences. **15**: 197-204.

Nwankwo, D.I. and Akinsoji, A. (1992). Epiphyte community of water hyacinth, *Eichhornia crassipes* (MART) Solms in coastal waters of South Western Nigeria. *Archiv fur Hydrobiologie.* **124**(4): 501-511.

Nwankwo, D.I., Onyema, I.C. and Adesalu, T.A. (2003). A survey of harmful algae in coastal waters of south-western Nigeria. *Journal of Nigerian Environmental Society.* **1**(2): 241 – 246.

Lawson, G.W. and John, D.M. (1982). *The marine algae and coastal environment of tropical West Africa*. Bei hertazur Nor. Hedingia. Heft. **70**: J. Cramer.

Nwankwo, D.I., Owoseni, T.I., Usilo, D.A., Obinyan I., Uche, A.C. and Onyema, I.C. (2008). Hydrochemistry and plankton dynamics of Kuramo lagoon. *Life Science Journal*. **5** (3): 50 – 55.

Nwankwo, D.I. (2004). The Microalgae: Our indispensable allies in aquatic monitoring and biodiversity sustainability. University of Lagos Press. Inaugural lecture seris. 44pp.

Odiete, W.O. (1999). *Environmental Physiology of Animals and Pollution.* Diversified Resources Ltd., Lagos. 261pp.

Ogamba, E.N. Chindah, A.C., Ekweozor, I.K.E. and Onwuteaka, J.N. (2004). Water quality of phytoplankton distribution in Elechi creek complex of the Niger delta. *Journal of Nigerian Environmental Society*. **2**(2): 121 – 130.

Olaniyan, C.I.O. (1969). The seasonal variation in the hydrology and total plankton of the lagoons of South West-Nigeria. *Nigerian Journal of Science.* **3**(2): 101-119.

Onyema, I.C. (2008). A checklist of phytoplankton species of the Iyagbe lagoon, Lagos. *Journal of Fisheries and Aquatic Sciences*. **3**(3): 167 – 175.

Onyema, I.C. and Emmanuel, B.E. (2009). Fishing impairment and *Spirogyra africanum* (Fruda) in a freshwater lagoon. *Estonian Journal of Ecology.* **58 (1): 1 – 7.**

Onyema, I.C. and Nwankwo, D.I. (2009). Chlorophyll a dynamics and environmental factors in a tropical estuarine lagoon. *Academia Arena*. **1**(1): 18 – 30.

Onyema, I.C., Otudeko, O.G. and Nwankwo, D.I. (2003). The distribution and composition of plankton around a sewage disposal site at Iddo, Nigeria. *Journal of Scientific Research Development.***7:** 11-26.

Onyema, 1.C., Okpara, C.U., Ogbebor, C.I. Otudeko, O. and Nwankwo, D.I. (2007). Comparative studies of the water chemistry characteristics and temporal plankton variations at two polluted sites along the Lagos lagoon, Nigeria. *Ecology, Environment and Conservation*. **13**: 1 – 12.

Sandison, E.E. (1966). The effect of salinity fluctuation on the life of *Balanus pallidus strusburi* (Darwin) in Lagos Habour, Nigeria. *Journal of Animal Ecology*. **35**: 365 – 378.

Sandison, E.E. and Hill, M.B. (1966). The distribution of *Balanus pallidus* Strusburi (Darwin), Gryphaea gasar (Adanson) Dautzenbergi, *Mercierella enigmatica* farvel and *Hydroides uncinata* (Philippi) in relation to salinity in Lagos Harbour and adjacent creek. *Journal of Animal Ecology.* **38**: 235-258.

Suzuki, M.S., Figueiredo, R.O., Castro, S.C., Silva, C.F., Pereira, E.A., Silva, J.A. and Aragon, G.T. (2002). Sand bar opening in a castal lagoon (Iquipari) in the Northern region of Rio De Janeiro state: Hydrological and hydrochemical changes. *Braz. J. Biol*., **62** (1): 51 – 62.

Webb, J.E. (1958). The Ecology of Lagos lagoon. 1: The lagoons of the Guinea Coast. *Philosophical Transaction Royal Society London.* **Ser B**: 241-283.

Yoloye, V. and Adegoke, O.S. (1977). A new species of *Neritina* (Archaeogastroda, Neritidae) from the Lagos lagoon. *Malacologia.* **16**(1): 303 – 309.

Applications of Remote Sensing in Land Use/Land Cover Change Detection in Puer and Simao Counties, Yunnan Province

Yacouba Diallo[1], Guangdao Hu[1], Xingping Wen[2]
1. Institute for mathematics geosciences and Remote Sensing, Faculty of Earth Resources, China University of Geosciences, Wuhan, 430074, Hubei, P.R. CHINA

2. Kunming University of Science and Technology, Kunming, 650093, Yunnan, P.R. CHINA
yacdial2005@hotmail.com

Abstract
Digital change detection is the process that helps in determining the changes associated with land use and land cover properties with reference to geo-registered multi temporal remote sensing data. Puer and Simao, where land use has been greatly affected by recent government policies that aim to balance the need to encourage rural development with ecological stability. These policies include promoting livestock livelihoods, altering grazing practices, the removal of compulsory grain crop quotas and banning commercial logging. The counties remained important in Yunnan Province, Simao is of the six demonstration sites of sustainable forest management.The province harbors a large pool of biodiversity, mostly constrained to a few locations amongst which, Puer and Simao play a major role. For all those reasons, nonetheless, disproportionate Land use/cover change processes are taking place. This paper is an attempt to assess the changes in land use/land cover in this southern part of Yunnan over a nine year period. The study made use of Land Sat imageries of 1990 and 1999. The images were classified using Maximum Likelihood classification method in ENVI 4.3 and mapped using ArcGIS. The results indicated that severe land cover changes have occurred in croplands (+24.90%), forest or shrub land (-18.77%) and building (+16.72%) areas has been knowledgeable and unused area constituted the most extensive type of land use/land cover in the study period. This paper highlights the importance of digital change detection in apprehending the environmental situation in this southern part of Yunnan Province (China). [Journal of American Science 2009;5(4):157-166]. (ISSN: 1545-1003).

Key words: Remote sensing, county, change detection, LULC, classification scheme

I. INTRODUCTION

Digital change detection is the process that helps in determining the changes associated with land use and land cover properties with reference to geo-registered multi temporal remote sensing data. Throughout Southeast Asia, the expansion and intensification of agricultural activities are the principle reasons for land use land cover change (LULC) change particularly in tropical regions (Geist and Lambin 2002). Underlying causes of LULC changes leading to deforestation and land degradation include rapid economic development, population growth and poverty (Giri *et al.* 2003, Bolland et al., 2007). In China inappropriate institutional and development policies have also been major contributing factors (Xu et al., 1999). More specifically, (Lambin *et al.,* 2003) surmised that it is people's responses to economic opportunities as mediated by institutional factors that drive land use/ cover change. Puer and Simao, two counties of Yunnan Province in China, where land use/cover has been greatly affected by recent government policies that aim to balance the need to encourage rural development with ecological stability (Xu and Wilkes 2004; Xu and Ribot 2004). These policies include promoting livestock livelihoods, altering grazing practices, the removal of compulsory grain crop quotas and banning commercial logging. The counties remained important in Yunnan Province; Simao is of the six demonstration sites of sustainable forest management. The province harbors a large pool of biodiversity, mostly constrained to a few locations amongst which, the study area plays major role. Furthermore there is of the most famous Puer Tea Mountains areas in the Province. For all those reasons, nonetheless, disproportionate LULC change processes are taking place. Inventory and monitoring of LULC changes are indispensable aspects for further understanding of change mechanism and

modeling the impact of change on the environment and associated ecosystems at different scales (Wilson and Sader, 2002, Willson, 2005). Large scale changes are difficult and expensive to quantify through fieldwork.

The collaboration of remotely sensed data and field observations can accomplish land cover classification and change detection, faster and cheaper than either alone. This paper entails classifying the land cover of counties, in two Landsat TM scenes from 1990 and 1999, and assessing the changes that have occurred between them. Successful utilization of remotely sensed data for land use and land cover change detection requires careful selection of appropriate data set and methods.

The supervised classification technique is preferred, because the data of the study area is available and the author has a prior knowledge of the study area. LULC changes are investigated by using of Remote Sensing and Geographic Information Systems (GIS) in Rize, a mountainous region in North-East Turkey (Reis, 2008). For this purpose, the supervised classification technique is applied to Landsat images acquired in 1976 and 2000. Image Classification of six reflective bands of two Landsat images is carried out by using maximum likelihood method with the aid of ground truth data obtained from aerial images dated 1973 and 2002. The same methods were applied to classify and to map land cover in Himalayan region with high mountain peaks having elevations up to 4785 m above mean sea level (Saha et al. 2005). All Those methods gave satisfactory results with good classification overall accuracy.

Maximum Likelihood algorithm is a common method, but it is appropriate and efficient method in such uneven study area. It is still one of the most widely used supervised classification algorithms (Wu and Shao, 2002; McIver and Friedl, 2002). The results and accuracy using other methods were found to be insufficient. The change detection technique, which was employed in this study, was the post-classification comparison. Most of studies have addressed that post-classification comparison was found to be the most accurate procedure (Mas et al 2004, Yuan et al. 2005).

Our objectives were:

(1) Determine with accurateness the area LULC classification in two Landsat TM images in 1990 and 1999, (2) Perform post-classification change detection analysis of the classified images and quantify the changes in each land cover class. The rest of the paper is organized as follow: section 2 presents materials and methods used in this study, Section 3, presents our results and discussions and finally section 4, conclusions.

II. MATERIALS AND METHODS

2.1 Study area

The study was conducted in Puer and Simao, two counties of the southern part of Yunnan Province. The area is situated between Longitudes 100°20′ 07”-101°36′17” E and Latitudes 22°49’32”-22°52′11” N (Fig.1). Puer, called Simao before January 21, 2007 is a major town with a population of 75 000. Simao Metropolitan County contains four urban townships, two rural townships and two ethnic rural townships. The climate is subtropical monsoon without hot summers or harsh winters. The mean annual rainfall of the area is around 1300 to 1400 mm, while the mean annual temperature is around 15°C to 18°C. It is neither extremely hot in summer nor terribly cold in winter. The topography is extremely irregular. The major landforms are mountains, highlands, small basins and valleys**.** The vegetative cover is of the type of savanna or tropical arid shrubby steppe. Puer Tea is grown in the mountainous forests of subtropical and tropical areas with an altitude of 1200 to 1400 meters. The shrubs include governorsplum (Flacourtia indica), boxleaf atalantia (Atalantia buxifolia) and the grasses are dominated by tangle head (Heteropogon pers). The soils are part of a series, which belongs to the group of Red Soils with erosion and water loss. According to the classification works (Vogel, Mingzhu and Huang, 1995), the soil is called Ferralic Cambisol or Haplic Phaeozem. It is called Aridic Haplustoll, according to the USDA soil taxonomy, 1992 or Haplic Dry Red Soil after Chinese Soil Classification system-Soil Taxonomic Classification Research Group, 1993. It has been called savanna red soil, red brown soil, red cinnamon soil or purple soil. Without irrigation the soils can be used for planting xerophilous plants like sisal, or produce low yields of traditional crops. With irrigation the soils can be used for rice, sugar-cane, flowering quince, water melon and peanut.

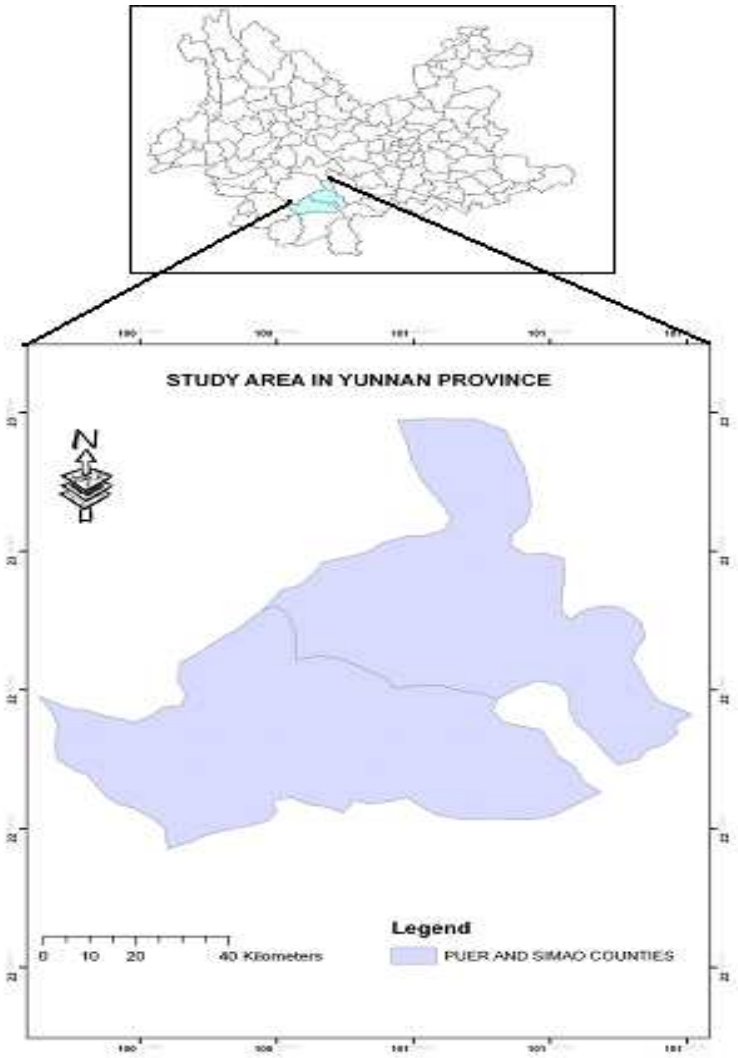

Figure 1: Location of the Study area in Yunnan Province

2.2 Data sources

An area of 6900 km^2 was delineated on the LandSat scene covering the study area. The LULC mapping for the area was based on LandSat 5 Thematic Mapper (TM) of July 1990 and December 1999 data. Obtaining images at near anniversary dates is considered important for change detection studies (Jensen, 2007). However, the summer image in 1999 was unavailable. Both time series were from Landsat TM, path 130, row 044 with. The images were corrected to remove atmospheric effects and then geo-rectified using ground control points collected by GPS. The images were re-sampled to 30m pixel size for all bands using the nearest neighbor method. The resultant root mean squared error was found to be 0.53 pixel (about 16 m on the ground) for the 1990 image, 0.51 pixel (about 15 m on the ground) for the 1999 image. All the data were projected to an Universal Transverse Mercator (UTM) coordinate system, Datum WGS 1984, zone 49 North using 1:50 000 topographic map of the study area.

2.3 Image classification and Accuracy assessment statistical criteria

In our study, two dated Landsat images were compared supervised classification technique. Once the training sites were determined, a supervised classification was performed on both images using Maximum Likelihood algorithm in ENVI 4.3. The supervised classification technique is preferred, because the data of the study area is available and the author has a prior knowledge of the study area. The Maximum Likelihood decision rule is still one of the most widely used supervised classification algorithms (Wu and Shao, 2002; McIver and Friedl, 2002). It is considered to give very accurate results (Mengistu, 2007; Reis, 2008). From there the LULC maps were derived with the following six classes: 1. building area, 2. forest or shrub land 3.water, 4. cropland, 5. fallow, 6. unused area (Table 1).

Table1. Land use/land cover classification Scheme.

Land use/cover types	Description
Building area	Areas that have been populated with residential, commercial, industrial, transportation and facilities.
Forest or shrub land	Areas covered with mature trees, shrubby plants and other plants growing close together.
Water	Areas covered with water such as rivers and lakes.
Croplands	Rain fed cropping, planted and irrigated cropping areas
Fallow	Areas covered mainly with herbaceous vegetation with shrubs
Unused area	Mountainous or hilly areas, areas with no vegetation cover or degraded agricultural lands

Three standard criteria were used to assess the accuracy of the classifications:

(1) The User accuracy was defined as the proportion of the correctly classified pixels in a class to the total pixels that were classified in that class. It indicates the probability that a classified pixel actually represents that category in reality.

(2) The Overall accuracy was defined as the total number of correctly classified pixels divided by the total number of reference pixels (total number of sample points) (Rogan *et al.* 2002)

(3) Kappa coefficient was defined as a statistical measure of accuracy that ranges between 0 and 1, it measures how much better the classification is compared to randomly assigning class values to each pixel. For example, a Kappa of 0.76 means the classification accuracy is 76% greater than chance (Miller and Yool, 2002).

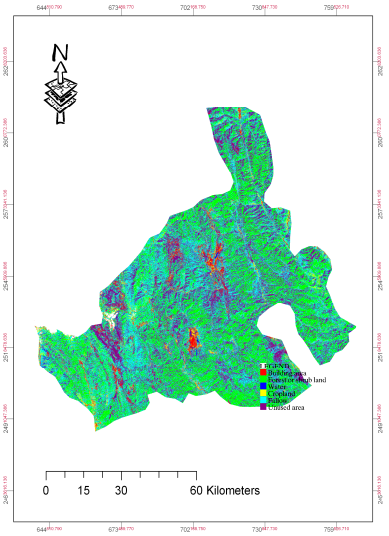

Figure2: Land use/cover Map, 1990

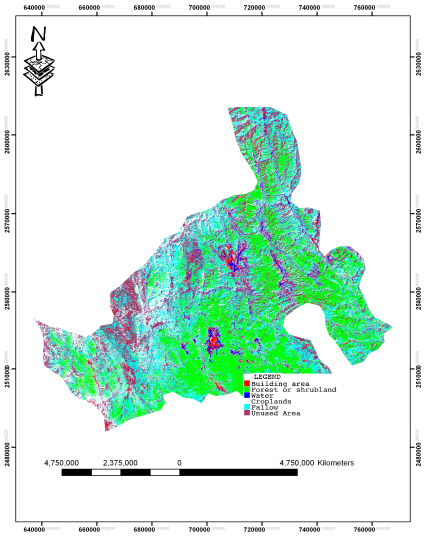

Figure 3: Land use-cover Map, 1999

III. RESULTS

3.1 Accuracy Assessment

Table 2 shows all two classification dates achieved satisfactory overall accuracies of 83.2% for1990 and 85.1% for 1999. In 1990 the unused area received the lowest accuracy score; with only 78.8% of pixels being correctly classified (Table 3). This is because several unused areas pixels were miss-classified as croplands and fallow. The fallow land cover type also presented a relatively low accuracy score of 79.7%, as some pixels were incorrectly classified as unused area and cropland. Similarly in 1999, unused area and fallow had the lowest accuracy scores of 79.2% and 79.5% respectively. For classifying croplands, there was some confusion with fallow and for classifying fallow; there was confusion with unused area (table 3).

Table 2: Summary of classification accuracy assessment

LULC types	1990		1999	
	User	Kappa	User	Kappa
Building area	81.2%	.805	85.3%	.814
Forest or shrub land	98.7%	.973	100%	1.000
Water	80.0%	.720	85.1%	.793
Croplands	80.9%	.826	81.4%	.823
Fallow	79.7%	.788	79.5%	.779
Unused area	78.8%	.786	79.2%	.805
Overall	83.2%	.816	85.1%	.836

3.2 Changes in land use/land cover (1990-1999)

Figures 2 and 3 show the LULC maps of the study area for 1990 and 1999. Tabulations and area calculations provide a comprehensive data set in terms of the overall landscape changes, which have occurred (Tables 3). The class area was measured by the number of pixel multiplied

by the Landsat TM4-5 spatial resolution, i.e. 30m. The pixel number was given by the post-classification analysis. The change was calculated as a pixel number difference between two dates (1990 and 1999). The last column of table3 indicates an average rate of change; it was computed by the pixel number divided by the study period multiplied by 100. The change matrix (table 4), that contributes to facilitate the understanding of the change types (conversion, transformation) processes, came from post classification statistics output data .

In the periods considered, unused area constituted the most extensive type of LULC in the study area. Accordingly, it accounted for about 32.48 and 31.78% of the total area in 1990 and 1999 respectively, followed by forest or shrub land and fallow, occupying 26.94 and 14.50 of the total area respectively. LULC units under croplands, building and water covered 9.44, 9.07 and 7.55% of the total area respectively. In 1999 however, the unused area decreased marginally to about 31.78% of the total area. Forest or shrub land and fallow occupied 21.88 and 16.27 %, respectively. The remaining area was occupied by croplands, building and water, which accounted for about 12.57, 10.89 and 6.60 % respectively. It was not possible to discriminate a famous Tea Mountain area from forest and shrub land. The average rate of changes is summarized in table 3.where the areas covered with forest or shrub land, water and unused area were receding at an average rate of 2.08, 1.39 and 0.4% per annum respectively, while building area, cropland and fallow were, respectively expanding at rates of 1.85, 2.77 and 1.20% per annum over the 9 years period.

Further, the from- to change matrix as seen in table 4 show that the most significant changes in the area were from *Unused area* into Fallow (98917 ha), from *Fallow* into Unused area (89182ha), from *Forest or shrub land* into Cropland *(60570 ha),* from *Building* area into Cropland *(11893 ha) and* from *Building area* into Forest or shrub land (11000 ha).

Table3: Comparison of areas and rates of change of the six LULC classes between 1990 and 1999.

LULC Types	**1990**		**1999**		**Change in 1990-1999**		**Average rate of change**	
	Area ha^{-1}	**%**	**Area ha^{-1}**	**%**	**Area ha^{-1}**	**%**	**Ha yr^{-1}**	**%**
Building area	59874	9.07	71896	10.86	+12022	+16.72	+1336	+1.85
Forest or Shrub land	177840	26.94	144451	21.88	-33388	-18.77	-3710	-2.08
Water	49840	7.55	43573	6.65	-6267	-12.57	-696	-1.39
Croplands	62316	9.44	82987	12.57	+20670	+24.90	+2297	+2.77
Fallow	95719	14.50	107414	16.27	+11695	+10.88	+1299	+1.20
Unused area	214411	32.48	206708	31.78	-7703	-3.59	-8.56	-0.40
Total	660000	99.98	660000	99.98	----	-----	----	------

Table 4: Change matrix for the change in land cover types between 1990 and 1999 in hectares.

	1990						
1999	1	2	3	4	5	6	Total
1. Building area	**34530**	903	1	35362	60	1040	71896
2. Forest or shrub land	11000	**110261**	20	1000	0	0	144451
3. Water	560	2100	**40459**	22	32	400	43573
4. Croplands	11893	60570	10	**10514**	0	0	82987
5. Fallow	2	2000	50	0	**6445**	98917	107414
6. Unused area	1889	1006	300	302	89182	**114029**	206708
Total	59874	177840	49840	62316	95719	214411	657029

Note: Unchanged areas occupy the diagonal of the matrix, while changed areas are represented in the off diagonal elements of the matrix.

The fig.4 shows the LULC change rate between 1990 and 1999. The bars above zero represent the LULC types that expanded their surface area, whereas the bars below zero indicate the LULC types that lost their surface area. Within the period, more land was brought croplands, at the same time building area and fallow expanded at the expense of other land cover types. The area under forest or shrub land, water and unused area declined by 18.77, 12.57 and 3.59% respectively, while those under croplands, building, and fallow registered a net gain of 24.90, 16.72 and 10.88%, respectively.

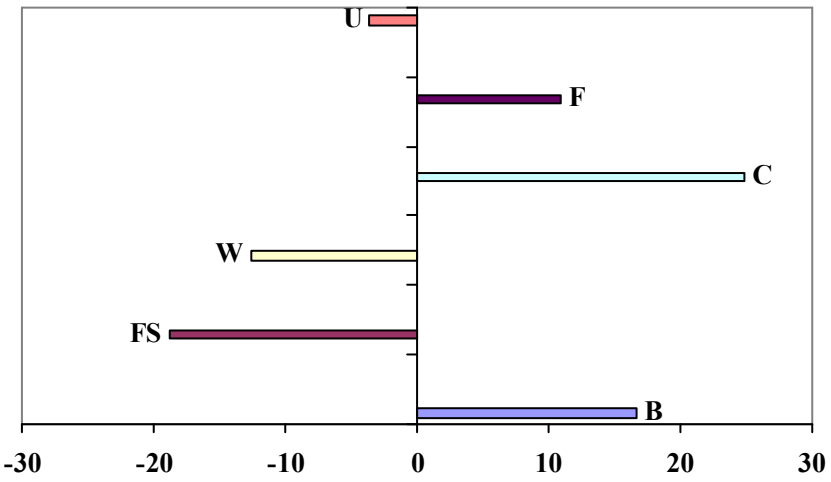

B= Building area FS= Forest or shrub land W= Water
C= Cropland F= Fallow U= Unused area

Fig.4: Land use land cover change expressed in percentage between 1990 and 1999

IV. DISCUSSIONS

4.1 Accuracy

The accuracies of classification were turned out to be better than expected. The reasonable overall accuracies of all classification process can be explained by the fact that the total number of correctly classified pixels was high. The LULC types were correctly chosen, the precision of the classification might be another if we tried to classify separately classes (i.e. forest and shrub land, or rain fed cropland and irrigated). The comparatively lower accuracy of unused area and fallow could be explained by the fact that several of fallow pixels were misclassified as unused area or vise-versa. That indicates the probability that a fallow classified pixel in the map represented that category in reality. In other words the spectral signatures of unused area and fallow were very similar. For classifying croplands, there was some confusion with fallow and for classifying fallow; there was confusion with unused area. That was found to be consistent with the range reported elsewhere (Hazeu and De Wit, 2004). But most classes had quite high accuracy scores. That indicates the classification process was done as expected.

4.2 Changes in land use/land cover (1990-1999)

The satellite-based analysis reveals some interesting trends as regards the land cover development in the period 1990 to 1999. From our results fig.4 it is clear that the study area had been subjected to intensive use influence and degraded with +24.90 % and -18.77% of change under cropland and forest or shrub land respectively. It is worth mentioning that most of the deforestation took place south and south-east of the study area in 1999. The increase in cropland area and the decrease in forest or shrub land was found as deforestation at the profits of cropland elsewhere (Mengistu and Salami, 2007, Reis, 2008). In line with this, the LULC data of the two years indicated a change. The retreating of areas covered with forest or shrub land, water and unused area and expanding of building area, cropland and fallow is common in the region. This indicates the encroachment of cropland, fallow and buildings towards forest areas, water and unused area; this was established by the field investigation. The phenomenon is found to be a forest clearing and caused by anthropogenic disturbance (Roy, Chowdhury and Schneider, 2004). In other words the additional people have placed considerable pressure on the land for new housing and for increased food production. In many cases, new building areas were constructed on prime agricultural land with the attendant loss in food production from the best lands. To replace food production lost from converted prime agricultural land, and to provide additional output for the increased population, marginal lands have been cultivated, many of them on steep hillslopes. A better scenario can be foreseen if local social initiatives devoted to the sustainable use of natural resources are enforced (Velazquez et al., 2001). LULC changes reflect the dynamics observed in the socio-economic condition of the study area. As saying up the changes might due to the government policies that aim to balance the need to encourage rural development, the removal of compulsory grain crop quotas, promoting livestock with ecological stability. That is found to be similar to the situation in a neighboring area Xishuangbanna Prefecture (Xu et al., 1999). The driving force for building area (urban) expansion of Puer as Chinese city might be the phenomenon of development zones that are created to host innovative activities and foreign investment. The same reasons are valuable for cropland expansion, where the change was extremely important 24.90%. This indicates that, despite the economic growth, many people are still greatly dependent on the management of soils and the traditional agriculture. It puts pressure on the others land cover types, this in turn leads to the opening up of more natural forests, water and unused area for cultivation. Hence, the expansion of cropland was partially responsible for the disappearance of the forest of the area in the study period, even if the 1999 image was taken in December in winter period. The relationships between the cropland and building areas expansion and the forest decrease were found to be consistent with the range reported elsewhere (Fearnside, 2001, Lambin et al. 2003, Velazquez and al., 2003).

V. CONCLUSIONS:

LULC change detection analysis derived from landsat imagery has provided an accurate account of the situation of the study area during the period 1990-1999. Land use activities were towards more agricultural production. Drivers of land use change are strongly influenced by changes in agricultural practices, which themselves are influenced by institutional and economics factors (public policy, infrastructure growth). This analysis confirmed by the results, indicated that forest or shrub land conversion and modification were intensifying, as the human population was increased and livestock promoting became more common. The results indicated that severe land cover changes have occurred in croplands (+24.90%), forest or shrub land (-18.77%) and building (+16.72%) areas have been knowledgeable and unused area constituted the most extensive type of LULC in the study period. This paper highlights the importance of digital change detection in apprehending the environmental situation in this southern part of Yunnan Province (China). Further research would be important to help us understand more about variations in deforestation rates across counties, as well as the conversion and modification mechanisms of the above classified land use land cover types.

ACKNOWLEDGEMENTS

The author is grateful to the China Scholarship Council and China University of Geosciences for their financial support.

Correspondence to: Diallo Yacouba,, Institute for mathematics geosciences and Remote Sensing, Geosciences
Faculty of Earth Resources, China University of

Wuhan, 430074, Hubei, P.R. CHINA
Telephone: +86-027-67885970
Mobile phone: +86-15827248937,
E-mail: yacdial2005@hotmail.com

REFERENCES

1. Bolland L. P., Ellis E.A., Gholz H.L., 2007 Land use dynamics and landscape history in La Montana, Campeche, Mexico, Landscape and Urban Planning, 82: 198-207

2. Fearnside, M.P., 2001. Saving tropical forests as a global warming countermeasure: an issue that divides the environmental movement.Ecological Economics 39, 167–184.

3. Geist, H., J., Lambin E.F., 2002, Proximate causes and underlying driving forces of tropical deforestation . BioScience 52(2): 143-150

4. Giri, C., Defourny, P., & Shrestha, S. (2003) Land cover characterization and mapping of continental Southeast Asia using multi-resolution satellite sensor data. *Int. J. Remote Sensing*, 24 (21): 4181-4196.

5. Hazeu G.W. and De wit A.W., 2004, Corine land cover database of the Netherlands: monitoring land cover changes between 1986 and 2000. In the proceedings of EARSel conference pp. 382-387.

6. Jensen,J.R., 2007. Introductory Digital Image Processing: a remote sensing perspective. 3rd Edn., science Press and Pearson Education Asia Ltd: Beijing ISBN:978703018819-9 pp. 467-494

7. Lambin EF, Geist H, Lepers E (2003). Dynamics of land use and cover change in tropical regions. Annual Rev. Environ. Resour. 28: 205–241.

8. Mas, J.F.; Velazquez, A.; Gallegos, J.R.D.; Saucedo, R.M., Alcantare, C.; Bocco, G.; Castro, R.; Fernandez, T.; Vega, A.P., 2004, Assessing land use/cover changes: a nationwide multidate spatial database for Mexico. International Journal of Applied Earth Observation and Geoinformation**,** 5: 249-2

9. McIver D. K. and M. A. Friedl, 2002, Using prior probabilities in decision-tree classification of remotely sensed data. Remote Sensing of Environment 81: 253-261

10. Mengistu D., A., and Salami A.T., 2007, Application of remote sensing and GIS inland use/land cover mapping and change detection in a part of south western Nigeria, African Journal of Environmental Science and Technology 1(5): 099-109

11. Miller, J.D. and Pool, S.R., (2002). Mapping forest Post-Fire canopy Consumption in several 12. Overstory Types Using Multi-Temporal Landsat TM and ETM data. Remote Sensing of the Environment, 82(2-3): 481-496

13. Reis S. 2008, Analyzing land use/land cover changes using remote sensing and GIS in Rize, North-East Turkey, *Sensors*, *8*: 6188-6202

14. Rogan, J., Franklin, J. & Roberts, D.A. (2002) A comparison of methods for monitoring multitemporal vegetation change using Thematic Mapper imagery. *Remote Sens. Environ.*, 80(1): 143-156.

15. Roy Chowdhury, R., Scheneider, L.C., 2004. land cover and land use classification and change analysis. In Turner II, B.L.,Geoghegan, J., Foster, D.(Eds), Integrated Land change Science and Tropical Deforestation in the Southern Yucatan: Final Frontiers.Clarendon Press/Oxford U.P., Oxford,pp.105-141.

16. Saha A. K., Arora M. K., Csaplovics E., Gupta R. P., 2005, Land Cover Classification Using IRS LISS III Image and DEM in a Rugged Terrain: A Case Study in Himalayas, Geocarto International, 20(2): 33-40

17. Velazquez A,Bocco G,Torres A (2001) Turning scientific approaches into practical conservation actions: The case of Comunidad Indigena de Nuevo San Juan Paranagrocutiro, *Mexico. Environmental Management* 27: 655- 665.

18. Velazquez, A., Durana E., Ramırez I., Mas J., F., Bocco G., Ramırez G., Palacio J., L., 2003, Land use-cover change processes in highly biodiverse areas: the case of Oaxaca, Mexico, Global Environmental Change 13: 175–184

19. Vogel, A.W., Wang Mingzhu and Huang Xiaoqing, 1995. people's Republic of China: Red Reference Soils of the subtropical Yunnan Province. Soil Brief China1. Institute of Soil Science-Academica Sinica, Nanjing, and International Soil Reference and Information Centre, Wageningen. pp. 10-27.

20. Willson A. 2005, Using remote sensing to measure forest conversion and land use changes in Xiaozhongdian Township, Northwest Yunnan Province, China, Center for Biodiversity and Indigenous Knowledge (CBIK) Working Paper, pp. 5-15 http//: www.cbik.ac.cn

21. Wilson, E.H. & Sader, S.A. (2002) Detection of forest harvest type using multiple dates of Landsat TM imagery. *Remote Sensing of Environment*, 80: 385-396.

22. Wu, W. and Shao, G. 2002; "Optimal Combinations of Data, Classifiers, and sampling methods for Accurate Characterizations of deforestation" Canadian Journal of Remote Sensing, 28(4): 601-609.

23. Xu, J., & Ribot, J.C. (2004) Decentralization and accountability in forest management: a case from Yunnan, Southwest China. *European Journal of Development Research*, Vol. 16(1): 153-173.

24. Xu, J., & Wilkes, A.. (2004) Biodiversity impact analysis in northwest Yunnan, southwest China. *Biodiversity and Conservation,* 13: 959-983.

25. Xu, J., Fox, J., Xing, L., Podger, N., Leisz, S., Xihui, A., 1999. Effects of swidden cultivation, state policies, and customary institutions on land cover in a Hani village, Yunnan, China. Mountain Research and Development 19 (2): 123–132.

26. Yuan, F.; Sawaya, K.E.; Loeffelholz, B.C.; Bauer, M.E. 2005, Land cover classification and change analysis of the Twin Cities (Minnesota) metropolitan areas by multitemporal Landsat remote sensing. *Remote Sensing of Environment 98*, 317-328.

Ethnomedicinal uses of Pteridophytes of Kumaun Himalaya, Uttarakhand, India

Kanchan Upreti[1], Jeewan S. Jalal[1], Lalit M. Tewari[1*], G. C. Joshi[2], Y.P.S.Pangtey[1] and Geeta Tewari[3]
1. Department of Botany, D.S.B.Campus, Kumaun University, Nainital 263001, Uttarakhand, India
2. RRI (AI) CCRAS, Tarikhet (Ranikhet), Uttarakhand, India
3. Department of Chemistry, D.S.B.Campus, Kumaun University, Nainital 263001, Uttarakhand, India
l_tewari@rediffmail.com

Abstract: The present study deals with the ethnomedicinal uses of Pteridophytes in the treatments of various diseases. The Pteridophytes are widely used by the local people of the Kumaun Himalaya. The present study documents ethnomedicinal uses of 30 Pteridophytes plants, which are prevalent in study area along with botanical name, family, plant parts and mode of ethnomedicinal use. [Journal of American Science 2009;5(4):167-170]. (ISSN: 1545-1003).

Keywords: ethnomedicinal; Kumaun Himalaya; pteridophytes

1. Introduction

Kumaun Himalaya occupies the central sector of Indian Himalaya and lies between 28°44'- 30° 49' N Lat. and 78° 45'- 81° and 1' E long. It has occupy an area 21,033 sq km and made up of six districts. Due to varied topography, climate, soil and vegetation this region is very rich in Pteridophytes. Kali valley, Gori valley, Ramganga valley, Pindari valley are the important area where these Pteridophytes are very abundant.

Pteridophytes are one of the oldest land plant groups on earth and constitute a vast group of vascular cryptograms. The position of the Pteridophytes as intermediate between the lower cryptograms and higher vascular plants has made the group fascinating. Pteridophytes have a long geological history on our planet. They were known as far back as 380 million years ago. In India, Pteridophytes are particularly distributed in the Himalayan and coastal regions. Khullar (1991, 1994) recorded 356 species of Pteridophytes from Western Himalaya. Pteridophytes prefer shady, moist habitats with moderate temperature but also occur through out a very diverse range of habitats from high altitude. Like other groups of plants, Pteridophytes are also show medicinal utility and many of them are being used medicinally from ancient time (Kumar and Kaushik 1999). The tribal communities, ethic groups and folklore throughout the world are utilizing plant parts like rhizome, stem, fronds, pinnae and spores in various ways for the treatment of various aliments since ancient time. The numbers of contribution about the taxonomy, ecology and distribution of Pteridophytes have been published from time to time but enough attention have not been paid towards their medicinal useful aspects (Dixit, 1975). In the present attempt have been made to explore ethnomedicinally important Pteridophytes and properly documented their useful aspect.

The pteridophytes (Ferns and fern allies) represented by over 1200 taxa belonging to 204 genera (ca10,000) species of the world, grow in varied climatic zones of different phytogeographical regions of India. Subhash Chandra in his ferns of India has enumerated 1100 species belonging to 144 genera under 34 families from the Indian regions. Chowdhary (1973) published an account of pteridophytes from Upper Gangetic plains, which include parts of Uttarakhand, plains o f Uttar Pradesh, Bihar and part of West Bengal. Khullar (1994, 2000) in his illustrated fern flora of Western Himalaya included 360 species of ferns. Pande and Pande (2002) reported ca 350 species of ferns and fern allies from Kumaun Himalaya. Dixit and Kumar (2002) listed 487 species and 32 infra specific taxa belonging to 108 genera under 50 families. Eighteen species are endemic to Uttarakhand, of these, 10 species and 2 varieties confined these distributions only to Uttarakhand state and remaining six taxa also show their occurrence in other parts of India beside Uttarakhand. About 57 species are relatively of rare occurrence being endemic, rare and endangered due to other anthropogenic factors.

As far as trade of medicinal plants is concerned only species of *Adiantum* is exploited as the trade

name Hansraj, Hanspadi, Myurshikha. The entire plant of this species is used as medicine in Ayurveda, Sidha and Unani. The species of *Lycopodium* is also used in Homeopathic industry.

2. Materials and Methods

The present study is the outcome of the four years of critical field survey in the different parts of Kumaun Himalaya in every season. Ethnomedicinal information was gathered by the local and tribal people and interviewed the local people. All the specimens were collected in duplicate forms and they were deposited in the Herbarium of Botany department of D. S. B. Campus, Kumaun University, Nainital. Descriptions of species and identification were done with the help of literature Khullar, S.P. (1994 and 2000), Khullar et al 1991 and Pande and Pande, 2002.

3. Results

All known 30 species of Pteridophytes are encountered for the Kumaun Himalaya. Botanical names, family name, mode of use and plant parts used are given below:

1. ***Actiniopteris radiata*** (Sw.) Link, (Actiniopteridaceae) Myursikha, Morphanki

Plant used as a styptic and anthelmintic also used in bronchitis and gynecological disorders. The dry leaves are used in tuberculosis.

2. ***Adiantum capillus-veneris*** L., (Adiantaceae) Hansraj, Hanspadi

The decoction of leaves is taken for acute bronchitis and fever. The fronds are used against cough and cold and also chewed for the treatment of mouth blisters. Frond extract mixed with honey is used as an eye ointment. The plant is also used as a demulcent, expectorant, diuretic, emenagogue, tonic and febrifuge.

3. ***Adiantum incisum*** Forsk., (Adiantaceae) Hanspadi

The leaf powder is mixed with butter and used for controlling the internal burning of the body. Also used in cough, diabetes, fever and skin diseases.

4. ***Adiantum philippense*** L., (Adiantaceae) Hansraj

Plant is demulcent, astringent and emenagogue. It is used in cough, asthma, fever, leprosy and hair falling.

5. ***Adiantum venustum*** D. Don, (Adiantaceae) Hansraj, Hanspadi

Fronds are used as tonic, expectorant, astringent, emetic, diuretic etc. and decoction of fronds is given in fever also used in scorpion bite.

6. ***Angiopteris evecta*** Hoffm. (Angiopteridaceae)

Fresh rhizome and rachis powdered mixed with water is used in diarrhea.

7. ***Asplenium nidus*** L. (Aspleniaceae)

Used in enlargement of spleen in continuance of urine, calculus, jaundice and malaria.

8. ***Asplenium trichomanes*** L., (Aspleniaceae)

This is a laxative medicine. The leaf is smoked for colds in head and chest, used as an expectorant.

9. ***Blechnum orientale*** **L.,** (Blechnaceae)

Used as poultice in boils and rhizomes as anthelmintic, rhizome is used in typhoid.

10. ***Botrychium ternatum*** (Thunb.) Sw. (Botrychiaceae)

The plant is used as a vulnerary. The root is prescribed in dysentery.

11. ***Cheilanthes bicolor*** (Roxb.in Griff.) Griff. ex Fras.-Jenk., (Sinopteridaceae)

Plant powder mixed with cow's ghee is used as an incense to keep off fear in children. Brown stipes is used by the children as nose and ear studs. Root used in sickness.

12. ***Cyathea spinulosa*** Wall. *ex* Hook., (Cyatheaceae)

Soft pith and roots are used in the preparation of local drinks. Fronds are used as fodder as well as thatching the huts.

13. ***Dicranopteris linearis*** (Burm. f.) Und., (Gleichinaceae)

Young rachises are eaten after boiling. Fronds are used for thatching the roofs and house walls. Decoction of plant is laxative. Fronds are used in asthma and aqueous extract of fronds possesses antibacterial activity. The plants are used as cushion for cattle shed. Used as an anthelmintic. The fronds of young plant are used to remove sterility in women by grinding them with cow milk.

14. ***Diplazium esculentum*** (Retz.) Sw., (Athyriaceae)

The rhizomes are kept in the granaries to check them from insect and pests. Young fronds are used as green vegetables and also used as salad or cooked as vegetables.

15. ***Diplazium maximum*** (D.Don) C.Chr., (Athyriaceae) Lingura, Lyona

Young fronds are eaten as vegetables after cooking and are commonly sold in the local market in high price.

16. *Equisetum ramosissimum* Desf. (Equisetaceae)

Plant paste applied in bone fracture.

17. *Helminthostachys zeylanica* **(**L.) Hook., (Helminthostachyaceae) Tharu name (Kamsaj)

The plant is considered as intoxicant, anodyne and used in sciatica. Fronds used as aphrodisiac.

18. *Lycopodiella cernua* (L.) (Lycopodiaceae)

The decoction of the plant is used in beri-beri as lotion, used in cough and skin eruption.

19.*Lycopodium japonicum* Thunb. (Lycopodiaceae)

Diuretic, antispasmodic, used in rheumatism and diseases of lungs and kidney.

20. *Lygodium flexuosum* (L.) Sw. (Lycopodiaceae)

Rhizome powder is used in skin diseases. Plants are used as expectorant, rheumatism, sprains, scabies, eczema and cut wounds. Fresh roots boiled with mustered oil used in casbundes and rheumatism.

21. *Marsilea minuta* L., (Marsileaceae)

Plant used in cough, spastic conditions of leg muscles, in sedation and insomnia. A macrocyclic ketone of sedative and convulsant properties has been isolated.

22. *Nephrolepis cordifolia* (L.) Presl, (Nephrolepidaceae)

Paste of the leaves is applied as wound to check bleeding. Fresh watery tubers are eaten to especially quench thirst. Decoction of tubers is given to cure cough and intestinal disorders. Fresh watery tubers used in stomach ulcer and acidity.

23. *Ophioglossum reticulatum* **L.,** (Ophioglossaceae)

The paste of plant is applied on burns as cooling agent. The extract of leaf is also used in the preparation of tonic used as vulnerary and as remedy for wounds.

24. *Pteris biaurita* L., (Pteridaceae)

A decoction of the rhizome and fronds has been given in chronic disorders.

25. *Pteris vittata* L., (Pteridaceae)

Leaves used in worship at the time of illness. Fronds are largely used as cushion for cattle sheds.

26. *Pteris wallichiana* Agardh, Recens. (Pteridaceae)

Young fronds are steamed and eaten as a flavoring material. Juice is stated to possess astringent properties. Decoction is given in dysentery and applied to glandular swellings. A roasted frond made into a paste with sesame oil is applied to skin affections of infants.

27. *Selaginella bryopteris* (L.) Bak., (Selaginellaceae) Sanjeevani

Plant is used as diuretic and in gonorrhoea. The dried plant along with tobacco, are smoked by tribal people for inducing hallucinations used as witch craft and worship.

28. *Sphenomeris chinensis* (L.) Maxon, (Lindsaeaceae)

Paste of the plant used in swelling and sprains. Dried fronds are used as a substitute for tea leaves used internally for chronic enteritis and used as diuretic.

29. *Tectaria coadunate* (J. Smith) C. Chr., (Tectariaceae)

Plant decoction useful in colitis. Decoction of rhizome is given to children in stomachache.

30. *Thelypteris arida* (D.Don) (Thelypteridaceae)

Plant paste applied in wounds and cuts.

4. Conclusions

The Pteridophytes are widely used by the local people of the Kumaun Himalaya for ethnomedicinal purpose. The study documented 30 pteridophyte plants of ethnomedicinal use.

Acknowledgment:

The authors are thankful to the Head of Botany Department, D. S. B. Campus, Kumaun University, Nainital and Director CCRAS for encouragement and facilities during this short field survey.

References

[1] Chowdhary NP, The Pteridophytic flora of the Upper Gangetic Plain. Navyug Traders, New Delhi. 1973.

[2] Dixit RD. Ferns a much-neglected group of medicinal plants. I. J. Res. Ind. Med. 1975:10:74-90.

[3] Dixit RD, Kumar Ramesh. Pteridophytes of Uttaranchal- A check list. Bishen Singh Mahendra Pal Singh, Dehradun. 2002.

[4] Khullar SP. An Illustrated Fern Flora of the West Himalaya. Vol. I & II. Dehradun. 1994 and 2000.
[5] Khullar SP, Pangtey YPS, Samant SS, Rawal RS, Singh P. Ferns of Nainital. Bisen Singh Mahendra Pal Singh, Dehradun. 1991
[6] Kumar A, Kaushik P. Antibacterial effect of *Adinatum capillaris veneris* Linn. Indian Fern J. 1999:16:72-74.
[7] Pande HC, Pande PC. An Illustrated Fern Flora of Kumaun Himalaya Vol. I & II. Bisen Singh Mahendra Pal Singh, Dehradun. 2002.

Local livelihoods and protected area conservation in Rwanda: A case study of Akagera National Park.

Nahayo Alphonse[1,*],Yansheng Gu[2]

1. School of Environmental Studies, China University of Geosciences, Hubei province, 388 Lumo Road, 430074, Wuhan city, P.R.China, nahayalfa@gmail.com, +86 27 59839745
2. School of Environmental Studies, China University of Geosciences, Hubei province, 388 Lumo Road, 430074, Wuhan city, P.R. China, Yansheng_gu@yahoo.com.cn, +86 27 67883160, Fax: 86 27 87436235

Abstract: This study aims at investigating the local people's perceptions towards the conservation of Akagera National Park located in East of Rwanda. Due to different human activities such as cultivation, overgrazing and hunting, there is a conflict of interest between local livelihoods and conservation of the park. This study provides an insight into understanding the socioeconomic factors around the park and how they relate to its conservation. It also establishes a basis for decision-making in its management. Data was collected using a questionnaire survey in the villages neighboring the park. In total, 75 household heads were randomly selected and interviewed about the conservation of the park, its resource exploitation and the local people's socioeconomic conditions. Data has been analyzed using Descriptive Statistics and Logistic Regression Analysis. The inter method results suggest that the household size, the total livestock income and the age have a positive relationship with the forest resource dependency. The land scarcity, the crop raiding are statistically significant ($p<0.05$) and have a positive relationship with the conservation attitude whereas the variables age, primary and secondary education, residency length and food insufficiency have a negative attitude towards conservation. We suggest that the government should keep on emphasizing the conservation of the park by taking into account the improvement of local people's welfare and providing the financial support to agricultural and livestock projects in the area. [Journal of American Science 2009; 5(4):171-178]. (ISSN: 1545-1003)

Key words: Local livelihoods, socioeconomic factors, forest resource dependency, conservation attitudes, Akagera National Park, Rwanda.

INTRODUCTION

While biodiversity conservation in Africa is complex (Vogel 2001), the Rwandan situation is even more complex because of the growing population pressure, rural poverty and land limited resources (Masozera 2002). Rwanda with a total surface of 26 338 sq. km, has approximately 8.4% of its land under protected areas (Figure 1). They include:

1) The Nyungwe Forest Reserve (970 sq. km) in the Southwest, which is the largest remaining lower mountain forest in Africa; 2) The Volcanoes National Park (425 sq. km) in the northern part, which harbors highly-endangered biota, including mountain gorillas and golden monkeys; and

3) The Akagera National Park in the East (900 sq. km), which is a complex of savanna and wetland that provide habitat for a diverse fauna, including nearly 600 species of birds (Rutagarama and Martin 2006). This park has suffered more than others because of the conflict of interest between local livelihoods and conservation. An aerial survey of the park showed that between 1994 and 2002, wildlife declined by 50–80% due to human activities, including cultivation, pastoralism and hunting (Kanyamibwa 1998). The same author mentioned that in the last few years, additional pressures have been created by the settlement of people and cattle through the Ministry of Lands, Resettlement and Environmental Protection. The government has had to consider degazetting the entire park and it has maintained only 90 000 of the 245 000 ha originally gazetted (Masozera 2002). Since 1999, support for managing this threatened protected area has come from the German aid agency GTZ, through their project 'Protection des Resources Naturelles'. However, this project faces complex problems and results to date have been mixed because the demand for land and grazing, together with conflicts between wildlife and

agriculture, continue to undermine conservation efforts (Kanyamibwa 1998). This study aims at investigating local community's perceptions on the conservation of Akagera National Park taking into account the economic and social status of the local people. Specific objectives are: To identify the socioeconomic factors determining Akagera National Park dependency and to assess local people's attitudes towards its Rwanda's protected area network currently covers 8.4% of the total land area of 26 338 sq. km. The Akagera National Park covers 900 sq. km of wetland and savanna habitats and has one of the most diverse avifauna of the African continent, with about 600 bird species recorded (Rutagarama and Martin 2006). This research was conducted during the summer 2008 in villages neighboring Akagera National Park namely Karangazi (north west of the park), Rugarama (west) and Rwinkwavu (south west).

conservation. On the completion of this study, the following questions will have been answered: Is there any forest resource dependency by the communities living around Akagera National Park? Do the human activities around Akagera National Park affect negatively its conservation?

MATERIALS AND METHODS

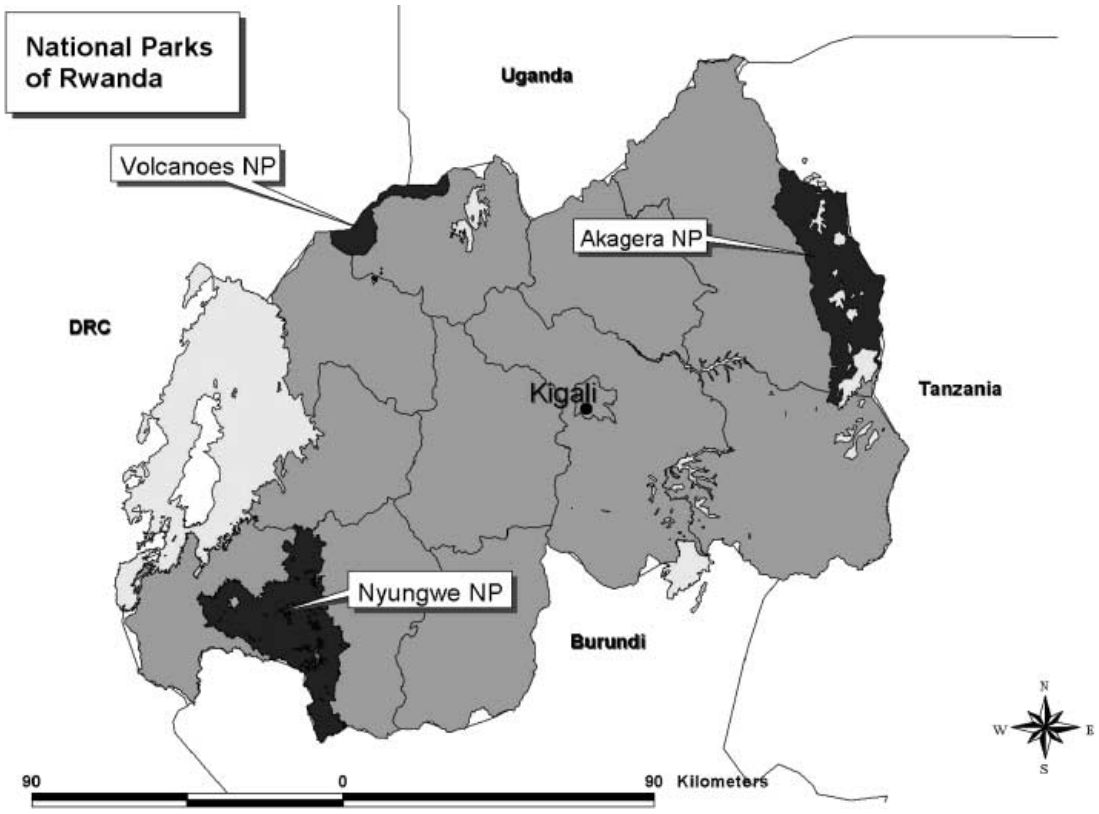

Figure1**:** National Parks of Rwanda (map by Jose Kalpers)

The primary and the secondary data have been collected. The primary data was collected using a questionnaire survey which was translated in Kinyarwanda and orally administrated. The secondary data was obtained from different documents already published about Akagera National Park conservation. Within each village, twenty five households were randomly selected for interview. In total, seventy five households were randomly selected from villages around the Akagera National Park. The survey was divided into three main sections. The first section included questions about attitudes towards Akagera National Park conservation. The respondents were asked to report on the different issues facing their daily economic life. The second section was composed of questions about Akagera National Park resource exploitation. The respondents were asked to report and quantify all items they collect from the forest. The third section dealt with questions about the socioeconomic conditions. Specifically, the

respondents were asked to report on the size of the land they own, education level, age, gender, household size, market accessibility, food availability, the main crops they grow, their annual crop and livestock output. In addition, the respondents were asked to list all capital assets they own. A combination of descriptive statistics and logistic regression analysis model are used to address stated research objectives. Logistic regression analysis is used to determine which independent variables are significant in predicting attitude towards conservation or forest resource dependency. The same technique has been used to assess the relationship between socioeconomic factors and conservation attitude (Masozera and Alavalapati 2004.

.

RESULTS AND DISCUSSION

Forest resource dependency

Table 1: Descriptive Statistics for forest resource dependency

Independent variables	Minimum	Maximum	Mean	Standard Deviation
Education level	1	3	1.38	0.59
Age	32	71	48.77	10.84
Gender	0	1	0.66	0.47
Land size	0.20	7.00	2.41	1.81
Total agricultural income	70	5400	487.85	1016.30
Total livestock income	67	9450	1310.06	2043.05
Market accessibility	0	1	0.31	0.47
Household size	2	8	5.4	1.40

Source: Data analysis 2008

66.66% of respondents have finished 6 years of primary education of whom 38% are women. Four men (5.33%) have graduated from university. Twenty one respondents (28%) have finished the secondary education of whom 28.57% are women. The age of respondents ranged from 32 to 71 and 66.66% are men. In total, 405 individuals have registered in the visited families and 69.34% of respondents live nearby the town (distance inferior to 10 km on foot) where the schools, hospitals and other different infrastructures are located. The land size of the respondents ranges from 0.2 to 7 ha and the average annual family income of the respondents was about 899 US$. By using enter method, we have got -2 log likelihood values of 46.112 for forest resource dependency and 65.316 for conservation attitude. This means that the model used fits the data better because the values of -2 log likelihood are small (George and Mallery2006).

Table 2: Logistic regression analysis for forest resource dependency

Independent variables	B coefficient	Standard error	Significance
Household size	1.246	0.398	0.002
Market accessibility	-1.373	0.976	0.159
Total livestock income	0.001	0.001	0.051
Total agricultural income	-0.002	0.001	0.142
Land size	-1.050	0.519	0.043
Gender	-0.594	0.814	0.466
Age	0.015	0.037	0.686
Primary education	-0.372	1.551	0.811
Secondary education	-21.576	7007.226	0.998

Source: Data analysis 2008

The table 2 shows the significance and B coefficient of each independent variable on the dependent variable. Five variables have got expected results namely the education level, the land size, the total agricultural income, the household size and the accessibility to the market.

It was hypothesized that the size of the household is directly related to forest resource dependency. The large families generally require many resources to satisfy their daily needs, therefore there is a higher tendency to extract forest resources. The variable household size has a positive relationship with forest dependency and it is statistically significant. This suggests that large families tend to rely on the forest resources in order to increase their income. Masozera and Alavalapati (2004) also found the same relationship between household size and Nyungwe forest resource exploitation.

It was also hypothesized that people's accessibility to the market reduces forest resource dependency. One the one hand, people living in isolated areas with limited access to external markets and infrastructure facilities are likely to remain poor and will continue to depend on surrounding forest resources. On the other hand, people living closer to the town may have a wide range of opportunities such as employment in small businesses. This study found that there is a negative relationship between people's accessibility to the markets and the forest resource dependency. Another study carried out by Gunatilake (1998) showed that the access to outside markets reduces forest dependency.

It was also hypothesized that the land size is inversely related to the forest resource. Families with a wide land are likely to raise their incomes by being engaged in off- farm activities and therefore depend less on forest resources. This study revealed this relationship with significance. Moreover, it is difficult for a big family to meet its daily needs without any other employment opportunities owing to the poor quality of land, the agricultural practices of land renting, lending and share- cropping.

The variable total agricultural income shows the negative relationship with the forest resource dependency, meaning that the family with higher agricultural income depends less on the forest resources. The same case was found around Nyungwe forest reserve where the agricultural income has got a negative impact on the forest (Masozera and Alavalapati 2004).

The negative coefficient of education level, both primary and secondary education suggests that educated people can easily get off farm employment opportunities than non- educated people. The education allows people to move away from subsistence agricultural activities. Hedge and Enters (2000) showed that high educated people will have greater off- farm employment opportunities than less educated ones.

The variable total livestock income has got a positive relationship with the forest resource dependency. This suggests that, due to a large number of heads of cattle in the area, the farmers

can sometimes enter the forest to fetch for water and pasture especially during the dry season.

The two variables namely age and gender have got the contrary results of what we expected to get. Indeed, the variable age which was supposed to be negatively related to the forest resource dependence showed a positive relationship because, even though illegal activities in the park are not allowed, people can sometimes take the risk of entering the forest. This study showed that aged people depend more on the forest resources than younger people. However, a study done around Nyungwe forest reserve revealed that younger households rely more on the forest resources to meet their daily needs (Masozera 2002). The variable gender which was supposed to have a positive relationship with the forest resources showed a negative value because both men and women have been sensitized on Akagera National Park conservation. However, around Nyungwe forest reserve, men are more dependent on the forest resources than women (Masozera and Alavalapati 2004). In Rwandan traditional society, there are some activities done especially by men like hunting and others by women like water collection.

Conservation attitude

Table 3: Descriptive Statistics for forest conservation attitude

Independent variables	Minimum	Maximum	Mean	Standard Deviation
Land scarcity	0	1	0.57	0.50
Water scarcity	0	1	0.76	0.43
Crop raiding	0	1	0.80	0.40
Food insufficiency	0	1	0.15	0.36
Inaccessibility to forest resources	0	1	0.21	0.41
Residency length	6	66	31.63	19.67
Dependency level	0	1	0.16	0.37
Education level	1	3	1.39	0.60
Age	32	71	48.77	10.85

Source: Data analysis 2008

Table 4: Logistic regression analysis for people's attitude towards conservation

Independent variables	B coefficient	Standard error	Significance
Land scarcity	1.842	0.756	0.015
Crop raiding	2.159	0.962	0.025
Water scarcity	0.880	0.818	0.282
Food insufficiency	-0.015	1.086	0.989
Inaccessibility to forest resources	0.515	1.106	0.641
Residency length	-0.034	0.023	0.134
Dependency level	0.583	1.445	0.687
Primary education	-2.544	1.466	0.083
Secondary education	-0.939	1.536	0.541
Age	-0.005	0.036	0.887

Source: Data analysis 2008

The table 4 shows the values of B coefficient (the magnitude of B indicates the effect of the predictor variable on the predicted variable), the standard error (the measure of the dispersion of B) and the significance of the wald test of all independent variables.

Though the land is not enough around the park, the variable land scarcity is no longer a threat against the conservation. However, the test is statistically significant with $p<0.05$. This is due to the recent decision of the government to redistribute equitably the land among the population living around the park and this was a long- term solution to the resettlement of new people in that area.

The crop raiding has not shown the negative attitude towards the conservation as it was expected. However, around the park, the crops are sometimes damaged by buffaloes and the compensation process was under discussion between the government and the population. The wildlife damage in the form of crop raiding has led to a negative attitude towards conservation of Nyungwe forest reserve (Masozera 2002).

The variable water scarcity has got a positive relationship with the conservation attitude. Even though Akagera National Park is located in semi arid region, the effort has been made to pump water from aquifer zone and make it available for daily domestic use. The shortage of water is not a common problem but it becomes serious during the dry season because of the presence of many heads of cattle in the area.

The variable food insufficiency has got a negative relationship with the conservation. People who do not meet their daily needs like food may not care about conservation (Masozera and Alavalapati 2004).

The residency length has got a negative relationship with the conservation because former residents are likely to hold a negative attitude towards the conservation. This is due to the poverty and the lack of diverse economic opportunities. Moreover, the aged people held a negative attitude towards Akagera National Park conservation because of their tradition according to which people adjacent to forest were living on the forest resources like hunting, honey, wood and water collection (Masozera and Alavalapati 2004).

The variable dependency level has got a positive relationship with the conservation because many people interviewed in the area do not highly rely on the forest resources for their daily needs. The ORTPN and the government have focused on Akagera National Park conservation by taking into account the improvement of community welfare around the park and providing the financial support to agricultural and livestock projects able to regenerate employments like Send a cow, PADEBEL (Dairy Cattle Development Support Project), PAPSTA (Agricultural Transformation Strategic Plan Support Project), RSSP (Rural Sector Support Project), PEDERCIU (Umutara Region Development Project) and EDPRS (Economic Development and Poverty Reduction Strategy) (MINAGRI 2003).

People who have finished primary and secondary education had demonstrated a negative attitude towards conservation because of the lack of variation in their education enabling them to find various employment opportunities in rural areas. Age is considered as important independent variable to determine conservation attitude. The negative value of B coefficient means that elderly people living around Akagera National Park have complained about the conservation initiatives because of the tradition according to which people were living by exploiting forest resources. This study showed that, due to the urban migration, younger people support conservation because most of them do not live permanently in the area. Harada (2003) showed that elderly inhabitants are less likely to support conservation than younger people.

CONCLUSION

In total 75 household heads were surveyed around Akagera Natonal Park where local people rely on agricultural and livestock activities. The study revealed that the people's dependency on forest resources is driven by many factors. The results show that the education level, the market accessibility, the total agricultural income, the land size, and the gender have got a negative relationship with the forest dependency. However, larger families are more dependent on the forest resources. Moreover, people having many heads of cattle together with aged people are likely to exploit the forest resources. The significance of the wald test showed that the

household size, the land size and the total livestock income are the most influencing factors for forest resource dependency. As far as Akagera National Park conservation is concerned, the variables land scarcity, crop raiding and education level are statistically significant. Though some respondents showed that the land scarcity is not actually a big threat against the conservation, there has been an overgrazing pressure on the land because of a large number of heads of cattle in the area. The variables primary and secondary education level, long-term residency length, food insufficiency and age have got a negative attitude towards the conservation of Akagera National Park.

In order to resolve the conflict between local livelihoods and the conservation of the park, the government has taken measures to increase agricultural and livestock production and generate off- farm employment opportunities for rural communities in general and around Akagera National Park in particular. This has been done through different support projects operating in the area. They provide many job opportunities and offer small credits to farmers. The government has also taken decision to provide 10% of its total annual ecotourism income in order to reinforce the community-based conservation projects.

ACKNOWLEDGEMENTS
I would like to acknowledge the financial support provided by China University of Geosciences (Wuhan) and the Student Financing Agency of Rwanda (SFAR).

***Correspondence to**
Nahayo Alphonse;Tel: 0086 27 59839745;
E- mail: nahayalfa@gmail.com
China University of Geosciences (Wuhan), School of Environmental Studies, 388 lumo Road, Wuhan, Hubei, 430074, P.R.China

REFERENCES

George, D. and Mallery, P. 2006. SPSS for Windows Step-by-Step.13.0. 6th edition, 0205480713, published by Pearson education, Inc, publishing as Allyn& Bacon. ISBN 978-7-5062-8219-2/R .128; 01- 2006- 1967; 386P.

Gunatilake, H.M. 1998. The role of rural development in protecting tropical rainforests: evidence from Sri Lanka. Journal of environmental management, 53(3):273-292; DOI:10.1006/jema.1998.0201; ISSN:0301-4797;Elsevier,Oxford,UK(1973);http://www.ingentaconnect.com/content/els/03014797/1998/00000053/00000003/art90201

Harada, K. 2003. Attitudes of local people towards conservation and Gunung Halimum National Park in West Java, Indonesia. Journal of Forest Research, 8(4): 271–282; ISSN: 1341-6979 (print) 1610-7403 (online), DOI: 10.1007/S10310-003-0037- Z; Springer Japan.

Hedge, R. and T. Enters. 2000. Forest products and household economy: A case study from Mudumalai Wildlife Sanctuary, Southern India. Journal of Environmental Conservation, 27(3):250-259; ISSN: 0376- 8929; Cambridge University Press, Cambridge, UK (1974)

Kanyamibwa, S. 1998. Impact of war on conservation: Rwandan environment and wildlife in agony.Journal of Biodiversity and Conservation, 7(11): 1399- 1406; ISSN: 0960-3115 (print) 1572- 9710 (online); DOI: 10.1023/A: 1008880113990; Springer; http://www.ingentaconnect.com/klu/bioc/1998/00000007 /00000011/00199211.

Masozera, M.K. and Alavalapati, J.R.R. 2004. Forest dependency and its implications for protected areas management: A case study from the Nyungwe Forest Reserve, Rwanda. Scandinavian Journal of Forest Research, 19 (Supplement 4): 85–92; ISSN: 1400- 4089; Taylor & Francis, Basingstoke, UK (1994).

Masozera, M. K. 2002. Socioeconomic impact analysis of the conservation of the Nyungwe forest reserve,
Rwanda. Thesis presented for the degree of Master of Science.University of Florida.103p.

MINAGRI 2003. Draft on National Forestry Policy Project. Ministry of Agriculture, Livestock and Forest.
Kigali, Rwanda.

Rutagarama, E. and Martin, A. 2006. Partnerships for protected area conservation in Rwanda. The
Geographical Journal, 172(4):291-305; DOI:10.1111/J.1475- 4959.2006.00217.xabout doi.

Vogel, G. 2001. No easy answers for biodiversity in Africa. Science magazine, 291(5513):2529-2530; DOI:10.1126/science.291.5513.2529a

Diversity of Aquatic Hyphomycetes as Root Endophytes on Pteridophytic Plants in Kumaun Himalaya

S.C. Sati, N. Pargaein and M. Belwal*
Department of Botany, Kumaun University, Nainital-263002
*manish_belwal@yahoo.co.in

Abstract: Present study was carried out to explore the diversity of endophytic hyphomycetes on living roots of healthy pteridophytic plants growing near ravine areas of Jeoli (1150m.asl) and Kilburry (2160m.asl), located at Nainital, Kumaun Himalaya. Root samples of pteridophytic plants were processed and incubated in the laboratory following standard technique. A total of 11 species of aquatic hyphomycetes belonging to 9 genera namely *Alatospora*, *Anguillospora*, *Campylospora*, *Clavariopsis*, *Heliscus*, *Lunulospora*, *Pestalotiopsis*, *Tetrachaetum* and *Tetracladium* were recorded as root endophytic hyphomycetes of pteridophytic plants. Four species namely, *Alatospora acuminata*, *Anguillospora crassa*, *Pestalotiopsis submersus*, and *Tetrachaetum elegans* are being reported for the first time as root endophytic hyphomycetes of *Equisetum*, fern and *Botrychium* plant roots. It was interesting part of the study that the roots of *Botrychium* were found to colonize the maximum number of endophytic hyphomycetes, while *Tetracladium setigerum* was recorded as a commonly occurring root endophyte on all the pteridophytic hosts. [Journal of American Science 2009; 5(4):179-182]. (ISSN: 1545-1003)

Key words: aquatic hyphomycetes, endophytes, sporulation, spore types

1. Introduction:

Microbes, which live with interior tissues of healthy plants without causing disease symptoms, are called endophytes. Endophytic fungi have been reported from different plants such as mosses, ferns, conifers and angiosperms (Sati and Belwal 2005). Endophyte occupies a unique ecological niche and has major influence on distribution, ecology, physiology and biochemistry of plants (Sridhar and Raviraja, 1995).

The aquatic hyphomycetes were first described by Prof. C.T. Ingold in 1942 as they complete their life cycle on submerged substrate in well aerated water, producing magnificent spore types (Belwal and Sati, 2005; Sati et al, 2002) while, Waid (1954) was the pioneer, for the first time reported some of these aquatic hyphomycetes from root surface too. Fisher et al (1986) recognized a separate group of aquatic hyphomycetes as Endophytic hyphomycetes and later Fisher et al (1991) confirmed their occurrence on the plant roots of aquatic habitats through experimental basis by examining the bark and xylem of aquatic roots of *Alnus glutinosa*. Similar reports have been made by some other mycologists on the endophytic aquatic hyphomycetes (Marvanova and Fisher, 1991; Marvanova et al, 1992; Pargaien, 2006; Sridhar and Barlocher, 1992; Sati et al, 2006, 2008) on different hosts. In the present paper aquatic hyphomycetes as endophyte of the Pteridophytic plant roots collected from Kumaun Himalaya were studied.

2. Materials and Methods:

'Three step sterilization' method of Fisher and Petrini (1989) was followed for the study of root endophytic fungi. Living roots of different tree plant species including herbs and shrubs growing in the ravine and wet areas located at Nainital Kumaun Himalaya were collected in 3 replicates of each. Nearly 10-15 cm long roots were cut off with a sharp sterile knife and washed with sterile water. These root samples were then keep in sterile polythene bags, brought to the lab and processed within 4-5 hours after collection. Root samples were washed under running tap water for about 10 minute to remove extraneous adhering soil particles and cut into 3-4 cm size segments. These were then rinsed with sterile water after surface sterilization with 90% alcohol for 2-3 minutes. The segments were incubated at 20 ± 2^0C for 5-20 days in sterile petri-dishes containing 30 ml of sterile water. Incubated dishes were observed periodically to detect the conidia of endophytic fungi under low power of microscope.

Simultaneously, some of the surface sterilized root segments were placed in 2% Malt Extract Agar, supplemented with streptopenicillin or tetramycin solution (250mg/l) and incubated for a few days depending upon the growth of emerging fungi following agar plate method. Fungal mycelia growing on agar blocks were transferred into another petri dishes containing sterile water for sporulation and identification.

3. Results and Discussion:

The present study was carried out to

investigate the diversity of aquatic hyphomycetes as endophytes from the living roots of pteridophytic plants growing near the selected ravine areas of Kumaun Himalaya. A total of eleven species belonging to 9 genera namely *Alatospora*, *Anguillospora*, *Campylospora*, *Clavariopsis*, *Heliscus*, *Lunulospora*, *Pestalotiopsis*, *Tetrachaetum* and *Tetracladium* of aquatic hyphomycetes were recorded as root endophytes, showing variation in the host diversity (Table 1; Fig. 1).

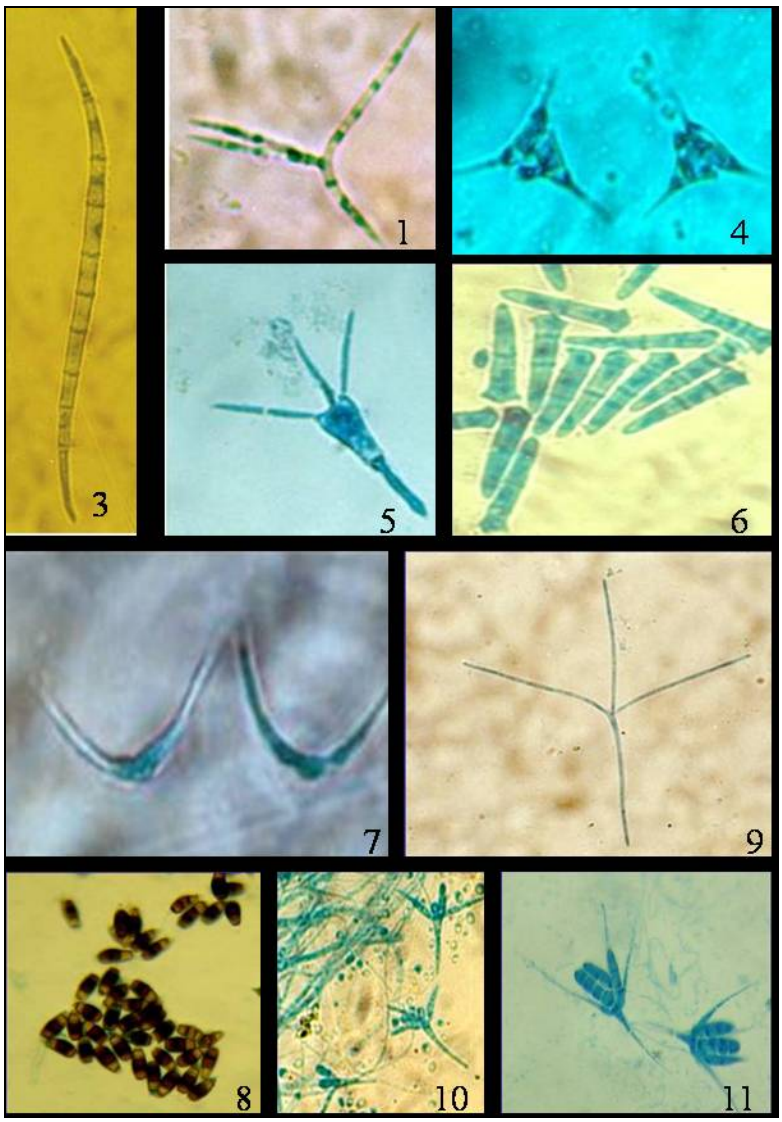

Fig. 1

(Figure no. are corresponding to table 1)

Table 1. Aquatic hyphomycetes isolated from pteridophytic plant of Kumaun Himalaya as root endophytes

S. No.	Root Endophytes	Host*	Locality**
1.	*Alatospora acuminata*	Eq / F	Jl / Kil
2.	*Anguillospora crassa*	Eq / F	Jl / Kil
3.	*A. longissima*	Bot	Jl / Kil
4.	*Campylospora purvula*	Bot	Jl / Kil
5.	*Clavariopsis aquatica*	Bot / F	Kil
6.	*Heliscus lugdunensis*	Bot	Jl / Kil
7.	*Lunulospora curvula*	Bot	Jl / Kil
8.	*Pestalotiopsis submersus*	Eq/F	Jl / Kil
9.	*Tetrachaetum elegans*	Bot	Jl / Kil
10.	*Tetracladium marchalianum*	F	Jl
11.	*T. setigerum*	F / Eq / Bot	Jl / Kil

* Eq = *Equisetum*, Bot = *Botrychium*, F= Fern,
** Jl = Jeoli, Kil = Kilburry

As evident from table 1, out of eleven species, 7 species were also reported by the earlier workers as commonly occurring endophyte. In the present investigation, however, these were found with their new host records. Two species namely, *Anguillospora longissima* and *Tetracladium marchalianum* which were earlier reported from Strawberry plant roots (Nemec, 1969) as well as from Lyonia ovalifolia and ferns (Sati and Belwal, 2005) were also recorded to colonize the roots of fern and *Botrychium* species, in the present study. *Campylospora purvula* and *Clavariopsis aquatica* was earlier reported by Fisher and Petrini (1989,1990), Sridhar and Barlocher (1992) and Sati and Belwal (2005) were also isolated here from *Botrychium* species. *Heliscus lugdunensis* was isolated from *Botrychium* and fern species in this study however, Fisher et al (1991), Sridhar and Barlocher (1992) and Sati and Belwal (2005) reported it from the roots of *Alnus glutinosa, A. spicatum, Betula papyrifera, Picea glauca Lyonia ovalifolia* and unknown pteridophytic plants. *Lunulospora curvula* was earlier reported by Sridhar and Barlocher (1992) and Sati and Belwal (2005), but in our study it was isolated from *Botrychium* and fern roots. *Tetracladium setigerum* was found as frequently occurring root endophyte as it was isolated from all Pteridophytic plants studied, however, Watanabe (1975) and Sati and Belwal (2005) recorded it from strawberry roots, *Lyonia ovalifolia , Murrya koenjii* and Fern roots. *Botrichium* roots were highly colonized by endophytic aquatic hyphomycetes followed by fern and *Equisetum*. In the present study, the staurosporus conidial forms were found most prevalent followed by variation in forms in order of occurrence (Fig. 1).

Acknowledgement:

The authors thank head, Department of Botany, Kumaun University Nainital, for providing lab facilities. Financial support of DST, New Delhi is greatly acknowledged.

References:

Belwal, M. and Sati, SC. 2005. Fungal flora of two altitudinally different streams of Kumaun Himalaya, In "*Recent Mycological Researches*" (Ed. **S. C. Sati**) I. K. International Pvt. Ltd., New Delhi, pp 3-21.

Fisher PJ and Petrini O. 1989. Two aquatic hyphomycetes as endophytes in *Alnus glutinosa* roots. Mycological Research, 92: 367-368.

Fisher PJ and Petrini O. 1990. A comparative study of fungal endophytes in xylem and bark of *Alnus* species in England and Switzerland. Mycological Research, 94: 313-319.

Fisher PJ, Anson AE and Petrini O. 1986. Fungal endophytes in *Ulex europaeus* and *Ulex gallii.* Trans. Brit. Mycol. Soc., 86:

153-156.

Fisher PJ, Petrini O and Webster J. 1991. Aquatic Hyphomycetes and other fungi living aquatic and terrestrial roots of *Alnus glutinosa*. Mycol. Res., 95: 543-547.

Ingold CT. 1942. Aquatic Hyphomycetes of decaying alder leaves. Trans. Brit. Mycol. Soc., 25: 339-417.

Nemec S. 1969. Sporulation and identification of fungi isolated from root rot diseased Strawberry plants. Phytopathology, 59: 1552- 1553.

Pargaien, N., Sati, S.C. and Belwal, M. 2006 Endophytic aquatic hyphomycetes of roots from forested plants of Nainital, Kumaun Himalaya. In "*Plant Science Research in India: Challenges and Prospect*:" (Ed. S. Kumar) pp 213-220.

Sati, S C, Tiwari, N. and Belwal, M. 2002. Conidial aquatic fungi of Nainital, Kumaun Himalaya, India. Mycotaxon 81: 445-455.

Sati SC and Belwal M. 2005. Aquatic Hyphomycetes as root endophytes of Riparian plant roots. Mycologia, 97(1): 45-59.

Sati, SC, Pargaein, N. and Belwal, M. 2006. Three species of aquatic hyphomycetes as new root endophytes of temperate forest plants. Nat. Acad. Sci. India 29 (2): 9-10.

Sati, SC, Belwal, M. and Pargaien, N. 2008. Diversity of water borne conidial fungi as root endophyte in temperate forest of western Himalaya. Nature and Science, 6 : 59-69.

Sridhar KR and Barlocher F. 1992a. Aquatic hyphomycetes in spruce roots. Mycologia, 84: 580-584.

Sridhar KR and Barlocher F. 1992b. Endophytic aquatic hyphomycetes of roots of Spruce, Birch and Maple. Mycol. Res. 96: 305- 308..

Sridhar KR and Raviraja NS. 1995. Endophytes- A crucial issue. Curr. Sci., 69: 570-571.

Waid JS. 1954. Occurrence of aquatic hyphomycetes upon the roots surface of beech grown in woodland soil. Trans. Brit. Mycol. Soc. 37: 420-421.

Watanabe T. 1975. *Tetracladium setigerum* an aquatic hyphomycetes associated with gentian and Strawberry roots. Trans. Mycol. Soc. Japan, 16: 348-350.

Flavonol Glycosides of *Cheilanthes anceps* Roxb.

[1]Rachana Mishra[*] and D. L. Verma[2]
[1&2]Department of Chemistry, Kumaun University,
SSJ Campus, Almora-263601, (Uttarakhand) India.
[*]Email- 09411102476m@gmail.com
Phone Numbers: +91-9411102476[1], +91-5962-233849(R)[2]

Abstract: *Cheilanthes anceps* Roxb, a member of Silva-back group of fern of the family, Sinopteridaceae, is a fern constituent of pine forest of Central Himalaya, ranging altitude from 2000m to 3000m. It has been recognized as a traditional medicine by the tribal inhabitants of Central Himalaya. The aqueous extract of the fern has been used for curing number of human ailments like cough, bronchitis, diabetes, inflammatory and healing wounds. The aqueous-ethanolic extract of fern fronds of *C. anceps* was concentrated and partitioned with CH_2Cl_2 and n-BuOH. The flavonoid positive fraction derived from 30% HOAc fractionation of BuOH soluble gave antioxidative activity against the methanolic solution of free radical, DPPH by the standard thin layer autobiography and UV-VIS spectrophotometer assay. Two flavonol glycosides, kaempferol – 3 – O – α- L- rhamnopyranosyl (1→2) – α - L-rhamnopyranosyl (1→6) – β – D - galactopyranoside and quercetin- 3 – O -α -L- rhamnopyranosyl (1→2)- α -L-rhamno pyranosyl(1→6)-β-D-galactopyranoside, were isolated and identified from antioxidative activity guided fraction and named as compound [1] and [2] respectively. The compound [2] was found to be more active than the compound [1] using quercetin as a reference substance. Both the compounds [1] and [2] showed lower activity than reference substance, quercetin. [Journal of American Science 2009;5(4):183-188]. (ISSN: 1545-1003).

Key words: Ferns, *Cheilanthes anceps*, Roxb, Central Himalaya

1. Introduction

Genus *Cheilanthes*, a group of Silva-back ferns of the family, Psinopteridaceae, is widely distributed in temperate and humid environs of Central Himalaya ranging altitude from 2000m to 3000m. Eighteen species of genus *Cheilanthes* have been reported from the hills of Kumaun Himalaya of newly created state Uttarakhand. Some *Cheilanthes* species, native of Himalaya have been recognized as a traditional medicine by some ethnic groups of the region (Pande, 1992). Various extracts derived from *Cheilanthes* species have been identified for antimicrobial activities (Nickell, 1959; Bhakuni *et al.*, 1969). Similar studies on different kind of medicinal plants have been reported by Verma and his co-workers (Khetwal and Verma, 1983, 1984, 1986, 1990; Khetwal *et al*., 1985, 1986; Mishra, 2009a, Mishra and Verma, 2009b and Mishra and Verma, 2009c). *Cheilanthes anceps*, an abundant fern constituent of the pine forests of Central Himalaya, has been identified as a traditional medicine by the local Kumaun people of the region and aqueous extract has been used for curing human ailments like cold, cough, asthma, bronchitis, diabetes, inflammatory and heeling wounds (Banerjee and Sen, 1980).

Naturally occurring flavonoidal compounds have a vital role as antioxidants (Oleszek, 2002). These compounds have widely been used to cure diseases related to oxidative stress like, diabetes, stroke, arthritis, cancer, cardiovascular and inflammatory (Kapiszewska *et al.*, 2005). These natural antioxidants are an integral constituent of angiosperm food and fodder plants. The objective of present chemical investigation is to investigate new natural products responsible for antioxidative activity from non-flowering and not a usual food and fodder plants like ferns. Attributing a traditional medicinal uses of *C. anceps* for curing number of ailments, the present communication revealed the isolation and characterisation of flavonol glycosides. *C. anceps* is a rich source of flavonoids and produces in general a number of methylated flavonols, flavonol-O-glycosides of quercetin and kaempferol that have been reported in the literature (Erdtman *et al.*, 1966; Salatino and Prado, 1998). *C. anceps* has neither been reported for biological activities and nor been reported for active secondary metabolites.

2. Material and method

Fern fronds of *Cheilanthes anceps* Blanford was collected from 3000m height of pindari glacier route of Kumaun Himalaya and authentification of the species was made by Prof. P. C. Pande, Botany Department of Kumaun University, S. S. J. Campus, Almora (Uttarakhand). Its vouch. (Specimen No. 13) has been deposited in the Chemistry Department of Kumaun University at SSJ Campus, Almora, Uttarakhand, India.

About 1kg air dried and powdered fronds of *Cheilanthes anceps* was extracted sequentially with 70% aqueous ethanol and 50% aqueous ethanol by cold percolation method for six days. These two were combined and concentrated under reduced pressure until only a small H_2O layer (approx. 50ml) remained. It was partitioned with CH_2Cl_2 and BuOH successively. The BuOH fraction was adsorbed on cellulose CC (Merck) and it was eluted initially with H_2O then increasing polarity with HOAc. On eluting CC with 30% HOAc, three dark fluorescent bands were observed on CC and each was eluted and collected separately by monitoring with UV light. The eluents derived from faster, middle and slower moving bands represent Frac-I, Frac-II and Frac-III, respectively.

3. Antioxidative screening of Frac-I, Frac-II and Frac-III

Each fraction was evaporated to dryness under reduced pressure at 70^0C. The residue of each fraction was dissolve in MeOH and evaluated for antioxidative activity against DPPH free radical solution with UV-VIS spectrophotometer and the quenching of fluorescence was measured at 515nm. Besides the spectrophotometer evaluation, the thin layer autobiographic methods using SiO_2 TLC plate of the fraction developed with suitable solvent and sprayed with methanolic solution of DPPH. The methanolic solution of Frac-I afforded active spots (yellow spots in purple background) while Frac-II and Frac-III did not produce any active spot.

Frac-I, an antioxidative active fraction was adsorbed on Whatman No. 3 PC and fractionated with BAW (n-BuOH-AcOH-H_2O, 4:1:5, V/V, upper layer) as a developing solvent. On inspecting PC under UV light, two dark purple fluorescent bands were observed and each was cut and eluted with 70% EtOH. The eluate of faster moving component produces two antioxidative active spot on TLC was separated by Sephadex LH-20 CC using 40% MeOH as an eluent. Two compounds [1] and [2] were isolated. The compound [2] was found more antioxidative compound than compound [1] using quercetin as a reference substance.

4. Result and discussion

Compound [1], a grey-yellow amorphous solid, gave positive results in Molish and Mg+HCl test. It appeared as a dark purple fluorescent spot on PC under UV light and changed to yellow-green after fuming with NH_3 vapours, indicating the presence of free hydroxyl groups at C-4'and C-5. When cellulose TLC of the compound was sprayed with methanolic solution of Naturstoffreagenz A (NA) reagent, the spot turned to yellow, indicating the presence of a free hydroxyl group at C-4' but absence of ortho-di-hydroxyl group in the B-ring. Its UV spectrum in MeOH showed characteristic absorption at 268nm (band II) and 361nm (band I), indicting 3-O-substituted flavonol skeleton (Markham, 1982) and analysis with the usual flavonoid shift reagents, NaOMe (282, 396); $AlCl_3$ (267, 305, 345); $AlCl_3$/HCl (267, 305, 344); NaOAc (270, 351); NaOAc/H_3BO_3 (270, 310, 314) and $ZrOCl_2$+citric acid (282, 396), suggesting the presence of free hydroxyl groups at positions, C-4', C-5 and C-7 (Markham, 1982). The mono-saccharides obtained after complete acid hydrolysis were identified as glucose and rhamnose by paper chromatographic comparison with their standards.

FABMS (-ve) of the compound [1] gave a molecular ions at m/z 739 $[M-H]^-$ calculated for $C_{33}H_{40}O_{19}$ and prominent ions observed at m/z 447 $[m/z\ 739\text{-}2x\ rham]^-$ and m/z 285 $[m/z\ 447\text{-}galac]^-$ supporting the release of two molecules of rhamnose and one molecule of galactose from kaempferol. H_2O_2 oxidation of compound gave kaempferol (CoPC) and a tri-saccharide sugar on PC at Rf 16 in BAW (n-BuOH-AcOH-H_2O, 4:1:5, V/V, upper layer) which on partial acid hydrolysis released rhamnose first then glucose. Partial acid hydrolysis of compound [1] with 0.1N-HCl gave three dark purple fluorescent compounds on PC at Rf, 48, 46 and 56 in BAW (n-BuOH-AcOH-H_2O, 4:1:5, V/V, upper layer), representing compounds [1(a)], [1(b)] and [1(c)] respectively. These three constituents were isolated by RPPC using BAW as a developing solvent followed by their final purification on Sephadex LH-20 CC.

The compound [1(a)] and [1(b)] were identified as a kaempferol - 3 - O - di - glycoside by their chromatographic behaviour, UV spectral data in MeOH and with diagnostic shift reagents (Mabry *et al.*, 1970; Markham and Mabry, 1975). The structure of [1(a)] and [1(b)] were identified as a kaempferol -3- O- α- L-rhamnopyranosyl $(1\rightarrow6)$ – β – D - galactoside and kaempferol – 3 – O – α – L - rhamnopyranosyl $(1\rightarrow2)$ – β – D - galactoside, respectively by their ^{1}HNMR studies in (DMSO-d_6 and 400MHz), shown in table [1] and by comparison of the physico-chemical data with those of authentic samples on the reported values in the literature (Yasukawa and Takido, 1987; Cui *et al.*, 1993).

Table 1. ^{1}HNMR of compound [1(a)] and [1(b)] in DMSO-d_6 (400MHz).

Shift (Multiplicity) of [1(a)]	Shift (Multiplicity) of [1(b)]	Identification
6.15 (1H, d, J=2.0Hz)	6.16 (1H, d, J=2.0Hz)	H-6
6.36 (1H, d, J=2.0Hz)	6.38 (1H, d, J=2.0Hz)	H-8
6.83 (2H, d, J=8.5Hz)	6.87 (2H, d, J=8.5Hz)	H-3', 5'
8.04 (2H, d, J=8.5Hz)	8.04 (2H, d, J= 8.5Hz)	H-2', 6'
12.60 (1H,s)	12.60 (1H,S)	5-OH
5.33 (1H, d, J=7.4Hz)	5.66 (1H, d, J=7.5Hz)	H-1"
4.48 (1H, d, J=1.5Hz)	5.10 (1H, d, J=7.5Hz)	H-1"'
2.90-4.10 (m)	2.95-4.00 (m)	Remaining protons of sugar moieties
1.10 (3H, d, J=6.0Hz)	1.15 (1H, d, J=8.3Hz)	6"-OCH_3

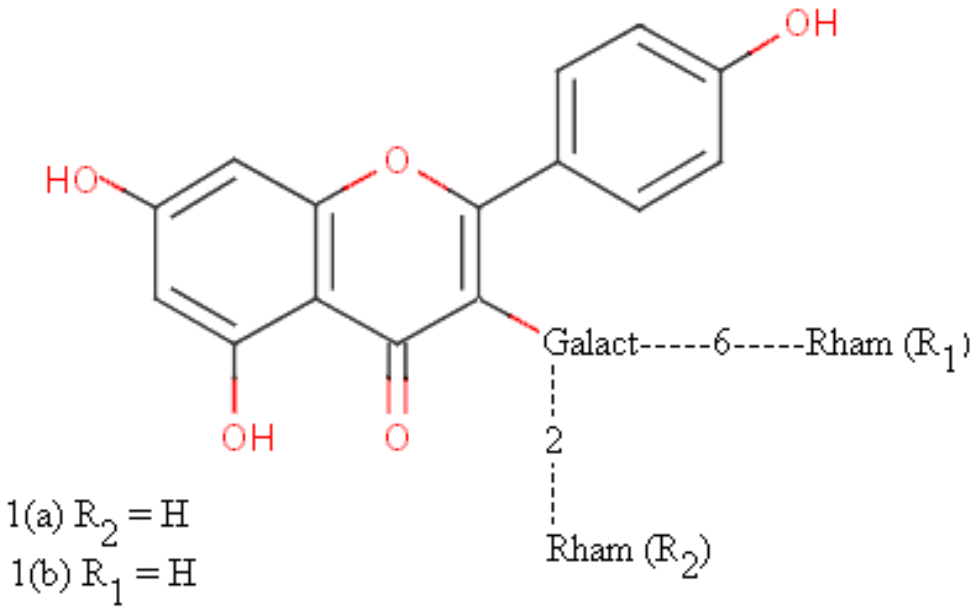

The compound [1(c)] was identified as kaempferol-3-O-β-D-galactoside by comparison on PC with its standard. The similar product was also identified from enzymatic hydrolysis of compound [1] with α-rhamnosidase. On the basis of chromatographic behaviour, UV spectral data, FABMS and hydrolytic methods, the compound [1] was identified as kaempferol-3-O-(2, 6-di-O-α-L-rhamnopyranosyl -β-D- galactopyranoside).

Finally, the structure of compound [1] was confirmed by ^{1}HNMR studies in (DMSO-d_6 and 400MHz): ^{1}HNMR of compound [1], as discussed in table (2), showed two ortho coupled symmetrical doublets appeared at δ 6.20 (1H, d, J=2.0Hz) and δ 6.42 (1H, d, J=2.0Hz) representing for H-6 and H-8 respectively of A-ring and two ortho coupled symmetrical doublets appeared at δ 6.87 (2H, d, J=8.5Hz) and δ 8.10 (2H, d, J=8.5Hz) assignable to H-2', 5' and H-2', 6' respectively of B-ring. A broad singlet appeared at δ 12.62 represent chelated 5-OH of A-ring. In aliphatic region , an anomeric proton signal appeared at δ 5.68 (1H, d, J=7.5Hz) attributed to a galactose (β-configuration) sugar moiety directly attached to aromatic ring and two high field anomeric proton singlets appeared at δ 5.12 (1H, S) and δ 4.46 (1H, S) were attributed to two rhamnosyl moieties (α-configuration) linked to the 2" and 6" positions respectively of 3-O-galactosyl moiety (Overend, 1972; Altona and Haasnoot, 1980). The rhamnosyl methyls appeared as doublets at δ 0.90 (3H, d, J=6.0Hz) and δ 1.12 (3H, d, J=6.0Hz). The remaining sugar protons were observed in the range δ 3.0-4.0.

Table 2. ^{1}HNMR spectra of compound [1] in DMSO-d_6 (400MHz)

Shift (δ)	Multiplicity	Identification
6.20	1H, d, J=2.0Hz)	H-6
6.42	1H, d, J=2.0Hz)	H-8
6.87	2H, d, J=8.5Hz)	H-3', 5'
8.10	2H, d, J= 8.5Hz)	H-2', 6'
5.68	1H, d, J=7.5Hz	H-1"
5.12	1H, d, J=7.5Hz	H-1"'
4.46	1H,s	H-1""
0.90	3H, d, J=6.0Hz	6"'-CH_3
1.12	3H, d, J=6.0Hz	6""-OCH_3
3.00-4.00	(m)	Remaining protons of sugar moieties

On the basis of ^{1}HNMR studies, the compound [1] was identified as kaempferol-3-O-α- L- rhamnopyranosyl (1 → 2) - α – L - rhamnopyranosyl (1 → 6) – β – D - galactopyranoside.

^{13}CNMR data chemical shift of sugar unit with those of kaempferol-3-O-galactoside showed glycosylation shift for C-2" by 5.9 ppm and C-6" by 5.5 ppm in the residual galactose unit. The signals at δ 76.2 and at δ 66.3 were attributed to C-2" and C-6" of inner galactose linked to two molecules of rhamnose as rhamnosyl (1→2) – β – D - galactopyranoside and rhamnosyl (1→6) – β – D - galactopyranoside respectively (Markham *et al.*, 1978).

Compound [2] gave positive reactions with Mg+HCl and α-naphthol. Complete acid hydrolysis of [2] with 2N-HCl gave quercetin (CoPC), galactose (CoPC) and rhamnose (CoPC). FABMS (-ve) of the compound [2] gave a molecular ions at m/z 755 $[M-H]^-$ calculated for $C_{33}H_{40}O_{20}$ and prominent ions were observed at m/z 463 [m/z 755-2x rham]$^-$ and m/z 301[m/z 463-galac]$^-$ supporting the abstraction of two molecules of rhamnose and one molecule of galactose from quercetin.

H_2O_2 oxidation of compound [2] afforded quercetin (CoPC) and a tri-saccharide, 2, 6-di-rhamnpside of galactose which was identified by comparing with its standard on paper chromatogram. Enzymatic hydrolysis of compound [2] with α-rhamnosidase gave quercetin-3-O-β-D-galactoside CoPC) and rhamnose (CoPC). Partial acid hydrolysis of compound [2] with 0.1N-HCl gave three compounds, quercetin – 3 - robinobioside, quercetin – 3 – α – L – rhamnopyranosyl (1 → 2) – β – D - galactoside and quercetin – 3 – O – β – D - galactopyranoside were identified by comparison of the physico-chemical data with those of authentic samples or the reported values in the literature (Yasukawa *et al.*, 1989; Nawwar *et al.*, 1989).

Finally, the structure of compound [2] was confirmed by ^{1}HNMR studies in (DMSO-d_6 and 400MHz) as discussed in table (3): ^{1}HNMR data of compound [2] in sugar region were found similar to the corresponding sugar region of compound [1]. Thus, the compound [2] was identified as quercetin-3-O-α-L-rhamnopyranosyl (1→2)-α-L-rhamnopyranosyl(1→6)-β-D-galactopyranoside.

Table 3. ^{1}HNMR spectra of compound [2] in (DMSO-d_6, 400MHz)

Shift (δ)	Multiplicity	Identification Protons
6.24	1H, d, J=2.0Hz	H – 6
6.43	1H, d, J=2.0Hz	H – 8
6.84	1H, d, J=8.5Hz	H – 5'
7.56	1H, d, J=2.0Hz	H – 2'
7.64	1H, dd, J=2 and 8.5Hz	H – 6'
12.60	1H (S)	5-OH
5.65	1H, d, J=7.5Hz	H – 1"
5.10	1H, d, J=1.0Hz	H – 1"'
4.45	1H (S)	H – 1""
0.92	3H, d, J=6.0Hz	CH_3 at 6"'
1.10	3H, d, J=6.0Hz	CH_3 at 6""
3.0-4.0	(m)	Remaining protons of sugar moieties

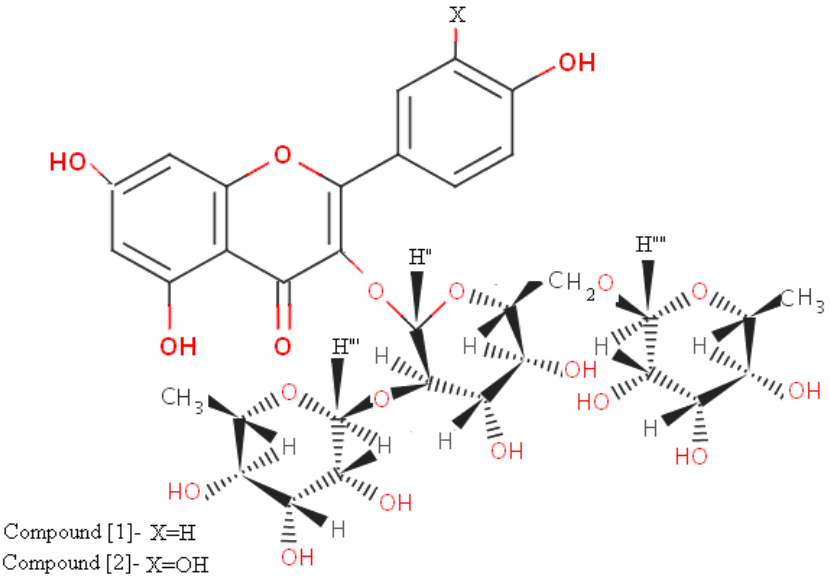

Acknowledgement:

We thank to the authority of Central Drug Research Institute (CDRI), Lucknow (U. P.), India for their kind co-operation in the structural analysis of flavonoids by [1]HNMR, UV and MS spectral studies.

Correspondence to:

[1]Mrs. (Dr.) Rachana Mishra, Department of Chemistry, SSJ Campus, Almora-263 601, Uttarakhand (India).

[2]Dr. D. L. Verma, Associate Professor of Chemistry, Department of Chemistry, SSJ Campus, Almora-263 601, Uttarakhand (India).

Telephone[2]: +91-5962-233849(R)

Cellular phone[1]: +91-9411102476

Email[1]: 09411102476m@gmail.com

References

1. Altona C. and Haasnoot C. A. G. Org. Mag. Resonance. 1980; 13: 417.
2. Banerjee R. D. and Sen S. P. Economic Botany. 1980; 34(3): 284-298.
3. Bhakuni D. S., Dhar M. L., Dhar M. M., Dhawan B. N. and Mehrotra B. N. Screening of Indian Plants Biological Activity. Indian Journal of Experimental Biology. 1969; 7: 250-262.
4. Cui B., Kinjo J. and Nohara T. Chem. Phar. Bull. 1993; 41: 553.
5. Erdtman H., Novatny L. C., Rumanuk M. Flavonols from the fern *Cheilanthes farinose.* Tetrahedron (sup.). 1966; 8: 71-74.
6. Kapiszewska M., Soltys E., Visioli F., Cierniak A. and Zajac G.. The Protective Ability of the Mediterranean Plant Extracts against the Oxidative DNA Damage: The Role of the Radical Oxygen Species and the Polyphenolic Content. Jour. of Physio. and Pharma. 2005; 56: 183-197.
7. Khetwal KS, and Verma DL. Natural and Applied Science Bulletin. 1983; 34(4): 337-338.
8. Khetwal K. S and Verma D. L. Indian J. of Pharmaceutical Sciences. 1984; 46(1): 25-26.
9. Khetwal KS, Verma DL and Tandon AK. Indian Drugs. 1986; 24: 116-117.
10. Khetwal KS, Verma DL, Pathak RP, Manral K, Tandon AK and Manju Joshi. Indian Drugs. 1985; 23(3): 126-128.
11. Khetwal KS and Verma DL. Fitoterapia. 1986; LVII(2): 128.
12. Khetwal KS and Verma DL. Indian Drugs. 1990; 28(2)**:** 99-100.
13. Mabry T. J., Markham K. R. and Thomas M. B. The Systematic Identification of Flavonoids; Springer Verlag: Berlin. 2005.
14. Markham K. R. and Mabry T. J. The

Flavonoids: In J. B. Harborne, Mabry, T. J. and H. Mabry, Chapman and Hall, London, 1975: 48-63.

15. Markham K. R. Techniques of Flavonoid Identification: A.P. London; 1982.
16. Mishra R. Chemical investigation of some ferns of Kumaun Hills, Ph. D. Thesis, Kumaun University, Naini Tal, 2009a.
17. Mishra R. and Verma DL. Nature and Science. 2009b; 7(6): 82-85.
18. Mishra R. and Verma DL. New York Science Journal. 2009c; 2(5): 93-95.
19. Mishra R. and Verma DL. (to be published); Mishra R. and Verma DL. (to be published).
20. Nawwar M. A. M., El-Mousallamy A. M. D. and Barkat H. H. Quercetin 3-glycosides from the Leaves of *Solanum nigrum*. Phytochemistry. 1989; 28(6): 1755-1757.
21. Nickell L. S. Antimicrobial Activity of Vascular Plant. Economic Botany. 1959; 13: 281-381.
22. Oleszek K. Dietary Phyto -chemicals and Human Health. Phytochemistry. 2002; revised 1: 163 -166; Overend W.G. In the Carbohydrates Chemistry and Biochemistry. (eds., W. Pigman and D. Horton) Academic Press: New York, 1972: 308-09.
23. Pande H. C. Systematic of the Ferns Flora of Kumaun Himalaya. Ph. D. Thesis, Kumaun University, Nainital, 1992.
24. Salatino M. L. F. and Prado J. Flavonoid Glycosides of Pteridaceae from Brazil, Biochem. Sys. and Ecol. 1998; 26: 761-769.
25. Yasukawa K. and Takido M. Phytochemistry. 1987; 26: 1224.
26. Yasukawa K., Sekine H. and Takido M. Phytochemistry. 1989; 28: 2215.

Progress In Dracunculiasis Eradication: Ogun State, South-West Nigeria As Case Study

Morenikeji Olajumoke * and Adekolu Abimbola

Parasitology unit, Department of Zoology, University of Ibadan, Nigeria.
E-mail: jumokemorenikeji@yahoo.co.uk
Telephone: +234 805 527 5915

Abstract: Studies on dracunculiasis at the threshhold of its eradication was carried out in 8 infected and at-risk non-infected villages in Obafemi Owode Local Government Area(LGA) of Ogun State between January and December 2005. Current prevalence status of the villages were determined, pretested and standardised questionnairres were administered to head of households(HOHs) to assess Knowledge, Atitude and Practice(KAP) in the management of guinea worm and water samples were collected for cyclops identification. 158 people were examined in 3 infected villages, cyclopoid copepods were recovered from all ponds in the study villages and 76 HOHs were interviwed. The overall prevalence of infection was 5.07%. There was no significant difference in the prevalence of infection between sexes, 5.04% and 4.76% in the females and males respectively (χ^2 = 0.03,P>0.05).The period of infection coincided with the dry season. Uninfected *Halicyclops* and *Thermocyclops* species of cyclops were recovered. Majority(74.1%) of HOHs in infected and 38.8% HOHs in at-risk villages had been infected before. Most(68.4%) HOHs believe the infection is from drinking water. Filtering of water was mostly practised. Studies show that with persistent eradication efforts the 2009 daedline for eradication of the guinea worm disease from the country will be met. [The Journal of American Science. 2009; 5(4):189-193]. (ISSN 1545-1003).

Keywords : Dracunculiasis, Guinea worm prevalence, Cyclops, Nigeria.

Introduction

Dracunculiasis is one of the oldest diseases known to man. Although it is not a killer disease, it is a disease of high morbidity and complications found mostly in farming populations(Brieger and Guyer,1990). Its health, social, educational and economic cost to the individual, the household and the community which is considerable and it's transmission cycle are well documented (Belcher *et al*,1975; Kale,1977). Key intervention strategies to eradicate guinea worm are safe water supply, vector control using abate, health education and case management.

The complete eradication of the guinea worm disease which is still endemic among the poorest rural communities in areas without safe water supplies in Sub-Saharan Africa will require sustained high level political,financial and community support (Diamenu and Nyaku,1998). There has however been tremendous progress towards the eradication of the disease.The World Health Assembly in 1986 reported that an estimateed 3.5 million persons in 20 countries had the disease and approximately 120 million persons were at risk of infection in 1986. By the end of 2002,annual incidence of the disease had been reduced by more than 98%. The burden of guinea worm disease today occurs in Sudan,Ghana and Nigeria.These three countries account for 93% of all cases worldwide (Department of Health and Human Services,2003).

This study is on the epidemiology of dracunculiasis at the threshhold of its eradication in eight infected and at-risk non-infected villages in Obafemi Owode Local Government Area(LGA) of Ogun State.

Materials and Methods

Study Area

The study area, Obafemi Owode LGA is one of the two LGAs found to be endemic for guinea worm disease in Ogun state, south-west Nigeria. The other being Odeda LGA (Morenikeji and Alade,2006). Obafemi Owode LGA is located between Latitude 6^0 45^1 and6^0 53^1 north of the equator and Longitude 3^0 40^1 and 3^0 54^1 east of the Greenwich meridien. The people in the LGA are predominantly farmers and Yoruba speaking with Egba dialect.

The villages under survey are Agbedi, Jibowu, Olowotedo, Onibata, Oduro, Oluwo oke, Sapala, Makinde, and Eleruja. These villages are known to have a long experience of guinea worm infection. However, at the time of this survey, Agbedi, Jibowu and Olowotedo were the villages infected while the other villages were at risk of infection.They were at risk of infection because they were located around villages infected in

2005,they had been infected before until 2005 and were under surveillance by Global 2000.

Main water sources in the villages include rivers and ponds, deep wells and a borehole in Agbedi. Some villages are supplied water weekly from the LGA office.

Methods

The prevalence of dracunculiasis was determined in the three infected villages after ascertaining that people in the study villages had been residing in the area for at least one year.Prevalence of infection was determined in relation to age and sex and compared to the data for previous year got from Global 2000 Carter Centre,South-West Zonal office,Nigeria.

Questionnaire Administration

Pretested and standardised questionnaires were administered to all heads of households (HOHs) in infected villages and randomly administered to HOHs in villages at risk of infection. Questionaires were used to record the respondents village and demographic information. Source and treatment of water in households was recorded.Their perception of the cause/ seriousness and prevention of the disease was also recorded.

The questions were asked in Yoruba language assisted by Global 2000 field staff and village-based Health Workers (VBHWs). Eradication activities and measures in the villages were noted.

Collection of Water Samples For Cyclopoid identification

Water samples were collected in the evenings when villagers came to fetch water from ponds. Water samples were taken from 7 different ponds in the study area. Agbedi, Olowotedo,Jibowu, and Onibata use a common pond, Semore pond. Other ponds include Ganta and Morocco in Oduro,Iporo pond in Oluwo Ake, Orisunbare pond and Oripako pond in Sapala Makinde and Agodo pond in Efunjo.

Water samples were collected and examined for Cyclops types and infection rates according to methods described by Falode and Odaibo (2002). Morphological identification was done by the illustrated keys of Jeje and Fernando (1986) and Boxshall and Braide (1991).

Data analysis involved frequency and distribution statistics. The results were tested with Pearson's χ^2 to determine variability in the distribution of categorical variables for each study outcome, with an α – level of $P < 0.05$ indicating statistical significance.

Results

A total of 158 people were examined in the three infected vilages under study , 84 males and 74 females. 8(5.07%) were infected, 3.2% in Agbedi, 1.3% in Olowotedo and 0.6% in Jibowu. Out of those infected,4(50%) and 4(50%) were males and females respectively. Although the prevalence in males (4.76%) was lower than females (5.40%), it was not statistically significant (χ^2=0.03,d.f.=1,p>0.05). Infection was found in three age groups; 11-20(37.5%),21-30(37.5%) and 61-70(25%) (Table 1).

The location of guinea worm infection was in the lower limbs. The number of emerging worms was between 1 and 3. Incapacitation lasted for a period of two weeks to a month after the blister bursted. Of those infected, there were four farmers (50%),one trader (12.5%) and three students (37.5%). The cases were recorded in the months of March and April towards the end of dry season. A total of 42 and 13 cases were recorded in the three infected villages in 2003 and 2004 respectively. There were 83 and 15 cases in all in the LGA in 2003 and 2004 respectively, 81% and 90% reduction in the number of cases from 2003 to 2005 in the three infected villages and LGA respectively.

For the KAP studies in the infected and at-risk non-infected villages, 76 households were sampled in 8 villages. 35.5% households in three infected villages and 64.4% in five at- risk non-infected villages. 54(71.1%) respondents were males while 22(28.9%) were females. More respondents were between 61-70 years (36.8%) followed by those aged 51-60 years (18.4%), 41-50(15.8%), 31-40(14.5%), 21-30(7.9%) and 71+(6.6%). Most(71.1%) of the respondents were farmers,17.1% were traders while 11.8% did other things like tailoring and carpentry.

Most (74.1%) of the respondents in infected villages had been infected before while only 38.8% were infected before in the villages at risk of infection. 51.3% had been infected before in all the villages. Majority(76.3%) still consider guinea worm disease a serious problem in their village.

When rerspondents were asked what they perceived as the cause of infection,81.5% of those from the infected villages knew infection was from drinking infected water, while 61.2% knew in the villages at risk of infection. For treatment, apart from the winding of the worm around a stick, most from all villages(69.2%) claimed they used antibiotics while 12.8% used shea butter, another 12.8% used herbs and 5.2% used nothing.

87.2% of those infected before claimed that the infection had very serious effect on their farming activities, 79.5% said effect of infection on their

econonmic well being for the period of infection was very high and 71.8% claimed it had very serious adverse effect on their social activities.

Majority (65.8%) of the respondents get their drinking water from ponds, 15.8% from boreholes and a few(18.4%) from the well during the dry season. Some claim to harvest rain water during the rains. The water treatment mostly practised by the respondents that treat water(67(88.2%)) was filtering (85.7%), a few boil(7.1%) and a few(7.1%) add alum to their water.

Table 2 shows the number and the species of Cyclops recovered from a total of 7(5 litres) water samples from the ponds in the infected and at-risk villages. No infected Cyclops were found in all samples. *Thermocyclops* and *Halicyclops* species were recovered from ponds.

Table 1: Age And Sex Distribution Of Persons Infected With Guinea Worm In Obafemi Owode LGA, Ogun State.

	Male		Female		Total	
Age Group (years)	No Examined (%)	No Infected(% Prevalence)	No Examined (%)	No Infected(% Prevalence)	No Examined	No Infected
0-10	11(13.1)	0(0)	10(13.5)	0(0)	21(13.3)	0(0)
11-20	09(10.7)	0(0)	08(10.8)	3(4.05)	17(10.8)	3(37.5)
21-30	10(11.9)	2(2.38)	13(17.6)	1(1.35)	23(14.6)	3(37.5)
31-40	17(20.2)	0(0)	09(12.2)	0(0)	26(16.5)	0(0)
41-50	07(8.3)	0(0)	12(16.2)	0(0)	19(12.0)	0(0)
51-60	10(11.9)	0(0)	08(10.8)	0(0)	18(11.4)	0(0)
61-70	20(23.8)	2(2.38)	14(18.9)	0(0)	34(21.5)	2(25)
TOTAL	84(100)	4(4.76)	74(100)	4(5.40)	158	8(100)

Table 2: Cyclopoid Copepods in Ponds in Obafemi Owode LGA, Ogun State

Ponds	Villages that use the Pond	Species of Cyclops	No present per 5 litres of water
Semore	Agbedi,Jibowu, Olowotedo and Onibata	*Thermocyclops oblongatus nigerianus*	2
Gamta	Oduro	*Thermocyclops oblongatus nigerianus*	9
Morroco	Oduro	*Thermocyclops oblongatus nigerianus*	5
Iporo	Oluwo ake	*Halicyclops korodiensis*	2
Orisumbare	Sapala Makinde	*Halicyclops korodiensis*	18
Oripako	Sapala Makinde	*Halicyclops korodiensis*	12
Agodo	Efunjo	*Halicyclops korodiensis*	15

Discussion

The study shows that dracunculiasis is still present in the study area and it also shows the efficacy of eradication measures in reducing the disease prevalence. This can be seen in the number of infections recorded in the previous years (2003 and 2004) as compared with the present status of infection. The decline in guinea worm cases is commendable. This reduction of cases may be attributed mainly to the provision of safe drinking water to these infected villages. Udonsi(1987) and Hopkins (1998) found similar effects in their studies. However efforts must be intensified to combat the last few cases considering the fact that a small foci of infection can bring about a resurgence of the disease.

The study showed that there was no significant difference in the prevalence of infection rate between males and females ($p>0.05$) which conforms with other reports (Onabamiro,1952; Anosike *et al*, 2001).

The period when cases occured was towards the end of dry season (March and April). This dry season is often associated with the consumption of water from ponds or water holes formed (or dug) in the bed of seasonal rivers when flow has ceased.

In many studies,ponds have been claimed to be the ideal source of dracunculiasis transmision (Onabamiro,1952, Kale,1977). Two species of Cyclops with no infection were found during the period of study probably due to the low infection rate in human population which is due to control measures in place.

The study shows that inspite of alternative water sources in some villages such as boreholes and wells,it is almost impossible to stop villagers from going to the ponds. Most HOHs(81.5%) claimed villagers still drink the infested water without filtering especially on their way to or from the farm. Old villagers stated they prefer the "natural" taste of pond water. The presence of the disease in the infected villages is probably as a result of the three infected villages sharing a common pond.

Some villages that had no other source of water other than the ponds like Oduro with only two ponds (Gamta and Morroco) rely solely on these ponds. Onibata and Jibowu villages relied on water that is supplied to them fortnightly by the Government. Hence, the Government's inability to regularly supply safe water also forces inhabitants to revert to these contaminated ponds at the period of high water needs. The only village that had one functional borehole constructed by the government was Agbedi, being the most infected village.

Most of the respondents think that the infection is caused by contaminated pond water because cases of infection reduced when pond treatment and filtering of drinking water started.

Most of the respondents think all ages are susceptible to the infection as they said there was no age or sex spared at the time of high endemicity. In Agbedi however, a few respondents claimed that females are more susceptible than males.

The eradication measures in the villages include usage of cloth and pipe filters supplied monthly by Global 2000 staff, provision of boreholes and wells, application of abate to ponds and most importantly health education,without which these other eradication measures would have failed.

Filters were seen hung outside each household after usage to dry after washing. Water filters though wildly acclaimed to be cheap and the most simple eradication measure, has to be highly distributed to be highly effective. Village based health workers (VBHWs) were trained in each village to treat their ponds with Abate. They do this on monthly basis as long as Abate is given to them by health officials. As noted by Amali (2000), the intensified Abate treatment in 1999/2000 in Ebonyi and Oziba might have caused more than 90% reduction in the number of cases.

Health education has played the most important role in reduction of the disease to a minimal level. It is very important for the success of every component of the intervention strategies and it is a continuous process. For instance, it was observed that in the endemic communities, series of health education were done to enable the villagers accept the treatment of their ponds with Abate which brought about a reduction in the density of cyclopoid copepod population. The combination of both persistent education to change behaviour patterns and implementation of measures to provide safe water has been shown to be effective in the reduction of the disease in previous studies (Nwobi and Ibe,1996; Hopkins,1998).

Correspondence to
Dr Olajumoke Morenikeji
Parasitology unit,
Department of Zoology,
University of Ibadan,
Nigeria.
E-mail: jumokemorenikeji@yahoo.co.uk
Telephone: +234 805 527 5915

References

1. Brieger,W.R. and Guyer, J. Farmers' loss due to guineaworm disease: a pilot study. J.Trop. Med. Hyg 1990; 93: 106-111.

2. Belcher, D.W. , Wurapa, F.K.,Ward, W.B. and Lourie, I.M. Guinea worm in Southern Ghana: it's epidemiology and impact on agricultural productivity. Amer. J. Trop. Med. Hyg 1975; 24, 444-449 .

3. Kale, O.O. Clinico-epidemiological profile of guinea worm in the Ibadan District of Nigeria. Amer. J. Trop. Med. Hyg 1977; 26,208-214.

4. Diamenu, S.K. and Nyaku,A.A.. Guinea worm disease- A chance for successful eradication in the Volta Region, Ghana. Social Science Medicine 1998; 47(3): 405-410.

5. Department of Health and Human Services. Guineaworm wrap-up No 132. Centres for Disease Control and Prevention 2003; www.cdc.gov/ncidod/dpd/parasites/guineaworm/wrap-up/word.

6.Morenikeji O.A and Alade A.O. Guinea worm disease and its persistence in some rural communities of Nigeria. Nigerian Journal of Parasitology 2007; 28(1) : 15-19

7. Falode O. A. and Odaibo A.B. Cyclopoid Copepods in domestic water sources in three villages in Akinyele Local Government Area of Oyo State, Nigeria. The Zoologist 2002;1(2):16-22.

8. Jeje, C.Y. and fernando,C.H. A practical guide to the identification of Nigerian zooplankton (Cladocera,Copepoda and Rotifera) 1986; Pp 120-132.

9. Boxshall,G.A, and Braide, E.I. The fresh water cyclopoids copepods of Nigeria, with an illustrated key to all species. Bull. Br. Mus. Nat. His. (zool) 1991;57(2):185-212.

10. Udonsi,J.K.. Control of endemic dracontiasis by provision of water supply in rural communities of Imo State,Nigeria. Public Health 1987;100: 63-70.

11. Hopkins,D.R. The guinea worm eradication effort: lessons for the future.Emerg. Infect. Dis 1998; 4(3): 414-415.

12. Onabamiro S.D. The geographical distribution and clinical features of *Dracunculus medinensis* in Southwest Nigeria. Ann. Trop. Med. Parasitol 1952; 45: 1-10.

13. Anosike, J.C , Nwoke, B.E.B., Dozie, I.N.S., Oku,E.E., Asor,J.E., Nzeoma,L.G. ,Ameh,G.,Ogbusi,F.I., Adeiyongo,C.M.,Osunwa,C.O., and Ikpeama, C.A. The endemicity of dracunculiasis,transmission pattern and ecology of cyclopoid copepods in the Northwestern part of Ebonyi,Nigeria. International Journal of Natural and Applied Sciences 2001; 1(1): 57-67.

14. Amali, O. Report of Global 2000 guinea worm consulting, Ebonyi Local Government area of Ebonyi State,Nigeria 2000; April 17-28,2000.

15. Nwobi,B.C. and Ibe,K.K. Dracunculiasis transmission and variations in geological formation. A preliminary study in Afiko-Amasiri-Okposi region of South Eastern Nigeria. The Nigerian Journal of Parasitology 1996; 17: 75-81.

Different Technique of Microcalorimetry and Their Applications to Environmental Sciences: A Review

Mohammad Russel [1], Jun Yao[1,*], Huilun Chen[1], Fei Wang[1], Yong Zhou[1], Martin M. F. Choi[2,*], Gyula Zaray[3] and Polonca Trebse[4]

[1] *School of Environmental Studies & Key Laboratory of Biogeology and Environmental Geology of Chinese Ministry of Education & Sino-Hungarian Joint Laboratory of Environmental Science and Health, China University of Geosciences, 430074 Wuhan, P.R. China*
[2] *Department of Chemistry, Hong Kong Baptist University, Kowloon Tong, Hong Kong SAR, P.R. China*
[3] *Department of Chemical Technology and Environmental Chemistry, Eötvös University, H-1518 Budapest, P.O. Box 32, Hungary*
[4] *Laboratory for Environmental Research, University of Nova Gorica, Vipavska 13, 5000 Nova Gorica, Slovenia*

School of Environmental Studies, MOE Key of Biogeology and Environmental Geology Laboratory, Sino-Hungarian Joint Laboratory of Environmental Science and Health, China University of Geosciences, Wuhan, P. R. China, 430074.
Tel: +86 27 67883036, +86-13207152128
Fax: +86 27 87436235
E-mail: yaojun@cug.edu.cn

Abstract: Microcalorimetry plays a significant role with its thermodynamic capacity across a broad range of environmental research fields. Recently developed instrumental methods are easily applied to different fields of study through microcalorimeters and they are commercially available. The effective area of application includes investigation into trace elements, living organisms, solute-solvent interactions, sorption processes and the identification of technical products stability. The combination of microcalorimetry with different specific analytical techniques has taken an effective role in solving the complex study of environmental sciences. Although microcalorimetric analyses have secured a place industrially for quality production, it is still not widely used in industrially. In our understanding it is also possible to apply in ecotoxicological fields of environmental sciences such as wastewater treatment. [The Journal of American Science. 2009;5(4):194-208]. (ISSN: 1545-1003).

Keywords*:* Microcalrimeter; Isothermal titration; Spectrophotometer; Double twin microcalorimeter; Chip microcalorimeter.

1. INTRODUCTION

All chemical, physical and biological processes result in either heat production or heat consumption. Microcalorimetry is a versatile technique for studying these thermal activities in terms of heat, heat flow and heat capacity. Microcalorimetry can be completely nondestructive and non-invasive to the sample. It seldom requires any prior sample treatment nor does it limit analysis to a physical state of the sample. Solids, liquids and gases can all be investigated. Microcalorimetry does not require a sample that has a particular characteristic to enable measurement like FTIR, UV-VIS, NMR, etc. Microcalorimetry is a direct and continuous measurement of the process under study. Unlike other analytical techniques that give "snapshots" of data, microcalorimetry gives real-time data continuously as the process proceeds. Fig. 1 displays the heat measuring principle of a microcalorimeter.

All calorimeters are thermodynamic instruments but some are also used in kinetics or as analytical tools. Differential scanning calorimetry (DSC) has for a long time been one of the most important techniques in thermal analysis and more recently 'isothermal microcalorimeters' are gaining an increasing importance as analytical instruments, in particular in some applied fields. Up to four independent calorimeters can be used simultaneously with Thermal Activity Monitor (TAM III), to perform repetitive or different types of experiments. TAM III is totally modular and enables a smaller system to be added to increase sample capacity or functionality. With the addition of a multi-calorimeter, holding six independent mini-calorimeters, the sample throughput is increased. While the standard version may be sufficient for many applications, the 48 channel version of TAM III, which enables as many as 48

simultaneous measurements, is recommended for high sample throughput. TAM III is simple to use and seldom requires much sample preparation. Since measurement is continuous, there are no breaks in the data collected. All sample set-up and data acquisition steps are performed by a dedicated software package, TAM Assistant™, which can also perform most common types of data analyses. In the isothermal mode, the high level of control enables for both long and short-term experiments to be performed with excellent baseline stability. The step isothermal mode is used to perform isothermal experiments at a number of temperatures in one single experiment. Because the instrument records data continuously, also during the temperature change, phase transitions or other temperature dependent effects will be detected. The scanning mode operates a linear ramp of temperature with time. Since the scanning rate is very slow the sample can be considered to be in thermal, chemical and physical equilibrium during measurement. In kinetic studies, the slow scanning rate ensures that the reaction follows the Arrhenius relation, i.e. the actual reaction rate takes place without significant overshoot in temperature. Fig. 2 shows one unit of TAM III multi-channel isothermal micro calorimeter. Most isothermal micro-calorimeters in current use are of the heat conduction type, for details of heat conduction micro-calorimeter see the references (Backman et al 1994; Wadsö 1994).

Currently calorimeters designed for work in the microwatt range conducted environmental research work under isothermal conditions. Nano-calorimeters, the name of which usually indicates a detection limit approaching one nano-watt, are included here in the group of micro-calorimeters. Recent developments in isothermal microcalorimetry have been substantial and several “easy to use” instruments are now commercially available. When complex processes are characterized by calorimetric measurements, for example in technical products or in biotic materials, it may not be possible to express the results in terms of thermodynamic or kinetic quantities by referring to well-defined reaction steps. In such cases, isothermal micro-calorimeters have found important, but so far limited use, as general ‘process monitors’ (Wadsö 1997).

This review will discuss microcalorimetric technology and its wide range application in environmental research. Its not cover all the applications of microcalorimetric technique in respect of environmental issue. Due to this limitation we apologize. Special attention will focus on different microcalorimeter techniques as process monitors in applied areas and where specific analytical measurements are conducted with the calorimetric experiments. Finding suitable microcalorimetric technique to reduce the environmental waste management and safe our environment.

2. MICROCALORIMETRIC AND OTHER METHODS FOR ENVIRONMENTAL STUDIES

2.1. Flow Microcalorimetric Technique

The microcalorimeter contained one flow through type reaction vessel operated at a constant flow rate and another vessel that could be used for mixing. A bubble of air was allowed to enter the flow system before an experiment; this showed the boundary between the liquids, acted as a marker and also helped to clean the reaction vessel before the new liquid entered.

Morgan and Bunch (2000) suggest that the microcalorimeter plays an excellent role in recovering oral microflora. The oral care market is one of the most important in the pharmaceutical sector, toothpaste sales alone were worth nearly $1 billion per annum a decade ago (Zeeve 1991). Microcalorimetry can be used to measure the heat associated with chemical or biochemical reactions (Buckton et al 1991; Chowdhry et al 1983). It has been to be a useful tool for examining many types of cellular activities in a wide range of organisms (Kemp 1991; Criddle et al 1991; Beezer et al 1977). The advantage of microcalorimetry is that the microorganisms can be challenged with various concentrations of the agent and any response is immediately registered. Microcalorimetry can be used to indicate a wider range of metabolic events that are inhibited by assessment percentage. Indeed, microcalorimetry has provided useful information for the synthetic drug design (Huang et al 1998) and has been used in deriving quantitative structural activity relationships (QSARs) (Montanari 1999). In their study it is proposed that microcalorimetry with cryopreserved cells could be used as a method for rapidly assessing the potential of individual or mixtures of components for commercial preparations designed to control oral microflora.

2.2. Combination Techniques

2.2.1. Flow Microcalorimetry and Spectrophotometry

Debord and others (2005) used a flow microcalorimeter to study enzyme (arylesterase) reactions. The enzyme activity is usually determined by spectrophotometry at 270 nm, using phenyl acetate as substrate. During there studies with various inhibitors of this enzyme, they experienced some limitations of the spectrophotometric

technique, due to the high absorption of some inhibitors. So that they are selected microcalorimetry as a suitable alternative technique, since it does not display such limitations. Their main object was to summarizing the theoretical aspects of the microcalorimetric method, taking advantage of recent mathematical developments concerning the integrated Michaelis equation (Schnell & Mendoza 1997; Goudar et al 1999; Barry et al 1995) in order to validate the microcalorimetric study of arylesterase through comparison with the standard spectrophotometric method. Johnson and Biltonen (1975) have shown that the validity of this hypothesis depends on the existence of a thermal equilibrium between the exiting solution and the body of the calorimeter cell. Determining the thermodynamic and kinetic parameters of enzyme reactions is very useful to follow special references (Beezer et al 1972; Beezer & Stubbs 1973; O'Neill et al 2003; O'Neill et al 2004a; O'Neill et al 2004b). The microcalorimetric analysis of enzyme reactions often requires application of the integrated Michaelis equation. This application or integration was previously performed mostly by linear regression applied to a linearized form of the equation (Juszkiewicz et al 1998; Kot et al 2000; Todd & Gomez 2001; Stödeman & Schwartz 2002; Stödeman & Schwartz 2003). The results show that flow microcalorimetry could be a useful method for kinetic studies of arylesterase.

2.2.2. Differential Scanning and Isothermal Titration Microcalorimetry

The capabilities of contemporary differential scanning and isothermal titration microcalorimetry (ITC) for studying the thermodynamics of protein unfolding/refolding and their association with partners, particularly target DNA duplexes, were considered (Privalov & Dragan 2007). Contemporary DSC instruments are characterized not only by high sensitivity but by the high stability of their baseline and the ability to scan aqueous solutions up to and above 100 $^{\circ}$C under excess pressure and by super cooling down below 0 $^{\circ}$C. The wide operational range is important because changes of many macro molecules take place over a very broad temperature range. The main specificities of the contemporary ITC instruments are their sensitivity (*i.e.*, the nanomolar consumption of material for experiment), the stability work at various fixed temperatures and fast equilibration at reloading the sample and changing the temperature at points whose measurements are conducted. The combined use of the isothermal titration and differential scanning microcalorimeters is critical. One of the important results from that study is the revealed qualitative difference in the energetic signatures of protein binding to the minor and major grooves.

2.2.3. Differential Calorimeter and Respirometer

So far only a few studies have been conducted about wastewater pollution based study in respect to the microcalorimetric analytical method in this specific field. One of these studies has used a combination method with differential calorimeters for animal wastewaters (AWW). The animal wastewaters were sampled from a pig-fattening farm (Dziejowski1995). Long-term and heavy application of AWW to soil may cause the pollution of ground waters, eutrophication of surface waters and biological, chemical and physical changes in soil (Middlebrooks 1974). Animal wastewaters from pig farms are characterized by high values of chemical oxygen demand (COD) and biochemical oxygen demand (BOD), and contain significant amounts of organic and inorganic compounds, N, P and other elements (Middlebrooks 1974). Studies of the microbial decomposition and mineralization of AWW are vital for environmental protection. An important research fact for the calorimetry of soil microbial processes has been concerned with the decomposition of sugars in soil (Yamano & Takahashi 1983; Ljungholm 1979). The main goal of this work is to show the usefulness of a high-volume calorimeter (0.5 dm^3) as an applied method for characterization of the decomposition of AWW in soils.

Soil microorganisms play an essential role in the environment due to their role in cycling mineral compounds and in the decomposition of organic material (Silvana et al 2004). Soil microorganisms and their controlled processes are essential for the long-term sustainability of agricultural systems (Aikio et al 2000). However, many studies of agricultural effects on microbiota in soil are short-term. On the other hand, microorganisms also play an important role in degrading many agrochemicals. This action in the soil can promote a decrease in the toxicity of many organic compounds and influence the health of soil. The microbial activity measured in soils can indicate its degree of fertility and quality for agricultural management (Dumontet et al 2001). This procedure leads to the recommendation of desirable soil management, in order to favor agricultural uses (Kushwaha et al 2001). Knowledge of the dominant microbial processes in agricultural soils requires a great number of measurements at different conditions, which also requires a great number of samples and accurate methods (Turner et al 2001). A usual method to quantify microbial activity in soils

consists in measuring soil respiration as carbon dioxide evolution or molecular oxygen consumption, which depends on microbial biomass composition in the soil, ambient temperature and moisture content. These methods employed for monitoring the microbiology of soil, have some advantages and limitations with a common characteristic that consists of measuring a given final product (Klein & Paschke 2000). The investigation of soil microbial activity is the use of a calorimetric technique, which has recently increased due to its facility in data collection. Some calorimetric investigations have been compared with classical methods for soil microbiology, referring to temperate soils. Calorimetric measurements for a metabolic process have become a method important for studying microorganisms, but the interpretation of the thermal effect observed requires additional biochemical information, including the simultaneous knowledge of molecular oxygen consumption and carbon dioxide evolution. The thermal effect involved can be followed through power–time curves and the great advantage of this procedure is the evaluation of the enthalpy values. Another advantage of the calorimetric method is related to the fact that it is simple and the measurement does not affect the sample. The signal is continuously recorded and enables to follow measurement of the same sample, a procedure which is not possible for other methods. The lowest incubation time presented smaller correlation values than those from longer incubation times and the best correlation data is verified after 103 days of incubation (Silvana et al 2004). The lowest correlations may be attributed to bioreactions that can be occurring simultaneously with the respiration process. The close correlation between respirometric and calorimetric values suggests that both methods are appropriate for assessing the relationship between the microbial activity and some properties in soils. Based on the obtained calorimetric results, it can be proposed that this technique should be as a useful analytical method for determining the microbial activity in soils.

Control of the utilization of soil for economic purposes is of the utmost importance for sustainable development. The Kyoto protocol states that CO_2 emissions due to soil utilization must be controlled and appropriate methodologies introduced that are rational and allow the monitoring of soil activity. Most studies focused soil microbial activity employ the CO_2 dissipated and the biomass as indicators. The methodologies to quantify CO_2 and soil biomass are very laborious, and provide results only after very long experimental phases. These studies have only an empirical focus, since it is very difficult to obtain quantitative indicators of soil microbial activity. The main consequence of the methodological limitations has been inappropriate soil management, which in many cases has been responsible for important losses in soil fertility (George et al 2002; O'Connor et al 2005; Stewart et al 2005). Thus, there is need for new methodologies to contribute to a better understanding of the biochemical reactions related to the fertility of soil. Calorimetry appears to be an important option for determination of both biomass and activity. The latest results show that this method can provide qualitative (Critter et al 2002a; Critter et al 2002b; Barros et al 2003) and quantitative (Prado & Airoldi 2002; Barros & Feijóo 2003) indicators of soil microbial activity that could be used as early warning signals of soil deterioration. Calorimeters are sensitive enough to detect very low heat rates. They can continuously monitor soil microbial activity in terms of dissipated heat, which is a direct product of the degradation of the soil organic matter. Preparation of the samples is clean and easy, avoiding the use of reagents that may affect the results and that may be pollutants. Barros and Feijóo (2006) took a further step towards quantitative application of calorimetric methods for the evaluation of the environmental impact of $NH_4FePO_4.H_2O$ (AIP) on soil microbial reactions. This work shows a model and analyzes the power–time curves recorded from soil samples under the effect of different amounts of AIP. For phosphorous and iron contents were determined with an ICP-MS and quantify the percentage of soil organic matter by DSC. Using combination technique they get effective result due to the application of AIP on soil microbial metabolism. It is believed that this information can be very useful for the agriculture industry and its newly assumed obligations with respect to the Kyoto protocol.

2.2.4. Isothermal Titration Microcalorimetry and Atomic Absorption Spectrometry

A great variety of crystalline inorganic layered compounds have been employed as host nanomaterials due to favorable organic substance insertions into the interlayer nanospaces, with the purpose to synthesize inorganic–organic supramolecular systems, which enable applications in many fields, such as chemical surface modifications with functionalized agents, catalysis, toxic substance removal from the environment or compound preparations based on guest polymer intercalation into the layered nanostructures (Çapková & Schenk 2003). The intercalation reaction takes place due to acid–base interaction (Nunes & Airoldi 2000), whose progress of reaction can be easily followed through X-ray diffraction

patterns. The chemical interaction of these invited species with the matrix can provide an explanation related to the intercalation chemistry as well as the interlayer organization of the guest species and the host–guest interactions (Eypert-Blaison et al 2001; Nunes & Airoldi 2000; Fudala et al 2000). The calorimetric technique has been used as a direct method for measuring the enthalpy of the host–guest interactions in many systems (Lima & Airoldi 2003). However, the complete thermo chemical data for systems comprising the intercalation of polar organic molecules into the cavities of lamellar compounds are, nevertheless, very limited in the literature. Thermodynamic data involved with the host/guest interaction of a chosen molecule or with a series of guest molecules and the inorganic polymeric lamellar matrix can give information of the acid–base reactions. From the experimental view point, calorimetric techniques can be successfully applied to such kinds of heterogeneous systems and the effectiveness of the interactive effect that is established at the solid–liquid interface can be determined (Macedo & Airoldi 2006; Ruiz & Airoldi 2004; Lazarin & Airoldi 2006; ; Lazarin & Airoldi 2005). Lazarin and Airoldi (2007) studied hydrated layered crystalline barium phenylarsonate, $Ba(HO_3AsC_6H_5)_2 \cdot 2H_2O$ as host for intercalation of *n*-alkylmonoamine molecules $CH_3(CH_2)n\text{-}NH_2$ (n = 1–4) in aqueous solution. These new intercalated compounds were characterized through physical and thermal methods and some correlations of these data correlate with the energetic of intercalation were observed. Using combination technique and they try to give a new dimension such kind research work. They are getting positive result in respect of that kind of research work. As a result hydrated lamellar crystalline barium phenylarsonate can be used as host support for organic polar molecules. The data obtained from calorimetric determinations are consistent with processes involving *n*-alkylmonoamines and the phenylarsonate nanocompound at the solid–liquid interface, with thermodynamically favorable values from the viewpoint of negative Gibbs free energy, exothermic enthalpy values and also positive entropic results. The correlations between interlayer distances of guest/host enthalpy and interactions with the carbon atom numbers of the aliphatic amine chain can be useful to infer properties for intercalation of undetermined *n*-alkylmonoamines.

2.3. Heat Conduction Microcalorimeter Technique

2.3.1. Single Twin Isothermal Microcalorimeter

In recent years, growing concern has been expressed about chemicals such as heavy metals and organic compounds due to their possible effects on the environment and threats to human health (McGulnness & Georges1991). Acute toxicity tests are the first steps in determining accurate toxicological information. An acute toxicity study can establish the relationship between the dose of a toxicant and the effect it has on the tested organism. In respect to this information**,** Liu and others (2000) has provided substantial data and obtained positive results in the field of environmental ecotoxicology. Microcalorimetry is a quantitative, inexpensive, and versatile method for toxicology research. Miles and Beezer (1986) demonstrated that microcalorimetric studies of bacterial growth reveal temporal details not observable by other techniques. Microcalorimetry can also be used to study the metabolism of mitochondria and the effects of toxicants on mitochondrial metabolism (Liu et al 1996; Tan et al 1996; Xie et al 1993; Wang et al 1991; Liu 1997). Thus, microcalorimetry could be helpful in safeguarding our environment by improving the performance and the operational safety of wastewater treatment plants.

Study of mitochondria is not only of theoretical significance, but also of applied value. Many aspects of the relations between mitochondria and the hardiness of plants, cytoplasmic male sterility of plants, disease and aging have been studied in recent years (Wallace 1992). Moreover, few microcalorimetric studies on the energy release of mitochondria isolated from plants have been previously reported. Zhou and others (2001) studied the energy release of rice mitochondria using a LKB 2277 Bioactivity Monitor under different conditions. After obtaining data on thermodynamic and kinetic behavior of rice mitochondria the results indicated that the lower the temperature the slower the energy release of the rice mitochondria. One can use this method and these results to characterize the ability of rice and other plants to release mitochondrial energy under different conditions.

Isothermal microcalorimetry (IMC) is a rapid technique for measuring changes in the susceptibility of a material to physicochemical change and the aggregate rate of such changes. Changes in heat content accompany all chemical and physical changes, including material degradation (Angberg & Nystromn 1988; Buckton & Beezer 1991;Koenigbauer et al 1992). IMC was utilized to measure the exothermic heat flow from specimens of ultra-high-molecular-weight polyethylene. Charlebois et al. (2003) used Willson's method for interpreting IMC data. It was based on continuous measurement of heat flow at the temperature of interest for an extended period of time. The method involves obtaining an empirical equation as follows

Percent reaction=$H_p/H_t \times 100\%$ (1)

The equation is then integrated from time 0 to ∞ to obtain the total theoretical heat content (H_t) for the test specimen-medium. The applied equation is then re-integrated from 0 to some specified time to give the heat produced (H_p) over that time (Willson et al 1995). They demonstrate in this paper the usefulness of IMC as a viable method for studying the stability of polymeric implant materials.

2.3.2. Double Twin Microcalorimetric Technique

Double twin isothermal microcalorimeter provides a new dimension for the environmental research field. It is a heat conduction microcalorimeter (Wadsö & Markova 2000). In this instrument two twin microcalorimeters are placed adjacent, one on top of the other. The size of the instrument is the same as that of a commercial single twin microcalorimeter and each of the twin parts has similar properties to one normal twin microcalorimeter. There have however, also been reported more advanced measurements where a second calorimeter has been used to assess a secondary parameter characterizing the same process. One example is the number of sorption calorimeters where water vaporized in one calorimeter and absorbed by a sample in another calorimeter (Calvet 1953; Duisterwinkel & Bokhoven 1995; Wadsö & Wadsö 1996; Wadsö & Wadsö 1997). The two important key functions that will be beneficial for the use of this type of microcalorimeter: (1) it is very sensitive with small changes in temperature; (2) with comparison to reference sample side it is consume the time to get steady state for analyzing the sample (fig 3). The advantage with a double calorimeter is that one may easily perform two related calorimetric experiments at the same time and in close proximity.

2.3.3. Multi-channel Isothermal Microcalorimetric Technique

Techniques of isothermal micorcalorimetry have been greatly improved during the past two decades (Wadsö 2002). In addition to their use in fundamental research, applications of practical importance have been established in other areas. However, no significant use of isothermal microcalorimetry has yet been seen in practical applications of biology, despite many methodological studies reported from that discipline. Significant progress has recently, however, been made in the design of multi-channel isothermal microcalorimeters and in techniques where specific analytical methods have been combined with isothermal microcalorimetery.

A microcalorimeter that measures total heat output (μW) was used to determine the total metabolic rate (aerobic and anaerobic) and the cost of feeding (specific dynamic action, SDA) in larval Atlantic cod (*Gadus morhua*) (McCollum et al 2006). This study provides new information on individual measurements of total heat output in larval Atlantic cod. Previously there had been many studies undertaken by measuring oxygen uptake by respirometry (Fyhn & Seristag 1987; Finn et al 1995a; Finn et al 1995b, Finn et al 2002; Herbing & Boutilier 1996; Herbing et al 2001). This study shows that the metabolic cost of feeding increased with development and remained elevated suggesting that cod larvae allocate a large part of their energy budget to growth in order to meet the demands of their fast growth rates.

Using multichannel microcalorimetry Wang fei, et.al (2008) recent work to evaluate the toxic effect of Heavy metal ion Iron (iii) on different biological model. It is an ideal work for concentrate the environmental toxicological issue. They are main object to focus on the microbial ecology of bacteria and fungi in ecological niches. The presences of high metal concentrations have significant adverse effects on whole soil microbial biomass and activity (Preston et al 2000) and soil hydrolase activities (Renella et al 2004, Renella et al 2005). The major scientific and medical interest in iron is based on the essential bio-element, but toxicological considerations are also important in terms of accidental acute exposures by sensitive and accurate methods to assess the microbial activities in vitro. So that using multichannel microcaloriemtry to get power-time curves from thermal effect of different microbial activity. The results also will be useful to understand the tolerance of prokaryotes and eukaryotes to iron overload.

2.3.4. Multi-channel "Chip Calorimeters"

Chip calorimeters are heat power sensors which are developed in MEMS technology (*micro-electromechanical systems*), i.e. all essentially components of a calorimeter such as well defined heat conductance and heat sink, temperature sensors, sensors for the detection of temperature differences, heating resistors and sample containers are integrated on one single chip. A detailed overview of common technologies of chip fabrication for calorimetric devices is given in (Herwaarden 2005). Typically it is made from silicon, silicon nitride, silicon oxide and polymer foils. The design is based on a silicon chip which is etched in the central part in order to obtain a thin membrane (Fig.4).

Microcalorimetric methodology is used widely in the pharmaceutical field for quality production. It is a perfect instrument for pharmaceutical chemical

analysis. We would like to interpret the recent advances in the study of solid state pharmaceutical materials and the importance of microcalorimeter application. The practical example selected is that of formulated products containing benzoyl peroxide – a treatment for acne and athlete's foot (Beezer et al 2004). A newly developed procedure for data analysis is outlined and preliminary results from chemo metric-based analysis of complex solid state reaction schemes are presented. Those solid state reactions are not described by integral reaction orders but through non-integral fitting parameters (Ng 1975, Urbanovici & Segal 1999) that indicates a mechanism for the solid state reaction process is another rather significant limitation. The purpose of this study is to outline new approaches that may ameliorate some of these limitations. Microcalorimetric determinations of stability offers significant time saving relative to traditional high temperature storage studies as these take months to years to complete (Aulton 1988). In contrast, microcalorimetric studies may require, only some 50 hours to yield the appropriate rate constant data (Willson et al 1995, Beezer et al 2001). The overall conclusions of the study were that experimentation was 24 hours faster and this was sufficient to identify solid-state reaction rate coefficient and other relative factors (Zaman et al 2001a, Zaman et al 2001b). Finally, the microcalorimetric requirements for such stability studies are contrasted with the newly emerging multi-channel "chip calorimeters" that operate in the nanorange with high throughput potential.

Recently Johannes Lerchner analyzes the chip microcalorimeter potentiality for biochemical and cell biological investigation (2008).Essential progress in the development and application of chip calorimeters was made due to the growing technological potential evolved during the last decade. It is evident that the invention of chip calorimeters led to a considerable extension of the application field of calorimetry. Thus, it is hardly possible to determine heats of fusion of nano-scaled single crystals without using chip calorimeters (Kwan et al 2001). For the measurement of heats of reaction in nanoliter droplets chip calorimeters are favourable too (Torres et al 2004). Furthermore, chip calorimetry is the method of choice for investigations of absorption phenomena in thin films (Lerchner et al 2004). The membrane serves as sample carrier and contains temperature sensors and heater elements. The thickness of the membrane depends on the kind of application and ranges from several nanometers for high-speed temperature scanning experiments to a few micrometers for isothermal operations. The main advantages of chip calorimeters are their low costs, the ability of multiplex operations, the short sample transfer time and the simple construction. The latter enables the application as control device in bioreactors. Limitations arise from the restricted volume-specific heat power resolution.

2.4. Polarized Microcalorimeter Energy Dispersive X-Ray Spectrometric Technique

The use of microcalorimeter increases day by day according to its versatile analytical properties (Redfern et al 2002). Here we introduce a new type of microcalorimeter which is used commercially for trace metal element. The requirement for improvement in x-ray detector technology has been a major necessity for the semiconductor industry is their long term goal to address the analytical requirements of particles down to 35 nm as discussed in the 1997 National Technology Roadmap for semiconductors (NTRS 1997). To achieve these analytical requirements, the National Institute of Standards and Technology developed a transition edge sensor (TES) Microcalorimeter (Wollman et al 1996). To introduce this exiting technology to industrial applications, EDAX INC and CSP

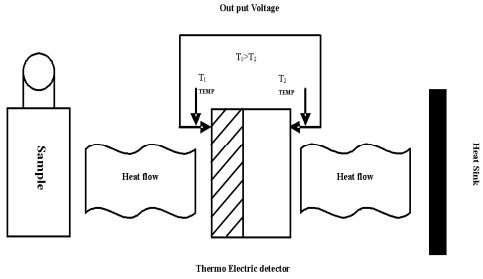

Fig. 1 Principle of measuring the heat by Microcalorimeter.

(Cryogenic Spectrometers) GmbH established a partnership to develop a commercially available microcalorimeter and installed the first beta unit at Infineon Munich.

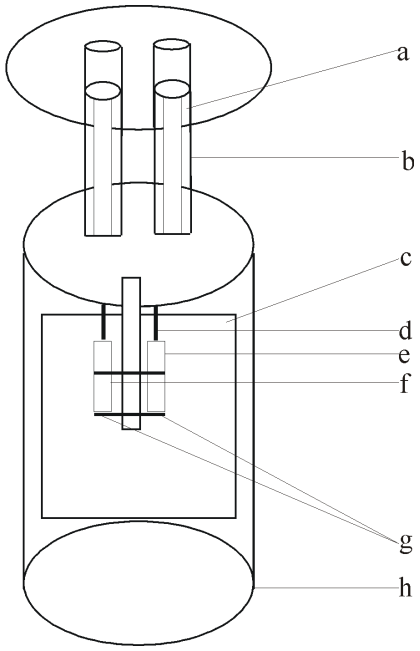

Fig.2 One unit of TAM III multi-channel isothermal micro calorimeter ; (a) Ampoule Lifter; (b) Equilibration Tube; (c) Heat Sink; (d) Ampoule lifter; (e) Sample measuring cup;(f) Reference measuring cup; (g) Thermoelectric modules; (h) Cylinder.

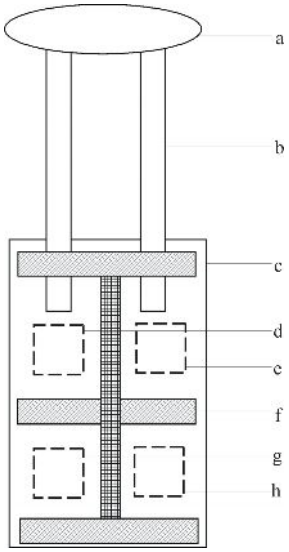

Fig.3 Cross sections of the double twin microcalorimeter; (a) Ampoule lifter ; (b) Tubes through which the calorimeters are charged; (c) Steel can; (d) Top reference ampoule position; (e) Top measuring ampoule position; (f) Heat flow breaker. (g) Bottom reference ampoule position; (h) Bottom measuring ampoule position.

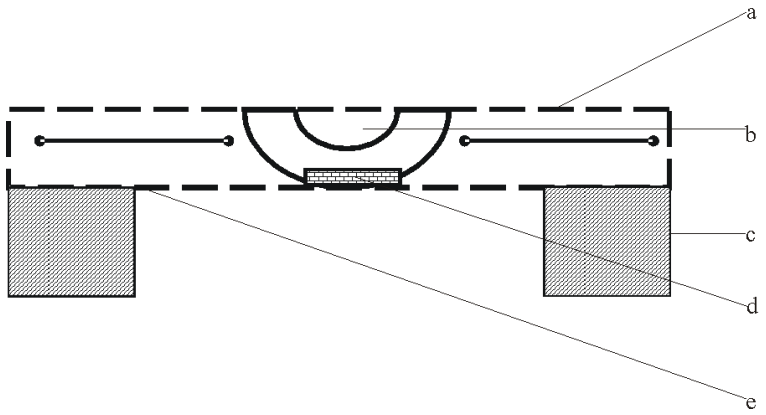

Fig.4 Schema of a chip calorimeter device with a thermopile as temperature sensor; (a) Membrane; (b) Sample; (c) silicon frame; (d) Chip heater; (e) Thermopile.

Table 1 Main application of microcalorimetric analysis and combined techniques to environmental sciences

Application	Techniques	Reference
Identified antimicrobial agents in respect of oral microorganism	Flow microcalorimeter	(Morgan & Bunch 2000)
Enzyme kinetics	Flow microcalorimeter and spectrophotometer	(Debord et al 2005)
Study the biological macromolecules	DSC and Isothermal titration microcalorimeter	(Privalov & Dragan 2007)
Study the animal wastewaters soil characteristics	Differential calorimeter and electolytical respirometer	(Dziejowski 1995)
Determine the soil properties	TG and DSC	(Barros et al 2006)
Determination of process involving at solid/ liquid interface	Isothermal micorcaloriemeter , AAS and X-ray diffraction pattern	(Lazarin & Airoldi 2007)
Determine the metabolism of cells	Heat conduction microcalorimeter	(Liu et al 2000)
Determine energy released from the mitochondria	Heat-Flow microcalorimeter	(Zhou et al 2001)
Studying the stability of polymeric implant material	Isothermal microcalorimeter	(Charlebois et al 2003)
Physical, chemical, biological change can be measured	Double twin isothermal microcalorimeter	(Wadsö & Markova 2000)
Working on living materials	Multi-channel isothermal microcalorimeter	(Wadsö 2002)
Study the metabolic cost of feeding in atlantics cod (larvae) and Evaluate the toxic effect of heavy metal ion on different biological model	Multi-channel isothermal microcalorimeter	(McCollum et al 2006; Wang 2008)
Study the solid state reaction of pharmaceutical importance and Biochemical and cell biological investigation	Multi-channel “chip calorimeter”	(Beezer et al 2004; Lerchner et al 2008)
Determine metal ion	Polaris microcalorimeter energy dispersive x-ray spectrometer	(Redfern et al 2002)

3. CONCLUSION

After overall discussion it is clear that microcalorimetric techniques are dramatically changed from inception to present. This overview cannot cover all applications of microcalorimetric techniques in environmental sciences, aim, however at showing the improvement of the current microcalorimetric analysis techniques regarding qualification, reproducibility and automation as well as the new emerging combined techniques. Table 1 summarizes the current applications of microcalorimetric techniques. Combination of the microcalorimetry methodology with other applications, such as high performance liquid chromatography, inductively coupled plasma mass spectrometry, and various spectroscopic analyses, would help better understand of the intrinsic mechanisms of various surface reactions, ligand-binding processes, microbial activity, and the interactions among soil constituents. In our opinion, the application of this equipment is insufficient for wastewater treatment. Therefore, it is essential to research application methods which can be combined with microcalorimetry for the safety of our environment.

4. ACKNOWLEDGEMENTS

This work was supported in part by grants from the Sino-Italian, Sino-German PPP Governmental International Scientific and Technological Cooperation Project (Annex No.3, 20063139, respectively), National Natural Science Foundation of China (No. 40425001, No.40673065), the Specialized Research Fund for the Doctoral Program of Higher Education (20060491508), the Key Project of Chinese Ministry of Education (107077), and the Hubei Key International Cooperation Project (2006CA007).

Corresponding authors:
Prof. & Dr. Jun Yao,
School of Environmental Studies
& Key Laboratory of Biogeology
& Environmental Geology of Chinese Ministry of Education
& Sino-Hungarian Joint Laboratory of Environmental Science and Health,
China University of Geosciences, Wuhan 430074, P.R. China.

Dr. Martin M. F. Choi,
Department of Chemistry,
Hong Kong Baptist University,
224 Waterloo Road, Kowloon Tong,
Hong Kong SAR, P.R. China
Tel.: +86 27 6788 3036 (J. Yao), +852 3411 7839 (M.M.F. Choi);
Fax: +86 27 6788 5032 (J. Yao), +852 3411 7348 (M.M.F. Choi).
E-mail: yaojun@cug.edu.cn (J. Yao), mfchoi@hkbu.edu.hk (M.M.F. Choi)

School of Environmental Studies,
MOE Key of Biogeology and Environmental Geology Laboratory,
Sino-Hungarian Joint Laboratory of Environmental Science and Health,
China University of Geosciences, Wuhan, P. R. China, 430074.
Tel: +86 27 67883036, +86-13207152128
Fax: +86 27 87436235
E-mail: yaojun@cug.edu.cn

5. REFERENCES:

1. Aikio, S., Väre H., and Strömmer R. (2000).Soil microbial activity and biomass in the primary succession of a dry heath forest. Soil Biology Biochemistry 32, 1091-1100.
2. Angberg, M. and Nystrom, C. (1988). Evaluation of heat-conduction microcalorimetry in pharmaceutical stability studies. Acta Pharmaceutica Suecica 25, 307-320.
3. Aulton, M.E. (1988). Pharmaceutics. Churchill Livingstone.
4. Backman, P., Bastos, M., Hallen, D., Lönnbro, P., and Wadsö, I. (1994). Heat conduction calorimeters: time constants, sensitivity and fast titration experiments. Journal of Biochemical and Biophysical Methods 28, 85-100.
5. Barry, D.A., Barry, S.J. and Culligan-Hensley, P. (1995). Algorithm 743: WAPR: A fortran routine for calculating real values of the w-function. Acm Transactions on Mathematical Software 21, 172-181.
6. Barros, N., Feijóo, S., and Fernández, S. (2003). Microcalorimetric determination of the cell specific heat rate in soils: relationship with the soil microbial population and biophysic significance. Thermochimica Acta 406, 161-170.
7. Barros, N., and Feijóo, S. (2003). A combined mass and energy balance to provide bioindicators of soil microbiological quality. Biophysical Chemistry 104, 561-572.
8. Barros, N., Airoldi, C., Simoni , J. A., Ramajo, B., Espina, A., and García, J. (2006). Calorimetric determination of the effect of

ammonium-iron(II) phosphate monohydrate on *Rhodic Eutrudox* Brazilian soil.Thermochimica Acta 441,89-95.
9. Beezer, A.E., Chowdhry, B.Z., Newell, R.D. and Tyrrell, H.J.V. (1977). Bioassay of antifungal antibiotics by flow micorcalorimetry. Analytical Chemistry 49, 34-37.
10. Beezer, A.E., Tyrrell, H. and Steenson, T. (1972). Protides of the Biological Fluids. Pergamon Press, p. 563.
11. Beezer, A.E. and Stubbs, C. (1973). Application of flow microcalorimetry to analytical problems—I Determination of organophosphorus pesticides by inhibition of cholinesterase. Talanta 20, 27-31.
12. Beezer, A.E., O'Neill, M.A.A., Urakami, K., Connor, J.A. and Tetteh, J. (2004). Pharmaceutical microcalorimetry: recent advances in the study of solid state materials. Thermochimica Acta 420, 19-22.
13. Beezer, A.E., Morris, A.C., O'Neill, M.A.A., Willson, R.J., Hills, A.K., Mitchell, J.C. and Connor, J.A. (2001). Direct determination of equilibrium thermodynamic and kinetic parameters from isothermal heat conduction microcalorimetry. Journal of Physical Chemistry 105, 1212-1215.
14. Buckton, G., Russell, S.J. and Beezer, A.E. (1991). Pharmaceutical calorimetry: a selective review. Thermochimica Acta 193, 195-214.
15. Buckton, G. and Beezer, A.E. (1991). The applications of microcalorimetry in the field of physical pharmacy. International Journal of Pharmaceutics 72, 181-191.
16. Chowdhry, B.Z., Beezer, A.E. and Greenhow, E.J. (1983). Analysis of drugs by microcalorimety: isothermal power-conduction calorimetry and thermometric titrimetry. Talanta 30, 209-243.
17. Criddle, R.S., Breidenbach, R.W. and Hansen, L.D. (1991). Plant calorimetry: how to quantitatively compare apples and oranges. Thermochimica Acta 193, 67-90.
18. Critter, S. A. M., Freitas, S. S., and Airoldi, C. (2002a). Microbial biomass and microcalorimetric methods in tropical soils. Thermochimica Acta 394,145-154.
19. Critter, S. A. M., Freitas, S. S., and Airoldi, C. (2002b). Comparison between microorganism counting and a calorimetric method applied to tropical soils. Thermochimica Acta 394, 133-144.
20. Çapková P., and Schenk H., (2003). Host–guest Complementarity and Crystal Packing of Intercalated Layered Structures . Journal of Inclusion Phenomena and Macrocyclic Chemistry, 47, 1-10.
21. Charlebois, S.J., Daniels, A.U. and Lewis, G. (2003). Isothermal microcalorimetry: an analytical technique for assessing the dynamic chemical stability of UHMWPE. Biomaterials 24, 291-296.
22. Calvet, E. (1953). Adaptation of a microcalorimeter of four elements to the thermogravimetry of adsorption. C R Academic Science (Paris) 236, 486-488.
23. Debord, J., Harel, M., Bollinger, J., Verneuil, B., Merle, L. and Dantoine, T. (2005). Flow microcalorimetric study of enzyme reactions: application to arylesterase from human serum. Thermochimica Acta 427, 85-91.
24. Dziejowski, J.E. (1995). Calorimetric and respirometric characteristics of the decomposition of animal wastewaters in soil. Thermochimica Acta 251, 37-43.
25. Dumontet, S., Mazzatura, A., Casucci, C., and Perucci, P. (2001). Effectiveness of microbial indexes in discriminating interactive effects of tillage and crop rotations in a Vertic Ustorthens. Biology and Fertility of Soils 34, 411-416.
26. Duisterwinkel, A.E. and Bokhoven, J.J.G.M. (1995). Water sorption measured by sorption calorimetry. Thermochimica Acta 256, 17-31.
27. Eypert-Blaison, C., Sauzéat, E., Pelletier, M., Michot, L. J., Villiéras, F., and Humbert, B. (2001) Hydration Mechanisms and Swelling Behavior of Na-Magadiite. Chemistry of Materials 13, 1480-1486.
28. Fudala, Á., Kónya, Z., Kiyozumi, Y., Niwa, S. I., Toba, M., Mizukami, F., Lentz, P. B., Nagy J., and Kiricsi, I. (2000). Preparation, characterization and application of the magadiite based mesoporous composite material of catalytic interest. Microporous and Mesoporous Materials 35, 631-641.
29. Fyhn, H.J. and Seristag, B. (1987). Free amino acids as energy substrate in developing eggs and larvae of the cod (*Gadus morhua*). Marine Biology 96, 335-341.
30. Finn, R.N., Fyhn, H.J. and Evjen, M.S. (1995a). Physiological energetics of developing embryos and yolk-sac larvae of Atlantic cod (*Gadus morhua*). I. Respiration and nitrogen metabolism. Marine Biology 124, 355-369.
31. Finn, R.N., Hendersen, J.R. and Fyhn, H.J. (1995b). Physiological energetics of

developing embryos and yolk-sac larvae of Atlantic cod (*Gadus morhua*). II. Lipid metabolism and enthalpy balance. Marine Biology, 124 371-379.
32. Finn, R.N., Ronnestad, I., van der Meeran, T. and Fyhn, H.J. (2002). Fuel and metabolic scaling during the early life stages of Atlantic cod (*Gadus morhua*). Marine Ecology-Progress Series 243, 217-234.
33. Goudar, C.T., Sonnad, J.R. and Duggleby, R.G. (1999). Parameter estimation using a direct solution of the integrated Michaelis-Menten equation. Biochimica et Biophysica Acta -Protein Structure Molecular Enzymology 1429, 377-383.
34. George, T., Magbanua, R., Garrity, D. P., Tubaña, B. S., and Quiton J. (2002). Rapid Yield Loss of Rice Cropped Successively in Aerobic Soil. Agronomy Journal 94, 981-989.
35. Huang, Z.Y., Liu, Y., Qu, S.S. and Feng, Y. (1998). A comparative study on half-inhibitory concentration of Schiff base-metal complexes reacting with bacteria. Thermochimica Acta 320, 121-126.
36. Herbing, H. V. I. and Boutilier, R.G. (1996). Activity and metabolism of larval Atlantic cod (*Gadus morhua*) from the Scotian Shelf and Newfoundland source populations. Marine Biology 124, 607-617.
37. Herbing, H. V. I., Gallager, S.M. and Halteman, W. (2001). Metabolic costs of pursuit and attack in early larval Atlantic cod. Marine Ecology-Progress Series 216, 201-212.
38. Herwaarden, A.W.C. (2005) Overview of calorimeter chips for various applications, Thermochimica Acta 432, 192–201.
39. Johnson, R.E. and Biltonen, R.L. (1975). Determination of reaction rate parameters by flow microcalorimetry. Journal of the American Chemical Society 97, 2349-2355.
40. Juszkiewicz, A., Kot, M. and Zaborska, W. (1998). Calorimetric study of inhibition of urease by 2-mercaptoethanol: procedures based upon integrated rate equations. Thermochimica Acta 320, 45-52.
41. Kemp, R.B. (1991). Calorimetric studies of heat flux in animal cells. Thermochimica Acta 193, 253-267.
42. Kot, M., Zaborska, W. and Juszkiewicz, A. (2000). Inhibition of jack bean urease by thiols: calorimetric studies. Thermochimica Acta 354, 63-69.
43. Kushwaha, C. P., Tripathi, S. K., and Singh, K. P. (2001). Soil organic matter and water-stable aggregates under different tillage and residue conditions in a tropical dry land agro ecosystem. Applied Soil Ecology 16, 229-241.
44. Klein, D. A., and Paschke, M. W. (2000). A soil microbial community structural-functional index: the microscopy-based total/active/active fungal/bacterial (TA/AFB) biovolumes ratio. Applied Soil Ecology 14, 257-268.
45. Koenigbauer, M.J., Brooks, S.H., Rullo, G. and Couch, R.A. (1992). Solid-state stability testing of drugs by isothermal calorimetry. Pharmacological Research 9, 933-944.
46. Kwan, A.T., Efremov, M.Yu., Olson, E.A., Schiettekatte, F., Zhang, M., Geil, P.H. and Allen, L.H. (2001). Nanoscale calorimetry of isolated polyethylene single Crystals. Journal of Polymer Science B 39, 1237–1245.
47. Ljungholm, K., Norėn, B., Sköld, R., Skold, R. and Wadso, J. (1979). Use of microcalorimetry for the characterisation of microbial activity in soil. Oikos 33, 15-2.
48. Lima, C. B. A., and Airoldi, C. (2003).Crystalline calcium phenylphosphonate thermodynamic data on n-alkylmonoamine intercalations. Thermochimica Acta 400, 51-59.
49. Lazarin, A. M., and Airoldi, C. (2006) Host hydrated barium phenylphosphonate/guest heterocyclic amine intercalation energetics by calorimetric titration. Thermochimica Acta 445 57-60.
50. Lazarin, A. M., and Airoldi, C. (2005). Calorimetric data on intercalation of some aromatic amines into barium phenylphosphonate at the solid/liquid interface. The Journal of Chemical and Thermodynamics 37, 243-248.
51. Lazarin, A. M. and Airoldi, C. (2007). Thermochemistry of intercalation of *n*-alkylmonoamines into lamellar hydrated barium phenylarsonate. Thermochimica Acta 454, 43-49.
52. Liu, Y., Li, X., Qu, S.S. And Shen, P. (2000) Microcalrimetric investigation of the toxic action of Cd^{2+} on *Rihizopus nigricans* growth. Journal of Biochemical and Biophysical Methods 45, 231-239.
53. Liu, Y., Wang, X.Q., Xie, C.L., Qu, S.S., Deng, F.J. and Guo, Y. (1996). Microcalorimetric study of metabolic inhibition by humic acids in mitochondria from Oryctolagus cuniculus domestica liver cells. Chemosphere 33, 99-105.
54. Liu, Y. (1997). Thermochemical studies on

the metabolic characteristics of bacteria and mitochondria. Wuhan University, Wuhan, China: Ph.D. Thesis.
55. Lerchner, J., Maskow, T. and Wolf, G. (2008) Chip calorimetry and its use for biochemical and cell biological investigations. Chemical Engineering and Processing 47, 991–999.
56. Lerchner, J., Kirchner, R., J. Seidel, Waehlisch, D. and Wolf, G. (2004). Determination of molar heats of absorption of enantiomers into thin chiral coatings by combined IC calorimetric and microgravimetric (QMB) measurements. I. IC calorimetric measurement of heats of absorption, Thermochimica Acta 415, 27–34.
57. Morgan, T.D. and Bunch, A.W. (2000). Cryopreservation of *Streptococcus mutans* for microcalorimetry based applications. Thermochimica Acta 349, 9-15.
58. Montanari, M.L.C., Beezer, A.E. and Montanari, C.A. (1999). QSAR based on biological microcalorimetry: the interaction of *Saccharomyces cerevisiae* with hydrazides. Thermochimica Acta 328, 91-97.
59. Middlebrooks, E.J. (1974). Animal wastes management and characterization. Water Research, 8, 697-712.
60. Macedo, T. R., and Airoldi, C. (2006). Host lamellar silicic acid magadiite for some heterocyclic amine inclusions and quantitative calorimetric data. Microporous and Mesoporous Materials 94, 81-88.
61. McGulnness, M.S. and Georges, B.B. (1991). Acute toxicity measurements on aquatic pollutants using microcalorimetry on tissue-cultured cells. Environmental Science & Technology 25, 1092-1098.
62. Miles, R.J., Beezer, A.E. and Lee, D.H. (1986). Growth of mycoplasma mycoides subspecies mycoides on media containing various sugars and amino sugars: An ampoule microcalorimetric study. Microbios 45, 7-19.
63. McCollum, A., Geubtner, J. and Herbing, H. V. I. (2006). Metabolic costs of feeding in Atlantic cod (*Gadus morhua*) larvae using microcalorimetry. Ices Journal of Marine Science 63, 335-339.
64. NTRS. (The National Technology Roadmap for Semiconductors). (1997). The semiconductor industry association, 4300 Stevens Creek Boulevard, Suite 271, San Jose, CA 95129.
65. Nunes, L. M., and Airoldi, C., (2000). The Intercalation of Some Heterocyclic Amines into α-Titanium Hydrogenphosphate—Structural and Calorimetric Data. Journal of Solid State Chemistry 154, 557-563.
66. Ng, W.L. (1975). Thermal decomposition in the solid state. Australian Journal of Chemistry 28, 1169-1178.
67. O'Neill, M.A.A., Beezer, A.E., Labetoulle, C., Nicolaides, L., Mitchell, J.C., Orchard, J.A., Connor, J.A., Kemp, R.P. and Olomolaiye, D. (2003). The base catalysed hydrolysis of methyl paraben: a test reaction for flow microcalorimeters used for determination of both kinetic and thermodynamic parameters. Thermochimica Acta 399, 63-71.
68. O'Neill, M.A.A., Beezer, A.E., Mitchell, J.C., Mitchell, J.C., Orchard, J.A. and Connor, J.A. (2004a). Determination of Michaelis–Menten parameters obtained from isothermal flow calorimetric data. Thermochimica Acta 417, 187-192.
69. O'Neill, M.A.A., Beezer, A.E., Vine, G.J., Kemp, R.P., Olomolaiye, D., Volpe, P.L.O. and Oliveira, D. (2004b). Practical and theoretical consideration of flow-through microcalorimetry: determination of "thermal volume" and its flow rate dependence. Thermochimica Acta 413, 193-199.
70. O'Connor, G. A., Elliott, H. A., Basta, N. T., Bastian, R. K., Pierzynski, G. M., Sims, R. C., and Smith, J. E., Jr.,(2005). Sustainable Land Application: An Overview. Journal of Environmental Quality 34, 7-17.
71. Privalov, P.L. and Dragan, A.I. (2007). Microcalorimetry of biological macromolecules. Biophysical Chemistry 126, 16-24.
72. Prado, A. G. S., and Airoldi, C. (2002). The toxic effect on soil microbial activity caused by the free or immobilized pesticide diuron. Thermochimica Acta 394 155-162.
73. Preston, S., Coad, N., Townend, J., Killham, K. and Paton, G.I.(2000). Biosensing the acute toxicity of metal interactions: are they additive, synergistic, or antagonistic. Environmental Toxicology and Chemistry 19, 775–780.
74. Ruiz, V. S. O., and Airoldi, C. (2004). Thermochemical data for n-alkylmonoamine intercalation into crystalline lamellar zirconium phenylphosphonate.Thermochimica Acta 420, 73-78.
75. Renella, G., Mench, M., Van der Lelie, D., Pietramellara, G., Ascher, J., Ceccherini, M.T., Landi, L. and Nannipieri, P.(2004)

Hydrolase activity, microbial biomass and community structure in long-term Cdcontaminated soils. Soil Biology and Biochemistry 36, 443–451.
76. Renella, G., Landi, L., Mench, M. and Nannipieri, P. (2005). Microbial activity and hydrolase synthesis in long-term Cd-contaminated soils. Soil Biology and Biochemistry 37, 133–139.
77. Redfern, D., Nicolosi, J., Höhne, J., Weiland, R., Simmnacher, B. and Hollerich, C. (2002). The microcalorimeter for industrial applications. Journal of Research of the National Institute of Standards and Technology 107, 621-626.
78. Schnell, S. and Mendoza, C. (1997). Closed form solution for time-dependent enzyme kinetics. Journal of Theoretical Biology 187, 207-212.
79. Stödeman, M. and Schwartz, F.P. (2002). Importance of product inhibition in the kinetics of the acylase hydrolysis reaction by differential stopped flow microcalorimetry. Analytical Biochemistry 308, 285-293.
80. Stödeman, M. and Schwartz, F.P. (2003). Temperature dependence of the kinetics of the acylase hydrolysis reaction by differential stopped flow microcalorimetry. Analytical Biochemistry 321, 1-7.
81. Silvana, A.M., Critter , Sueli, S., Freitas and Airoldi, C. (2004). Comparison of microbial activity in some Brazilian soils by microcalorimetric and respirometric methods. Thermochimica Acta 410, 35-46.
82. Stewart, W. M., Dibb, D. W., Johnston, A. E., and Smyth T. J. (2005). The Contribution of Commercial Fertilizer Nutrients to Food Production**.** Agronomy Journal 97, 1-6.
83. Todd, M.J. and Gomez, J. (2001). Enzyme kinetics determined using calorimetry: A general assay for enzyme activity. Analytical Biochemistry 296, 179-187.
84. Turner, B. L., Bristow, A. W., and Haygarth, P. M. (2001).Rapid estimation of microbial biomass in grassland soils by ultra-violet absorbance. Soil Biology and Biochemistry 33, 913-919.
85. Tan, A.M., Xie, C.L., Qu, S.S., Ku, P. and Guo, Y. (1996). Microcalorimetric study of mitochondria isolated from fish liver tissue. Journal of Biochemical and Biophysical Methods 31, 189-193.
86. Torres, F.E., Kuhn, P., Bruyker, D. D., Bell, A.G., Wolkin, M.V., Peeters, E., Williamson, J.R., Anderson, G.B., Schmitz, G.P., Recht, M.I., Schweizer, S., Scott, L.G., Ho, H.J., Elrod, S.A., Schultz, P.G., Lerner, R.A. and Bruce, R.H. (2004). Enthalpy arrays, PNAS 101, 9517–9522.
87. Urbanovici, E. and Segal, E. (1999). General kinetic equation for solid state reactions. Journal of Thermal Analysis and Calorimetry 55, 919-924.
88. Wadsö, I. (1994). In *Solution calorimetry*, ed Marsh K N and O'Hare PAG, Blackwell, Oxford, p 267.
89. Wadsö, I. (1997). Trends in isothermal microcalorimetry. Chemical Society Reviews 26, 79-86.
90. Wang, X.Q., Xie, C.L., Qu, S.S. and Zhou, Z.J. (1991). Microcalorimetric study of mitochondrial metabolism. Thermochimica Acta 176, 69-74.
91. Wallace, D.C. (1992). Mitochondrial genetics: a paradigm for ageing and degenerative disease. Science 256, 628-632.
92. Willson, R.J., Beezer, A.E., Mitchell, J.C. and Loht, W. (1995). Determination of thermodynamic and kinetic parameters from isothermal heat conduction microcalorimetry: applications to long term reaction studies. Journal of Physical Chemistry 99, 7108-7113.
93. Wadsö, L. and Markova, N. (2000). A double twin isothermal microcalorimeter. Thermochimica Acta 360, 101-107.
94. Wadsö, I. and Wadsö, L. (1996). A new method for determination of vapour sorption isotherms using a twin double microcalorimeter. Thermochimica Acta 271, 179-187.
95. Wadsö, I. and Wadsö, L. (1997). A second generation twin double microcalorimeter: measurements of sorption isotherms, heats of sorption and sorption kinetics. Journal of Thermal Analysis and Calorimetry 49, 1045-1052.
96. Wadsö, I. (2002). Isothermal micorcalorimetry in applied biology. Thermochimica Acta, 394, 305-311.
97. Wang, F., Yao, J., Chen, H., Zhou, Y., Chen, Y.J., Chen, H., Gai, N., Zhuang, R., Tian, L., Maskow, T., Ceccanti, B., Trebse, P. and Zaray, G. (2008), Microcalorimetric measurements of the microbial activities of single and mixed species with trivalent iron in soil. Ecotoxicology and Environmental Safety, doi:10.1016/j.ecoenv.2008.01.012
98. Wollman, D.A., Hilton, G.C. and Irwin, K.D. (1996). Proceedings of Microscopy and Microanalysis pp. 488-489
99. Xie, C.L., Tan, A.M., Song, Z.H., Qu, S.S.,

Ku, P. and Quo, Y. (1993). Microcalorimetric study on mitochondrial metabolism inhibited by toxicant. Thermochimica Acta 216, 15-18.
100. Yamano, H. and Takahashi, K. (1983). Temperature effect on the activity of soil microbes measured from heat evolution during the degradation of several carbon sources. Agricultural Biology and Chemistry 47, 1493-1499.
101. Zeeve, R.N. (1991). Toothpaste market-feeling the squeeze. Soap/Cosmet/Chem Specialities 67, 41-44.
102. Zhou, P.J., Zhou, H.T., Liu, Y., Qu, S.S., Zhu, Y.G. and Wu, Z.B. (2001). Studies on the energy release of rice mitochondria under different conditions by means of microcalorimetry. Journal of Biochemical and Biophysical Methods 48, 1-11.
103. Zaman, F., Beezer, A.E., Mitchell, J.C., Clarkson, Q., Elliot, J., Nisbet, M. and Davis, A.F. (2001a). The stability of benzoyl peroxide formulations determined from isothermal microcalorimetric studies. International Journal of Pharmaceutics 225, 135-143.
104. Zaman, F., Beezer, A.E., Mitchell, J.C., Clarkson, Q., Elliot, J., Davis, A.F. and Willson, R.J. (2001b). The stability of benzoyl peroxide by isothermal microcalorimetry. International Journal of Pharmaceutics 227, 133-137.

The Journal of American Science

ISSN 1545-1003

Marsland Press

2158 Butternut Drive
Okemos, Michigan 48864
The United States
Telephone: (517) 349-2362

Emails: editor@americanscience.org;
americansciencej@gmail.com

Websites: http://www.americanscience.org;
http://www.sciencepub.net

ISSN 1545-1003

9 771545 100203